



University of Kentucky  
UKnowledge

---

Theses and Dissertations--Microbiology,  
Immunology, and Molecular Genetics

Microbiology, Immunology, and Molecular  
Genetics

---

2017

## NOVEL ROLE OF PROSTATE APOPTOSIS RESPONSE-4 TUMOR SUPPRESSOR IN B-CELL CHRONIC LYMPHOCYTIC LEUKEMIA

Mary Kathryn McKenna

University of Kentucky, [mkmckenna@uky.edu](mailto:mkmckenna@uky.edu)

Digital Object Identifier: <https://doi.org/10.13023/ETD.2017.445>

[Right click to open a feedback form in a new tab to let us know how this document benefits you.](#)

---

### Recommended Citation

McKenna, Mary Kathryn, "NOVEL ROLE OF PROSTATE APOPTOSIS RESPONSE-4 TUMOR SUPPRESSOR IN B-CELL CHRONIC LYMPHOCYTIC LEUKEMIA" (2017). *Theses and Dissertations--Microbiology, Immunology, and Molecular Genetics*. 17.  
[https://uknowledge.uky.edu/microbio\\_etds/17](https://uknowledge.uky.edu/microbio_etds/17)

This Doctoral Dissertation is brought to you for free and open access by the Microbiology, Immunology, and Molecular Genetics at UKnowledge. It has been accepted for inclusion in Theses and Dissertations--Microbiology, Immunology, and Molecular Genetics by an authorized administrator of UKnowledge. For more information, please contact [UKnowledge@lsv.uky.edu](mailto:UKnowledge@lsv.uky.edu).

## **STUDENT AGREEMENT:**

I represent that my thesis or dissertation and abstract are my original work. Proper attribution has been given to all outside sources. I understand that I am solely responsible for obtaining any needed copyright permissions. I have obtained needed written permission statement(s) from the owner(s) of each third-party copyrighted matter to be included in my work, allowing electronic distribution (if such use is not permitted by the fair use doctrine) which will be submitted to UKnowledge as Additional File.

I hereby grant to The University of Kentucky and its agents the irrevocable, non-exclusive, and royalty-free license to archive and make accessible my work in whole or in part in all forms of media, now or hereafter known. I agree that the document mentioned above may be made available immediately for worldwide access unless an embargo applies.

I retain all other ownership rights to the copyright of my work. I also retain the right to use in future works (such as articles or books) all or part of my work. I understand that I am free to register the copyright to my work.

## **REVIEW, APPROVAL AND ACCEPTANCE**

The document mentioned above has been reviewed and accepted by the student's advisor, on behalf of the advisory committee, and by the Director of Graduate Studies (DGS), on behalf of the program; we verify that this is the final, approved version of the student's thesis including all changes required by the advisory committee. The undersigned agree to abide by the statements above.

Mary Kathryn McKenna, Student

Dr. Subbarao Bondada, Major Professor

Dr. Ken Fields, Director of Graduate Studies

NOVEL ROLE OF PROSTATE APOPTOSIS RESPONSE-4 TUMOR SUPPRESSOR  
IN B-CELL CHRONIC LYMPHOCYTIC LEUKEMIA

---

DISSERTATION

---

A dissertation submitted in partial fulfillment of the  
requirements for the degree of Doctor of Philosophy in the  
College of Medicine  
at the University of Kentucky

By  
Mary Kathryn McKenna

Lexington, Kentucky

Director: Dr. Subbarao Bondada, PhD  
Professor of Microbiology, Immunology, and Molecular Genetics  
and Markey Cancer Center  
University of Kentucky, Lexington, Kentucky

2017

Copyright © Mary Kathryn McKenna 2017

## ABSTRACT OF DISSERTATION

### NOVEL ROLE OF PROSTATE APOPTOSIS RESPONSE-4 TUMOR SUPPRESSOR IN B-CELL CHRONIC LYMPHOCYTIC LEUKEMIA

Chronic Lymphocytic Leukemia (CLL) is defined by the accumulation of clonally expanded CD5+ and CD19+ B lymphocytes in blood and secondary lymphoid organs with impaired apoptotic mechanisms. CLL represents one third of all leukemia cases with an average age of 72 years at diagnosis making it the most common adult leukemia. The E $\mu$ -Tcl1 mouse serves as an excellent model to study the development of CLL as they progress to a CLL like disease by 9-14 months of age, due to overexpression of an oncogene, T cell Leukemia 1(Tcl1), specifically in B cells through the Ig VH promoter and E $\mu$  enhancer (Bichi et al. PNAS. 2002). In an adoptive transfer model, intravenous or intraperitoneal injection of primary CD5+CD19+ CLL cells from the E $\mu$ -Tcl1 CLL mouse into recipient syngeneic mice leads to the development of a CLL like disease within 3-8 weeks of transfer. We have characterized the growth of CLL cells in these mice by periodic submandibular bleeding, spleen ultrasonography and flow cytometry. We find that E $\mu$ -Tcl1 CLL cells express more Prostate apoptosis response-4 protein (Par-4), a known pro-apoptotic tumor suppressor protein, than normal B-1 or B-2 cells in mice. Par-4 is silenced by promoter methylation in more than 30% of all cancers and has been shown to be secreted and to induce apoptosis selectively in various types of cancer cells but not in normal cells. We found that CLL cells have constitutively active B-cell receptor signaling (BCR) and that inhibition of BCR signaling with FDA approved drugs causes a decrease in Par-4 protein, mRNA levels, and an increase in apoptosis. In particular, activities of Src family kinases, spleen tyrosine kinase and Bruton's tyrosine kinase are required for Par-4 expression in CLL cells, suggesting a novel regulation of Par-4 through BCR signaling in both E $\mu$ -Tcl1 CLL cells and primary human CLL samples. Consistent with this, lenti-viral shRNA mediated knockdown of Lyn kinase leads to a decrease in Par-4 expression in MEC-1 cells, a human CLL derived cell line. Ig $\alpha$  (CD79a) silencing in primary human CLL cells also results in down regulation of Par-4 expression. Additionally, we knocked down expression of Par-4 in MEC-1 cells which resulted in a decrease in cell growth that could be attributed to an increase in p21 expression and a reduction in the G1/S cell cycle transition. We have also observed this phenomenon by crossing mice deficient in Par-4 with the E $\mu$ -Tcl1 mouse where lack of Par-4 delays CLL growth in the mouse significantly (time to euthanization due to poor body condition - E $\mu$ -Tcl1: 8.9mo vs Par4-/-E $\mu$ Tcl1: 11.97 mo, p = 0.0472) and splenic B-CLL cells from these mice also have increased expression of p21. Since

mice in this cohort are whole body knockout for Par-4, the difference in survival times between the Par-4 +ve and Par-4 -ve E $\mu$ Tcl1 mice could be due to the influence of Par-4 on CLL cells as well as the effect of Par-4 secreted by the CLL cells on the microenvironment. There could be other potential roles for Par-4 in the context of CLL which are under further investigation. We have also investigated the site of CLL growth in mouse models to determine that the spleen is the primary organ to accumulate the CLL tumor burden. We have found that splenectomy significantly delays the development of CLL in the primary E $\mu$ -Tcl1 mouse model and prevents growth and development in the adoptive transfer model. Interestingly, splenectomy did not delay CLL development as significantly in animals deficient for Par-4 compared to C57BL/6 wild type mice. Par-4 appears to regulate a specific microenvironment required for CLL growth. Current studies are investigating the role of Par-4 in the microenvironment and the cell types that are critical for CLL growth within the splenic niche.

KEYWORDS: Chronic Lymphocytic Leukemia, BCR Signaling, Par-4, Growth Regulation, Splenic microenvironment

Mary Kathryn (Katie) McKenna

---

November 15, 2017

---

Date

NOVEL ROLE OF PROSTATE APOPTOSIS RESPONSE-4 TUMOR SUPPRESSOR  
IN B-CELL CHRONIC LYMPHOCYTIC LEUKEMIA

By

Mary Kathryn McKenna

---

Dr. Subbarao Bondada, PhD

Director of Dissertation

---

Dr. Ken Fields, PhD

Director of Graduate Studies

November 15, 2017

---

Date

DEDICATION

To the many cancer patients that have inspired me.

## ACKNOWLEDGEMENTS

First and foremost I would like to express sincere gratitude to my outstanding mentor, Dr. Subbarao Bondada. Without his guidance, encouragement, immeasurable patience, and support I would not have become the scientist that I am today. It was truly an honor to have the opportunity to train under his mentorship. I am especially thankful for his challenging and critical questions, promotion of independent thinking, and providing a jovial environment that allowed me to have fun in science. Dr. Bondada exemplifies high quality scholarship to which I aspire. I would also like to take this opportunity to thank my committee members Dr. John Yannelli, Dr. Brett Spear, Dr. Vivek Rangnekar, and Dr. Melinda Wilson for their constructive suggestions and guidance over the years that have helped to shape this dissertation. I also thank Dr. John D’Orazio for agreeing to serve as my outside examiner for my dissertation defense.

I would not have been able to complete this work without the help and support from all current and previous Bondada Lab members. I am forever grateful for the scientific guidance, honest opinion, and friendship of Dr. Sunil Noothi whom I worked very closely with on these projects. I thank Ms. Beth Gachuki for teaching me many lab techniques and providing unyielding support and genuine friendship throughout my program. I am sincerely appreciative for the help of Ms. Kathryn Perry as a student and I know she will continue to do outstanding things in her future. Thank you to Mr. James Collard for his optimism and friendship. I will never be able to express my true gratitude for Dr. Karine Oben and Dr. Sara Alhakeem. It is rare to have the friendships I have made with these women and it is a true honor to have them as my colleagues. I am tremendously proud to have worked with them during our doctoral program and owe my success to them.



I thank the Microbiology, Immunology, and Molecular Genetics Department professors, staff and students for all of their support during my tenure as a student. The department has fostered a wonderful educational environment that I am indebted to and very thankful to experience. I thank the Chair, Dr. Beth Garvy for her generous support of students and Ms. Kate Fresca for her delightful encouragement and friendship. I thank Dr. Greg Bauman and Ms. Jennifer Strange in the Flow Cytometry Core for all of their help in data collection and analysis for which I would not have been able to do research. I want to particularly thank Dr. John Yannelli for his unyielding friendship and kindness as I would not have pursued my degree if it was not for his mentorship. I express my sincere and heartfelt thanks to my friends and fellow graduate students, especially Kate Townsend Creasy, Nikhil Hebbar, Grant Jones, Will Arnold, Michelle Pitts and Maria Dixon whose company and support over the years made this an exceptional experience.

Finally, I express my deepest gratitude to my husband, Michael Maniskas and my family. I am very blessed to have found a partner in life that shares my passion for scientific research and look forward to where life takes us. I could not do anything without the encouragement of my sister, Dudley Napier, who has paved the way for me to excel in life and I try to match her every day. My parents, Mark and Cindy McKenna have been the greatest support system of them all with unconditional love and sacrifice, I thank you for everything.

## TABLE OF CONTENTS

ACKNOWLEDGEMENTS.....	iii
LIST OF TABLES.....	viii
LIST OF FIGURES.....	ix
ABBREVIATIONS.....	xi
CHAPTER 1 .....	1
<b>Introduction.....</b>	<b>1</b>
1.1 B cells and B cell Malignancies.....	3
1.1a Normal B cells .....	3
1.1b B Cell Malignancies .....	4
1.2 Chronic Lymphocytic Leukemia .....	6
1.2a History, Staging, and Etiology .....	8
1.2b Cell of Origin.....	12
1.2c B cell receptor and signaling .....	15
1.2d CLL microenvironment.....	22
1.2e Current Treatment for Chronic Lymphocytic Leukemia .....	26
1.3 Prostate Apoptosis Response -4 .....	28
1.3a Par-4 Tumor Suppressor .....	31
1.3b Par-4 and Apoptosis.....	34
1.3c Secretion of Par-4.....	36
1.3d Par-4 and Chronic Lymphocytic Leukemia.....	37
1.4 Study of Chronic Lymphocytic Leukemia .....	38
1.4a T cell leukemia 1.....	39
1.4b E $\mu$ -Tcl1 Mouse .....	40
1.4c Cell lines of CLL.....	42
1.5 Premise of this study.....	42
CHAPTER 2 .....	44
<b>Materials and Methods.....</b>	<b>44</b>
2a) Mice .....	44

2b) Cells and Tissues .....	45
2c) Patients .....	46
2d) Reagents .....	46
2e) Flow Cytometry and Cell Sorting .....	47
2g) Immunoblot Analysis .....	48
2h) Measurement of apoptosis induced by secreted Par-4 .....	49
2i) shRNA Lentiviral Infection.....	50
2j) Knocking out selected SFKs using CRISPR- Cas 9 techniques.....	51
2k) CD79 siRNA Knockdown Study.....	53
2l) In vivo tumor study .....	53
2m) Cell Cycle Analysis.....	53
2n) Quantitative Real-time PCR (qRT-PCR) .....	54
2o) Tissue Histology .....	54
2p) Ultrasound Imaging .....	55
2q) Splenectomy .....	56
2r) Statistical Analysis .....	56
CHAPTER 3 .....	58
E $\mu$ -Tcl1 CLL cells have elevated expression of Par-4.....	58
3a) E $\mu$ -Tcl1 B-CLL spleen cells have elevated levels of Par-4 expression.....	60
3b) Primary human CLL cells express elevated Par-4 levels .....	61
3c) Expression of Par-4 in adoptive transfer mouse model of CLL .....	62
3d) Par-4 is secreted by CLL cells and is functional in inducing apoptosis .....	63
Summary .....	87
Novel Regulation of Par-4 through BCR signaling in CLL .....	89
4a) Constitutive BCR signaling in CLL cells .....	90
4b) BCR inhibition leads to decreased Par-4 expression in mouse and human CLL cells.....	90
4c) Lyn knockdown in CLL cells results in decreased Par-4 expression .....	91
Summary .....	107
CHAPTER 5 .....	110
Novel Role of Par-4 in regulating the Growth of CLL.....	110
Summary .....	129
Splenic microenvironment and Par-4 expression is important for the .....	131

development of CLL in the mouse .....	131
Summary .....	161
Discussion .....	163
7.1 Increased expression of Par-4 in CLL and novel regulation through BCR signaling .....	164
7.2 Role of p21 in pro-growth function of Par-4 in CLL .....	171
7.3 Par-4 in the tumor microenvironment .....	173
7.4 Summary .....	175
<b>REFERENCES</b> .....	179
Vita .....	194

## LIST OF TABLES

Table 1: Staging of CLL.....	9
Table 2: Primer list for mouse genotyping.....	44
Table 3: Designed Guide RNA oligonucleotide sequences for CRISPR-Cas9.....	52
Table 4: List of qRT-PCR primers.....	54
Table 5: Human CLL Patient information.....	73
Table 6: FACS markers of WT, E $\mu$ -Tcl1, and Adoptive Transfer recipient spleens.....	80
Table 7: Summary of splenectomized E $\mu$ -Tcl1 mice.....	153

## LIST OF FIGURES

Figure 1.1: Number of cancer related articles published and cancer mortality in the US.....	2
Figure 1.2: Number of new CLL cases in the US compared to total articles published on PubMed covering CLL.....	7
Figure 1.3: Survival of CLL patients with various cytogenetic abnormalities.....	11
Figure 1.4: BCR signaling in CLL.....	17
Figure 1.5: Interactions of the CLL cells with surround microenvironment.....	25
Figure 1.6: Diagram of Par-4 domains.....	30
Figure 1.7: Endogenous role of Par-4 in normal and cancer cells.....	31
Figure 1.8: Par-4 mediated apoptosis.....	37
Figure 1.9: Tcl1 expression construct.....	40
Figure 3.1: E $\mu$ -Tcl1 B-CLL spleen cells and human CLL cells have elevated levels of Par-4 expression .....	65
Figure 3.2 Human CLL samples express elevated Par-4 protein levels.....	74
Figure 3.3 Expression of Par-4 in Adoptive Transfer Mouse Model of CLL.....	77
Figure 3.4 Par-4 translocates to the nucleus, secreted from CLL cells and is functional in inducing apoptosis.....	81
Figure 4.1 Constitutive BCR signaling in CLL cells.....	94
Figure 4.2 BCR inhibition leads to decreased Par-4 expression.....	96
Figure 4.3 Specific knockdown of Lyn leads to reduced expression of Par-4 in CLL cell lines.....	101
Figure 5.1 Knockdown of Par-4 in vitro leads to reduced CLL growth.....	115
Figure 5.2 Par-4 knockdown leads to G1 cell cycle arrest and increased p21 expression.....	120
Figure 5.3 Loss of Par-4 delays development of CLL in vivo.....	123
Figure 5.4 Par-4 <sup>-/-</sup> E $\mu$ -Tcl1 spleens have increased levels of p21 expression.....	127
Figure 6.1: Spleen is primary site of growth in CLL mouse models.....	139
Figure 6.2 Growth of CLL in spleen in the adoptive transfer model.....	141

Figure 6.3 Injection of hROR1+CLL cells to monitor location of CLL growth in adoptive transfer model.....	144
Figure 6.4 Human xenograft in NSG mice .....	147
Figure 6.5 Splenectomy delays the development and growth of CLL.....	149
Figure 6.6 Splenectomy in adoptive transfer model results in delayed CLL growth.....	154
Figure 6.7 CLL cells do not require B, T, or NK cells in the microenvironment niche.....	156
Figure 6.8 Adoptive transfer of CLL cells in Par4 <sup>-/-</sup> vs Par4 <sup>+/+</sup> recipient mice.....	157
Figure 6.9 CLL develops faster in splenectomized Par-4 <sup>-/-</sup> recipients.....	159
Figure 7.1 Summary of the Role of Par-4 in B-cell Chronic Lymphocytic Leukemia.....	176

## ABBREVIATIONS

AKT – Protein Kinase B  
ALL – Acute Lymphoblastic Leukemia  
AML – Acute Myeloid Leukemia  
Bcl-2 – B cell lymphoma 2  
BCR – B Cell Receptor  
BM – Bone Marrow  
BTK – Bruton’s Tyrosine Kinase  
CD – Cluster of Differentiation  
CDK – Cyclin Dependent Kinase  
CLL - Chronic Lymphocytic Leukemia  
CML – Chronic Myelogenous Leukemia  
CxCL – C-x-C motif ligand, chemokine  
DAG – Diacylglycerol  
DLBCL – Diffuse Large B cell Lymphoma  
DNA – Deoxyribonucleic Acid  
ERK – Extracellular signal-related kinases  
FADD – Fas-associated protein with death domain  
FasL- Fas Ligand  
FO – Follicular B cells  
GRP78- Glucose Related Protein 78 kDa  
HL – Hodgkin’s Lymphoma  
HSP – Heat Shock Protein  
Ig – Immunoglobulin  
IL – Interleukin  
IP – Intraperitoneal  
ITAM – Immunoreceptor tyrosine based activation motif  
IV – Intravenous  
JNK – c-Jun n-terminal kinase  
KD - Knockdown  
KO – Knockout  
LN – Lymph Node  
MAPK – Mitogen Activated protein kinases  
MCL – Mantle Cell Lymphoma  
Mcl1 – Myeloid Leukemia Cell Differentiation Protein  
M-CLL – Mutated Chronic Lymphocytic Leukemia  
MEFs – Mouse embryonic fibroblasts  
MIF – Macrophage inhibitory factor  
MZ – Marginal zone B cells  
NCBI - National Center for Biotechnology Information  
NCI - National Cancer Institute  
NF- $\kappa$ B – Nuclear factor kappa-light-chain-enhancer of activated B cells  
NHL - Non Hodgkin’s Lymphoma  
Par-4 - Prostate Apoptosis Response-4  
PB – Peripheral Blood  
PBMC – Peripheral Blood Mononuclear Cells



PI3K – phosphoinositide- 3 Kinase  
PIP<sub>3</sub> – Phosphatidylinositol 3,4,5-trisphosphate  
PKC – Protein Kinase C  
PLC $\gamma$ 2 – Phospholipase C $\gamma$ 2  
PTEN – Phosphatase and Tensin Homolog  
RNA – Ribonucleic Acid  
ROR1 – Receptor tyrosine kinase-like orphan receptor  
SAC – Selective for Apoptosis domain  
SEER - Surveillance, Epidemiology, and End Results Program  
SFK – Src Family Kinase  
SNP – Singly Nucleotide Polymorphism  
SpX - Splenectomy  
SQ – Subcutaneous  
Syk – Spleen Tyrosine Kinase  
Tcl1 – T cell leukemia 1  
TLR – Toll-Like Receptor  
TNF – Tumor necrosis factor  
U-CLL – Unmutated Chronic Lymphocytic Leukemia  
WT – Wild type  
XIAP – X-chromosome linked inhibitor of apoptosis

## CHAPTER 1

### Introduction

Cancer is defined as the abnormal growth of cells that have the ability to spread into surrounding tissues of the body[1]. It is a very heterogeneous disease with over 100 different types of cancers currently defined; some forming solid tumors and others derived from the blood, known as leukemias. Cancer is one of the leading causes of death worldwide and it is projected that from 2012 to 2030 cancer incidence will increase 50% with 22 million new cancer cases diagnosed [2]. This increase will lead to approximately 40% of the population being diagnosed with cancer during their lifetime and attribute to nearly 1 in 6 deaths [3]. In the United States, the overall cancer rate has declined in last several years but it is estimated that in 2017 there will still be 1,688,780 new cancer cases diagnosed [4]. While dramatic progress has been made over the last few decades in cancer research, these numbers are still astronomical and continue to support the need for innovative new research in cancer biology.

Since 1960, the number of cancer related articles that are available on the NCBI PubMed data base has grown significantly each decade indicating the increased research efforts to further understand this disease. More peer reviewed articles have focused on cancer research which in turn is helping to decrease cancer related deaths in the United States as reported by the NCI SEER database (Figure 1.1)[2]. While cancer mortality has decreased, the American Cancer Society predicts that about 1,650 people will die per day in 2017 due to cancer, making it an incurable disease [5].

Extensive research has allowed us to understand the mechanisms that underlie the development of cancer which led to definition of the now famous “six hallmarks of cancer” by Hanahan and Weinberg. These include 1)sustaining proliferative signaling 2)evading growth suppressors 3) activating invasion and metastasis 4) enabling replicative immortality 5) inducing

angiogenesis and 6) resisting cell death [6]. With the addition of two emerging hallmarks that include the reprogramming of energy metabolism and immune evasion, these acquired biological functions allow for the persistence of malignant cells and metastasis[7]. Furthermore, the tumor microenvironment has been found to play a role in sustaining the growth of both solid tumors and hematological malignancies which introduces other supportive factors that provide survival signals for cancer cells [8, 9]. All cancers have the hallmarks of self-replication and avoidance of cell death mechanisms, or apoptosis, which leads to an increased tumor burden. Specifically, Chronic Lymphocytic Leukemia (CLL) is characterized to have a defect in apoptosis that facilitates the accumulation of malignant cells in the secondary lymphoid organs and peripheral blood. This dissertation will focus on understanding the survival pathways supporting CLL and specific regulatory proteins, such as Prostate Apoptosis Response-4 (Par-4) that we have found to promote the growth of this malignancy.

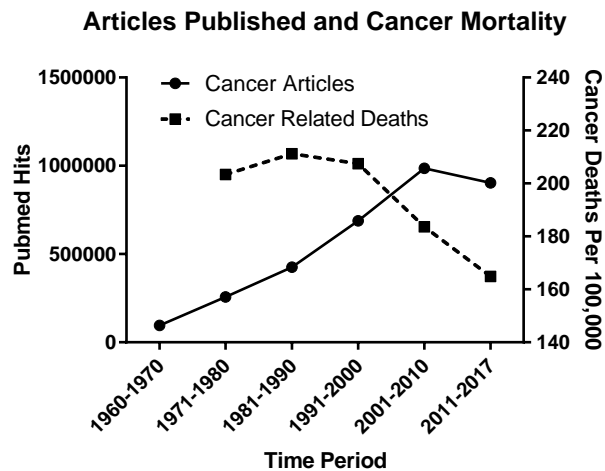


Figure 1.1: Number of cancer related articles published and cancer mortality in the United States. Article values generated through PubMed search via “cancer” for each decade (Left Y-axis). Number of cancer related deaths per 100,000 reported in SEER database per year (Right Y-axis).

## 1.1 B cells and B cell Malignancies

### 1.1a Normal B cells

A B cell is a type of lymphocyte that is derived from a hematopoietic precursor in the bone marrow [10]. B cells function primarily within the adaptive immune system, specifically humoral immunity, to secrete antibodies and present antigen to other effector cells such as T cells in order to provide protection against infectious agents. B cells develop from stem cells within the adult bone marrow, but are also derived from fetal liver precursors within the embryo [11]. B cells can be subdivided into two populations known as B1 and B2 cells. B1 cells are unique and thought to mainly play a role in the innate immune system by producing immunoglobulins (primarily IgM) that recognize self-antigen and are therefore self-reactive, although they also recognize evolutionarily conserved epitopes on pathogens [12]. B1 cells can be classified into two subgroups based on surface marker expression: B1-a are defined as IgM<sup>+</sup> CD11b<sup>+</sup> CD5<sup>+</sup> and B1-b are defined as IgM<sup>+</sup> CD11b<sup>+</sup> CD5<sup>-</sup> [13]. B1 cells were first described in mice around 1983 by the Herzenberg group and originally called Ly-1 B cells based on the expression of CD5, a pan T cell marker [14]. B1 cells are abundantly located in the peritoneal cavity of mice making up nearly 70% of the B cell population [15, 16]. In humans, B1 cells are more prominently found in the tonsils, mucosal sites, and pleural cavity [17]. B1 cells are thought to derive from the fetal liver providing evidence for the “layered immune system” or “lineage hypothesis” suggested by Herzenberg et al. This hypothesis suggests that B1 and B2 cells are from separate lineages derived from different time points in development [18]. The more conventional B2 cells originate from the bone marrow and then migrate to secondary lymphoid organs such as the lymph node and spleen, where they complete maturation. Within the bone marrow, B cell development is tightly regulated with the functional rearrangement of the immunoglobulin gene segments [19]. During this stage of development, B cells begin to

express a  $\kappa$  or  $\lambda$  light chain associated with the  $\mu$  heavy chain to make up the B cell receptor (BCR) and express surface IgM; they then begin to egress from the bone marrow as immature B cells. If these cells come in contact with antigen during the immature state, the B cell undergoes anergy and apoptosis (clonal deletion) rather than clonal expansion. It is important for B cells to express an additional immunoglobulin, IgD, on the surface of their membrane to become mature as they progress through a transitional state in the spleen. Depending on the strength of BCR derived signals, B cells become either marginal zone (MZ) or follicular (FO) B cells. Once MZ B cells come in contact with antigen, these cells develop into short lived plasma cells that secrete antibody in order to neutralize the pathogen. Follicular B cells form germinal centers with T helper cells that result in B cells becoming memory B cells or plasma cells as they undergo somatic hypermutation and class switching, but may also participate in an extrafollicular response that does not involve somatic hypermutation [20]. B cells are reliant on tonic signals through the BCR for their survival in the periphery [21]. These steps are strictly controlled in order for B cell activation to occur correctly and to generate a primary or secondary immune responses. If B cell development is dysregulated during VDJ rearrangement or if B cells escape self-antigen recognition and clonal deletion, autoimmunity may develop resulting in overproduction of auto-antibody secretion. Additionally, if dysregulation occurs during gene arrangement resulting in chromosomal translocations, oncogenic transformations may occur and therefore lead to the development of B cell malignancies [22].

### *1.1b B Cell Malignancies*

B cell malignancies encompass both lymphomas and leukemia. Lymphoma is a cancer of white blood cells that develops in the lymphatic system and is the 7<sup>th</sup> most common cancer in the US [23]. There are two primary types of lymphoma classified as Hodgkin's (HL) and non-Hodgkin's lymphoma (NHL). Hodgkin's lymphoma is characterized by large abnormal Reed-

Sternberg cells that accumulate in the lymph nodes and is one of the most curable forms of cancer with more than 75% of cases entering remission after chemotherapy and radiation[24]. There are over 30 different subtypes of NHL that originate from B, T, and NK cells but 85% of NHL is B cell in origin [25]. NHL is considered a very aggressive disease or slow growing, depending on the subtype. Diffuse large B cell lymphomas (DLBCL) account for about 60% of NHL and are aggressive in nature while follicular lymphomas are more indolent and slow progressing. Some of these subtypes can be classified according to chromosomal translocations that potentially result in enhanced expression of proliferative and survival genes under the control of the Ig loci regulatory regions. For example, mantle cell lymphoma (MCL) results from a translocation between chromosomes 11 and 14 allowing for overexpression of cyclin D1, a cell cycle regulator, by being brought under the control of the IgH promoter [22].

According to the SEER database, leukemia is the 9<sup>th</sup> most common cancer in the US and contributed to 4.1% of all reported cancer deaths [23]. The word leukemia originated in the mid-19<sup>th</sup> century from the Greek words “leukos” (≈white) and “haima” (≈blood), further designating an accumulation of white blood cells [26]. As a cancer of the blood, abnormal leukemic cells accumulate and do not die, suppress the function of normal immune cells, and eventually out populate other hematopoietic cell types resulting in anemia. Leukemia may be classified as chronic (slow progression of mature cells) or acute (rapid growth of primarily immature cells) and can affect both the myeloid or lymphoid white blood cells. Patients that are diagnosed with acute leukemia will normally start treatment as soon as possible while patients with chronic leukemia may be placed under a “watch and wait” status until symptoms progress. Subtypes of leukemia include: Acute Lymphoblastic Leukemia (ALL), Chronic Lymphocytic Leukemia (CLL), Acute Myelogenous Leukemia (AML), and Chronic Myelogenous Leukemia (CML). Both AML and CML are more common in adults than children and have distinct cytogenetic abnormalities,

especially the aberration noted in CML known as the Philadelphia Chromosome. Many CML patients respond well to imatinib, a small molecule targeting the kinase resulting from fusion of the BCR/ABL genes located on the Philadelphia chromosome [27]. Patients with AML have almost a 70% chance to attain a complete response after chemotherapy treatment with a traditional regimen of cytarabine and anthracycline [28]. ALL is more commonly seen in children and young adults. Recent advances in treatment have led to nearly a 98% remission rate and an overall 5-year survival of 90% in ALL patients [29, 30]. CLL is the most common adult leukemia in the Western world and like all leukemia, patients are grouped into fast or slow progressing disease based on prognostic indicators. Many patients with CLL may live a relatively normal life without symptoms, while others may only survive months to years after diagnosis or treatment initiation. Patients with CLL do have an 82% 5-year survival rate but experts in the field classify CLL as incurable [31].

## **1.2 Chronic Lymphocytic Leukemia**

Chronic Lymphocytic Leukemia (CLL) is defined by the accumulation of clonally expanded CD5<sup>+</sup> CD19<sup>+</sup> B lymphocytes with impaired apoptotic mechanisms in the blood, bone marrow, and secondary lymphoid organs [32]. In 2017, it is estimated that there will be 20,110 newly diagnosed cases of CLL leading to 4,660 deaths in the United States [31]. According the national SEER database, CLL contributes to 1.2% of all new cancer cases but of the over 3.5 million cancer articles available on PubMed, only 0.6% are related to CLL (Figure 1.2A) further substantiating the need to better understand the mechanisms of this disease to serve the population of patients. Additionally, it is predicted that 4.7 people per 100,000 will be diagnosed with CLL per year (Figure 1.2B) with an estimated 1.3 deaths per 100,000[23].

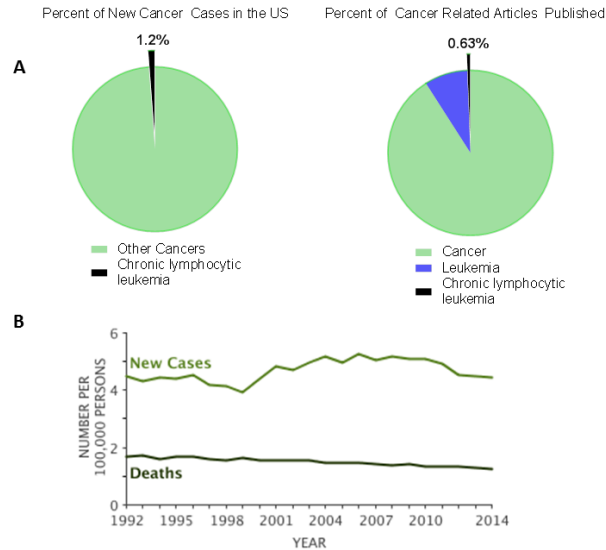


Figure 1.2: Comparing the number of new CLL cases in the US to the number of total articles published on PubMed covering CLL. A) Left: CLL represents 1.2% of all new cancer cases diagnosed in the US as reported to the NIH SEER registry. Right: CLL publications only comprise 0.63% of the total 3.5 million cancer articles available on PubMed. Values obtained by “Leukemia” and “Chronic Lymphocytic Leukemia” searches on PubMed. B) Number of new cases of CLL reported per 100,000 people is 4.7 per year. Adapted from SEER Cancer Stat Facts: Chronic Lymphocytic Leukemia. National Cancer Institute. Bethesda, MD, <http://seer.cancer.gov/statfacts/html/clyl.html>

The median age of diagnosis for CLL is 72, primarily affecting the older population and very rarely seen in patients under the age of 40 [31]. The incidence in men is almost twice that as observed in women[33]. CLL is classified within the Non-Hodgkin’s Lymphoma family of diseases. Leukemia is primarily characterized by an increase in the absolute lymphocyte count in the peripheral blood with  $\geq 5000$  lymphocytes per microliter of blood, and in many cases CLL is diagnosed through incidental blood counts [32]. Immunophenotyping is required to successfully



diagnose CLL to distinguish it from other unknown lymphocytosis or different types of lymphomas. Specifically, CLL cells are a distinct population of B cells which express CD19, CD20<sup>lo</sup>, CD5, CD23 and low levels of surface IgM/IgD molecules, as well as a clonal light chain restriction (kappa or lambda) [34]. These cell number requirements and surface markers help distinguish CLL cells from related diseases such as small lymphocytic lymphoma (SLL), B-cell prolymphocytic leukemia (PLL), monoclonal B cell lymphocytosis (MBL), and various B cell lymphomas such as Marginal Zone Lymphoma that also express CD5 (MZL).

CLL is a highly heterogeneous disease in terms of clinical course as some patients may live decades past initial diagnosis and likely die from other complications such as infections, while others may progress more rapidly. This heterogeneity can be attributed to mutations found within the variable gene segments of the BCR [35]. CLL can be classified into mutated (M-CLL) and un-mutated (U-CLL) forms, the latter resulting in increased BCR signaling, more aggressive disease, and worse prognosis. This BCR signaling pathway is a desirable target as it is required for the survival of malignant B cells and is constitutively activated in many CLL cases [36, 37]. Additionally, the microenvironment has been found to play a key role in promoting the growth of B cell malignancies, including CLL, by providing proliferative signals and promoting drug resistance [9, 38]. BCR signaling and microenvironment make CLL a very complex disease to study and treat but also allows for new targets to be explored for therapeutic potential.

### *1.2a History, Staging, and Etiology*

Leukemia was first described by Rudolph Virchow in 1845 after a 50-year old cook presented with an enlarged spleen and “pigmented to colourless corpuscles” found in her blood [39]. Chronic lymphocytic leukemia was not characterized until 1903 by Turk who differentiated CLL from lymphosarcoma [40] and in 1924, Minot and Issacs characterized the clinical features of CLL predicting a median survival time of 40 months post diagnosis [41]. In the mid-1970s

Galton and Dameshek defined CLL as a disease of progressive accumulation of lymphocytes that are not rapidly proliferating and are functionally inert [42]. This definition has been refined since then as Hamblin et al. discovered the mutational status of the Ig variable region genes to play a prognostic role in classifying aggressive and indolent CLL cases [43]. Some patients may remain symptom free for the majority of their disease while others may experience fatigue, weight loss, night sweats, abdominal fullness, increased frequency of infections, anemia, or thrombocytopenia [44]. Additionally, aggressive disease may result in enlarged lymph nodes, splenomegaly, and hepatomegaly. Two types of disease staging are accepted in the medical field including the Rai System and Binet System. A summary of the staging is provided in Table 1 [45-47].

Table 1: Staging of CLL.

<b>Rai System</b>			
Stage	Risk Category	Clinical Features	Treatment
0	Low	Lymphocytosis > 15 x 10 <sup>9</sup> /L	Watch and Wait
I/II	Intermediate	Lymphocytosis, enlarged LN at any site, Splenomegaly and/or Hepatomegaly	Treatment Considered
III/IV	High	Disease associated anemia (Hb ≤ 11 g/dL) or thrombocytopenia (platelets ≤ 100 x10 <sup>9</sup> /L)	Treatment Required
<b>Binet System</b>			
Stage	Risk Category	Clinical Features	Treatment
A	Low	Lymphocytosis, Hb 10g/dL or more, up to two areas involved*	Watch and Wait
B	Intermediate	≥ 3 areas of lymphadenopathy*, organomegaly greater than stage A	Treatment Considered
C	High	Anemia (Hb < 10 g/dL) or thrombocytopenia (platelets < 100 x10 <sup>9</sup> /L)	Treatment Required
*Binet areas of involvement: Head/Neck, Axillae, Groin, Spleen, Liver			

Two classifications used include Rai (typically used in US) and Binet (Europe).

Information adapted from Rai et. al. 1975, Binet et. al. 1981, and Hallek et. al. 2008. (Hb indicates hemoglobin, normal levels are 13.8-17.2g/dL)

The etiology of CLL is not precisely known, but genetic factors are thought to contribute to the development of disease as 9% of patients with CLL also have a diagnosed relative [48]. It is important to note that multiple genome wide association studies (GWAS) have identified various single nucleotide polymorphisms (SNPs) within loci that are associated with heritable CLL risk [49]. Many of the biological pathways associated with the SNPs involve apoptosis and enhance the resistance to cell death [50]. SNPs and chromosomal deletions are common among CLL cases even though the genome is considered relatively stable in CLL compared to other cancers [51]. Some identified mutations have been excellent prognostic indicators; for example, deletion of 13q14 is a frequent genetic aberration that is associated with a more favorable outcome in patients but it is also the site of microRNAs 15a and 16-1 that work to suppress ZAP-70 and Bcl-2 [48, 52]. Some of the more frequent chromosome abnormalities include Trisomy 12, 13q deletion, 13q14 translocation, 17p deletion, and 11q22/23 band deletions [34]. In a study examining 325 cases of CLL, 82% of patients had detectable chromosomal aberrations, some of which led to worse prognosis and decreased median survival times (Figure 1.3) [53]. On average, patients with the 17p deletion only live 32 months past their point of diagnosis making it a very aggressive disease with splenomegaly and extensive lymphadenopathy. The 17p deletion is associated with loss of the tumor suppressor p53 in CLL and other lymphoid malignancies [54]. p53 is well-known for its role as guardian of the genome by its ability to regulate cell cycle, and its loss in CLL cases leads to rapid disease progression [55]. Patients with loss of 11q are associated with defects in the ATM (ataxia telangiectasia mutated) gene which is a key kinase that is recruited to recognize DNA double strand breaks in order to repair damage [56]. The addition of chromosome 12 is the third most common genetic aberration in CLL and has been linked to a variety of genetic irregularities [51]. A recent GWAS study also identified multiple loci aberrations in CLL compared to other B cell malignancies, including multiple

myeloma and Hodgkin's Lymphoma, and found pleiotropic associations at 3q22.2. This region is associated with T cell activation and the PI3K/Akt pathway. Additional polymorphisms were identified in HLA regions that are critical for antigen presentation and T cell receptor binding [57]. There are currently 33 common loci genetic variations that influence the risk of CLL development but with the recent GWAS studies, more are being identified that include SNPs involved in B cell immune response and signaling[58].

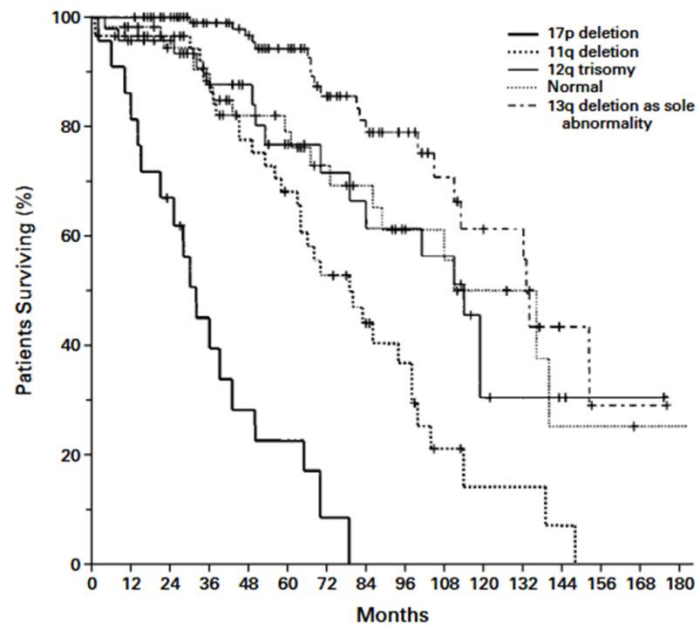


Figure 1.3 Adapted from Dohner et. al. 2008, NEJM 344(26): 1910-1916, Figure 1 with permission: Survival of patients with various cytogenetic abnormalities. 17p deletion is the most aggressive aberration resulting in a decreased life expectancy compared to other mutations. Reproduced with permission from New England Journal of Medicine, Copyright Massachusetts Medical Society.

Next generation sequencing has revealed alterations in the NOTCH1, SF3B1, and BIRC3 genes along with the previously known alteration in the ATM gene associated with the 11q22 deletion [59]. NOTCH signaling is constitutively activated in CLL cells compared to normal B cells, leading to apoptosis resistance [60]. NOTCH is a cell surface receptor that responds to Delta-like

and Jagged ligands leading to nuclear translocation of an intracellular subunit that regulates DNA binding proteins and transcriptional complexes [61]. This pathway is known to regulate cell proliferation, differentiation and some mechanisms of cell death. In CLL, NOTCH has been found to promote the expression of Mcl-1, an anti-apoptotic protein, leading to increased CLL survival [62]. NOTCH overexpression is associated an intermediate survival risk and is also found to be expressed in unmutated IGHV patients with trisomy 12 [63, 64]. *SF3B1*, which encodes a component of the spliceosome that plays a key role in pre-mRNA splicing [65], has been found to be associated with intermediate risk patients and 11q deletions [63]. Loss of BIRC3, located within the 11q deleted region, is linked to high risk patients [66]. BIRC3 negatively regulates NF- $\kappa$ B and loss of BIRC3 is very common in patients that are refractory to chemotherapy treatments [63, 67]. Many of these mutations are associated with a shorter time to treatment and used as prognostic indicators [68].

Interestingly, other than age and gender, no other lifestyle or dietary factors have been associated with the increased incidence of CLL. Of note, a few studies found that exposure to Agent Orange and insecticides increased the risk of developing CLL [48, 69, 70].

### *1.2b Cell of Origin*

Even with the incredible discoveries made in the field of Chronic Lymphocytic Leukemia over the last few decades, the cellular origin of the disease is still debated today. CLL cells distinctively express CD19, CD5, CD23, as well as surface Ig molecules [71]. CD19 is a surface antigen that is expressed on both normal and neoplastic B cells and is critical for intrinsic B cell signaling through BCR interactions as well as BCR independent signaling [72]. CD5 is also a cell surface molecule that is expressed on thymocytes, mature T cells, and differentiates B1 cells from the conventional B2 population [73]. Previous studies have also indicated that CD5 is found on some activated human B cells that are autoreactive [74]. CD5 is thought to be a negative

regulator to mitigate signaling in order to prevent over activation of signaling downstream of the TCR or BCR [75]. CD23 is a reliable marker for CLL cells to differentiate between other lymphomas that also express CD5 (mantle cell lymphomas). CD23 is an IgE receptor that is normally expressed on mature resting B cells and some activated B cells [76].

The co-expression of low IgM and IgD levels on the surface of CLL cells originally suggested that these cells arise from naïve antigen-inexperienced B cells [77]. After Hamblin and colleagues classified CLL into two subgroups, M-CLL and U-CLL defined by mutations in the variable gene segments of the BCR indicating that 50-60% of CLL cells had undergone somatic hypermutation (M-CLL), hypotheses arose that CLL cells are derived from two cellular origins [43, 78]. Seifert and colleagues suggest that U-CLL cells are derived from unmutated mature CD5+ B cells as their IgV sequence is less than 2% different from germline, whereas M-CLL cells are derived from a distinct CD5+CD27+ post germinal center B cell [79]. An additional study investigating phenotypic markers found that CLL cells express more of an activated state (CD69+CD25+CD71+) independent of their Ig mutational status when compared to normal CD5+ B cells in humans, suggesting that CLL cells are mature antigen experienced cells [77]. Antigen experienced cells can be derived from cells that undergo somatic hypermutation within a germinal center but may also develop in a T cell-independent manner which may account for CLL cells that have unmutated Ig variable regions [78, 80]. Further support for antigen experienced B cells to be CLL precursors comes from studies that have examined the BCR repertoire in multiple CLL samples. It is well accepted that CLL cells have constitutive BCR signaling, but CLL cells also respond to antigen [81, 82]. Recent studies have found that 30% of BCR immunoglobulins within the CLL patient population are quasi-identical resulting in a stereotypy of BCRs [81, 83, 84]. This indicates that these malignant B cells from unrelated patients recognize similar antigens suggesting that there are a few common epitopes which activate

CLL cells. Not many antigens have been identified to stimulate CLL cells, but one potential candidate is non-muscle myosin heavy chain IIA which is an intracellular protein that interacts with actin to provide cellular movement and therefore is considered a self-antigen [85]. This is interesting as B1 cells are thought to be self-reactive and respond to autoantigens supporting the idea that CLL cells are derived from B1 cells [78].

B1 cells are primarily found within the peritoneal cavity of mice but are also present in the spleen, albeit at a lower level [16]. As mentioned before, B1 cells express self-reactive BCRs but respond poorly to BCR cross-linking to prevent against self-activation that is suggested to be mediated through CD5 [75, 86]. B1 B cells also express restricted BCRs with a predominance of V<sub>H</sub>12 promoting B1 phenotype [87] and are known to produce antibody quickly in response to infection, primarily IgM, independent of T cell help (similar to U-CLL) [88]. Additionally, B1 cells are divided into B1a (CD5+) and B1b (CD5-) subsets where B1a cells are the primary source of natural IgM production and B1b cells respond to antigen in mice [16, 89, 90]. It has been suggested that B1a cells serve as the normal counterpart for CLL cells. Adoptive transfer studies of young/early B1a populations into immunocompromised recipient mice led to development of CLL like disease [91]. CLL development in this study was independent of oncogene expression but a follow-up study was able to confirm that early B1a cells expressing the oncogene, Tcl1, also led to the development of CLL in recipient mice [92]. These authors did note that not all B1a cells result in CLL development, but were restricted to specific BCRs that were later identified in promoting CLL growth [91, 92]. Additional studies favoring the B1a population serving as CLL normal counterpart provide evidence that both B1a cells and CLL cells secrete significant amounts of the cytokine Interleukin-10 that works to suppress the immune response [86].

Controversy regarding the normal counterpart of CLL has been focused on the inability to identify a human B1 population that is similar to mouse B1 cells [93]. Recently, reverse

engineering has allowed researchers to identify a human B1 cell population within the umbilical cord blood and adult peripheral blood [94]. Rothstein et al summarized evidence showing that mouse and human B1 cells share similar phenotypes and also express autoreactive antibodies that protect against infections. Seifert and colleagues compared normal CD5+ B cells from healthy human donors with both populations of CLL cells, M-CLL and U-CLL, and confirmed that CD5+ B cells are the normal B cell subset that are most similar to CLL [79].

Besides B1 cells, other hypotheses for the CLL precursor include marginal zone B cells as well as immature pre-B cells and transitional B cells [35, 93]. While the data indicating CD5+ B cells is strong in supporting the normal counterpart of CLL, it is important to keep these other origins in mind as CLL cells may arise from different cell populations based on their BCR repertoire.

Recently, a case report involving a 65y male with stage IV CLL identified a “Side Population” of CLL cells identified through flow cytometry that were proposed to be precursors to leukemic development [95]. Ablation of these cells through vaccination after CD40L stimulation diminished the bulk of the disease 12months after treatment. The “side population” of cells were CD5 and CD19 positive and thought to be similar to the cancer stem cell population characterized in other types of tumor models [96]. True identification of this “side population” would be of great benefit to determine if the likely B1 cells give rise to the malignant counterpart.

### *1.2c B cell receptor and signaling*

For normal B cells to be functionally active in an immune response, their BCR must recognize a specific antigen for BCR cross-linking to occur and differentiation to antibody secreting plasma cells or memory B cells [20]. With the millions of potential antigens that initiate an immune response, the B cell must have a large repertoire of BCR sequences to



recognize most of the possible different epitopes. Each B cell clone that is generated has a unique B cell receptor but the diversity between clones is spectacular. Diversity is generated through somatic recombination of the variable gene segments, random recombination of VDJ joining, and combination of light and heavy chains for maturation of the BCR followed by somatic hypermutation during the course of the immune response [10]. The two different CLL subsets, M-CLL and U-CLL, are defined by mutations found within the variable gene segments that compose the Ig molecules that comprise up the B cell receptor.

The entire BCR complex is made of the surface Ig molecule and the signaling Ig $\alpha$  (CD79A) and Ig $\beta$  (CD79B) heterodimer that conduct cytoplasmic downstream signaling and other co-receptors like CD19 [97]. The BCR is critical for the survival of both normal and malignant B cells despite their oncogenic transformation [21, 36, 98]. B cells can receive both tonic (no external signal) and antigen dependent signaling that initiates phosphorylation of ITAM motifs located on Ig $\alpha$ / $\beta$  heterodimer by the Src Family Kinase (SFK) Lyn. This creates a scaffold for other kinases such as Syk (spleen tyrosine kinase) to become activated and promote downstream signaling [99]. Syk then triggers activation of multiple kinases such as BTK (Bruton tyrosine kinase), AKT (Protein Kinase B), PI3K (Phosphoinositide 3-kinase), other protein kinases shown in Figure 1.4 as well as PLC $\gamma$ 2 (Phospholipase C 2), BLNK (B cell linker protein) that promote NF- $\kappa$ B and MAPK signaling for survival and proliferation [100, 101].

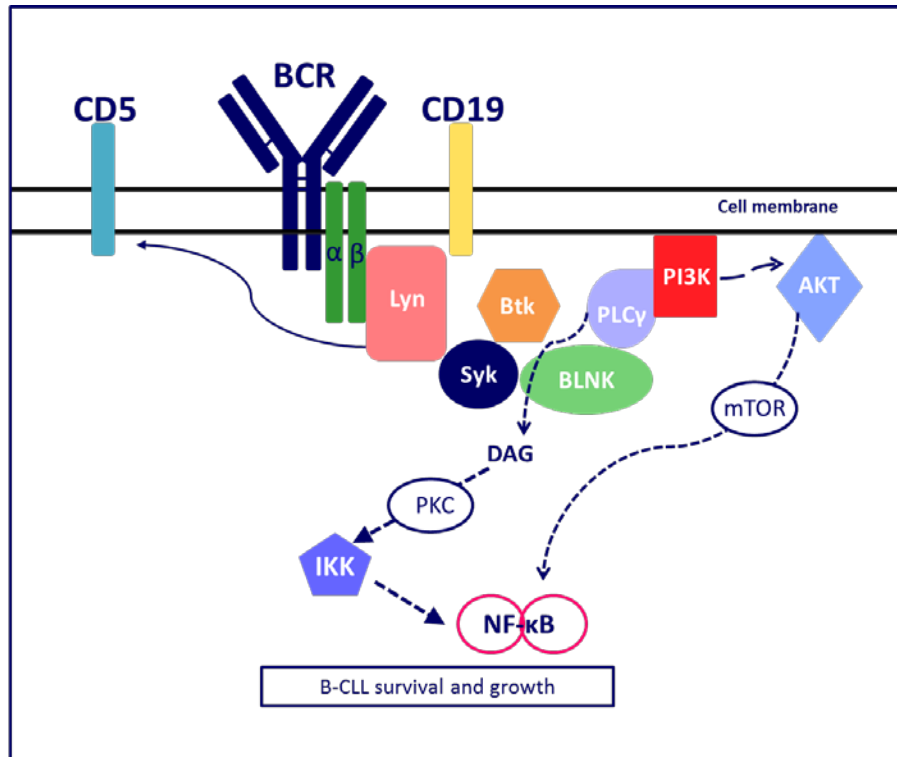


Figure 1.4: BCR signaling in CLL. Simplified model of the BCR signaling pathway in CLL cells and key kinases involved in downstream pathways that promote survival and proliferation. Adapted from Hallek, M. *Blood*. 2013 88(9): 803-816.

The two subsets of IGHV mutational status in CLL are also associated with varying levels of BCR signaling, with U-CLL cells having higher levels of BCR activation compared to M-CLL [102]. Mutational status has also been associated with ZAP-70 expression. ZAP-70, a protein tyrosine kinase that is involved in signaling downstream of the T cell receptor, is more highly expressed and is associated with enhanced signaling in U-CLL [35, 103]. The BCR pathway provides the survival signals necessary for CLL but also provides multiple potential therapeutic targets for disease treatment.

*Lyn*:

The Src Family Kinases (SFK) play an important role in BCR signaling. These proteins contain specific domains characterizing them as SFKs, including SH1, SH2, SH3, and SH4 motifs [104]. Most important are the SH2 and the catalytic SH3 domains that regulate activation through binding and phosphorylation of the ITAMs (immunoreceptor tyrosine based activation motifs) on Ig $\alpha$ / $\beta$  of the BCR complex. Multiple members of the SFKs include Lyn, Fgr, Lck, Blk, Fyn, Hck, Yes, and Src but Lyn is known to be the primary SFK in B cells [104]. There are two alternately spliced forms of Lyn resulting in 53kDa and 56kDa protein isoforms [105]. Lyn is a complex kinase known to have paradoxical roles as both a positive and negative regulator of signaling [106]. In addition to recruitment and activation of Syk in BCR signaling, Lyn mediates phosphorylation of the co-receptor, CD19, promotes activation of PI3K dependent signaling such as AKT activation. Conversely, Lyn is also known to phosphorylate the co-receptor CD22 that recruits SHP-1, a phosphatase that attenuates BCR signaling [104]. B cells from Lyn<sup>-/-</sup> mice are found to be hyper-responsive and autoreactive suggesting the important role of Lyn in negative regulation of B cells [101]. Lyn is also known to phosphorylate FC $\gamma$ R [107], CD5 [108], and other negative regulators of BCR signaling [106].

In CLL, Lyn is found to be highly overexpressed at the protein level with increased basal activity compared to normal B cells [109]. Contri and colleagues found that Lyn activation is not increased with BCR cross-linking which is thought to be due to the increased basal activity of Lyn present in the CLL cells. However, inhibition of Lyn decreased survival of leukemic cells. In 2013, Wang et al investigated 92 patients with CLL to determine if expression levels of kinases involved in the BCR signaling cascade correlated with patient prognosis, treatment response and survival. Results suggested that mRNA levels of all the kinases involved in proximal BCR signaling were elevated but Lyn expression was further increased in patients that were being treated and resulted in decreased treatment free survival [110, 111]. The increased Lyn activity in CLL cases

could be a contributing factor to the tonic BCR signaling in CLL cells as Lyn is the first kinase immediately downstream of the BCR and also responsible for the prolonged survival of leukemic cells as it inhibits apoptosis [37, 109]. Additionally, Lyn has been shown to provide survival signals within the CLL microenvironment [112]. One study transferred CLL cells into mice that are null for Lyn expression and found that disease developed at a slower rate compared to WT animals. The lack of Lyn provided by macrophages in the microenvironment impaired CLL cell expansion suggesting that this kinase has multiple functions in CLL [113]

Data indicating Lyn as a key proponent in CLL pathogenesis has led to the development of targeted inhibitors. Drugs such as PP2 and SU6656 that target the activity of SFKs result in down regulation of phospho-src and inhibition of Lyn expression in B cell lymphomas and CLL [109, 114, 115]. Dasatinib, an approved FDA drug targeting the activity of all SFKs, has also shown potential as a therapeutic option for CLL patients [116, 117].

*Syk:*

Spleen Tyrosine Kinase (Syk) is essential in BCR signaling, leading to intracellular calcium flux and activation of downstream signaling cascades [118]. Animals that lack Syk exhibit embryonic hemorrhage and perinatal lethality but also have impaired B cell development at the pre- B cell level [101]. Syk is a 72kDa protein that can bind to phosphorylated ITAMs to provide a scaffold for other kinases involved in the pathway and is also activated by the upstream kinase, Lyn. Syk couples BCR activation to downstream signaling by activating BTK and PLC $\gamma$ 2. Activation of these kinases enhances the survival of B-cells by promoting DAG, AKT and Mcl1 [118, 119]. Syk is also involved in pathways independent of the BCR in normal and malignant cells such as cellular adhesion and vascular development [120, 121].

In CLL, Syk is found to have elevated constitutive activity that promotes cell survival through the BCR pathway and is associated slightly more with unmutated status of the IGHV

region [119]. Elevated Syk activation is also associated with CD38 positivity in CLL cells [122]. CD38 is a transmembrane glycoprotein that promotes intracellular calcium signaling and cell-cell adhesion. Expression of CD38 on CLL cells is also a prognostic indicator of aggressive disease in patients [35, 71]. Benkisser-Petersen et al. found that CD38 expressing cells had elevated Syk activity and treatment with R406, a Syk inhibitor and active metabolite of Fostamatinib, decreased CD38 mediated migration and CLL cell survival. Studies examining the regulation of Syk activity in CLL cells after CD40L stimulation discovered that Syk inhibition prevented the anti-apoptotic signals mediated through T helper cells via CD40L [123]. Syk inhibition has also been found to block the cross-talk between CLL cells and stromal cells independent of BCR signaling inhibition, making this kinase a promising therapeutic target [124]. Currently, Fostamatinib is the only FDA approved drug targeting Syk in CLL and other B cell malignancies and its objective response rate is a promising 55% [37].

*BTK:*

Bruton's tyrosine kinase (BTK), a 77kDa protein that is a member of the Tec family of kinases, is primarily expressed in B cells [125]. Patients with X-linked agammaglobulinemia lack peripheral blood B cells due to a defect in BTK function, confirming the importance of this kinase in B cell development and survival [37]. BTK is important in B cell development at the transition between pre-B cell to immature B cell suggesting it may have a role in the signaling required for Ig light chain arrangement [126]. BTK is also important in mature B cells as BCR activation promotes PLC $\gamma$ 2 phosphorylation leading to calcium mobilization, NF- $\kappa$ B and MAPK signaling. Additionally, BTK has also been found to amplify the PI3K/AKT pathway in B cells [127]. BTK signaling has also been shown to promote B cell migration through chemokine receptors and adhesion molecules playing an important role in tissue homing.

In CLL, BTK is found to be over-expressed and shown to be a promising target for therapy as it is involved in tonic BCR signaling [128]. Ibrutinib is the most notable inhibitor in that it irreversibly binds to the active site of BTK and results in decreased NF- $\kappa$ B activity [101]. In vivo, Ibrutinib treatment has been very successful with a 54% overall response rate. Ibrutinib has been known to cause lymphocytosis of CLL cells or egress of cells from nodal compartments suggesting that treatment also blocks the homing capacity of CLL cells [129]. Ibrutinib treatment is the most promising FDA approved therapy for patients with aggressive disease, such as cases with the 17p deletion that otherwise have no other treatment options [130]. However, Ibrutinib also blocks TEC kinases family member, IEK, involved in T-cell activation. Currently small molecules that target BTK, but not IEK, are being developed.

*Other Kinases:*

The PI3K/AKT pathway is known to contribute to BCR-induced survival [131]. As described above, upstream activation of Lyn, Syk, and BTK leads to increased PI3K activity. Idelalisib, which specifically inhibits the PI3K $\delta$  isoform, is approved for treatment of patients with CLL. Idelalisib inhibits both PI3K and ERK activation in malignant B cells and induces apoptosis [101]. ERK signaling has been well defined and is critical for B cell development and proliferation downstream of BCR activation and has also been well studied as a therapeutic target in many cancers [132-134]. The RAF/MEK/ERK1/2 pathway is activated in CLL cells and drugs such as Sorafenib that target Raf kinases lead to decreased CLL survival in vitro [135].

The mammalian target of rapamycin (mTOR) is another kinase that is known to be a key regulator of downstream BCR signaling targets such as cell cycle proteins [136]. Treatment with rapamycin has led to the prevention of CLL cells entering the cell cycle ex vivo and also induces apoptosis in p53 mutated CLL cells.

Recent studies further investigating antigen-independent proliferation of CLL cells through BCR independent pathways have found that CLL cells respond well to TLR-9 and CD40 stimulation. TLR-9 stimulation via CpG induces proliferation of CLL cells, but treatment with BCR inhibitors such as Ibrutinib and entospletinib ( $\alpha$ -Syk) led to reduced viability [137, 138]. Additionally, CD40L with IL-21 stimulation generates CLL proliferation through the MAPK axis that leads to increased cyclin D2 expression via JAK/STAT signaling [138, 139]. Inhibition of BTK, PI3K, and JAK kinases after CD40L stimulation led to reduced survival of CLL cells further confirming that these kinases are critical for CLL survival independent of BCR.

#### *1.2d CLL microenvironment*

The original hallmarks of cancer proposed by Hannahan and Weinberg have been expanded to include the tumor microenvironment that promotes growth of cancer cells by avoiding apoptosis and evading immune suppression [7]. Both solid and hematologic tumors are very heterogeneous and comprise of multiple different cell types such as stromal cells, endothelial cells, tumor infiltrating macrophages and lymphocytes. These cells produce vascular growth factors and various cytokines and chemokines that support cancer cells [140]. Compelling evidence exists that recognizes the importance of the BCR signaling pathway in the survival of CLL, but microenvironment has emerged as another key factor in CLL survival. The microenvironment is of interest in CLL as primary CLL cells do not proliferate or survive in long-term *in vitro* cultures alone, suggesting that other factors and/or cell types provide support. The actual site of proliferation and the CLL microenvironment is still debated in the field. This could be because CLL cells are found within the peripheral blood, bone marrow and other secondary lymphoid organs in which the malignant cell comes into contact with a variety of accessory cells depending on their location. Several studies have identified proliferation centers in the bone marrow and lymph nodes. A study from the University of Nebraska performed extensive gene

expression profiling of CLL cells derived from the peripheral blood (PB), bone marrow (BM) and lymph nodes (LN) of patients. Results suggested that cells derived from the lymph node expressed genes enriched for BCR signaling, BAFF/APRIL proliferation, NF- $\kappa$ B signaling and immune suppression signatures compared to the PB and BM compartments [141]. These results confirmed an earlier study that examined Ki67 staining in PB, LN, and BM samples from 24 patients which found that the LN contained CLL cells with a greater proliferative capacity [142]. Although studies in human samples find that the lymph node is the site of CLL proliferation; questions are still raised based on the dramatic splenomegaly observed in mouse models [143, 144].

The CLL tumor microenvironment provides a physical location supporting the cross-talk between malignant cells and accessory cells that inhibit apoptosis and also provide resistance to drug treatment [145]. CLL is a slow progressing disease and was originally thought to simply be an accumulation of cells with defective apoptosis, but recent studies using deuterium labeling have determined that CLL cells proliferate at a rate of 0.1-1% per day suggesting that CLL is a dynamic disease of proliferation [146]. Pseudofollicular proliferation centers that are found throughout infiltrated tissues are the source of newly generated CLL cells [147]. Within this area, CLL cells depend on stimulation through a functioning BCR receptor as discussed above. It is well appreciated that CLL cells are activated through antigen independent and dependent manners but the microenvironment may be the source of antigen/stimulus [148]. These antigens are not specifically defined, but may include microbial antigens, natural antibodies, and auto antigens expressed by dying cells.

The CLL microenvironment promotes cell to cell interactions with a variety of different cell types. Direct interaction between B-CLL cells and T cells via CD40 on B-cells and CD40L on T cells provides a proliferative stimulus. [149]. CD40 signaling in B cells induces expression of anti-



apoptotic molecules and proliferative signaling through AKT, ERK, TRAF, and NF- $\kappa$ B. T cells also secrete cytokines such as IL-4, TNF $\alpha$ , and IL-2 that support CLL proliferation. Alternatively, the CLL microenvironment also supports immune evasion allowing CLL cells to dampen the immune function of cytotoxic T cells by secreting immunosuppressive cytokines like TGF $\beta$  and IL-10 [149].

Stromal cells derived from bone marrow or other secondary lymphoid tissues support the survival and proliferation of CLL cells [150]. This interaction provides a bi-directional cross talk that promotes the growth of both CLL and stromal cells. In cell culture, CLL cells actually migrate beneath bone marrow mesenchymal cells, a process known as pseudoemperipolesis, suggesting that this interaction is dependent on cell contact in order for CLL cells to survive. Cells known as Nurse-like cells can be found in the peripheral blood of patients that are derived from monocytes and become adherent in culture systems [151]. These cells express stromal cell derived factor – 1 (SDF-1) that binds to CXCR4 on CLL cells to prevent spontaneous apoptosis and promotes resistance of CLL cells to chemotherapies. CXCL12 is also secreted by nurse-like cells (NLCs) as well as mesenchymal derived stromal cells that attract CLL cells via CXCR4 towards proliferation centers within the secondary lymphoid compartments [48].

Tumor associated macrophages (TAMs) also play a key role in supporting the growth and survival of CLL cells. Depletion of TAMs in CLL models by targeting CSF1 or by clodronate treatment was found to decrease the engraftment of CLL resulting in leukemic cell death [152]. Reinart and colleagues found that plasma of CLL patients had increased levels of circulating MIF (macrophage inhibitory factor). By crossing a mouse lacking MIF to the well-known CLL mouse model, E $\mu$ -Tcl1, this group discovered that decreased expression of MIF significantly delayed disease development [153]. Absence of MIF decreased BCR signaling in CLL and rendered cells more susceptible to apoptosis, further confirming the necessity of BCR signaling stimulation of CLL cells in the microenvironment. In another mouse study examining the role of CXCR5 in the

homing of CLL cells, Heinig et al discovered that access to follicular dendritic cells was critical for disease proliferation [154].

Many additional cell types, chemokines and cytokines have been identified in the CLL microenvironment that support CLL growth and survival (briefly summarized in Figure 1.5, adapted from Kipps, 2017 Nature Primers [48]). The cross-talk between neoplastic CLL cells and the surrounding tissue provides more options for therapeutic targets.

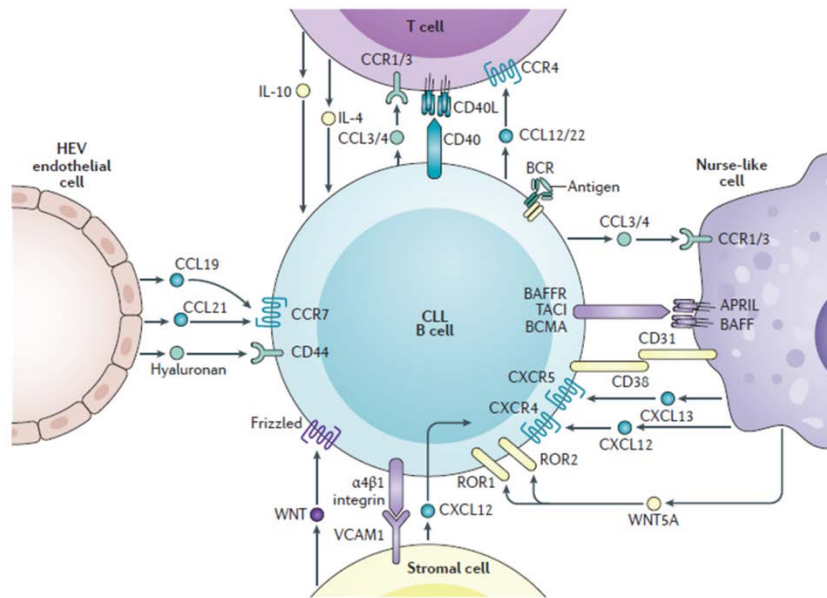


Figure 1.5: Interactions of the CLL cells with the surrounding microenvironment. CLL cells require the support of multiple cell types and survival factors for persistence. Neoplastic B cells interact with stromal cells, nurse-like cells, macrophages, lymphocytes, endothelial cells, and many others through direct cell to cell contact via receptor-ligand mediated interactions and through soluble mediators. Signals within the microenvironment stimulate the CLL cell through the BCR signaling pathway to promote survival and proliferation. Figure used with permission from Kipps, T. 2017 Nature Disease Primers: Chronic Lymphocytic Leukemia 3(16096).

### *1.2e Current Treatment for Chronic Lymphocytic Leukemia*

Vast improvements have been made over the past few decades in discovering new treatment modalities for patients with CLL as we learn more about the requirement of the BCR signaling pathway and microenvironment. Small molecule inhibitors targeting kinases such as SFKs, BTK, SYK, and PI3K as discussed earlier have proven successful in a number of cases in addition to the standard regimen of chemotherapeutics  $\pm$  anti-CD20 antibodies [48].

Next generation sequencing (NGS) has revealed many complexities among CLL patients and has enabled grouping of patients into prognostic categories. In addition to the IGHV mutational status, mutations such as TP53, SF3B1, and NOTCH1 indicates more aggressive disease triggering the need for more efficient treatment strategies [130]. FISH (fluorescence in situ hybridization) analysis has also improved the detection of genomic aberrations leading to worse prognosis of patients with 17p and 11q abnormalities [53]. These prognostic factors in addition to patient age and fitness determine the dose of treatment. As mentioned before, some patients do not require treatment and are only placed in the “watch and wait” category. There is no evidence suggesting that early treatment of asymptomatic cases can improve the overall survival of patients, therefore, preference is for monitoring of disease symptoms until progression is evident for treatment to start. Treatment is required immediately for patients classified as Stage III or IV, if they show signs of progressive bone marrow failure or have autoimmune cytopenias [155].

Standard treatment for patients includes chemotherapy combinations of fludarabine and cyclophosphamide with rituximab (FCR), but due to comorbidities or other exclusion criteria, not all patients are able to tolerate chemotherapy [156]. Current chemotherapies used for CLL treatment include purine analogues such as pentostatin and cladribine in addition to fludarabine. Other alkylating agents besides cyclophosphamide are chlorambucil or

bendamustine [48]. Immunotherapy options are primarily monoclonal antibodies that target CD20 surface receptors on the neoplastic B cells (rituximab, obintuzumab, and ofatumumab) as well as Campath-1 antibodies (alemtuzumab) that target CD52 and otlertuzumab, which targets CD37 [156]. Patients that are fit, have mutated IGHV status and no p53 mutation normally respond well to FCR, but if a patient is older and more prone to infections, bendamustine and rituximab are normally prescribed as they are more tolerable. Patients with unmutated IGHV status do not respond as well to FCR with only a 32% overall survival rate compared to 65% for M-CLL patients [42]. Patients that have p53 mutation have a worse response to standard chemotherapy treatment and are often treated initially with ibrutinib, a BTK inhibitor. If these 17p deletion/p53 mutated patients do not respond to ibrutinib, they will receive a combination of idealisib (PI3K inhibitor) and rituximab [130]. This combination is normally the last line of defense as it is very harsh and exponentially increases the patient's risk of infection. Patients may also be considered for allogeneic hematopoietic cell transplantation if they are in good physiological condition. Drugs targeting molecules involved in the apoptotic pathway have proven very successful in the treatment of CLL. Venetoclax, or ABT-199, targets the function of BCL-2 and prevents sequestration of Bim in order for the apoptotic cascade to proceed. This drug treatment has been helpful in refractory or relapsed patients [48]. Other refractory patients may receive a combination of chemoimmunotherapy options pending their last treatment regimen. Salvage treatment options include combinations of standard chemotherapies, immunotherapy, BCR inhibitors, and immunomodulatory drugs such as lenalidomide as well as steroids.

Impressive results have been obtained with genetically modified T cells known as CAR-T (chimeric antigen receptor) cell therapy that target hematological B-cell malignancies. These T cell have been engineered to target known tumor antigens or in the case of B cells, CD19, and

are expanded in vitro before intravenous injection back to the patient. CD19-CAR-T cells have led to long term disease free remission in multiple clinical trials [157].

Patients with CLL have about a 5-10% chance of developing Richter's syndrome which usually leads to a very poor prognosis with a median survival time of about 10 months [158]. Richter's transformation is due to the development of lymphoma after being diagnosed with CLL. Most patients present with hepatosplenomegaly and are primarily diagnosed with diffuse large B cell lymphoma that is aggressive and difficult to treat as it varies from the de novo DLBCL with known genetic abnormalities [48]. Retrospective studies have examined the incidence of secondary cancers in CLL patients. There is a slight increase in melanoma, sarcoma, lung, renal, and prostate cancer in patients with CLL [34, 159].

Therapy for Chronic Lymphocytic Leukemia has improved extensively over the past few decades leading to better outcomes, but CLL still remains incurable. Further studies about the role of BCR signaling and microenvironment in CLL are warranted to improve the current success of these drugs and to design even more effective therapies that can lead to cures.

### **1.3 Prostate Apoptosis Response -4**

One of the original hallmarks of cancer is to evade apoptosis and many cancers master this skill by down regulating tumor suppressors and pro-apoptotic factors [6]. Prostate Apoptosis Response-4 (Par-4) is a well-defined tumor suppressor that is found to be repressed by promoter methylation in about 30% of all cancers including Acute Lymphoblastic Leukemia (ALL) [160]. Par-4 was originally identified by Sells and colleagues by its upregulation during ionomycin induced apoptosis of androgen independent and dependent prostate cancer cells in 1994 [161]. Shortly after, using a yeast two-hybrid assay and HEK-293 mammalian cells, Johnstone et. al. discovered that Par-4 interacts with the Wilm's Tumor-1 protein, a transcriptional suppressor [162]. Additional early studies found that Par-4 also interacts

physically with atypical protein kinase c (aPKC) and over expression of Par-4 in NIH 3T3 fibroblasts led to an apoptotic morphological change [163]. These initial studies defined Par-4 as a pro-apoptotic factor and tumor suppressor.

The human Par-4 gene is located on chromosome 12q21 and contains 7 exons, encoding a 340 amino acid, 43-47kDa protein [164, 165]. Par-4 is ubiquitously expressed in tissues of different species and Johnstone et al. found that mouse Par-4 shows 83% and 91% identity to human and rat Par-4 respectively [164]. Interestingly, the leucine zipper domains, carboxy terminal region, and nuclear localization sequences (NLS) exhibit 100% conservation across species [166]. The leucine zipper domain allows Par-4 to interact with other proteins as either a homo- or heterodimer. The nuclear localization sequences suggest that Par-4's function is dependent on nuclear. However, in normal tissues, Par-4 is localized mostly to the cytoplasm [167]. The NLS2 sequence is very interesting in Par-4 as it is sufficient to allow nuclear translocation alone but it is also part of a domain that is necessary for the apoptosis-inducing properties of Par-4, termed selective for apoptosis of cancer cell (SAC) domain [168]. SAC is a core domain of 59 amino acids in length and includes a threonine residue that is the site of phosphorylation via Protein Kinase A [169]. Activation of Par-4 through phosphorylation indicates that its function is tightly regulated by post-translational modification. PKA, a broad spectrum serine/threonine kinase regulated by cAMP signaling, is associated with cell proliferation, and is frequently overexpressed in cancer cells. Par-4 is able to utilize the PKA upregulation in cancer cells to specifically induce apoptosis of cancer but not normal cells [169]. This selective ability of Par-4 makes it an attractive therapeutic target. Additionally, Par-4 is negatively regulated by AKT activity through phosphorylation at serine 249, which is located between the SAC domain and leucine zipper region [165]. A simplified diagram of the Par-4 domains is found in Figure 1.6 (Adapted from Hebbar et al. 2012).

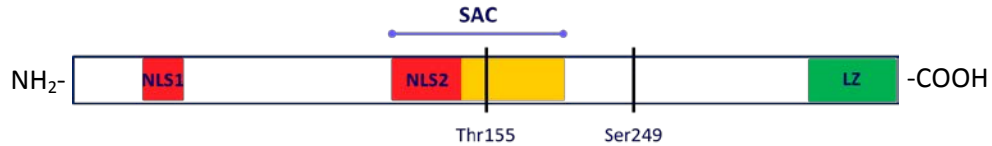
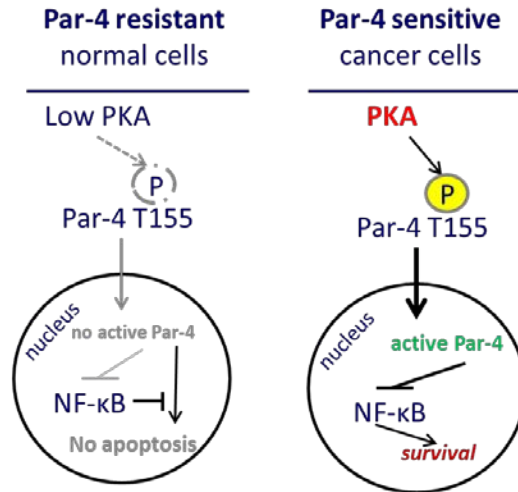


Figure 1.6: Diagram of Par-4 domains. Par-4 contains two nuclear localization sequences with NLS2 contained within the SAC domain. PKA phosphorylates Par-4 at threonine 155 for activation and is inhibited at serine 249 by Akt phosphorylation. A nuclear export sequence is also found within the N-terminal region. Amino acid residue numbers represent Rat Par-4, but domains are conserved across species.

Phosphorylation of Par-4 via AKT is required for cancer cell survival, as phosphorylation of Par-4 by Akt leads to binding of the chaperone 14-3-3, retaining Par-4 in the cytoplasm [170]. Many studies have linked the pro-apoptotic activity of Par-4 to its ability to inhibit NF- $\kappa$ B transcriptional activity. Activated Par-4 prevents  $\zeta$ PKC from phosphorylating I $\kappa$ B, which is necessary for RelA translocation to the nucleus [163, 171, 172]. Another mechanism of NF- $\kappa$ B inhibition is due to a direct repressive effect of Par-4 in the nucleus but the exact mechanism still needs to be elucidated. A summary of Par-4 activation is shown in Figure 1.7 [169].



Gurumurthy, 2005. Mechanism of Cancer Selective Apoptosis by Par-4

Figure 1.7: Endogenous role of Par-4 in normal and cancer cells. As described by Gurumurthy et al., Par-4 remains in the cytoplasm of normal cells. In cancer cells with elevated PKA activation, Par-4 is phosphorylated at Thr155 and translocates to the nucleus to inhibit NF-κB transcriptional activity. Figure modified from Gurumurthy, Sushma, "MECHANISM OF CANCER SELECTIVE APOPTOSIS BY PAR-4" (2005). University of Kentucky Doctoral Dissertations. 471.

### 1.3a Par-4 Tumor Suppressor

Par-4 has a dynamic relationship with Akt, a key survival kinase that is activated by the second messenger phosphatidylinositol 3,4,5-trisphosphate (PIP3)[173]. Akt is also phosphorylated by PDK1, which is activated by PIP3 at Thr308 and by TORC2 at Ser473, two residues critical for Akt enzymatic activity [174, 175]. Akt phosphorylates a number of effector proteins such as mTOR, IKK, and Mdm2 for activation and is found to inhibit other molecules such as Bad, p27, p21, GSK3β, and transcription factors including Foxo3a [173, 176]. Akt is inhibited by the tumor suppressor PTEN (phosphatase and tensin homolog) that converts PIP3 back to PIP2 to prevent Akt activation. Akt inhibits Par-4 activation through phosphorylation in



many studies as mentioned earlier [170, 177]. Conversely, Par-4 has also been found to inhibit Akt. In a mouse model of lung cancer, Joshi and colleagues show that lack of Par-4 led to increased Akt as well as NF- $\kappa$ B activity leaving cells more sensitive to Ras induced oncogenesis [178]. In Ras expressing lungs, the lack of Par-4 led to an increase in 75% of tumor tissue compared to 12% in WT mice. Increased tumor burden was also correlated with increased NF- $\kappa$ B signaling and thought to be regulated by the increased PKC $\zeta$  activity that is normally suppressed by Par-4 [163, 178]. Increased levels of Akt activity were confirmed by increased Ser473 and Thr308 phosphorylation in the Par-4 KO lungs. Increase in Akt activation was not due to an increase in PI3K activity and studies suggest that lack of Par-4 results in phosphorylation of Akt at Ser124 via PKC $\zeta$  which modulates Akt activation [178]. In another study, Gurumurthy et al., confirmed that Akt directly binds to Par-4 through immunoprecipitation assay and phosphorylates Par-4 at Ser249 (rat) to inhibit its translocation to the nucleus [170]. Additionally, they found that Par-4 expression is necessary for PTEN inhibition of Akt and apoptosis. Other studies have also noted that PTEN haploinsufficiency also led to a loss of Par-4 expression [179, 180].

In addition to the study by Joshi et al., other groups have noted the connection between Par-4 and Ras. Ras has been shown to regulate Par-4 expression through the Raf-MEK-ERK pathway [181]. In studies with immortalized fibroblast lines containing inducible Ras expression, Qiu and colleagues discovered Ras expression downregulated Par-4 expression whereas inhibition of the Raf-MEK-ERK pathway with the inhibitor PD98059 restored Par-4 levels. Par-4 was also found to inhibit expression and activation of ERK1/2 proteins which prevented the oncogenic Ras-transformation, showing a full negative regulatory loop between Par-4 and Ras [181].

Par-4 has also been found to interact with topoisomerase 1 (TOP1) by binding directly through its leucine zipper domain [182]. Topoisomerases relax DNA by making single strand nicks in order for DNA replication, transcription, and recombination to occur [183]. TOP1 protein levels are elevated in proliferating cells and also increased in several types of cancers. Goswami and colleagues found that Par-4 binds to TOP1 to attenuate its DNA relaxation activity to prevent cellular transformation [182].

Par-4 tumor suppressor function is also observed in vivo as Par-4 null animals are found to have increased spontaneous tumors with 80% of females developing endometrial hyperplasia and males developing prostatic lesions [172]. The *par-4* gene was disrupted via homologous recombination by inserting a neo cassette that eliminated exons 1 and 2 of the *par-4* gene completely abolishing Par-4 expression [184]. The absence of Par-4 in mouse embryonic fibroblasts (MEFs) decreased sensitivity to TNF $\alpha$  and cyclohexamide mediated apoptosis, further confirming that Par-4 is needed for the apoptotic response to these treatments. This result mirrored in vitro studies showing that downregulation of endogenous Par-4 elevated TNF $\alpha$  induced NF- $\kappa$ B activity [171]. Par-4 knockout MEFs also had reduced JNK and p38 activity after TNF $\alpha$  stimulation [184]. Par-4 null mice also exhibited increased levels of apoptosis inhibitor XIAP (X-chromosome linked inhibitor of apoptosis). XIAP is an E3 ubiquitin ligase and a known inhibitor of caspase activation [185]. XIAP is also downstream of NF- $\kappa$ B and thought to be increased in Par-4 null animals due to lack of Par-4 inhibition on the PKC $\zeta$ -NF $\kappa$ B-XIAP pathway [172, 184].

The average lifespan of Par-4 null mice is 18mo compared to 25mo for Par-4 WT animals with an 87% propensity to develop tumors [172]. These mice also exhibited normal B and T cell development but do have slight increase in total number of lymphocytes leading to an increased spleen size [186]. The proportions of B and T cells were not changed in young mice lacking Par-4,

but the proliferative response to BCR and TCR stimulants were increased compared to WT animals. Additionally, the lack of Par-4 in these mice led to hyperactivation of atypical protein kinases, blocking JNK signaling. Lack of JNK signaling in CD4+T cells resulted in increased IL-4 production and skewed the animal towards a Th2 response [186].

### *1.3b Par-4 and Apoptosis*

Apoptosis is a process of programmed cell death that is vital for many processes and is highly controlled [187]. There are two main pathways of apoptosis: the extrinsic or death receptor pathway and the intrinsic or mitochondrial pathway. Inappropriate apoptotic signaling can lead to different diseases, including cancer. Cancer avoids apoptosis by inhibiting apoptotic signals and promoting cell survival proteins. Par-4 is found to be silenced in multiple cancers including renal, neuroblastoma, endometrial, lung, prostate, and pancreatic mostly through promoter hypermethylation [188]. Par-4 has been shown to inhibit NF- $\kappa$ B activity as discussed earlier which results in an activation of the intrinsic apoptosis pathway and also plays a role in activating the extrinsic pathway through Fas/FasL. Over expression of Par-4 has been found to induce apoptosis in some sensitive cancer cell lines, but over expression of Par-4 in normal cells only sensitizes them to additional apoptotic signals, making Par-4 a cancer selective target [189].

Par-4 has been found to interact with Bcl-2, an anti-apoptotic molecule. An initial study investigating the levels of Par-4 in patients with ALL found that Par-4 expression was inversely correlated with Bcl-2 expression; similar results were found in leukemic cell lines [190]. Additionally, overexpressing Par-4 in PC-3 and NIH 3T3 cells reduced Bcl-2 protein levels [191]. These observations led to other studies defining the mechanism specifically in lymphoid malignancies as Bcl-2 overexpression is associated with DLBCL and follicular lymphoma pathogenesis [192]. Overexpression studies of Par-4 in Jurkat T lymphocytes led to a disruption in the mitochondrial membrane potential, downregulation of Bcl-2 and activation of caspase

mediated apoptosis [193]. Bcl-2 expression has been shown to increase after radiation induced insults via increased NF- $\kappa$ B activity in PC-3 cells, but enforced Par-4 expression prevented Bcl-2 induction [194].

Par-4 induces apoptosis by promoting the translocation of Fas and Fas Ligand (FasL) to the plasma membrane to recruit FADD, which activates downstream caspase-8 pathway [195]. PC-3 cells that were transfected with Par-4 exhibited an increase in Fas/FasL at the cell membrane and immunoprecipitation assay showed that Par-4 was bound to Fas and FADD, further confirming its important role in initiating the death pathway [195]. Activation of this pathway through Par-4 at normal levels is not sufficient to induce apoptosis alone, but Par-4's additional role in inhibiting NF- $\kappa$ B was also required for cell death. PKA phosphorylation of Par-4 at Thr155 is also essential for Par-4 induced trafficking of Fas/FasL to the membrane [169].

Activation of the Fas-FADD complex by Par-4 promotes caspase-8 dependent activation that leads to downstream activation of executioner caspases including 3, 6, and 7. Par-4 has also been found to be a substrate of caspase dependent cleavage by both caspase 8 and 3 [196, 197]. Studies utilizing cisplatin treatment resulted in decrease total Par-4 protein levels but a reciprocal increase in a 25kDa fragment suggesting Par-4 is cleaved [196]. Caspase-3, in particular, was found to cleave Par-4 at an unconventional site, leaving the fragment to accumulate in the nucleus and inhibit NF- $\kappa$ B activity. Caspase-3 inhibitors prevented Par-4 cleavage and cells lacking caspase-3 such as MCF-7 cells did not express cleaved Par-4. Another study found that UV-induced damage of HeLa cells resulted in a 17kDa and 28kDa fragments of Par-4 [197]. Treatment with cyclohexamide and TNF $\alpha$  also induced Par-4 cleavage through caspase-8 leading to nuclear accumulation of the c-terminal end of Par-4.

In addition to interacting with WT-1 (Wilm's tumor-1), and PKC $\zeta$ , Par-4 has also been found to interact with other anti-apoptotic proteins such as Dlk (DAP-like kinase)[162, 163, 198].

DAP Kinases are known to phosphorylate the regulatory myosin light chain II (MLC) that results in membrane blebbing during cell death [198]. Par-4 and DIK interactions are thought to result in cytoplasmic accumulation of the complex resulting in enhanced MLC phosphorylation and reorganization of the actin filament cytoskeleton.

### *1.3c Secretion of Par-4*

Seminal studies investigating Par-4 function led to the discovery that Par-4 is secreted from all cell types and can induce apoptosis of neighboring cells [199]. PC-3 cells were transfected with GFP labeled Par-4 as well as SAC domain-GFP to find that transfected cells underwent apoptosis but also cells that were not expressing GFP were dying as measured through caspase-3 activation. The Par-4 detected in the conditioned media was not due to dying cells as experiments performed in Par-4 transfected BPH-1 cells that are not sensitive to Par-4 apoptosis also resulted in secreted Par-4. This indicated that Par-4 secretion is independent of apoptosis. Par-4 secretion occurs through the classical ER-Golgi pathway as inhibition of the network with brefeldin A (BFA) blocked secretion [165, 199]. Par-4 secretion is associated with the ER stress response and was also found to associate with GRP78, a member of the heat shock protein family 70 (HSP70) that works to facilitate proper protein folding, prevent intermediate aggregates, target misfolded proteins for degradation, bind calcium, and serve as an ER stress signal regulator [200]. Burikhanov et al. showed that Par-4 and the SAC domain bind and associate with GRP78 at the plasma membrane in response to TRAIL (tumor necrosis factor related apoptosis inducing ligand). TRAIL is a known ER stress inducing factor and treatment of PC-3 cells with TRAIL led to increased GRP78/Par-4 at the cell surface and induced apoptosis [201]. Intrinsic Par-4 expression is also required for GRP78 expression on the surface of the cell but the lack of Par-4 does not alter total GRP78 protein levels [199]. BPH-1 cells that normally do not respond to extracellular Par-4, transfected with GRP78 were sensitive to apoptosis induced

by extracellular Par-4. Extracellular Par-4 is found to activate caspase-8 and caspase-3 through FADD[199]. Initiation of extracellular Par-4 mediated apoptosis results in a feedback loop that promotes more translocation of Par-4 and GRP78 to the surface of the cell. A simplified diagram of Par-4 mediated apoptosis is shown in Figure 1.8.

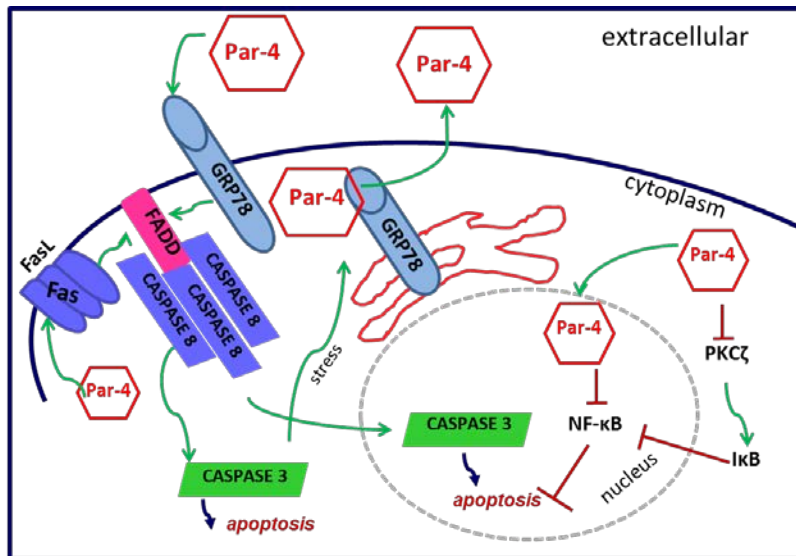


Figure 1.8: Par-4 mediated apoptosis. Par-4 binds and inhibits PKC $\zeta$  that prevents pro-survival signaling of NF- $\kappa$ B and leads to apoptosis. Under cellular stress, Par-4 and its chaperone, GRP78 are translocated from the ER to the plasma membrane where Par-4 is secreted. Extracellular Par-4 can bind to cell surface GRP78 that recruits FADD and initiates caspase-8 and caspase-3 activation. Cellular stress can then lead to increase in Par-4 secretion creating a robust feedback loop. Diagram adapted from Shrestha-Bhattarai, T. Cancer-selective apoptotic effects of extracellular and intracellular Par-4 *Oncogene* (2010) 29, 3873–3880.

### 1.3d Par-4 and Chronic Lymphocytic Leukemia

Several studies have examined Par-4 levels in CLL leading to prognostic predictions. Chow et. al. found that CLL patients that express high Par-4 levels respond better to imatinib treatment [202]. However, a 2011 study examining Par-4 levels in different CLL patient

populations found that Par-4 expression was elevated in the CD38<sup>+</sup> CLL subgroup and advanced stage patients [203]. Boehrer et. al. found 30/30 human CLL patient samples expressed detectable Par-4 protein levels but only 70% of acute lymphocytic leukemia samples expressed detectable Par-4 protein suggesting that Par-4 is not as frequently expressed in less mature lymphocytes [190]. Although Par-4 is expressed in CLL cells the mechanism of Par-4 regulation in CLL is yet to be studied.

#### **1.4 Study of Chronic Lymphocytic Leukemia**

CLL is a difficult disease to study as the culturing of primary CLL cells results in apoptosis. There is clear indication that the microenvironment is required for the survival and proliferation of these malignant B cells. Cell culture conditions have yet to be optimized to mimic the tumor microenvironment leaving *in vivo* models of CLL as the best way to study this cancer. Many mouse models are available to study the disease that represent findings in the clinic such as genomic aberrations (13q14 deletions) or overexpression of oncogenes such as Tcl1 [204]. Aged New Zealand Black (NZB) mouse shows development of a CLL-like disease with an expansion of IgM+CD5+ B cells, but serial passage of these cells results in lymphoma development in recipients [205]. The NZB model did suggest that lack of miR15a/16-1 leads to the development of CLL [206]. These two microRNAs are found at chromosome 13q14 which is commonly deleted in CLL patients, and loss of miR15a/16-1 is found in 68% of CLL patients and leads to CLL development in a mouse model [207]. Animals overexpressing APRIL, ROR1, and BCL2 also develop a CLL like disease [208-210]. There are additional mouse models of CLL but none as reliable as the E $\mu$ -Tcl1 mouse that overexpresses the human Tcl1 oncogene [204, 211].

#### *1.4a T cell leukemia 1*

The first transgenic mouse model to exhibit a CLL-like disease is the E $\mu$ -Tcl1 mouse developed in the early 2000's and is still widely used today [144]. This mouse expresses the human Tcl1 gene, T-cell leukemia 1, specifically in B cells through the Ig VH promoter and E $\mu$  enhancer. T cell leukemia 1 was first identified in a patient with ataxia telangiectasia that developed a T-cell chronic lymphocytic leukemia with a chromosomal translocation at 14q32 [212]. Normally, Tcl1 is expressed during embryogenesis and in fetal tissues, and in lymphocytes during the pro-B cell (CD34<sup>+</sup>CD19<sup>+</sup>) stage with peak expression found in the CD19<sup>hi</sup>IgM<sup>-</sup> naïve B cell population [213]. Tcl1 is also detected in CD4<sup>-</sup>CD8<sup>-</sup>CD3<sup>-</sup> immature thymocytes but not in mature T cells [213]. Narducci et al. found that Tcl1 was expressed in 75% of B-cell lymphoblastic lymphomas and 60% of diffuse large B cell lymphomas. This oncoprotein is also overexpressed in the majority of follicular and mantle cell lymphomas (Mino, Jeko cell lines), and Burkitt's lymphoma (Ramos, Daudi) which are all derived from germinal centers(GC) or post-GC B cells that normally express low levels of Tcl1[213-216]. Tcl1 is found to augment Akt1 kinase activity by physically interacting with the pleckstrin homology domain of the prosurvival protein [217]. It has been suggested that Tcl1 binding results in Akt1 oligomerization near the plasma membrane to promote transphosphorylation or phosphorylation via other kinases such as PDK1 at Thr308 residue and/or the mTOR complex at Ser473 [218]. Tcl1 also mediates the nuclear translocation of Akt1 [217]. Tcl1 promotes the activation of NF- $\kappa$ B in a 4-fold greater manner after treatment with wortmannin, a PI3K inhibitor, suggesting that it may interact with NF- $\kappa$ B co-activators such as CREB [219]. Pekarsky et al. also indicated that Tcl1 inhibited Activator Protein-1 complex (AP-1) dependent transcription by binding to cFos, cJun, and JunB [219].



A study at MD Anderson investigating the role of Tcl1 in human CLL cases found that nearly 90% were Tcl1 positive [220, 221]. While Tcl1 expression was variable among tumors, it was found to be closely associated with Zap-70 positivity and unmutated IGHV genes. Additional studies also found that Tcl1 expression led to increased BCR signaling capacity in patients due to elevated Lyn, Syk, Zap70, and PKC activity [222]. Herling and colleagues suggested that Tcl1 may be a biomarker indicating CLL patients with elevated BCR signaling that may respond better to kinase inhibitors. Because the E $\mu$ -Tcl1 mouse expresses high levels of the human Tcl1 gene, it is thought to be a representative model of U-CLL.

#### 1.4b E $\mu$ -Tcl1 Mouse

According to many different reviews, the E $\mu$ -Tcl1 mouse model is the most representative animal model of human CLL as these mice develop disease at late stages and exhibit similar genomic characteristics [204, 211, 221, 223, 224]. The Tcl1 oncogene was initially expressed in animals under the control of the *lck* promoter that led to T cell leukemia by the Croce group [225]. Bichi et. al. then utilized the Tcl1 oncogene to be expressed under the V<sub>H</sub> promoter and E $\mu$  enhancer to be expressed specifically in B cells and develop a CLL-like disease around the ages of 10-15 months (Figure 1.9)[144].

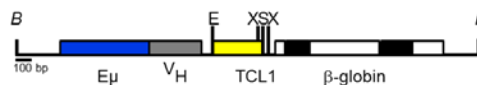


Figure 1.9: Tcl1 expression construct. The human Tcl1 350bp fragment was cloned and inserted into a plasmid with the mouse V<sub>H</sub> promoter and Ig  $\mu$  enhancer along with the poly A site of the human  $\beta$ -globulin gene. Figure adapted from Bichi et. al. 2002 PNAS 99(10): 6955-6960. Human chronic lymphocytic leukemia modeled in mouse by targeted TCL1 expression.

Penetrance of B cell malignancies is 100% in some but not all mouse studies [204]. It is important to note that at the same time the E $\mu$ -Tcl1 mouse was developed, another mouse expressing Tcl1 under the B29 promoter and  $\mu$  enhancer was developed by the Teitell group [226]. The B29-Tcl1 mouse developed malignancies in both the B and T cell compartments including DLBCL, follicular lymphoma, T cell lymphoma, and some cases of B cell leukemia. The E $\mu$ -Tcl1 mouse begins to exhibit a clonal expansion of CD5+IgM+ B lymphocytes in the peritoneal cavity at 2mo and the spleen and peripheral blood at the age of 3-4mo [144]. These mice continue to develop and exhibit splenomegaly with distorted histology and continued increased in the CD5+CD19+ population.

The E $\mu$ -Tcl1 mouse is an excellent model to study human disease as they express a similar BCR repertoire associated with aggressive disease [227], show similar response to treatment [228], and show dysregulated T cell function [229, 230]. Recently, with the development of the NSG (NOD/SCID gamma null) mouse, some groups have worked with xenograft models of CLL by taking human peripheral blood B-CLL cells and injecting them into immunodeficient animals for study but these cells exhibit minimal proliferation [231, 232].

While the E $\mu$ -Tcl1 mouse represents a similar course of disease as in humans, it does require time to develop. Due to this characteristic, we established an adoptive transfer model of primary E $\mu$ -Tcl1 splenic cells into syngeneic C56Bl/6 recipients without prior conditioning. We are able to monitor the progress of these animals by submandibular bleeding, flow cytometry and spleen palpation. We have compared the adoptive transfer cells to the primary E $\mu$ -Tcl1 cells by fluorescence-activated cell sorting (FACS) and found that they express similar cell surface molecules. Similarity is also observed in functional tests of primary and adoptive transfer CLL cells as well as spleen histology.

#### *1.4c Cell lines of CLL*

While the *in vivo* models of CLL replicate disease, *ex vivo* culturing of primary E $\mu$ -Tcl1 and adoptive transfer cells leads to apoptosis. Studies with *ex vivo* CLL cells are productive, but long term culture is challenging. Therefore, cell lines have been developed in order to study the biochemistry of this disease and define the mechanisms that promote CLL survival. The MEC-1 and MEC-2 cell lines were characterized in 1999 and were derived from the peripheral blood of an EBV-seropositive CLL patient [233]. These cells are highly utilized in the field as they express mature B cell markers and express VH4 Ig family that have not gone through somatic hypermutation. These cells are negative for CD5 expression but have the capacity to grow in *vivo* mouse models and MEC-1 cells also show other characteristics similar to *ex vivo* CLL cells such as high expression of Ig molecules [234]. Another cell line that has been used to study CLL is the OSU-CLL that was generated by EBV transformation of patient cells that expressed CD5 [235]. These cells were found to migrate similar to primary CLL cells and were also able to grow in immunodeficient NOG mice. A new cell line known as MDA-BM5 was recently generated from bone marrow of a CLL patient with the 17p and p53 deletion [236]. These cells are CD5+CD19+ and have undergone somatic hypermutation.

Cell lines have also been generated from mouse models, specifically the IgH.TE $\mu$  mouse that expressed the SV40 T oncogene [237]. Cell lines EMC2, 4, and 6 express CD5+CD43+IgM+CD19+ on their surface and are able to grow in Rag<sup>-/-</sup> mice [238]. Additionally, these mouse cell lines express constitutively active BTK and AKT.

#### **1.5 Premise of this study**

Although CLL has been very well characterized and new therapies have been developed to treat the disease, the cases of patient relapse are tremendous, warranting new pathways to be discovered. Par-4 has been documented to be expressed in CLL and related for a few

prognostic factors, but the actual role that Par-4 plays in CLL as well as its regulation has not been defined. We investigated the levels of Par-4 expression in primary mouse CLL cells, cell lines, and primary patient samples and found that these cells have elevated Par-4 expression when compared to normal B cell counter parts. Previous studies from our lab have shown the importance of BCR signaling in the survival of these cells and it is well known that CLL cells have elevated BCR signaling that promotes their survival [36, 114, 239]. This led us to hypothesize that constitutive BCR signaling could regulate Par-4 expression in CLL cells. Elevated levels of Par-4 protein expression also raised the question of why CLL cells were not sensitive to Par-4 induced apoptosis. Our studies show novel regulation of Par-4 through BCR signaling, and Par-4 plays a pro-growth rather than pro-apoptotic role in CLL, further confirming that this apoptotic pathway is dysregulated in CLL.

We made an additional observation about the importance of the spleen in the growth and development of CLL through our adoptive transfer model. Studies in the laboratory of injecting CLL cell through different routes (IV, IP, SQ) all led to severe splenomegaly. We were able to track the growth of CLL cells through a human ROR1 marker that allowed us to suggest that CLL cells home and grow primarily in the spleen. We hypothesized if removal of the spleen would alter the growth and development of CLL. Splenectomy of adoptive transfer recipients indeed prevented the growth of CLL after transfer in WT C57BL/6 mice. Splenectomy in the E $\mu$ -Tcl1 mouse at early and late stages also improved the overall survival time and delayed CLL development. But our surprising discovery was that splenectomy in the Par-4<sup>-/-</sup> mice enabled growth of CLL 50% of the time. This indicates that Par-4 does play a role in preventing the growth of CLL in secondary proliferation sites. Our studies show that intrinsic Par-4 works to promote the growth of CLL while extracellular Par-4 may act to suppress CLL in different microenvironments.

## CHAPTER 2

### Materials and Methods

#### 2a) Mice

$\text{E}\mu\text{-Tcl1}$  Mice and  $\text{Par-4}^{-/-}$  mice were described previously and were bred in house [144, 184].  $\text{E}\mu\text{-Tcl1}$  mice were provided by Dr. John Byrd (Ohio State University) and  $\text{Par-4}^{-/-}$  mice were provided by Dr. Vivek Rangnekar (University of Kentucky). C57BL/6 and NOD-scid IL2Rgnull-IL-3/GM-CSF (NSGS) and NOD-scid IL2Rgnull (NSG) mice were purchased from the Jackson Laboratory (Bar Harbor, ME) and bred in house.  $\text{E}\mu\text{-Tcl1}$  and  $\text{Par-4}^{-/-}$  mice were crossed for the F1 generation and the F1 mice were intercrossed to generate  $\text{Par-4}^{-/-}\text{Tcl1}^+$  offspring. Mice were confirmed for genotyping using primers listed in Table 2. The  $\text{Tcl1}$  amplified fragment is 320bp,  $\text{Par-4}$  WT fragment is 213bp and  $\text{Par-4}$  knockout fragment is 248bp in size.

Table 2: List of forward and reverse primers for PCR of genomic DNA of  $\text{Par-4}$  and  $\text{Tcl1}$ . Primer sequences were provided by collaborators at OSU ( $\text{Tcl1}$ ) and the Rangnekar lab ( $\text{Par-4}$ ).

Target Gene		Sequence (5' → 3')
Tcl1	Forward	GCC GAG TGC CCG ACA CTC
	Reverse	CAT CTG GCA GCA GCT CGA
Par-4 WT	Forward	GTG ATG ACG TCT TCT GAT TTC C
	Reverse	GAG ACT CCA GAA CTT AGT TGC
Par-4 KO	Forward	CGT CTC GGA ATG GAG G
	Reverse	GAG ACT CCA GAA CTT AGT TGC

Adoptive transfer models were carried out by injecting  $4\text{-}10 \times 10^6$  Ficoll-paque purified splenic  $\text{E}\mu\text{-Tcl1}$  CLL cells in 150 $\mu\text{l}$  volume with sterile PBS intravenously via retro-orbital route

while animals were under isoflurane anesthesia[240]. Animals were housed and maintained by the Department of Laboratory Animal Resources at the University of Kentucky (Lexington, KY) in specific pathogen free conditions in micro-isolator containers. All animal studies were approved by the Institutional Animal Care and Use Committee (under protocol number 2011-0904) and were carried out in accordance with the Animal Welfare Act. CLL development in E $\mu$ -Tcl1, Par-4<sup>-/-</sup>E $\mu$ Tcl1 and adoptive transfer recipients was monitored through submandibular cheek bleeding using sterile 5mm Goldenrod Animal lancets (Medipoint, Inc. Mineola, NY) collected in BD microtainer tubes with K<sub>2</sub>EDTA (Becton-Dickinson and Company, Franklin Lakes, NJ) [241]. When the percentage of CD5+CD19+ cells in the peripheral blood was >70%, E $\mu$ Tcl1 mice were carefully monitored for moribund body conditions and euthanized according to the IACUC standards. Body condition scores were generated by monitoring the weight of the mice and level of activity as previously described in [242]. Cells were isolated from the spleen of E $\mu$ -Tcl1 mice and confirmed for the CLL phenotype CD5+CD19+ by flow cytometry. Other characteristics to confirm CLL in the mice were through analysis of spleen histology by showing lack of follicular structures and expansion of proliferation centers with increased white pulp. Additionally, the ability to transfer the primary mouse spleen CLL cells into recipient mice confirmed the malignant qualities of the disease.

### *2b) Cells and Tissues*

Primary E $\mu$ -Tcl1 CLL single cell suspension was prepared by processing E $\mu$ -Tcl1 spleens through a 40 $\mu$ M cell strainer with the blunt end of a 5cc syringe in Hanks Buffered Salt Solution (HBSS). Other tissues were collected and processed in a similar manner including lymph nodes, liver, omental tissue, thymus, and any solid tumors. Tibiae and Femora were collected from mice and marrow was isolated by flushing with a 26G syringe with HBSS. Peritoneal cells for lysates and B cell subset sorting were obtained through peritoneal lavage with HBSS [15].

Peripheral blood mononuclear cells were isolated from 200-300µl collection and treated with RBC lysis buffer and HBSS washes. Cells were cultured in complete RPMI 1640 media (Corning #10-040-CV, New York, NY) supplemented with 10% Fetal Bovine Serum (FBS), 50µM beta-mercaptoethanol (2-ME), 1mM Sodium Pyruvate, and 50,000 Units Penicillin/Streptomycin.

Mec-1 cells were cultured in IMDM (Iscove's Modified Dulbecco's Medium) (ThermoFisher Scientific #12440061 Waltham, MA) supplemented with 10% FBS, 50µM 2-ME, 1mM Sodium Pyruvate, and 50,000 Units Gentamicin. OSU-CLL cells were cultured in completed RPMI 1640. NCI-H460, PC-3, SudHL-6, RAMOS, and NIH-3T3 cell lines were cultured in complete RPMI 1640 (H4-60, PC-3), IF-12 (SudHL-6, RAMOS), or DMEM (NIH-3T3) media.

### *2c) Patients*

Human Patients with CLL were recruited from the University of Kentucky, Markey Cancer Center Hematology and Oncology Clinic. Each patient gave informed consent approved through the University of Kentucky Institutional Review Board, IRB #15-0697. Peripheral blood CLL cells were purified through Ficoll-Paque density gradients (GE HealthCare #17-144-02, Pittsburgh, PA) and confirmed for CLL phenotype by CD45+CD5+CD19+ staining via flow cytometry. Healthy control donors were obtained from leukopack units purchased from the Kentucky Blood Bank (Lexington, KY) after quality testing and white blood cells were isolated through Ficoll-Paque density gradients. Human cells were cultured in completed RPMI 1640 described above.

### *2d) Reagents*

Dasatinib (0003-0528-11) was manufactured by Bristol-Myers Squibb Company (Seattle, WA). Syk inhibitor IV (Bay 61-3606) (57-471-42MG) was obtained from EMD Millipore Calbiochem (Billerica, MA). Ibrutinib (A3001) and ERK1/2 inhibitor, SCH772984 (A3805), were

obtained from ApexBio (Houston, TX). Dimethyl sulfoxide (DMSO) was obtained from Sigma Aldrich (D2438) (St. Louis, MO).

### *2e) Flow Cytometry and Cell Sorting*

Single cell suspensions of CLL cells and tissues from C57BL/6, E $\mu$ Tcl1 and Par4<sup>-/-</sup>E $\mu$ Tcl1 mice were analyzed for multicolor flow cytometry using the FACSCaliber and Becton Dickinson LSRII Flow Cytometer (BD San Jose, CA) in the University of Kentucky Flow Cytometry and Cell Sorting Facility.  $1 \times 10^6$  cells were incubated to block Fc $\gamma$  receptors using normal Rat Ig (10 $\mu$ g/ $1 \times 10^6$  cells) for 15 minutes at room temperature and then stained for 30 minutes on ice with fluorochrome-conjugated antibodies (all from BioLegend, San Diego, CA) towards CD5 (Cat # 100606 or 100608), CD19 (Cat # 115520 or 115508 or 115512), CD45 (Cat# 103114 or 103110). Peritoneal B cell subsets and spleen B cells were stained for CD19, CD5, and CD11b (Cat # 10121,) to distinguish B1a: CD5+CD19+CD11b+, B1b: CD5-CD19+CD11b+, and B2: CD5-CD19+CD11b- populations and sorted on the iCyt Synergy sorter system from Sony Biotechnology (San Jose, CA). Human CLL and normal peripheral blood samples were stained with antibodies specific to human CD5 (Cat # 364022), CD19 (Cat # 302208) and CD45 (Cat # 368512) for 1 hour on ice.

### *2f) Cell Survival and Proliferation Assays*

Cell survival and proliferation was determined by the 3-(4,5-dimethylthiazole-2-yl)-2,5-biphenyl tetrazolium bromide (MTT) assay[243]. Primary mouse and human CLL cells were cultured at  $2 \times 10^5$  cells/well in 96 well flat-bottom microtiter plates in 200 $\mu$ l. Mec-1 and OSU-CLL cells were cultured at  $2 \times 10^4$  cells/well. The cells were treated with 0-40 $\mu$ M Dasatinib, Fostamatinib, and Ibrutinib dissolved in DMSO for 48hr and then media was changed and incubated with MTT (0.5mg/ml; Sigma Aldrich, M5655) for 4hr. The formazin crystals were



solubilized in acidic isopropanol and optical density was measured at 560nm and 690nm. The OD values (560-690nm) of cultures without the drugs were set to 100%. DMSO concentration did not exceed 0.02% of culture medium and had no measurable effect on cell viability.

### *2g) Immunoblot Analysis*

Cells were lysed in Cell Signaling lysis buffer (Cat # 9803, Danvers, MA) supplemented with 1X protease inhibitor (Roche Cat # 5892953001, Indianapolis, IN), 1mM PMSF (Sigma#P7626), 2mM NaF (Sigma #S-1504), 2mM freshly made Na<sub>3</sub>VO<sub>4</sub> (Sigma #S-6508). Mec-1 shRNA cells were also lysed with RIPA buffer made by 10 mM Tris-Cl (pH 8.0), 1 mM EDTA, 1% Triton X-100 and 1X protease inhibitor. Nuclear and Cytoplasmic fractions were isolated using NE-PER Extraction Kit from ThermoScientific (#78833). Pierce BCA Assay was performed to detect the amount of protein in each sample and the diluted in 4x sodium dodecyl sulfate (SDS) sample buffer (100mM Tris-HCl, pH 6.8, 30% glycerol, 4% SDS, 5% 2-ME, and 0.01% weigh/volume bromophenol blue) resulting in 1X concentration and then boiled for 10 minutes followed by cooling on ice for 10 min. 30µg of protein was separated on an SDS polyacrylamide gel using the BIO-RAD Mini Protean Tetra System (Bio-Rad Cat #1658001EDU). 7µl of Precision Plus Protein dual color ladder (Bio-Rad Cat #1610394) ranging from 10-250kDa in size was used for each gel. Gel separation was run in running buffer (25mM Tris, 192 mM glycine, 0.1% SDS, pH 8.3) at 90V/3A for 10minutes followed by 150V/3A for approximately 45 minutes or until the loading dye reached the end of the gel. Gels were then transferred to polyvinylidene difluoride membranes (EMD Millipore Cat #IPVH00010) in transfer buffer (25mM Tris, 192mM glycine, 20% methanol, pH 8.3) at 90V/3A for 1.5hr at 4°C. Each membrane was blocked at room temperature for 1hr in 5% milk or 3% Bovine Serum Albumin (BSA) in 1X TBST (10X: 0.5M Tris, 1.5M NaCl, and 1% Tween-20). Membranes were then probed with respective primary antibodies at 4°C overnight, washed and then probed with horseradish peroxidase-conjugated

secondary antibodies for minimum 1hr at room temperature. Membranes were exposed to HyGLO chemiluminescence reagent (Denville Scientific Cat #E2400) and developed on HyBlot CL autoradiography film (Denville Scientific #E3012). Some difficult to detect proteins utilized BioRad Clarity Western ECL Substrate (Bio-Rad Laboratories Cat # 170-5060). Intensities of bands were quantified using the Gel Analysis method of the NIH Image J program. All band intensities were normalized to Glyceraldehyde 3-phosphate dehydrogenase (GAPDH) expression or  $\beta$ -actin or corresponding non-phosphorylated proteins. Phospho specific antibodies against Src (Y416) (#2101S), Akt (S473) (#9271L), Syk (Y525/526) (#2711), Btk (Y223) (#5082P), P-ERK (#9101) were obtained from Cell Signaling Technologies (Danvers, MA). Antibodies against total Akt (#9272S), Syk (#2712), Btk (#3533S), GAPDH (#2118S) were also obtained from Cell Signaling Technologies. Antibodies against total Lyn (#SC-15), Par-4 (#SC-1807), Col1A (#SC-28657), Tc11 (#SC-33550), p21 (F-5) (#SC-6246), ERK1/2 (#SC-94), Bcl2 (#SC-7382) and HDAC (Histone Deacetylase, #sc-7872) were obtained from Santa Cruz Biotechnologies (Santa Cruz, CA). Peroxidase coupled secondary antibodies were also obtained from Santa Cruz Biotechnologies (#SC-2004, SC-2005). Antibody against  $\beta$ -actin was obtained from Sigma Aldrich (Cat# A5441).

#### *2h) Measurement of apoptosis induced by secreted Par-4*

Primary E $\mu$ -Tc11 mouse CLL cells were cultured for 12-24hr in RPMI-1640 media and then media was collected and applied (400 $\mu$ l) to H4-60 lung cancer cell line. Apoptotic nuclei were defined by 6-diamidino-2-phenylindole (DAPI) staining (Cat #H-1200 Vector Laboratories, Inc., Burlingame, CA) [170]. 100nM Recombinant thioredoxin (TXR) and TXR-Par-4 fusion proteins were provided by Dr. Vivek Rangnekar (University of Kentucky) as a positive control and antibody towards Par-4 was used to block Par-4 mediated apoptosis. This assay was performed with the help of Dr. Nikhil Hebbar, University of Kentucky.

Primary E $\mu$ -Tcl1 mouse CLL cells and purified mouse splenic B cells were isolated via complement dependent T cell depletion: 25x10<sup>6</sup> total spleen cells in 10ml total volume were plated on 10cm petri dishes and incubated for 1hr at 37°C for macrophage depletion. Cells are then collected and RBCs are lysed at 100x10<sup>6</sup> cells per 1ml of RBC Lysis Buffer (Sigma Cat#R7757). Cells are then washed and re-suspended in antibody mix containing Thy1.2, Lyt2, and L3T4 at a cell density of 25x10<sup>6</sup>/ml and incubated for 40min on ice. 10ml of HBSS is then added to the antibody mixture with cells and centrifuged to wash. Rabbit IgG complement is then added at 1ml per 25x10<sup>6</sup> cells and incubated in 37°C water bath for 30 min. Cells were then washed in HBSS. Isolated B cells were then stimulated with 5 $\mu$ g/ml LPS (Millipore Sigma-Aldrich, St. Louis, MO) for 12 hrs in low serum (0.05%FBS) RPMI. Media was collected and concentrated using Amicon Ultra-4 centrifugal filter concentrators (Cat #UFC801024, EMD Millipore, Billerica, MA). The conditioned medium was probed for Par-4 and collagen (Col) 1A. Albumin was detected by Coomassie blue stain. The cells were also collected and the lysates were used to measure total cellular Par-4 levels.

### *2i) shRNA Lentiviral Infection*

Mec-1 CLL cells were transduced with lentiviruses expressing Lyn shRNA and Par-4 shRNA. Lyn shRNA gene set prepared by the RNAi Consortium was purchased through ThermoFisher Scientific (now with Dharmacon or open Biosystems) (Cat #RHS4533). We observed the highest knockdowns with Lyn shRNA clones # TRCN0000010101 and #TRCN0000010107, and hence were used in these studies. Par-4 shRNA constructs were cloned into the pLKO.1 lentiviral vector. Lentiviruses were packaged in HEK-293-T cells by cotransfection with pMD2.G (VSV G) envelope plasmid (Addgene Cat # 12259) and the Gag, Pol expressing psPAX2 packaging plasmid (Addgene #12260). Lentiviral particles were collected from the supernatants after 48hrs of transfection and then transduced in Mec-1 cells. 1.5x10<sup>6</sup>

Mec-1 cells were infected with the target shRNA lentivirus and 10µg/ml Polybrene (Cat # SC134220, Santa Cruz), in 4ml of complete IMDM media by centrifugation for 90 min at 2800rpm at 10°C (spinoculation technique). Viruses and cells were incubated for 24hrs at 37°C and then fresh media was replenished. Puromycin dose antibiotic selection began at day 3 and remained in culture for the entire period of experimentation after proper titration. Limiting dilution was performed earlier to determine that Mec-1 cells seeded at 0.5cells/well in 96 well plate were capable to of growing. shRNA infected cells were then added to 96 wells and clones were generated. Less than 15% of the wells generated knockdown clones that expanded. Gene silencing efficiency was analyzed by immunoblot for respective proteins. Control shRNA and Par-4 shRNA Mec-1 cell growth rate was monitored through counting and trypan blue exclusion using a hemacytometer. Total cell numbers were recorded with each passage and extrapolated total cell counts were calculated.

*2j) Knocking out selected SFKs using CRISPR- Cas 9 techniques*

R6-22 Lenti CRISPR V2 plasmid construct (Plasmid # 52961) included the Cas9 nickase and guide RNA and was obtained from Addgene (Cambridge, MA) along with R6-21 pCMV-VSV-G (Plasmid #8454) and R6-20 pLJM1-EGFP (Plasmid number 19319) for viral constructs in bacterial stabs. Cultures were grown up and plasmids were isolated using Omega EZNA Plasmid DNA Midi Kit (Omega Biotek Norcross, GA, Cat #D6915-03). Lenti CRISPR V2 plasmid was cut with BsmB1 restriction enzyme (NEB Biolabs Ipswich, MA, Cat #R0580S) to generate overhangs. Guide RNAs were designed using GeCKO (Genome scale CRISPR Knock-Out) program in the Lentiviral CRISPR toolbox provided by Zhang Lab at Massachusetts Institute of Technology (Cambridge, MA). NCBI RefSeq was used to confirm guide RNAs: Lyn NP\_002341, Fgr NP\_001036212, and Lck NP\_001036236. Oligonucleotide primer sequences of targets with BsmB1 sites were designed and obtained from IDT (Integrated DNA Technologies Coralville, IA)

(Table 3). Oligonucleotides were annealed and ends dephosphorylated before ligating oligo duplexes into BsmB1 cut Lenti-CRISPR V2 plasmid. Complete plasmid with target guide RNA was when ligated into NEB 10-beta Competent E. Coli (NEB Biolabs Cat # C3019H) and amplified in culture. Plasmids were cut to confirm that the target sequence was inserted correctly with SnaB1 restriction enzyme (NEB Biolabs Cat #R0130S) and also sequenced by ACGT Sequencing Services. Plasmids with Lyn, Fgr, and Lck target sequences were confirmed and then sent to the Genetic Technologies Core (GTC) at the University of Kentucky. Lentivirus titer was performed in the GTC and  $1.5 \times 10^6$  Mec-1 cells were infected with  $1 \times 10^6$  infection units in 4ml of complete IMDM media by centrifugation for 90 min at 2800rpm at 10°C. Cells were incubated with viruses for 24hrs at 37°C and then fresh media was replenished. Puromycin antibiotic selection began at day 3 and remained in culture for the entire period of experimentation after proper titration (1.5µg/ml). Gene silencing efficiency was analyzed by immunoblot for respective proteins.

Table 3: Designed Guide RNA oligonucleotide sequences for CRISPR-Cas9 knockout studies.

<b>Guide RNA</b>		<b>5' → 3'</b>
<b>Lyn1a</b>	Forward	<b>CACC</b> GTT CTT TCA GTA TTA CGT AC
	Reverse	<b>AAAC</b> GTA CGT AAT ACT GAA AGA AC
<b>Lyn4a</b>	Forward	<b>CACCG</b> TAA CCG CTC TGA CTC CCG TC
	Reverse	<b>AAAC</b> GAC GGG AGT CAG AGC GGT TA
<b>Fgr1</b>	Forward	<b>CACC</b> GGC GTG TCA GAG GCT ACC GC
	Reverse	<b>AAAC</b> GCG GTA GCC TCT GAC ACG CC
<b>Fgr2</b>	Forward	<b>CACC</b> GAA AAG CTA TAT AGA CGG TTA
	Reverse	<b>AAAC</b> TAA CCG TCT ATA TAG CTT TTC
<b>Lck1</b>	Forward	<b>CACC</b> GTG GTG GCT ACG ACG GCG AA
	Reverse	<b>AC</b> TTC GCC GTC CTA CGG ACC AC
<b>Lck2</b>	Forward	<b>CACC</b> GGT GGT GGC TAC GAC GGC GA
	Reverse	<b>AAC</b> TCG CCG TCG TAG CCA CCA CC

### *2k) CD79 siRNA Knockdown Study*

CD79 siRNA (Cat # SC-35025) and control siRNA (Cat # SC-37007) were obtained from Santa Cruz Biotechnologies. Human CLL samples obtained from peripheral blood collection were purified by Ficoll-paque density gradient.  $20 \times 10^6$  CLL cells were then transferred in 200  $\mu$ l PBS to a 0.4cm electrode gene pulser cuvette (Cat # 165-2008, BioRad, Richmond, CA) with 10  $\mu$ g of control or targeted siRNA. The cells were then pulsed at 220mV or 250mV, 960  $\mu$ F, 0  $\Omega$  and then quickly transferred to 4ml RPMI ( $5 \times 10^6$  cells/ml) for 24hr incubation and then collected for immunoblot analysis. Control siRNA was only pulsed at 250mV, 960  $\mu$ F, 0  $\Omega$ .

### *2l) In vivo tumor study*

Mec-1 CLL cells were transduced with lentiviruses expressing Par-4 shRNA or Control (scrambled) shRNA. Cells expressing shRNA constructs were selected with puromycin treatment for 26 days and knockdown was confirmed through immunoblot analysis.  $2 \times 10^6$  shRNA expressing cells were injected subcutaneously into flanks of NSGS mice with 1:1 ratio of matrigel (#354234, BD Biosciences) in 100  $\mu$ l volume. Par-4 shRNA cells were injected on the right flank and control shRNA cells were injected on the left flank with 6 mice for each group. Tumor volumes were measured using electronic caliper and tumor volumes were calculated by length (mm) x width<sup>2</sup>(mm). Significance was determined by student t-test for each day of measurement.

### *2m) Cell Cycle Analysis*

After selection and confirmed knockdown of Par-4, shRNA infected Mec-1 cells ( $5 \times 10^5$ ) were cultured in 48 well plates in triplicate for 48hrs and then analyzed for cell cycle stage after fixing with cold 70% ethanol for 1hr at 4°C and incubation with a mixture of 1  $\mu$ g/ml propidium iodide (PI) (Sigma Aldrich, P1470) and 25  $\mu$ g/ml RNase A (Sigma Aldrich, R6513) at 37°C for 30 min. The

level of PI fluorescence was measured with a FACSCaliber flow cytometer. Cell populations in G<sub>1</sub>, S, G<sub>2</sub>/M phase were calculated using ModFit Software.

### 2n) Quantitative Real-time PCR (qRT-PCR)

Total RNA was isolated from different cell populations using TRI reagent (Sigma Aldrich Cat #T9424) and quantified with ThermoScientific Nanodrop 1000 Spectrophotometer. A total of 0.5µg of RNA was then used to make cDNA with qScript cDNA SuperMix (Quanta Bioscience Cat #95048-100, Gaithersburg, MD). iTaq Universal SYBR Green Supermix (BIO-RAD Cat #172-5121, Hercules, CA) was used to carry out the RT-PCR reaction with indicated primers. Sequences are provided in Table 4 and primers were obtained from IDT technologies (Coralville, IA). RT-PCR was performed using BioRAD CFX96 Touch Real-time PCR Detection System.

Table 4: List of qRT-PCR primers

Target Gene		5' → 3'
<b>mPar-4</b>	Forward	GACTTGTGAGGCTGATGCAA
	Reverse	GCCCAACAACCTTCAAAAGA
<b>m18S</b>	Forward	CGCCGCTAGAGGTGAAATTCT
	Reverse	CGAACCTCCGACTTTTCGTTCT
<b>hPar-4</b>	Forward	GAAGATGCAATTACACAACAGAACAC
	Reverse	TAGCAGATAGGAACTGCCTGGAT
<b>hp21</b>	Forward	CAGACCAGCATGACAGATTTTC
	Reverse	TTAGGGCTTCCTCTTGGAGA
<b>h18s</b>	Forward	TTCGAACGTCTGCCCTATCAA
	Reverse	ATGGTAGGCACGGCGACTA

### 2o) Tissue Histology

Whole spleen tissues were collected from mice at the time of euthanasia and a fragment was cut for tissue analysis. Pieced spleen was placed in a tissue cassette and fixed in Buffered Formalde-Fresh 10% Formalin (Fisher Scientific Fair Lawn, NJ Cat #SF93-4). Tissues

were then processed and embedded in paraffin blocks by the Markey Cancer Center Biospecimen Procurement and Translational Pathology Shared Resource Facility (MCC BPTP SRF). Tissue blocks were cut and spleens were stained with Hematoxylin and Eosin staining. Gross morphological changes were noted by expanded white pulp and loss of follicular architecture within the tissue.

### *2p) Ultrasound Imaging*

Mice were sedated with isoflurane using an anesthetic vaporizer with a dial setting of 2-3% in the induction chamber followed by maintenance at 1.5% oxygen carrier gas at 4 liters/min at induction and at 1.5 to 2 liters/min as maintenance for a mouse weighing 300 grams. Mice were placed on a heated platform (capable of monitoring Heart rate) and the areas to be examined were shaved using a Wahl series 8900 cordless rechargeable animal trimmer and hair is further removed using a depilatory (Nair, Church & Dwight Company), approximately 0.1-0.5 ounces is applied using Q tips on the region of abdomen or thorax that was to be imaged. The depilatory was allowed to stay for 2-3 minutes and then wiped off with unscented baby wipes (PDI nice or M233XT Quick medical), and the skin was allowed to dry. Pre-warmed ultrasonic gel of about 0.5-2 ounces was applied. Mice were scanned using a solid-state transducer for the measurement of enlargement of spleen and any irregularities in the spleen and other abdominal organs if any. After scanning, the ultrasonic gel was removed/ wiped off and mice were placed back in the cage on padding to recover while being observed. The ultrasound machine, probe, nose cone, platform and surrounding areas were cleaned using a disinfectant (T-Spray II<sup>®</sup> by Pharmaceutical Innovations, Inc.) supplied by the manufacturer. The ultrasound machine (Vevo 2100), probes and equipment are manufactured by Visualsonics (FUJIFILM, Toronto, ON).



## *2q) Splenectomy*

Prior to surgery, the animal is assessed for normal activity and then the abdomen is shaved using a Wahl series 8900 cordless rechargeable animal trimmer and hair is further removed using a depilatory (Nair). Isoflurane (1-5% in O<sub>2</sub>) is inhaled through a nose cone at 1.5 to 2 liters/min. Artificial tear replacement ointment (Lacrilube) is placed on the eye of the mouse to prevent dehydration. Behavioral cues and respiratory rate are monitored closely during anesthesia. The animal is placed on a sterilized surgical pad on top of a heating pad to maintain body temperature. The animal is placed on its right side and scissors are used to make approximately a 2.0cm cut of the skin on the left side. Connective tissue is then gently moved away from the abdominal wall to where you can visual the spleen through the peritoneum. A 1.5cm incision is then made in the peritoneal wall and the spleen is gently pulled to the exterior. A 4-0 absorbable suture is used to look and tie off the splenic artery and the efferent venule. After vessel ligation, the spleen is removed. The peritoneal wall is closed with one or two absorbable sutures in a simple interrupted stitch. The skin is then closed with 9mm stainless steel wound clips (AUTOCLIP, Clay Adams Brand, Cat# 427631). The animal is then given sustained release buprenorphine (Animalgesics Labs) at 3.25mg/kg, subcutaneously once at the completion of surgery. Mice are then monitored daily for 3 days and checked twice weekly following. The wound clips are removed after 10-14 days, with triple antibiotic cream applied.

## *2r) Statistical Analysis*

Statistical analyses was performed using GraphPad Prism 7 (GraphPad Software, Inc., La Jolla,CA). Statistical significance of differences between groups was evaluated by Student's t-test, growth rates of cells were analyzed by linear regression analysis calculated through the slope, and Kaplan-Meier curves were analyzed by Log-Rank test and Gehan-Breslow-Wilcoxin

Test. Correlation statistics were tested by linear regression analysis. Experiments testing the means overtime were analyzed by two-way ANOVA. P values < 0.05 were considered significant.

## CHAPTER 3

### **μ-Tcl1 CLL cells have elevated expression of Par-4**

Prostate Apoptosis Response-4 (Par-4) is a known tumor suppressor that is down regulated by promoter methylation in about 30% of cancers including renal cell carcinoma and Acute Lymphoblastic Leukemia (ALL) [244, 245]. Par-4 was originally identified by its upregulation during apoptosis of prostate cancer cells and later was shown to have a cancer selective mechanism of inducing cell death through its specific SAC domain [168]. Par-4 has been shown to be activated by Protein Kinase A (PKA) phosphorylation at Thr155(rat)/Thr163(human) residue. This site is located in the SAC domain and allows Par-4 to translocate to the nucleus and inhibit NF-κB activity in cancer cells but not normal cells [169]. This specificity for cancer cell death makes Par-4 an attractive therapeutic target in many cancers that has resulted in clinical trials to enhance Par-4 mediated cell death in solid tumors [246]. To date, only three studies have examined Par-4 expression in CLL and these have led to some suggested prognostic indicators [190, 202, 203]. Initially, Boehrer et al. examined the levels of Par-4 in normal and neoplastic lymphocytes and found that all patients with CLL (n=30) expressed Par-4 protein levels, but only 63% were positive for Par-4 mRNA expression suggesting that there may be a difference in Par-4 regulation in different types of leukemia [190]. Previous studies had indicated that Par-4 and Bcl-2 are inversely correlated [191], but there was no relationship found between the expression of Par-4 and Bcl-2 protein expression in CLL patients. Next, Chow and colleagues found that CLL patients that lacked the Imatinib targets BCR-ABL, C-Kit, PDGFR were still sensitive to Imatinib treatment and that the response correlated with Par-4 expression [202]. Additionally, this study confirmed Boehrer et al. finding that there was no relationship between Par-4 expression and Bcl-2 in patients that did or did not respond to Imatinib treatment. Par-4 was also downregulated in the course of the treatment

with Imatinib when cells underwent apoptosis after caspase-8 and -3 activation [202]. Lastly, Borjarska-Junak and colleagues assessed the expression of Par-4 in CLL B-cells and found a positive correlation of Par-4 with Bcl-2, which is opposite of what is observed in non-hematopoietic cells. Par-4 was also positively correlated with DAXX (death associated protein), and ZIPK (zipper interacting protein kinase) expression [203]. Additionally, Par-4 was found to associate with LDH (lactate dehydrogenase) serum concentrations and was more highly expressed in CD38+ CLL patients who have a more aggressive form of CLL disease [35, 71]. These initial studies suggest that Par-4 in CLL may be regulated differently in this hematologic disease and have other regulatory mechanisms. Therefore studies presented in this chapter investigated the level of Par-4 expression in CLL cells from the E $\mu$ -Tcl1 mouse model compared to normal B cell subsets, specifically B1a cells, one of the suggested normal counterparts of CLL. We made the surprising finding that E $\mu$ -Tcl1 CLL cells express elevated levels of Par-4 that has been proven to be functional by inducing apoptosis of solid tumors, but CLL cells themselves were not sensitive to Par-4 mediated apoptosis. This observation also translated to human CLL samples that over expressed Par-4 compared to normal donor peripheral blood cells. Studies presented in this chapter also examined the expression of Par-4 in the primary CLL models as well as the adoptive transfer model of murine CLL.

## **Results**

### *3a) E $\mu$ -Tcl1 B-CLL spleen cells have elevated levels of Par-4 expression*

Although increased constitutive Par-4 expression has been described in CLL cells, most previous studies compared CLL cells to peripheral blood total B cells which are mostly made of B-2 cells. Hence we isolated CLL cells from the spleens of E $\mu$ -Tcl1 mice which were CD5+CD19+ (Figure 3.1A). B cell subsets were isolated from the peritoneum and spleens of C57BL/6 WT mice and FACS sorted into specific populations of B1a: CD19+CD5+CD11b+, B1b: CD19+CD5-CD11b+, and B2: CD19+CD5-CD11b- cells (Figure 3.1B) [15]. Immunoblot analysis indicated that E $\mu$ -Tcl1 CLL cells expressed high levels of Par-4 protein compared to all the normal B cell subsets (Figure 3.1C). B1a cells expressed more Par-4 compared to the other B cell populations but only ~33% of the observed levels in CLL. Par-4 mRNA expression was also elevated in CLL cells compared to B cell subsets, mirroring the levels of Par-4 protein expression (Figure 3.1D). Because E $\mu$ -Tcl1 CLL cells overexpress the Tcl1 oncogene, we questioned if the observed increase in Par-4 expression was associated with Tcl1. We isolated different B cell subsets from 2mo old E $\mu$ -Tcl1 mice that had no detectable levels of CLL in the peripheral blood and measured Par-4 levels compared to WT B cell subsets (Figure 3.1E). B1a E $\mu$ -Tcl1 cells expressed higher Par-4 protein levels compared to B1b and conventional B2 E $\mu$ -Tcl1 cells. This finding was similar to what was observed in WT B cell subsets. All the E $\mu$ -Tcl1 B cell subsets express Tcl1 as indicated in Fig. 3.1E and shown in reference [144], but Par-4 protein levels were not as highly expressed as compared to spleen cells from E $\mu$ -Tcl1 mice with >90% CD5+CD19+ CLL cells. This result led us to investigate if increased Par-4 expression resulted from leukemic progression in E $\mu$ -Tcl1 mice. As previously observed, CD5+CD19+ B cell percentage increased with the age of the mice in the peripheral blood and spleen (Figure 3.1F and [209]) and immunoblot analysis of whole spleen cells from the different aged E $\mu$ -Tcl1 mice indicated that Par-4 protein expression increased with CLL burden

(Figure 3.1G). We confirmed this correlation by examining the relationship between the percentage of CD5+CD19+ cells and Par-4 expression in the spleens of E $\mu$ -Tcl1 mice. This indicated a positive association between leukemic burden and Par-4 ( $r^2=0.7495$ ,  $p<0.0055$ ) (Figure 3.1H). On the other hand, Par-4 expression did not correlate with Tcl1 levels when both proteins were normalized to  $\beta$ -actin ( $r^2=0.003958$ ,  $p=.8824$ ) (Figure 3.1I). When comparing multiple different CLL samples that arose in individual mice, we also saw some variation in levels of Par-4 that also did not correlate with changes in Tcl1 expression (Figure 3.1J).

### *3b) Primary human CLL cells express elevated Par-4 levels*

We wanted to see if this elevated Par-4 expression was just a mouse phenomenon or if Par-4 was also highly expressed in human CLL. Primary human CLL peripheral blood samples were obtained through consent and IRB approval and compared to normal human donors summarized in Table 5. Such comparison to normal controls was not performed in previous studies. CLL was confirmed through CD5+CD19+ staining by flow cytometry (Figure 3.2A) and total protein was isolated and probed for Par-4 expression (Figure 3.2B). CLL samples expressed significantly higher levels of Par-4 protein when compared to normal donors. The Par-4 gene has been mapped to the middle portion of chromosome 12 that has also been implicated in CLL pathology as it is associated with about 16% of diagnosed CLL cases [164, 247, 248]. According to patient data indicated in Table 3.1, there does not appear to be a gene dosage effect of Par-4 expression in patients that express trisomy 12 (Figure 3.2C). For example, patients 11 and 14 are indicated to have trisomy 12, but appear to have less Par-4 than others that are not indicated to have cytogenetic abnormalities. With the help from our collaborators at Ohio State University, we were able to test the levels of Par-4 in patients with U-CLL and M-CLL (Figure 3.2D) ( $p=0.231$ ). It appears that Par-4 expression is slightly higher in the more aggressive U-CLL form

of CLL but it is not significantly different,  $p=0.231$ . However, more samples would be needed to further confirm this result.

### *3c) Expression of Par-4 in adoptive transfer mouse model of CLL*

We observed that Par-4 is highly expressed in the splenic B-CLL cells of the E $\mu$ -Tcl1 primary mouse model compared to the normal counter part of B1a cells [79, 93]. We have confirmed that the splenic CLL cells from the de novo primary E $\mu$ -Tcl1 mouse and the adoptive transfer CLL cells express almost identical cell surface molecules (Table 6), but we wanted to confirm that these cells retain similar Par-4 expression after transfer. Initially, we showed that the primary E $\mu$ -Tcl1 spleen and adoptive transfer spleen yielded similar total WBC counts and percent of CD5+CD19+ cells as shown in Figure 3.3A. Transfer of different primary E $\mu$ -Tcl1 CLL cells that arose de novo in individual mice may exhibit delayed or progressive variable growth patterns, but on average, these mice tend to develop CLL like disease in about 3-8 weeks. A representative growth curve of CLL in the peripheral blood is depicted in Figure 3.3B compared to normal peripheral blood CD5+CD19+ cells in WT mice. We are able to monitor CLL growth in recipient mice through submandibular cheek bleeding and FACs analysis over time. We isolated tissues from the recipient mice after CLL development and found that CD5+CD19+ CLL cells were present in the spleen, peripheral blood, lymph node, bone marrow, peritoneal cavity, liver, and omental tissues (Figure 3.3C, left). This is a dramatic increase compared to normal spleen, lymph node, and bone marrow tissues of a non-injected animal (Figure 3.3C, right). Additionally, we probed for Par-4 and Tcl1 expression in these tissues of CLL injected mice compared to the primary E $\mu$ -Tcl1 CLL cells that arose de novo (Figure 3.3D). All tissues expressed Tcl1, confirming the presence of CLL cells and there was high Par-4 expression as well.

### *3d) Par-4 is secreted by CLL cells and is functional in inducing apoptosis*

Par-4 is a known tumor suppressor in solid tumors and is able to induce apoptosis in an intrinsic as well as an extracellular manner [165, 244]. Because we observed that CLL cells expressed high levels of Par-4 but their survival is maintained, we questioned if Par-4 is able to translocate to the nucleus where it is known to interact with NF- $\kappa$ B. Nuclear and cytoplasmic compartments were isolated from multiple primary E $\mu$ -Tcl1 CLL samples and Par-4 was detected in both cellular locations (Figure 3.4A). Tcl1 expression was also located in both locations except for CLL #1. Presently we do not know why Tcl1 was absent in the nucleus of this one CLL sample. Additionally, the Mec-1 CLL cell line and primary human CLL samples were examined for Par-4 localization and the protein was also found within both compartments in these cells (Figure 3.4B).

Par-4 is also found to be secreted by many cells to induce apoptosis in an extracellular manner [199]. We found that CLL cells do secrete high amounts of Par-4 compared to normal and stimulated spleen B cells (Figure 3.4C). Because CLL cells undergo apoptosis quickly in culture, we questioned if the secreted Par-4 that we detected was just due to apoptosis of the cells. We cultured primary mouse E $\mu$ -Tcl1 CLL cells with or without LPS or  $\alpha$ IgM stimulation and measured Par-4 secretion. Additionally, we probed for GAPDH in the conditioned medium as an indicator of cell apoptosis and lysis because GAPDH is not supposed to be secreted (Figure 3.4D). GAPDH levels were very low in the concentrated medium in comparison to the cell lysates, whereas Par-4 levels in conditioned medium were almost as high as observed in total cell lysate.

Additionally, we adoptively transferred E $\mu$ -Tcl1 CLL cells into syngeneic C57BL/6 WT hosts and mice null for Par-4 [184] and detected similar levels of Par-4 in the plasma of WT and Par4<sup>-/-</sup> mice 4 weeks after transfer via western blot (Figure 3.4E). This confirmed that E $\mu$ -Tcl1 CLL

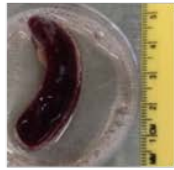


cells secreted Par-4 *in vivo*. We also examined the spleens of these recipient mice after termination to confirm that Par-4 and Tcl1 were expressed in the Par4<sup>-/-</sup> recipients to indicate CLL engraftment.

We next tested if Par-4 secreted from CLL cells was functional in inducing apoptosis of the Par-4 sensitive H460 lung cancer cell line. Conditioned medium from CLL cell culture applied to the H460 cell line induced apoptosis which was reduced by inclusion of anti-Par-4 antibody but not control IgG (Figure 3.4F). We also confirmed that human CLL samples secrete Par-4 with or without stimulation (Figure 3.4G).

Extracellular Par-4 requires the receptor GRP78 to bind and induce extrinsic apoptosis [199]. CLL cells have slightly lower levels of basal GRP78 protein compared to other cell lines and may be one reason why CLL cells are not sensitive to the known pro-apoptotic effects of Par-4 (Figure 3.2H) but further studies examining the location of GRP78 are required.

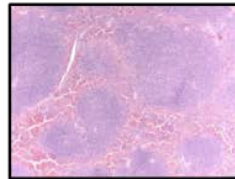
**Figure 3.1A**



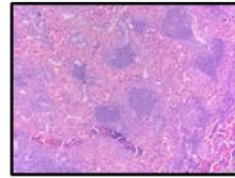
**Primary E $\mu$ -Tcl1 spleen  
13.6 mo**



**Normal spleen  
12.1 mo**



**E $\mu$ -TCL1 Spleen Histology**



**Normal Spleen Histology**

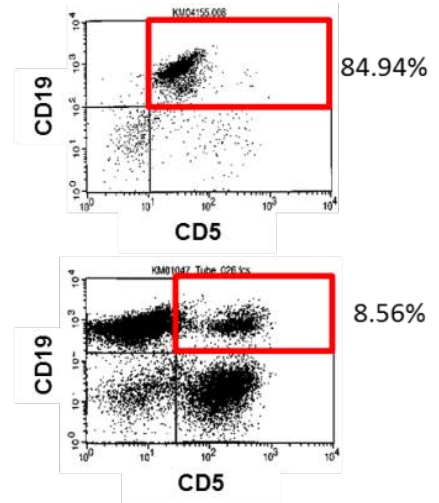


Figure 3.1B

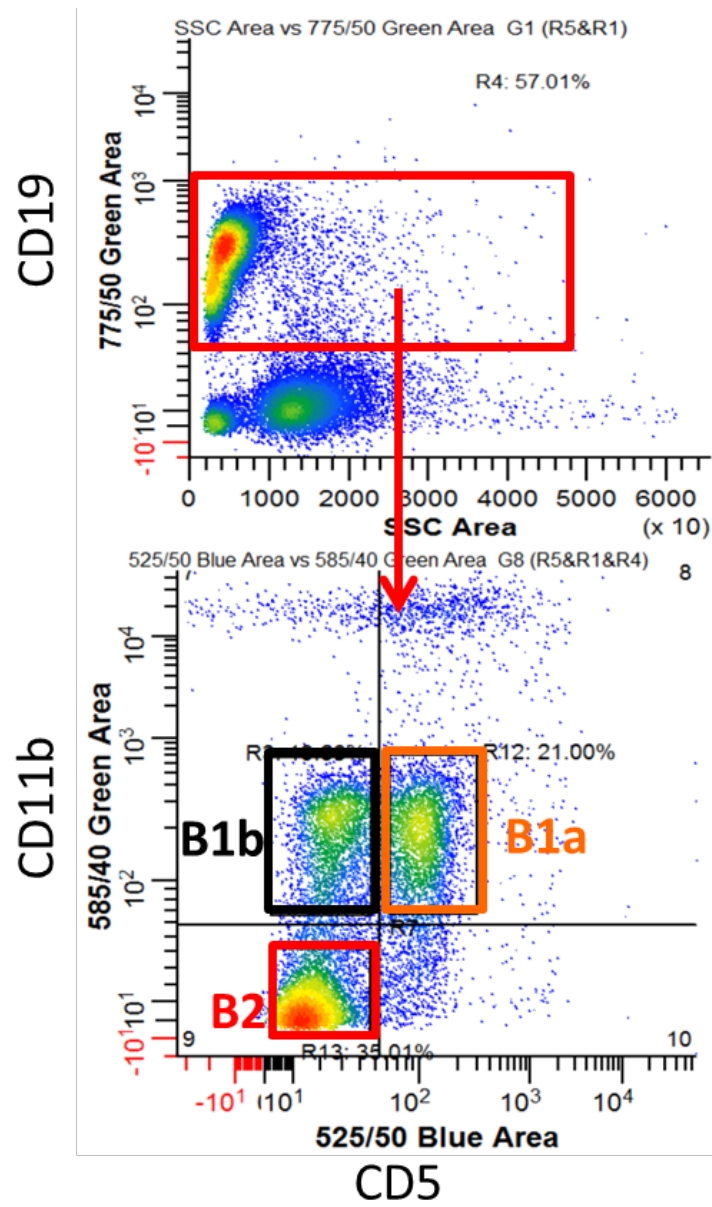


Figure 3.1C

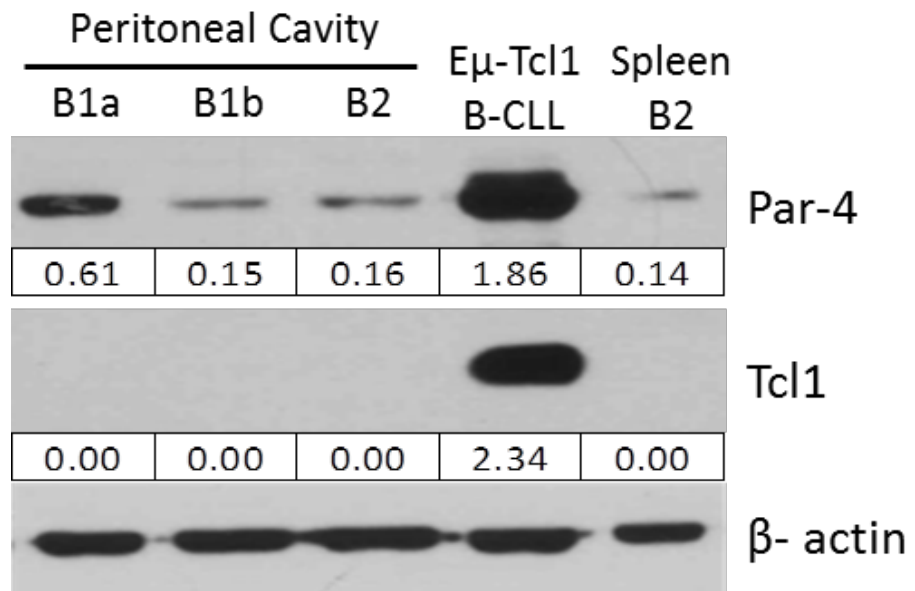
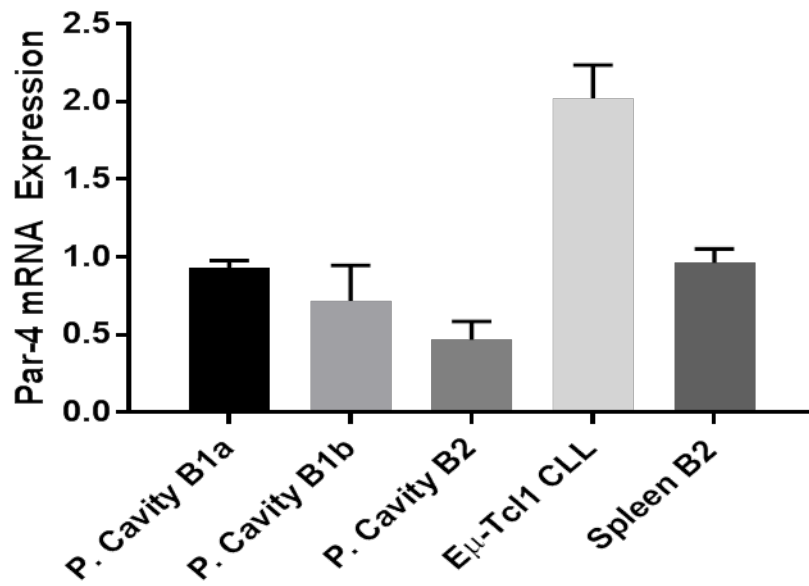
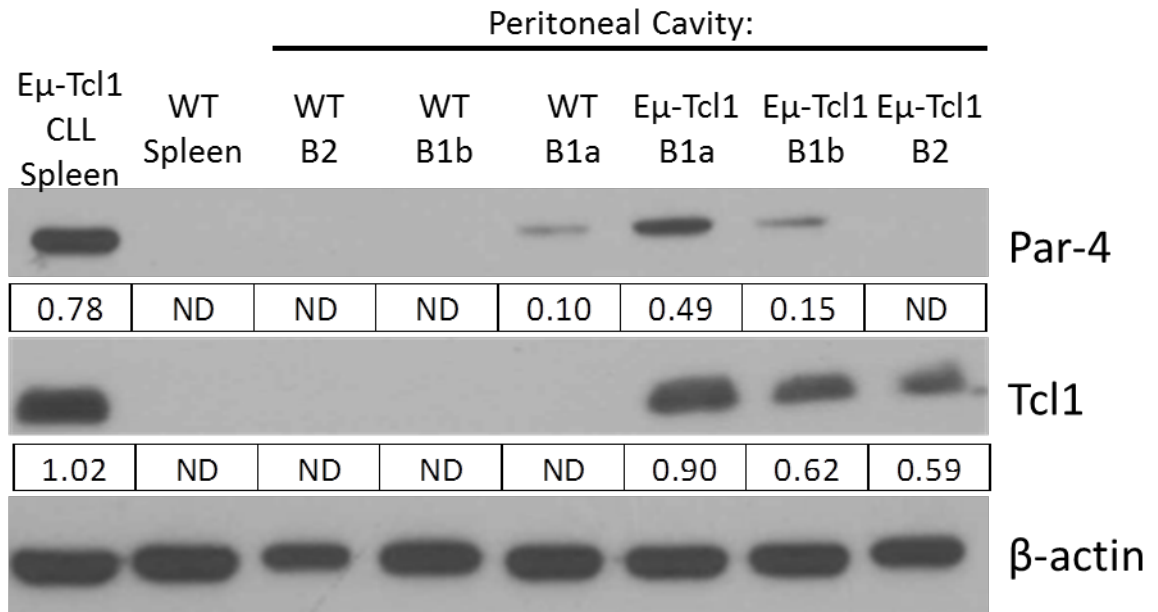


Figure 3.1D



**Figure 3.1E**



**Figure 3.1F**

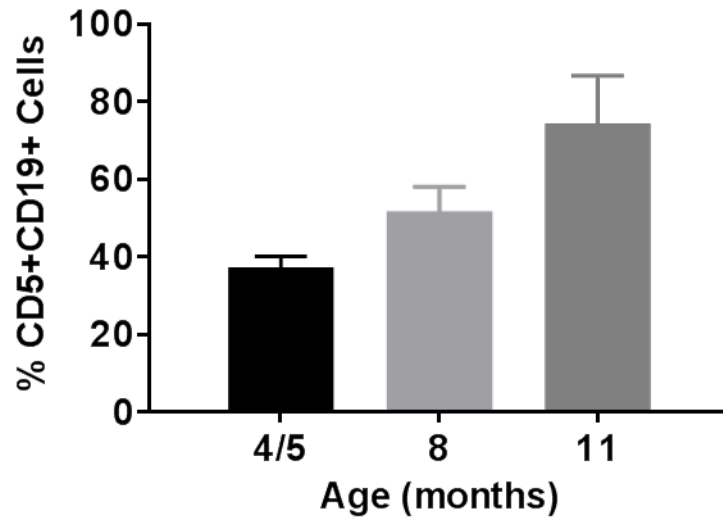


Figure 3.1G

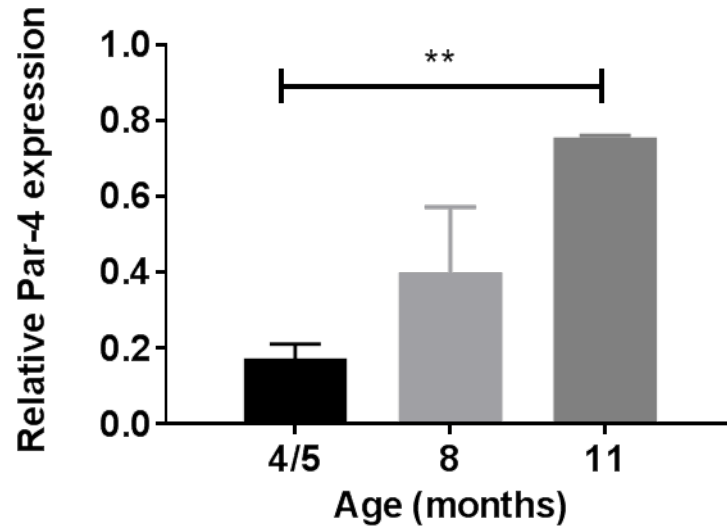
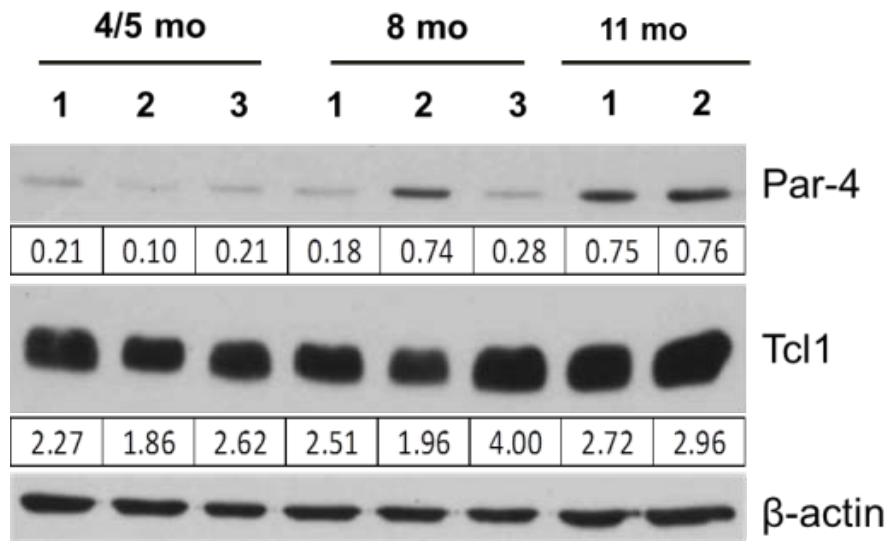


Figure 3.1H

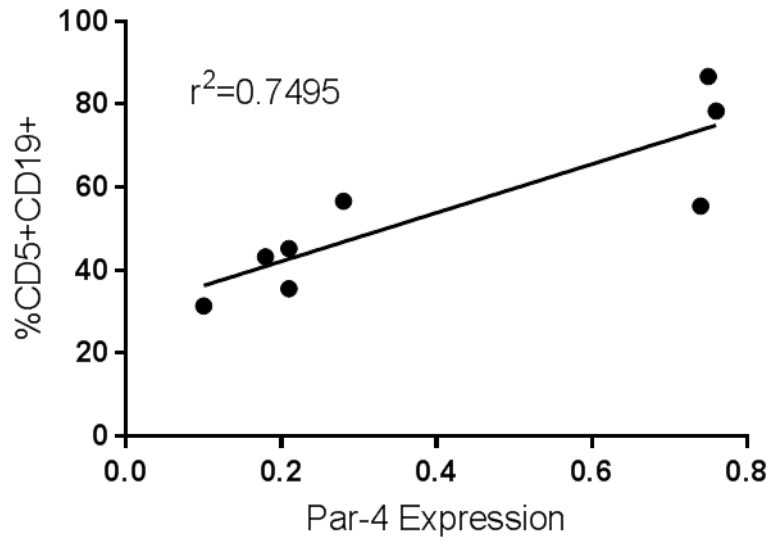
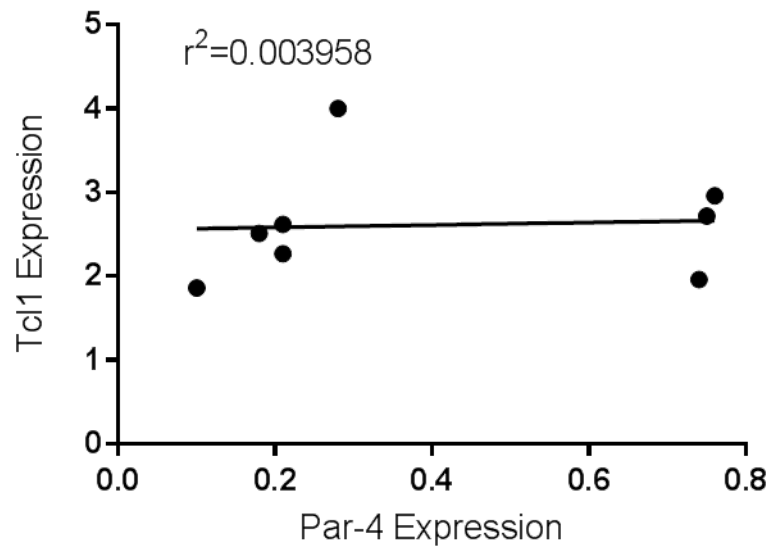


Figure 3.1I



**Figure 3.1J**

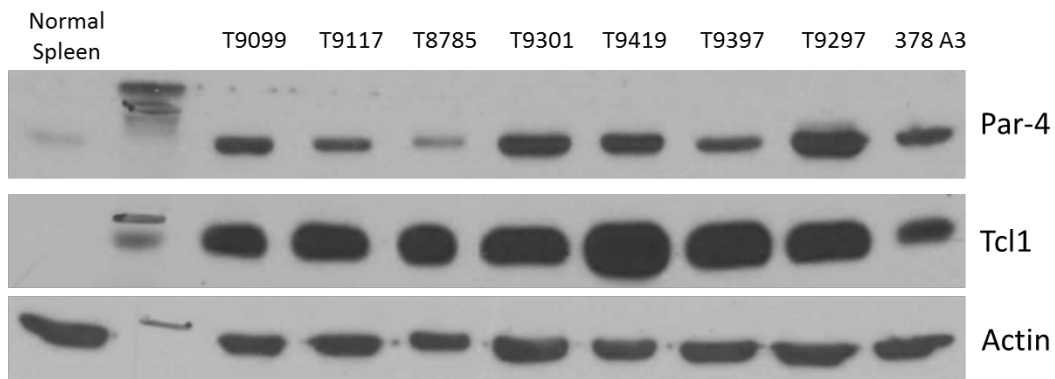


Figure 3.1: E $\mu$ -Tcl1 B-CLL spleen cells have elevated levels of Par-4 expression

A) Splens were collected from E $\mu$ -Tcl1 and C57BL/6 mice at similar ages. Tissue was processed and stained with H&E for histology analysis. Single cell suspensions from spleens were stained for CD45, CD5, and CD19. A representative FACs profile for a diseased mouse (10.1mo) is shown with 84.95% CD5+CD19+ cells compared to a normal 12.6mo WT mouse with 8.56% CD5+CD19+ cells. B) Peritoneal cavity cells were isolated from 20 WT 16 week mice and pooled together. Cells were stained for CD19, CD11b and CD5 and gated into B cell subsets as indicated and isolated by FACs sorting. C) Immunoblot analysis of peritoneal cavity B cell subsets, E $\mu$ -Tcl1 CLL spleen cells, and WT isolated B2 spleen cells probed for Par-4 and Tc1. Densitometry values are normalized to  $\beta$ -actin. D) Relative Par-4 mRNA expression measured in E $\mu$ -Tcl1 CLL cells and WT B cell subsets. Par-4 mRNA levels were normalized to mouse 18S mRNA expression. These values were normalized to B1a Par-4 mRNA expression. Results show mean  $\pm$  SE of triplicate samples. E) Peritoneal Cavity cells were collected from both WT (n=20) and E $\mu$ -Tcl1 mice (n=4) ranging in age of 2-3mo and sorted in to B cell subsets according to Fig 3.1b. Total protein was isolated. Immunoblot analysis was performed to determine the expression of Par-4 and Tc1 proteins. F) Total percentage of CD5+CD19+ cells in the spleens of E $\mu$ -Tcl1 mice



increase with age and CLL disease development. P value = <0.001 determined by One way ANOVA. G) Spleens were collected from mice at three different ages. Nine spleens collected from 4/5mo and 8mo each and 2 spleens from 11mo E $\mu$ -Tcl1 mice. Three spleens were pooled together and total protein was isolated and probed for Par-4 and Tcl1. Par-4 protein expression is normalized to  $\beta$ -actin. \*\* indicates p value = 0.0012 determine by student t test between 4/5mo and 11mo E $\mu$ Tcl1 mice. H) Correlation of Par-4 protein expression and percentage of CD5+CD19+ cells E $\mu$ Tcl1 mice. I) Correlation of Par-4 protein expression and Tcl1expression in the spleens of E $\mu$ Tcl1 mice at different ages. Each point represents an average of three mice.  $r^2$  value was determined by Pearson Coefficient test. p = 0.0055 (H) p =0.8824 (I) determined by linear regression analysis. J) Immunoblot analysis of Par-4 and Tcl1 expression in multiple E $\mu$ -Tcl1 CLL spleen samples compared to normal spleen. Lane 2 indicates gel loading ladder.

Table 5: Human CLL Patient information.

Patient Number	Age	Treated	CD38+	Zap70+	Cytogenetics	WBC (k/ $\mu$ l)	%CD5+CD19+
hCLL Patient #1	76	No	Positive		Trisomy 12	19.8	87.66
hCLL Patient #2	82	No	Negative	Negative		20.7	90.54
hCLL Patient #3	56	No					82.35
hCLL Patient #4	36	No	Negative		13q deletion	38.3	88.08
hCLL Patient #6	46	No	Negative	Negative	13q deletion	41	44.01
hCLL Patient #7	52	Yes				15.2	81.37
hCLL Patient #8	69	No	Positive		Normal	29	83.88
hCLL Patient #9	57	Yes				40	50.33
hCLL Patient #10	62	Yes			11.7% 17p deleted cells	83.7	10.55
hCLL Patient #11	69	No			Trisomy 12, 13q deletion	30.2	95.71
hCLL Patient #13	70	No				17.4	80.45
hCLL Patient #14	63	No			Trisomy 12	34.8	96.97
hCLL Patient #15	53	Yes	Positive		13 q deletion	12.1	84.73
hCLL Patient #16	55	Yes				6	13.64
hCLL Patient #17	76	Yes				36.6	37.23
hCLL Patient #18	80	Yes				142	97.73

Patient peripheral blood samples were obtained from the Markey Cancer Center Hematology/Oncology Clinic through IRB consent. Total peripheral white blood cell (WBC) counts at time of collection are indicated and the percent CD5+CD19+ cells were measured through flow cytometry after collection. Cytogenetics, CD38+, Zap70+ are indicated if known through previous diagnosis.

Figure 3.2A

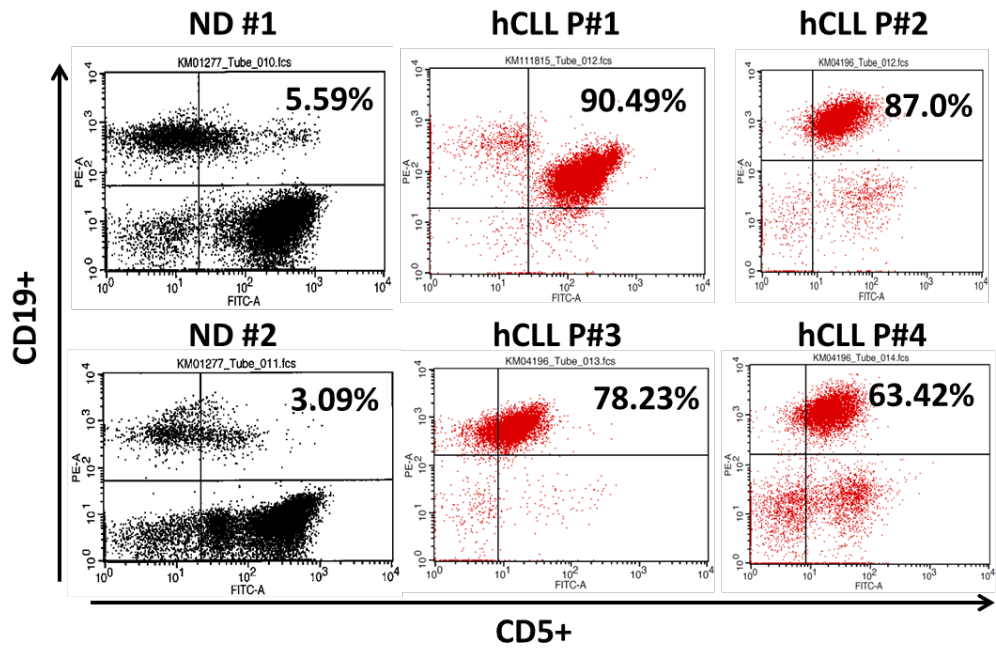


Figure 3.2B

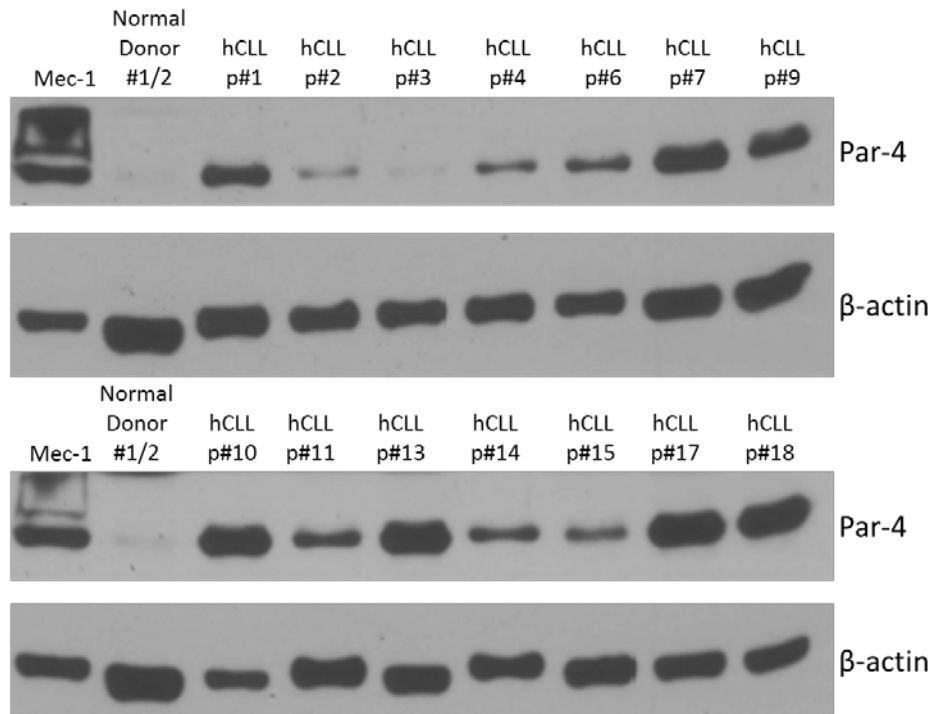


Figure 3.2C

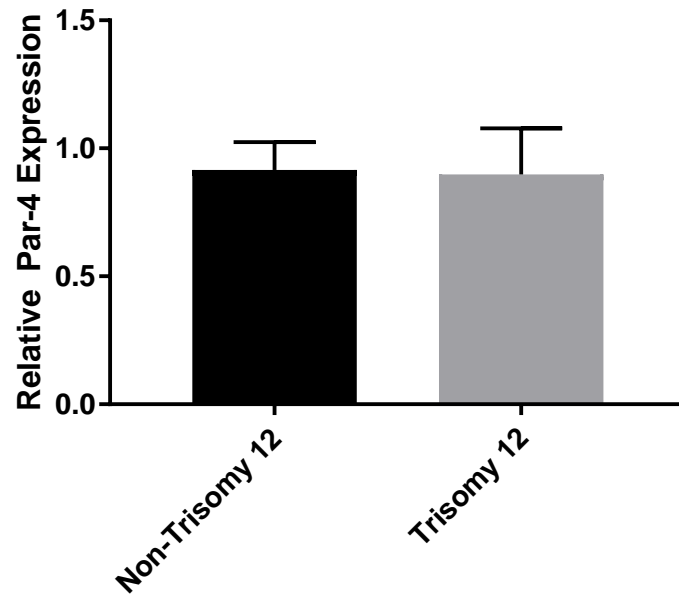


Figure 3.2D

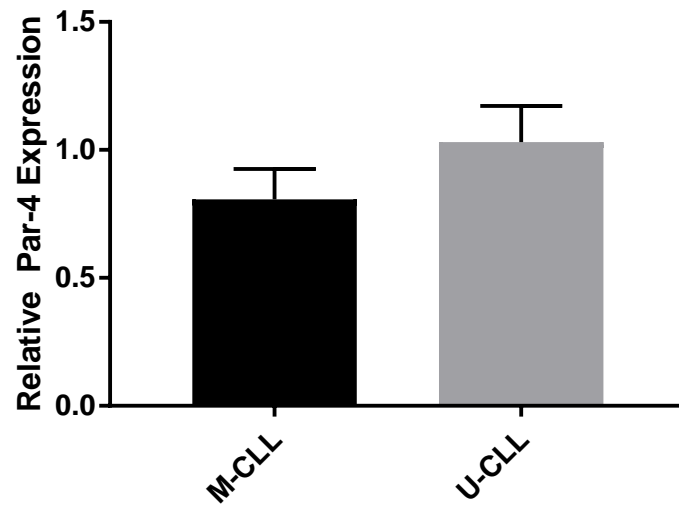


Figure 3.2 Human CLL samples express elevated Par-4 protein levels

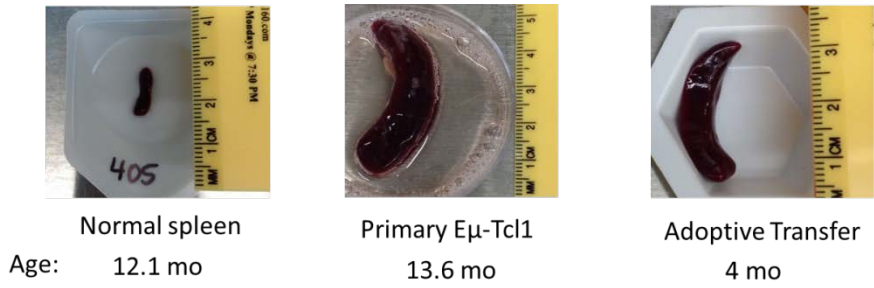
A) Representative FACS profiles of primary human peripheral blood samples diagnosed with B-CLL stained with antibodies to CD5 and CD19 compared to two normal donors (ND#1 and ND#2)

B) Immunoblot analysis of Par-4 protein expression levels in primary hCLL samples compared to a pooled whole peripheral blood lymphocyte lysate of two normal donors. Protein values were normalized to  $\beta$ -actin. C) Primary patient samples were collected and total protein was isolated from PBMC and analyzed by western blot to determine Par-4 expression. Densitometry was

determined by ImageJ analysis. Trisomy 12 levels were indicated from the patient's medical chart to subgroup patients. n=23 for non-trisomy 12 and n=7 for trisomy 12. p=0.879

determined by student t-test. D) Par-4 protein expression was determined by immunoblot analysis in C) and IGHV status was measured by PCR. Patients were grouped into U-CLL if the variable region was less than 2% different from the germline sequence. n= 16 for M-CLL and n=14 for U-CLL. p=0.231 determined by student t-test.

**Figure 3.3A**



	WBC Count	% CD5+/IgM-	% CD5-/IgM+	% CD5+/IgM+
Normal Spleen	$8.4 \times 10^7$	26.63	54.27	<b>10.95</b>
		% CD5+/CD19-	% CD5-/CD19+	% CD5+/CD19+
Primary Eμ-Tcl1	$1.3 \times 10^9$	2.1	0.23	<b>97.11</b>
Adoptive Transfer	$9.8 \times 10^8$	1.14	3.14	<b>93.79</b>

**Figure 3.3B**

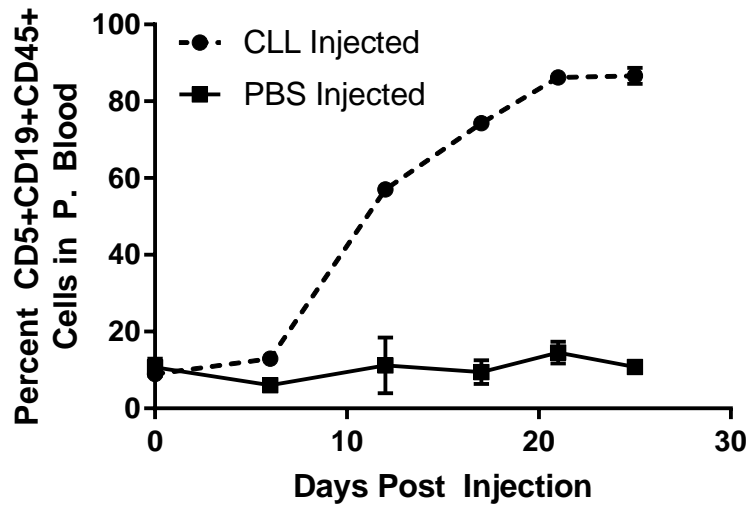


Figure 3.3C

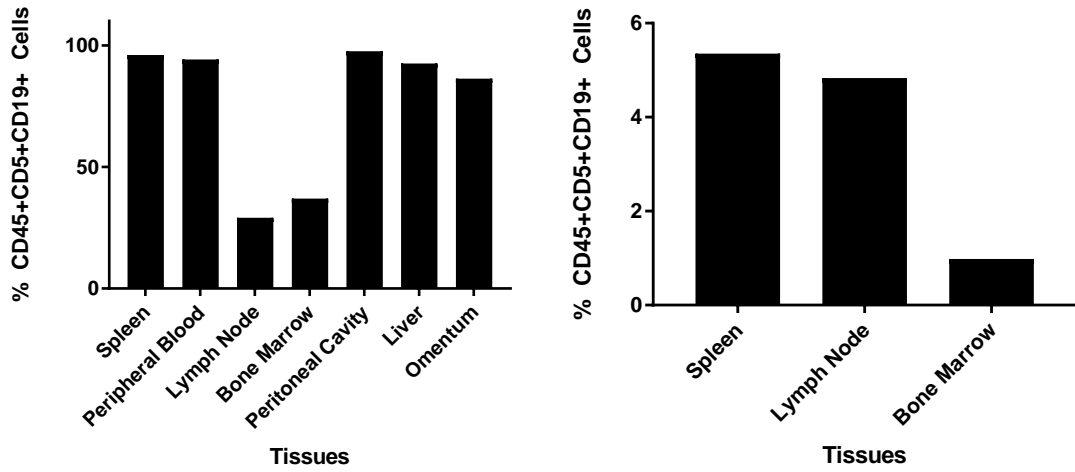
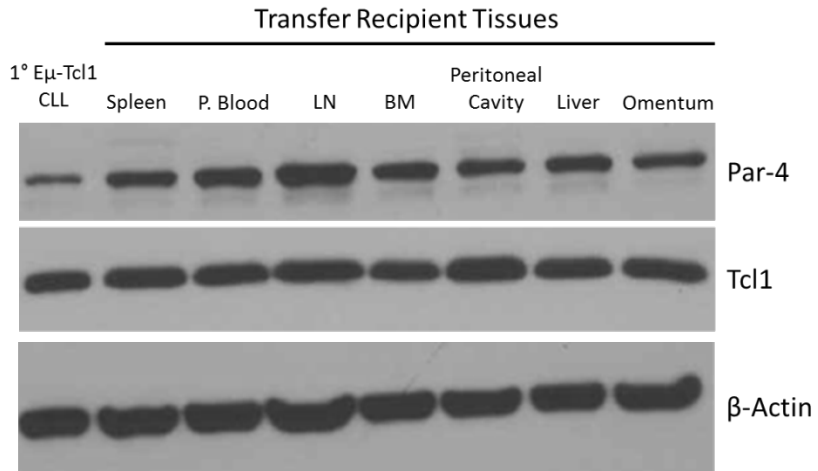


Figure 3.3D



### Figure 3.3 Expression of Par-4 in Adoptive Transfer Mouse Model of CLL

10 x10<sup>6</sup> E $\mu$ Tcl1 CLL cells were injected into C57BL/6 recipient mice which were monitored by regular submandibular bleeding. A) Representative spleen sizes of C57BL/6, E $\mu$ -Tcl1, and adoptive transfer recipient after development of CLL. Total viable cell numbers were calculated by hemacytomter using trypan blue exclusion and cells were stained for CD5, CD19 or IgM and gated on CD45 positivity. B) Representative growth of CLL in adoptive transfer recipients (n=4) measured through peripheral blood staining of CD5+CD19+ cells gated on CD45 compared to PBS-injected C57BL/6 mice (n=2). Points represent mean  $\pm$  SEM. C) Percent CD45+CD5+CD19+ cells in the tissues of adoptive transfer recipient mice 48 days post injection (Right) compared to normal C57BL/6 mouse tissues (Left). D) Immunoblot analysis of Par-4 expression in tissues of adoptive transfer recipient mice 48 days post injection compared to the primary E $\mu$ -Tcl1 CLL cells.

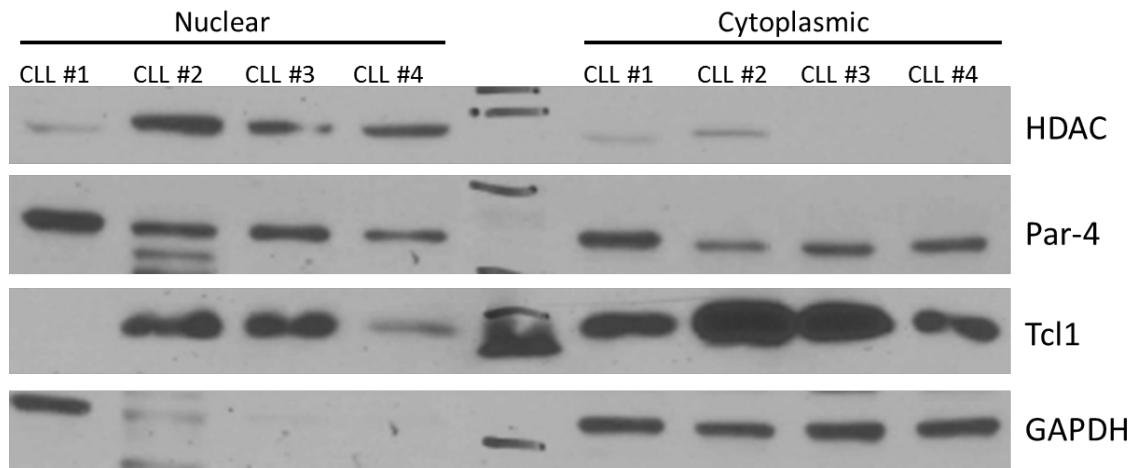


Table 6: Comparison of WT, E $\mu$ -Tcl1, and Adoptive Transfer recipient spleens.

	Normal Spleen (10 mo)	E $\mu$ -Tcl1 Spleen (14.2 mo)	10 week Adoptive Transfer Spleen
IgM+	43.27	77.25	72.18
CD5+	64.73	82.79	89.64
CD5+/IgM+	30.36	76.7	70.45
CD5+/IgM-	34.37	6.09	19.19
CD5-/IgM+	12.92	0.55	1.81
CD11b+	30.65	7.59	7.87
CD11b+/Ly6G+	17.89	4.98	4.16
F4/80+	5.17	6.06	1.18
CD138+	10.02	10.54	0.26
CD138+/IgG+	3.13	0.29	0.09
CD138+/IgG-	6.89	11.15	0.17
IgG+	15.19	0.39	0.53
B220+/IgG+	1.24	0.38	0.48
B220+/IgG-	47.73	76.02	53.34
IgD+	33.64	3.67	2.53
IgM+/IgD-	24.93	83.42	69.91
IgM+/IgD+	31.96	3.14	2.27
IgM-/IgD+	1.68	0.53	0.26
CD4+	10.14	1.68	6.76
CD8+	12.82	1.49	8.94
CD4+/CD8+	0.45	0.54	4.49

Whole spleens were crushed and stained for immune cell markers and analyzed by flow cytometry. Values represent percentage of cells in each population of total viable spleen cells.

**Figure 3.4A**



**Figure 3.4B**

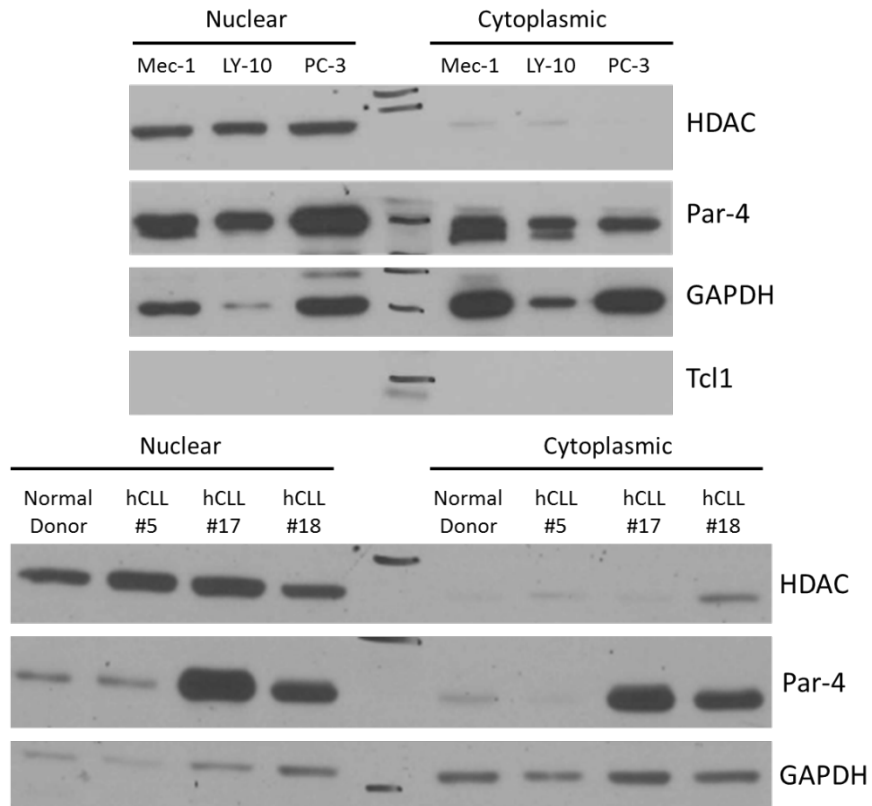


**Figure 3.4C**

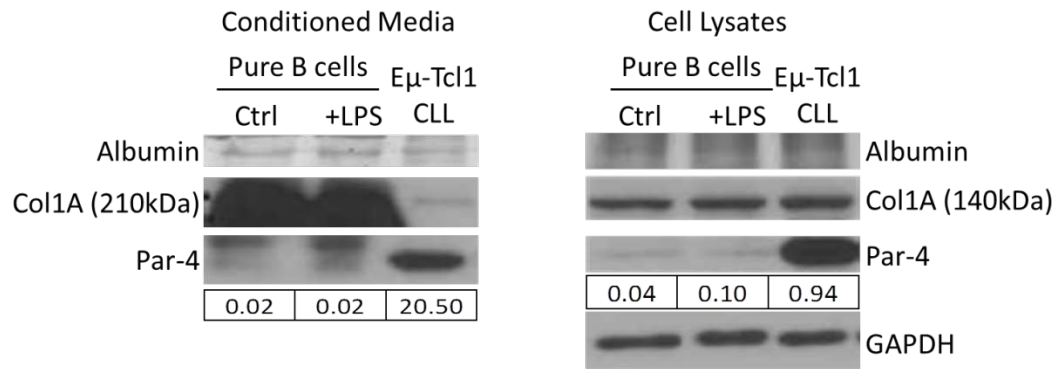


**Figure 3.4D**

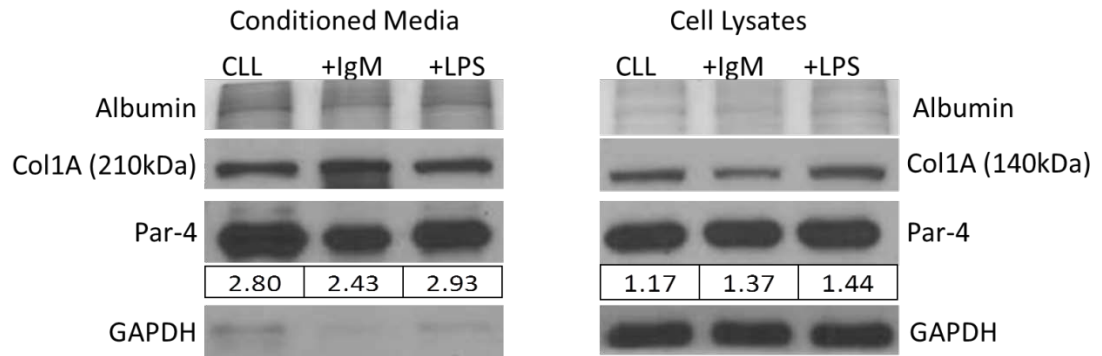


**Figure 3.4E**

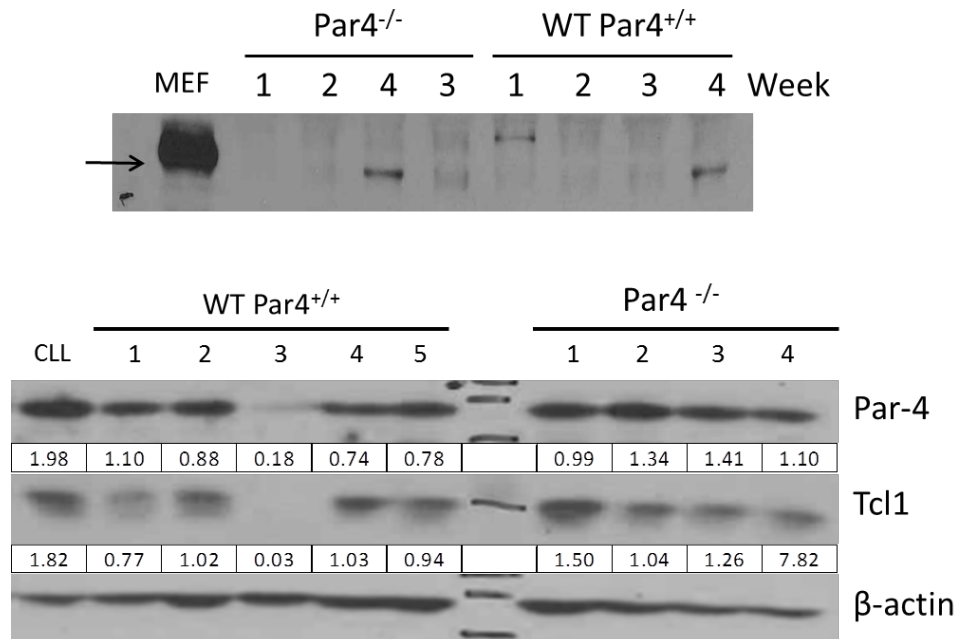


**Figure 3.4F**

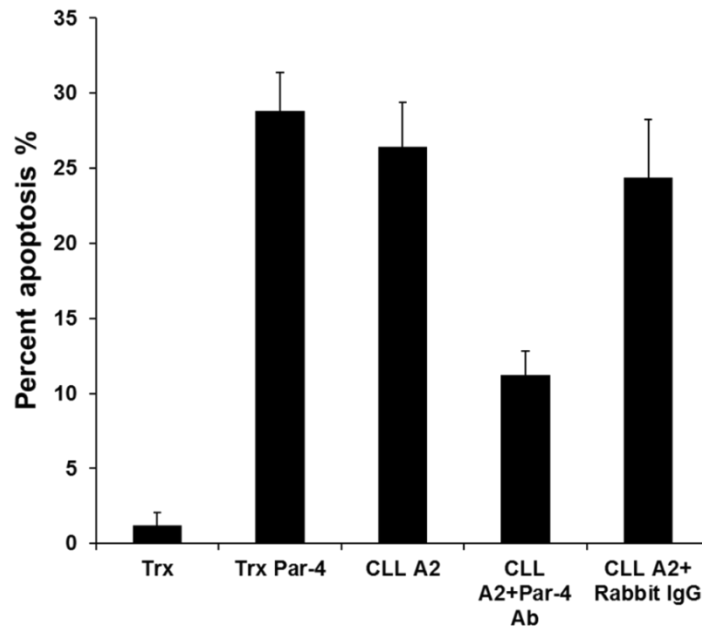


**Figure 3.4G**

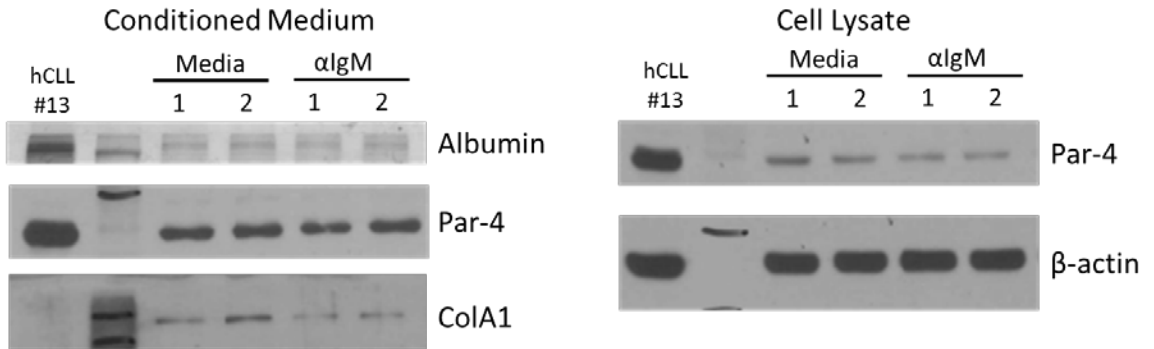


**Figure 3.4H**

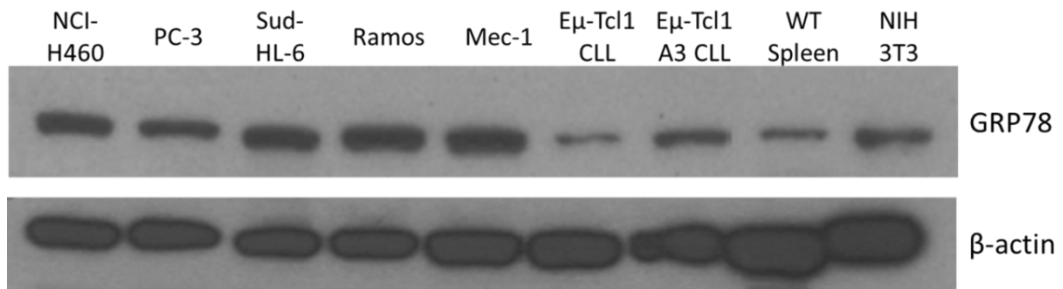


Figure 3.4 Par-4 translocates to the nucleus, is secreted from CLL cells and is functional in inducing apoptosis

A) Nuclear and cytoplasmic compartments were isolated from multiple primary E $\mu$ -Tcl1 CLL spleens, separated by SDS page, transferred to PVDF membrane and probed for Par-4, Tcl1, HDAC, and GAPDH. Lane 5 is the protein ladder control marker. B) Nuclear and cytoplasmic compartments were isolated from Mec-1, LY-10, and PC-3 CLL cell lines and Par-4 expression was analyzed by immunoblot (top). None of these cell lines express Tcl1. Lane 4 is the protein ladder marker. Primary human CLL nuclear and cytoplasmic fractions were probed for Par-4 (bottom). Lane 5 is the protein ladder marker. C) Conditioned medium (CM) was collected and concentrated from WT splenic B cells alone or stimulated with 5 $\mu$ g/ml LPS and E $\mu$ -Tcl1 CLL cells. CM and total protein lysate from the cells were analyzed by immunoblot analysis for Par-4, albumin, collagen 1A1, and GAPDH. D) E $\mu$ -Tcl1 CLL cells were cultured with or without 25 $\mu$ g/ml  $\alpha$ lgM or 5 $\mu$ g/ml LPS for 12hrs and CM was collected, concentrated, and separated by SDS-Page, and analyzed by immunoblot. CM Par-4 is normalized to Collagen 1A1 (Col1A1), a known secreted protein, and Par-4 in the total cell lysate was normalized to GAPDH. E) Top: Plasma was collected each week after adoptive transfer of E $\mu$ -Tcl1 CLL cells into C56BL/6 WT mice and Par4<sup>-/-</sup> animals. Plasma was diluted in 4X sample buffer and analyzed by immunoblot analysis for Par-4. Mouse Embryonic Fibroblasts (MEFs) were used as positive control of Par-4. Week 4 sample for Par4<sup>-/-</sup> plasma proteins are before week 3 due to loading error. Bottom: After 4 weeks of growth, spleens were collected from WT and Par4<sup>-/-</sup> animals injected with CLL cells and lysates were analyzed by immunoblot for Par-4 and Tcl1. Each lane represents one mouse. Par4<sup>+/+</sup> recipient #3 did not develop CLL. Densitometry values are normalized to  $\beta$ -actin. F) 400 $\mu$ l of conditioned medium from E $\mu$ -Tcl1 CLL cells was applied to H460 lung cancer cell line. H460 cells were treated with control recombinant protein 100nM thioredoxin (Trx), 100nM recombinant TRX Par-4

fusion protein, CLL CM, CLL CM with anti-Par-4 antibody, and isotype antibody for controls. Apoptosis was measured by immunocytochemistry and DAPI morphology. Results are presented as mean  $\pm$  SEM of triplicate determinations. G) Conditioned medium (CM) was collected and concentrated from human peripheral blood CLL cells alone or stimulated with 25 $\mu$ g/ml  $\alpha$ IgM. CM and total protein lysate from the cells were analyzed by immunoblots which were probed for Par-4. Lanes 1 and 2 represent duplicate samples. H) GRP78 expression in lysates from indicated cell lines, de novo and adoptive transfer E $\mu$ -Tcl1 CLL cells was determined by immunoblot analysis. The blots were probed for  $\beta$ -actin as loading control.

## Summary

Originally we initiated this study to define the tumor suppressive role of Par-4 in CLL, but made a surprising and exciting discovery that Par-4 is upregulated in both mouse and human CLL cells. CLL is classified by CD5 and CD19 positivity so it is important to compare these cells to the correct controls. Mouse B1a cells express both CD5 and CD19 making this subset of B cells a likely comparison as suggested by many other groups [93, 249]. CLL cells overexpress Par-4 compared to normal B cells and the increased expression is not related to the increased expression of the Tcl1 oncogene or the type of B cell subset. CLL cells and B1 cells express CD5 on the surface of their cells. In normal B1 cells, CD5 is thought to mitigate signaling through the BCR to prevent activation from weak signals. We did not investigate if increased Par-4 expression is related to CD5 expression in B cells but is unlikely as the human Mec-1 CLL cells also shows high levels of Par-4 but lack CD5 expression.

Our findings are consistent with studies presented by Boehrer and colleagues in that most CLL samples have detectable Par-4 protein levels [190]. We also find detectable levels of Par-4 mRNA in both mouse and human CLL samples. Our studies also showed that Par-4 in CLL is able to translocate to the nucleus of CLL cells and is secreted. Further examination of the Par-4 protein must be done to determine if it is phosphorylated at the Thr155/163 residue which is required for the known pro-apoptotic functions of Par-4 [169].

The ability of CLL cells to secrete Par-4 *in vitro* and *in vivo* is an interesting finding and begs the question of what cells in the microenvironment are sensitive to Par-4 mediated apoptosis. We show that CLL cells secrete Par-4 *in vivo* as detected in the plasma of Par-4 deficient mice injected with E $\mu$ -Tcl1 CLL cells containing Par-4. We surmise that CLL secreted Par-4 is not inducing an autocrine or paracrine apoptotic effect to other CLL cells as the tumor burden continues to grow similarly in wild type and Par4<sup>-/-</sup> recipients injected with CLL cells.



GRP78 expression is found to be slightly lower in CLL cells compared to other tumor cell lines and could be the reason CLL cells are not sensitive to Par-4 mediated apoptosis. Additional studies examining the location of GRP78 on CLL cells must be done to confirm this hypothesis.

## CHAPTER 4

### **Novel Regulation of Par-4 through BCR signaling in CLL**

Although Par-4 is synthesized in many tumor cells, mechanisms that regulate its expression have not been described thus far. Additionally, the function of Par-4 in normal cell homeostasis has not been investigated as the majority of its effector functions have been defined in cancer cells. Par-4 has been found to interact and bind to multiple proteins such as PKC $\zeta$  [163], WT1 [162], Akt [170], topoisomerase (TOP1) [182] and is downstream of ZIPK [198, 203] and Caspase-3 activation [196]. As shown in Chapter 3, CLL cells express high Par-4 levels compared to normal B cells, leading us to investigate its regulation. Since CLL cells have been shown to have elevated tonic BCR signaling [136, 227], we tested the hypothesis that Par-4 expression may be regulated by BCR signaling. The BCR pathway is required for the survival of both normal and malignant B cells despite their oncogenic activation, making it a therapeutic target in B cell malignancies [36, 99, 136]. Kinase inhibitors targeting SFK [250], Syk [124], BTK [127], and PI3K [130] have all been proven effective in the treatment of CLL as each inhibits required downstream survival signals. Anti-CD20 monoclonal antibodies such as rituximab have also been proven efficient with combination of other chemotherapies [251]. We utilized FDA approved therapies to target BCR signaling and examined the effects on Par-4 expression. Studies in this chapter resulted in a surprising finding that inhibition of the BCR survival pathway in CLL cells led to reduced Par-4 expression.

## **Results**

### *4a) Constitutive BCR signaling in CLL cells*

We first verified that E $\mu$ Tcl1 CLL cells have increased tonic BCR signaling by comparing p-SFK levels in CLL to those in various normal B-cell subsets. Surprisingly such a comparison, especially to normal B-1 cell subset has not been performed thus far either in human or mouse. As shown in Figure 4.1A, E $\mu$ Tcl1 cells indeed have increased p-SFK compared to both B-2 as well as B-1 cell subset in the WT and young E $\mu$ -Tcl1 mice. Additionally, mouse CLL cells express greater than two fold more total Lyn protein compared to other B cell subsets. We also observed high levels of activated SFK in human CLL samples but could not detect a significant difference compared to normal whole blood cells (Figure 4.1B). This could be because peripheral blood cells from healthy adults have very few B cells (5-10%) but a large majority of T cells (70-80%). T cells do have activated SFKs, which contributes to the SFK band seen in the normal whole peripheral blood cells [252]. There are very few T cells in the blood of CLL patients with the activated SFK coming primarily from neoplastic B cells.

### *4b) BCR inhibition leads to decreased Par-4 expression in mouse and human CLL cells*

CLL cells have increased BCR signaling and elevated Par-4 expression; therefore we hypothesized that kinases involved in the BCR signaling pathway may regulate Par-4 expression (Figure 4.2A). Treatment with dasatinib (SFK inhibitor), fostamatinib (SYK inhibitor), and ibrutinib (BTK inhibitor) all led to a decrease in E $\mu$ Tcl1 CLL survival measured through the MTT assay (Figure 4.2B). We additionally confirmed that these inhibitors were effective in reducing the survival of human CLL cells (Figure 4.2C). Immunoblot analysis shows that E $\mu$ -Tcl1 CLL cells treated with each kinase inhibitor led to reduced activation of its respective target (Figure 4.2D-F). In agreement with our hypothesis, this inhibition was accompanied by a decrease in Par-4

protein expression. We also observed decreased Par-4 mRNA levels after SFK and BTK inhibition, suggesting regulation at the transcript level (Figure 4.2G). Par-4 protein down regulation was replicated in primary human CLL samples after treatment with Dasatinib and Fostamatinib indicating that this is not just a mouse phenomenon (Figure 4.2H). Although the kinase inhibitors decrease CLL viability in 48 hour MTT assays, at 12-24 hours, when decrease in Par-4 levels could clearly be seen with the BCR signaling inhibitors, the cell viability was still 70-80%. Hence the decrease in Par-4 protein levels is unlikely due to nonspecific cell death.

#### *4c) Lyn knockdown in CLL cells results in decreased Par-4 expression*

We have observed that inhibition of BCR signaling in both mouse and human CLL cells results in a novel downregulation of Par-4 expression at the protein and mRNA levels. As mentioned before, primary CLL cells spontaneously undergo apoptosis in culture, making it difficult to study mechanisms of regulation. Therefore, we utilized the human CLL cell lines, Mec-1 and OSU-CLL for our studies. We first confirmed that these human cell lines were sensitive to BCR signaling inhibition by treating cells with Dasatinib. Both Mec-1 and OSU-CLL cells responded similarly to both primary mouse as well as human CLL cells (Figure 4.3A). The cell lines were slightly less sensitive to drug treatment compared to primary cells, which could be due to the background apoptosis occurring in primary CLL samples. Treatment of Mec-1 CLL cell line with Dasatinib also reduced the activity of SFKs compared to total Lyn expression and furthermore reduced Par-4 protein and mRNA expression (Figure 4.3B). Due to potential off target effects with kinase inhibitors, we also used lentiviral mediated shRNA to target Lyn, as it has been found to be important in the survival of B-CLL cells and required for BCR signaling [104, 106, 109]. Our first experiment led to a 60% knockdown of Lyn in the Mec-1 cell line and 50% knockdown of Par-4 (Figure 4.3C, Left). We repeated our experiment and attained a 50% knockdown of Lyn expression and a further reduction in Par-4 protein and mRNA expression

(Figure 4.3C, Right). We also observed similar results in the diffuse large B cell lymphoma cell line, LY-3, confirming that Lyn inhibition led to decreased Par-4 expression (Figure 4.3D).

We designed CRISPR-Cas9 constructs with guide RNAs targeting different SFKs expressed in the Mec-1 cell line, cloned them into lentivirus, and infected the cells with these viruses to knockout Lyn, Fgr, and Lck. Initial screening appeared to result in promising knockdowns of these particular Src family kinases, but complete knockout was not achieved. Attempts to single cell clone the knockouts were also made, but unfortunately, selection with puromycin did not yield productive results. The initial knockdown of Lyn in the Mec-1 cells with the CRISPR construct did reproduce the results with shRNA mediated knockdown that led to a decrease in Par-4 expression (Figure 4.3E). Interestingly, at day 8 of puromycin selection, Fgr levels were reduced by 72% which was maintained by day 13. Par-4 levels were down at day 8 but started to return by day 13. It is conceivable Fgr knockdown cells upregulate other SFKs such as Lyn that may rescue Par-4 expression. The trend was similar for Lck but less obvious (Figure 4.3F). This may suggest that Lyn, the primary SFK in B cells, is able to compensate for loss of the other SFKs or that other SFK members are not involved in Par-4 regulation.

For more specific targeting of BCR signaling, we used siRNA targeting CD79a (Ig $\alpha$ ), the molecule required for BCR expression on the cell surface and downstream signaling in B cells [36]. Inhibiting Ig $\alpha$  expression prevents activation of non-receptor tyrosine kinases required for BCR signaling and eliminates any pleiotropic effects of kinase inhibition with small molecules. We observed a dramatic decrease in Par-4 expression with Ig $\alpha$  silencing further confirming a novel regulation of Par-4 through BCR signaling in one patient sample (Figure 4.3G, left). In another patient sample, CD79a was difficult to detect, but we observed a slight down regulation of Par-4 after silencing (Figure 4.3G, right).

ERK signaling has been well defined to be critical for B cell development and proliferation downstream of the BCR activation and has also been well studied to be a therapeutic target in many cancers [132-134]. Because of its significance in B cell survival, we inhibited ERK1/2 with SCH772984, a well characterized ERK2 inhibitor. There was a decrease in Par-4 protein expression upon inhibition of ERK1/2 (Figure 4.3H)[253]. Interestingly, we did not see a decrease in Par-4 expression in PC-3 cells after ERK inhibition suggesting that Par-4 is downstream of a survival and proliferation pathway important in malignant B cells but not in epithelial cancers such as prostate cancer.

**Figure 4.1A**

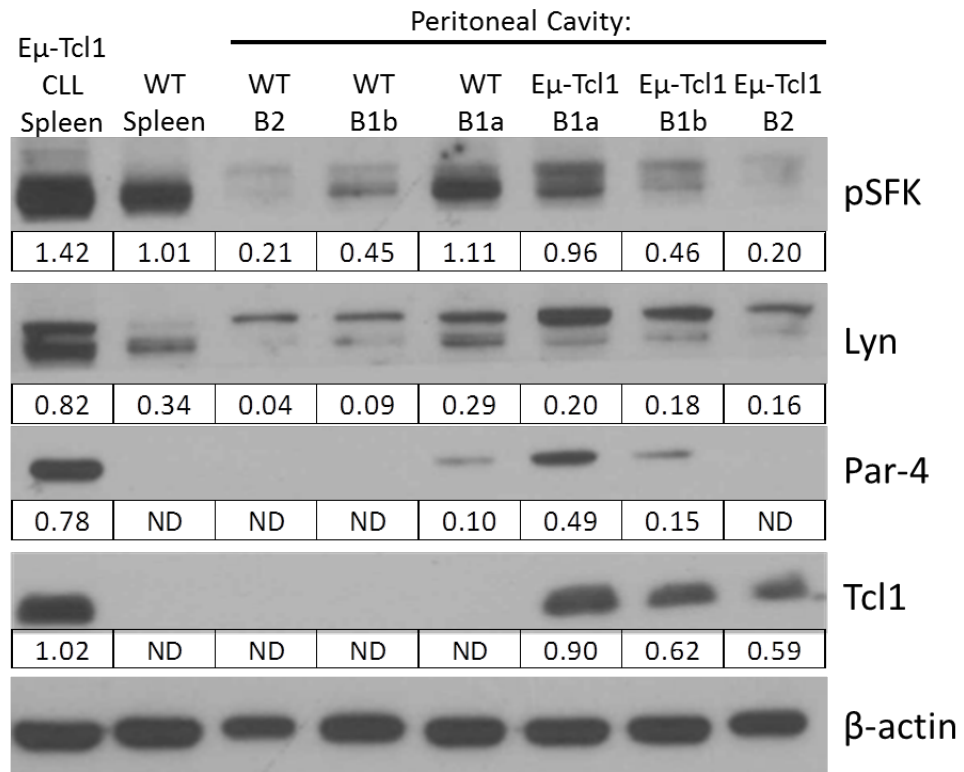


**Figure 4.1B**

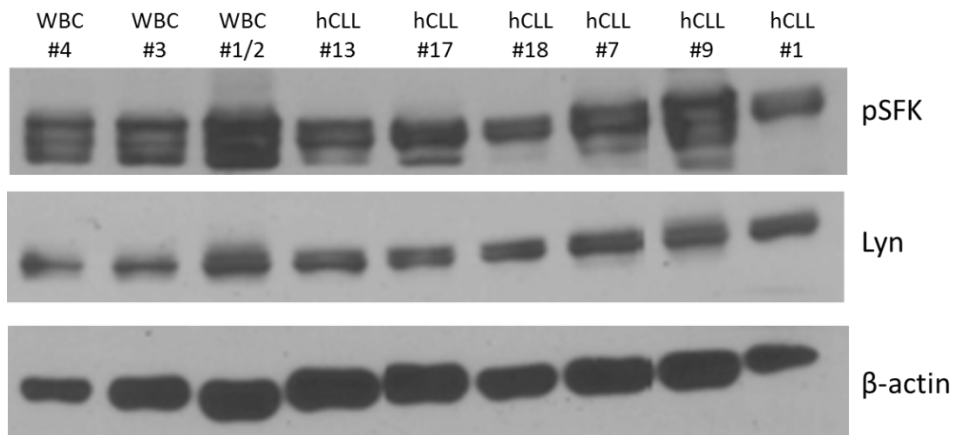


Figure 4.1 Constitutive BCR signaling in CLL cells

A) Immunoblot analysis of peritoneal cavity B cell subsets, E $\mu$ -Tcl1 CLL spleen cells, and WT isolated B2 spleen cells probed for pSFK and total Lyn. pSFK levels are normalized to total Lyn expression. Lyn, Par-4, and Tcl1 densitometry values are normalized to  $\beta$ -actin. B) Immunoblot analysis of activated SFK and total Lyn protein levels in primary hCLL samples compared to Ficoll purified peripheral blood lymphocyte lysate of four different normal donors (#1/2 pooled together, #3, #4). Results from one of two experiments with similar results are shown.



Figure 4.2A

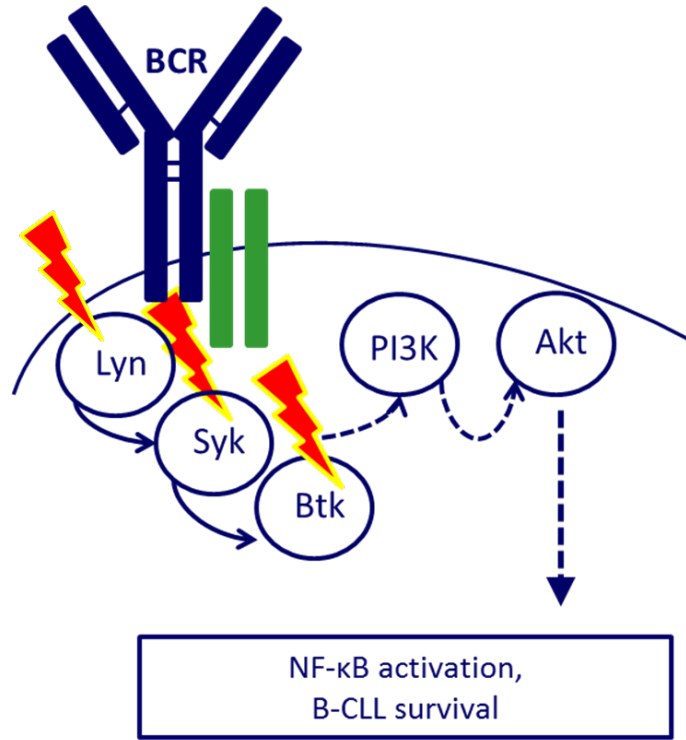


Figure 4.2B

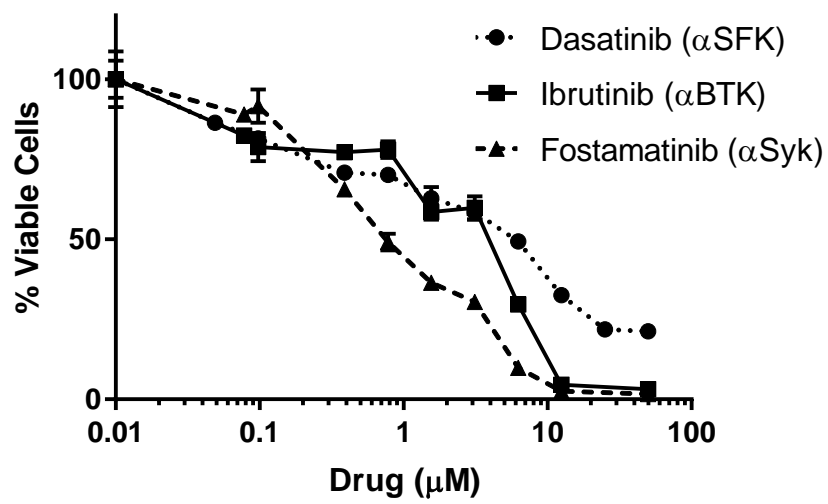


Figure 4.2C

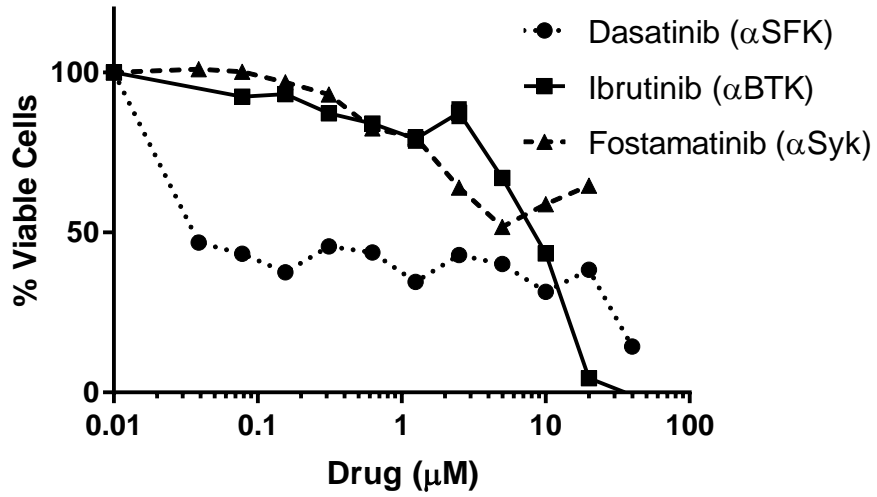
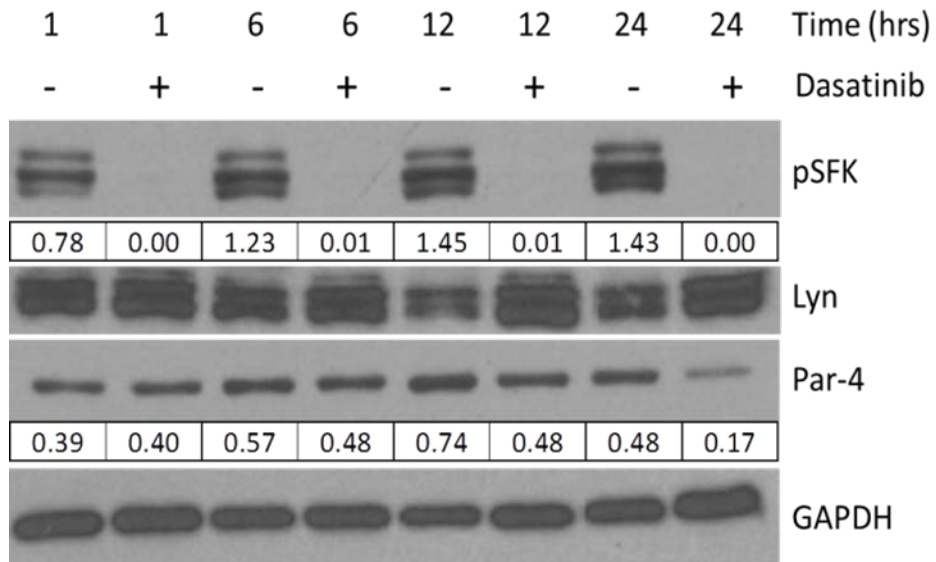
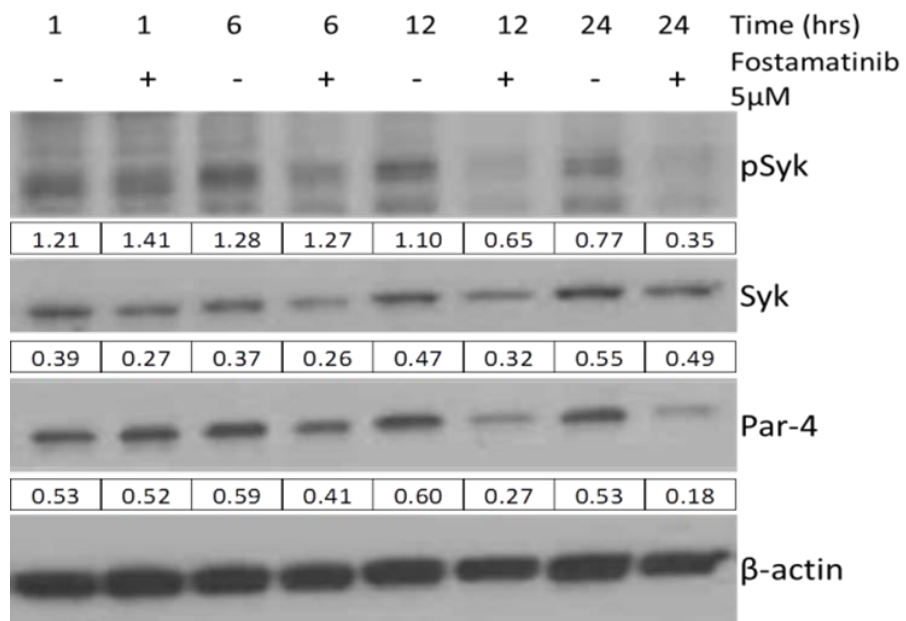


Figure 4.2D



**Figure 4.2E**



**Figure 4.2F**

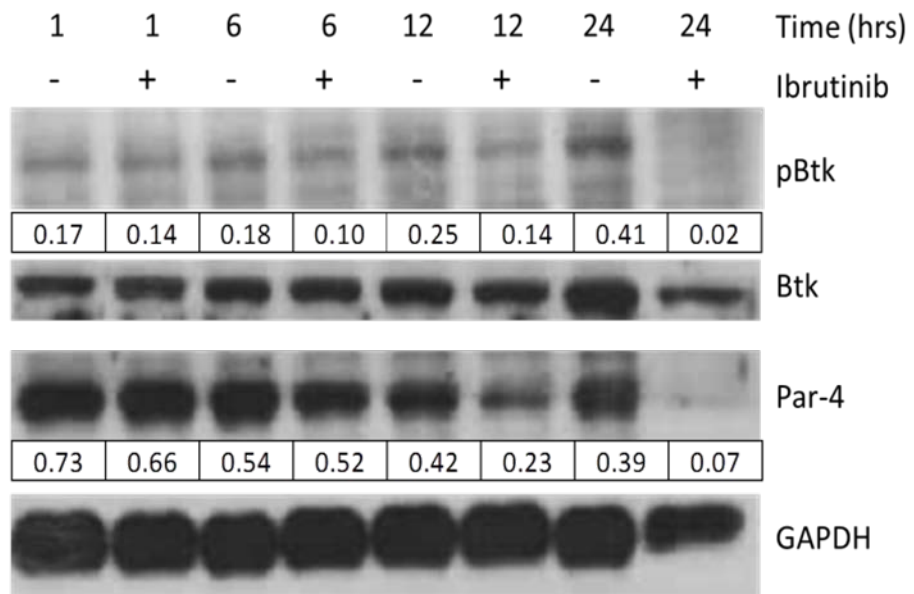


**Figure 4.2G**

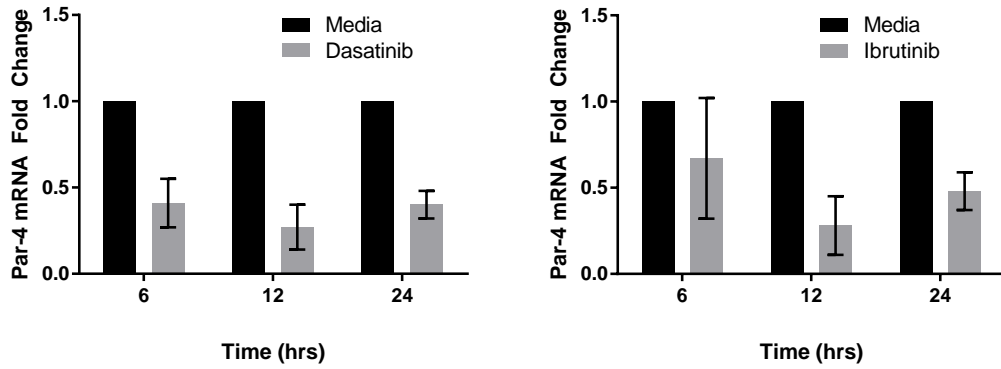


**Figure 4.2H**

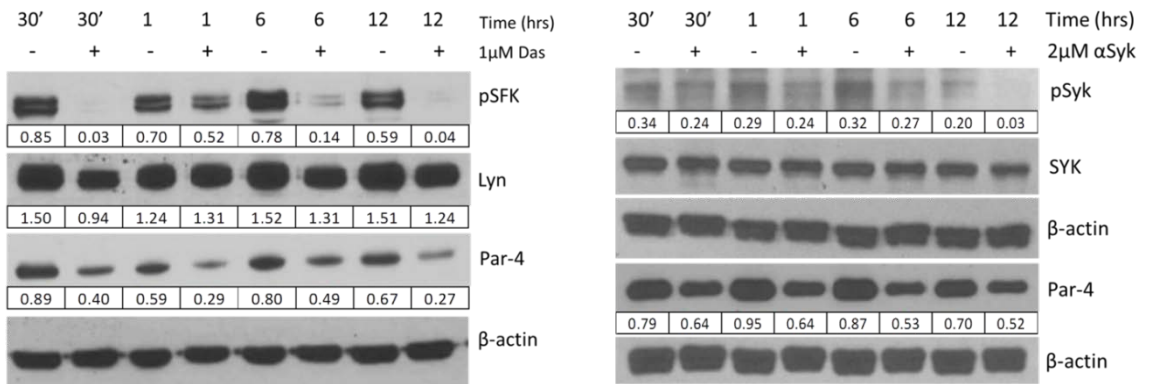


#### Figure 4.2 BCR inhibition leads to decreased Par-4 expression

A) Simplified diagram of BCR signaling indicating the kinases targeted with inhibitors: Lyn (Dasatinib), Syk (Fostamatinib), and BTK (Ibrutinib). B) E $\mu$ -Tcl1 CLL cells were treated with different concentrations of Dasatinib, Fostamatinib, or Ibrutinib for 48 hrs. Cell viability was measured through MTT Assay. Results represent an average of three experiments. C) Survival curves of human CLL cells treated with BCR signaling inhibitors. Data shown represents one of three experiments. D) Western blots of lysates of E $\mu$ -Tcl1 CLL cells treated with 1 $\mu$ M Dasatinib, E) 5 $\mu$ M Fostamatinib, and F) 5 $\mu$ M Ibrutinib. Phosphorylated SFK, P-Syk, and P-BTK were normalized to respective total proteins which were normalized to  $\beta$ -actin. G) Treatment of E $\mu$ -Tcl1 CLL cells with Dasatinib and Ibrutinib decreases Par-4 mRNA as measured by qRT-PCR. Par-4 mRNA is normalized to mouse 18S mRNA expression. H) Primary human peripheral blood B-CLL cells (97.7% CD5+CD19+) cells were treated with 1 $\mu$ M Dasatinib (left) and 2 $\mu$ M Fostamatinib (right). Phosphorylated SFK and Syk bands were normalized to total proteins respectively. Total Lyn, Syk and Par-4 were normalized to  $\beta$ -actin. Results are representative of at least two experiments.

Figure 4.3A

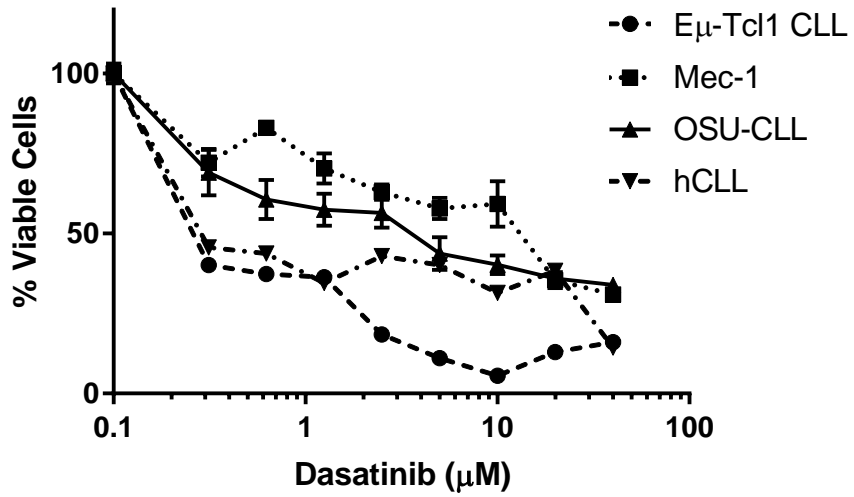
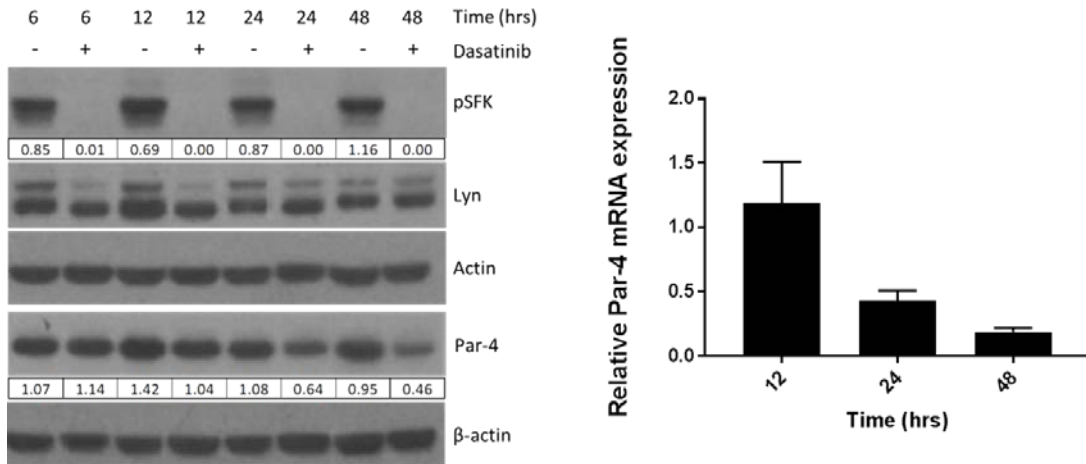
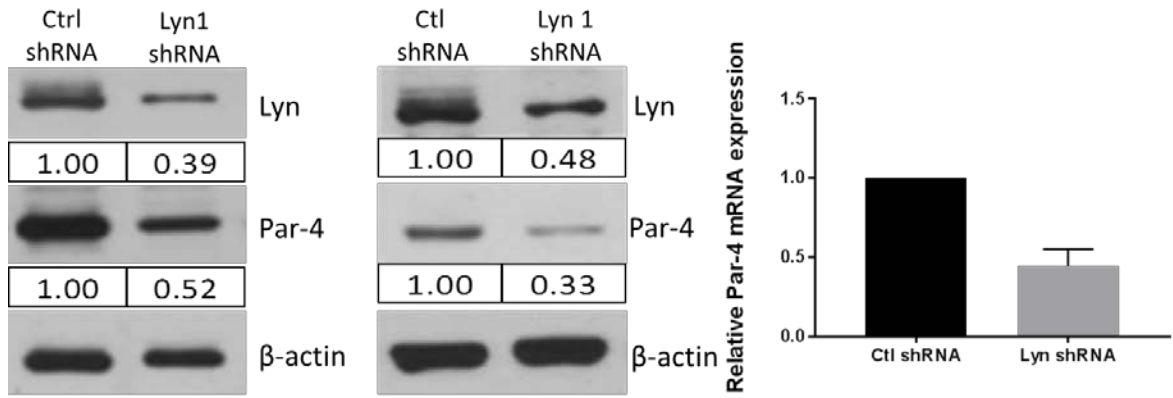


Figure 4.3B



**Figure 4.3C**



**Figure 4.3D**

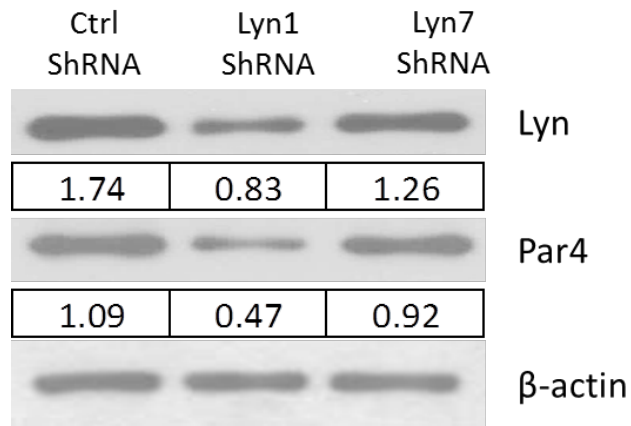


**Figure 4.3E**

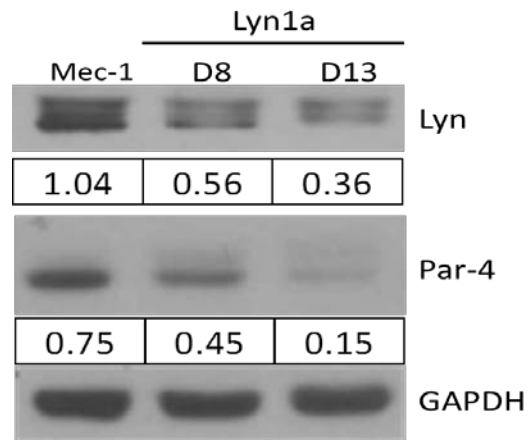


**Figure 4.3F**

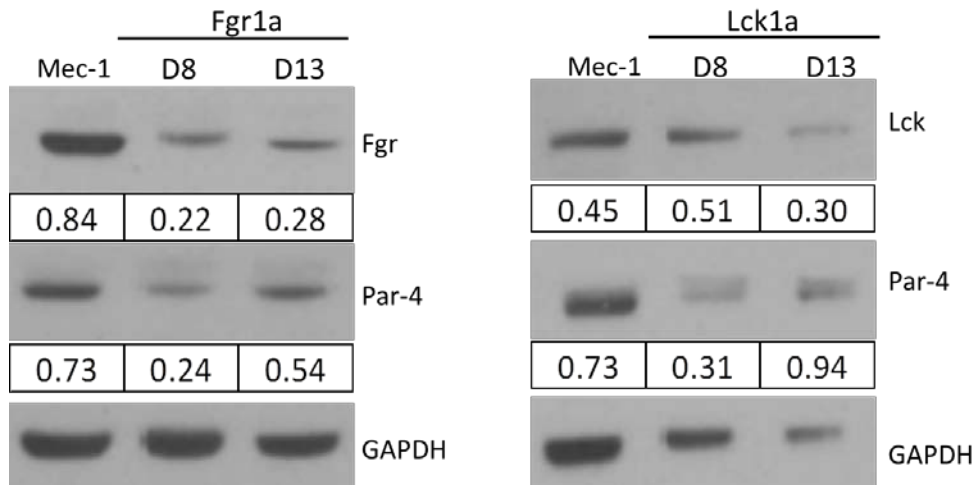




**Figure 4.3G**

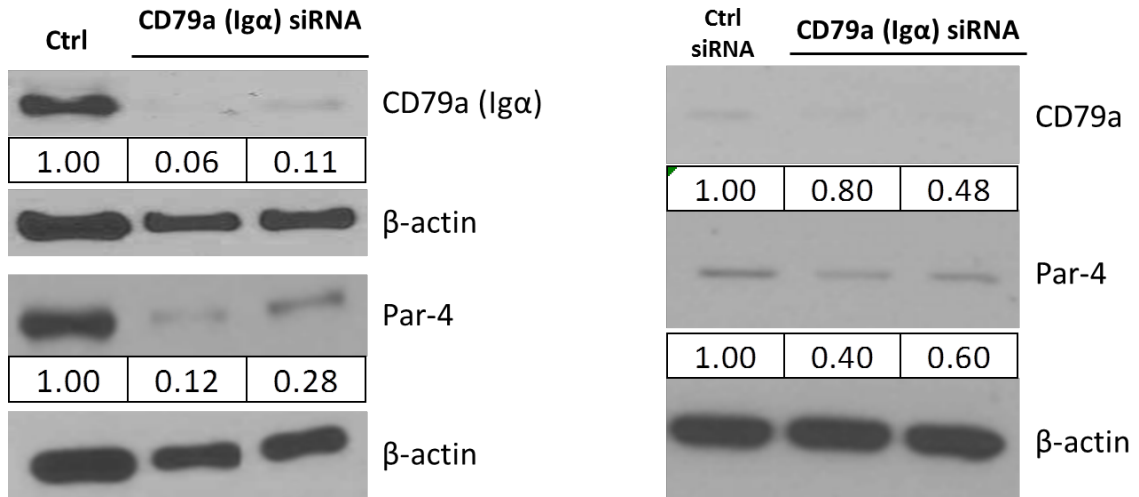


**Figure 4.3H**

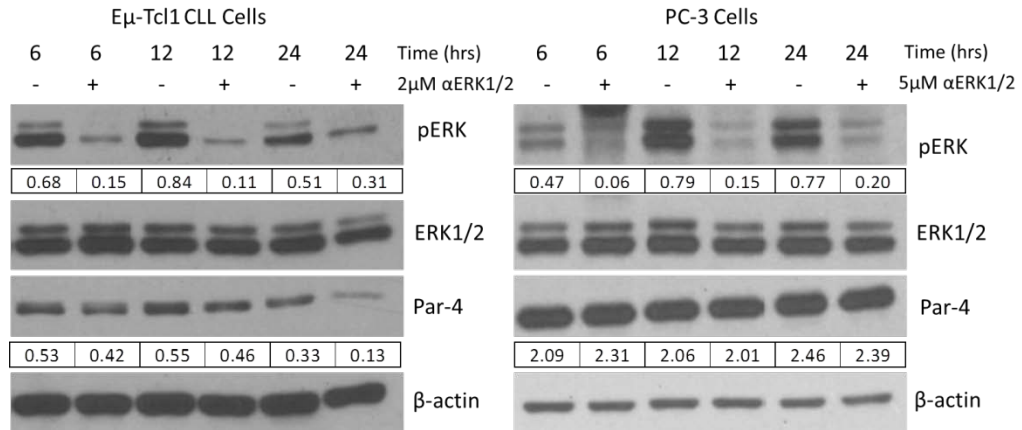


Figure 4.3 Specific knockdown of Lyn leads to reduced expression of Par-4 in CLL cell lines

A) E $\mu$ -Tcl1 CLL cells, two human CLL cell lines (Mec-1, OSU-CLL), and primary human B-CLL cells were treated with different concentrations of Dasatinib for 48hrs and viability was measured by MTT assay. Values represent mean  $\pm$ SE of triplicate cultures. Results represent a minimum of three experiments. B) Mec-1 CLL cell line was treated with Dasatinib (10 $\mu$ M) and for different time points. Total protein and mRNA were isolated. Levels of phosphorylated SFK and total Par-4 protein expression were analyzed by immunoblot analysis (left) and mRNA measured through qRT-PCR (right). mRNA values represent mean  $\pm$ SE in triplicates normalized to human 18s. C) Mec-1 CLL cell line was infected with control or Lyn specific shRNA lentivirus and selected for puromycin resistance. Viable cells were collected at Day 13 (Left, Experiment 1) and Day 17 (Middle, Experiment 2) and total protein and RNA was isolated. Left panel represents immunoblot analysis of Lyn protein. Right panel shows levels of Par-4 mRNA expression measured by qRT-PCR. D) Lentiviral mediated shRNA knockdown of Lyn on Par-4 expression in LY-3 lymphoma cell line. Western blot of lysates of control and Lyn shRNA treated cells probed for Lyn, Par-4 and  $\beta$ -actin is shown. (Provided by Dr. Sunil Noothi) E) Lyn targeting guide RNA was cloned into lentiviral plasmid (Lenti-CRISPR V2) containing CRISPR/Cas9 and puromycin resistance gene. Lentivirus was grown in HEK 293T cells. Mec-1 cells were infected with the lentivirus expressing Lyn specific guide RNAs and selected with puromycin. Lysates of puromycin resistant cells collected at day 8 or 13 after infection were analyzed by western blot to determine the degree of Lyn knockdown and Par-4 levels. F) Lentiviruses expressing CRISPR/Cas9 and guide RNAs targeting Fgr and Lck were used to infect Mec-1 cells. Lysates of puromycin resistant cells were analyzed by Western blots which were probed for target SFK and Par-4. Densitometry values were normalized to GAPDH. G) Human CLL cells were electroporated with CD79a siRNA and incubated for 24hrs. Different voltages were used for electroporation,

middle lane: 220mV, right lane: 250mV. Ctl siRNA voltage was 220mV. (Left: hCLL p#10, Right: hCLL p#15). Total protein was analyzed by SDS-PAGE and Western blots, which were probed for CD79a and Par-4. H) Par-4 expression is regulated through ERK signaling in E $\mu$ -Tcl1CLL cells but not PC-3 cancer cells. Western blots of lysates of E $\mu$ -Tcl1 CLL cells and PC-3 prostate cancer cells treated with ERK1/2 inhibitor, SCH772984, were probed for p-Erk, ERK1/2 and Par-4. pERK levels are normalized to total ERK1/2 and Actin. Par-4 protein expression is normalized to Actin. Blots represent one of three experiments.

## Summary

Our initial finding that CLL cells overexpress Par-4 compared to normal B cells led us to investigate how Par-4 might be regulated in this cancer. Due to the well-known activity of BCR signaling in CLL, we first focused on this pathway. Treatment of mouse and human primary CLL cells with inhibitors to SFKs, Syk, and BTK, led to reduced cell survival and a decrease in Par-4 expression. It is interesting to note that Par-4 down regulation is not seen until after 6hrs of treatment with BCR inhibitors with the greatest decrease in Par-4 expression at 12+hrs. Because Par-4 has been shown to interact with many different proteins such as Akt, PKC $\zeta$ , WT-1 and others, these proteins could be providing stability after cytotoxic agents until a threshold is met leading to Par-4 degradation. We and others saw reduced Akt activity and total protein after dasatinib treatment in CLL [254] suggesting that a decrease in Akt may not be responsible for immediate down regulation of Par-4 after BCR inhibition since Akt phosphorylation destabilizes Par-4. We have not investigated if PKC $\zeta$  or WT-1 are affected after BCR inhibition in CLL. Since much of the currently known regulation of Par-4 is through post-translational interactions, there could be other proteins that are bound to Par-4. Structural studies focusing on the regulatory interaction of Par-4 indicate that heterodimer interactions through the leucine zipper domain of Par-4 mediate more stable interactions [255]. Ternary structures and heterodimers of Par-4 could be responsible for the increased stability of Par-4 in B-CLL cells. One study proposed that Par-4 is involved in a ternary complex with PKC $\zeta$  and p62 to regulate NF- $\kappa$ B activation [256]. p62 is also known as the sequestosome (SQSTM1) which is important in autophagy and regulates transport of proteins between the nucleus and cytoplasm for proteasomal degradation [257]. Par-4 is known to inhibit NF- $\kappa$ B by blocking the activity of PKC $\zeta$ , but p62 has been found to antagonize this effect and prevent Par-4 mediated inhibition [256]. Dasatinib treatment has been found to result in autophagy-mediated cell death in ovarian cancer [258] and acute

myeloid leukemia [259], and therefore, could increase activation of autophagy initially that leads to increased p62 expression and further stability of Par-4 in CLL. Studies to confirm increase in LC3 lipidation after dasatinib treatment and measuring p62 levels must be done to validate this complex hypothesis but could explain why we do not see decreased Par-4 levels until later time points after BCR inhibition.

Par-4 is also known to be a target of caspase-3 activation and since BCR inhibitor treatment results in cell death, we questioned if down regulation of Par-4 is only through caspase-3 cleavage [196]. Our studies with Par-4 down regulation after specific Lyn shRNA knockdown in stably growing cells make this an unlikely possibility. We also observe Par-4 down regulation after Ig $\alpha$  silencing which leads us to suggest that BCR signaling inhibition through kinase inhibitors must activate other pathways that could result in Par-4 stabilization as discussed above.

This novel finding of Par-4 regulation by BCR signaling needs to be studied further to define the mechanisms of this control. Par-4 protein and mRNA levels are reduced after BCR signaling inhibition suggesting that Par-4 may be regulated at the transcriptional level in CLL. Assays to transfect Mec-1 CLL cell line with Par-4-Luc promoter were attempted to see if BCR inhibition led to reduced luciferase activity. Unfortunately, CLL cells were difficult to transfect and we were not successful in definitively answering the question. Preliminary findings showed that luciferase activity was slightly reduced after BCR inhibition treatment with dasatinib, but were not statistically significant. There was success in infecting Mec-1 cells with lentivirus carrying shRNA that targeted Lyn kinase. Down regulation of Lyn resulted in decreased Par-4 expression at both the protein and mRNA levels. Results targeting Ig $\alpha$  confirmed that Par-4 is downstream of BCR activation and regulated through this signaling pathway. Additional studies investigating the levels of Par-4 after ERK inhibition in CLL cells showed that Par-4 is further

downstream of the BCR signaling cascade. This result provides evidence that a well-defined survival signaling pathway is regulating the expression of Par-4 specifically in B cells since we did not see down regulation of Par-4 after ERK inhibition in PC-3 cells. Studies in Ras-transformed fibroblasts that expressed constitutively active ERK2 showed a decrease in Par-4 expression which is the opposite of what we observe in CLL cells [181]. While ERK1/2 are activated in PC-3 cells, we may not see an effect on Par-4 due to increased signaling upstream of ERK1/2 in PC-3 cells. Protein kinase c-alpha (PKC $\alpha$ ) and EGFR (epidermal growth factor receptor) signaling have both been found responsible for ERK1/2 signaling in PC-3 cells and could be masking the effect of ERK inhibition on Par-4 [260]. PKC- $\alpha$  is found to be variably expressed in CLL cells and potentially could not compensate for the inhibition of ERK1/2 signaling on Par-4 expression [261].

## CHAPTER 5

### **Novel Role of Par-4 in regulating the Growth of CLL**

We have shown that Par-4 expression is abnormal in CLL cells compared to its expression in other cancer types. Novel regulation of Par-4 expression in malignant B cells appears to be through the BCR signaling pathway. These observations have led us to question the role Par-4 in CLL. Previous studies have suggested that Par-4 regulation may be different in CLL cells as its mRNA levels did not match protein levels in patients [190]. Also, treatment of CLL cells with Imatinib led to reduced Par-4 expression and cell death [202]. Along with our findings, these two studies suggest that intrinsic Par-4 may not be playing its well-defined role as a tumor suppressor in CLL.

The original paper that identified Par-4 to be upregulated in response to calcium mobilization in prostate cancer cells also identified the entire family of prostate apoptosis response genes (Par-1, Par-3, Par-4, and Par-5) [161]. They discovered the genes involved in cell death mechanisms were divided into two components: specific apoptosis response genes (*par-4*) and genes induced by growth regulatory factors (*par-1*, *par-3*, and *par-5*). AT-3 cells (prostate carcinoma) starved from serum and then stimulated with serum resulted in an induction of *par-1*, *par-3*, and *par-5* but not *par-4*. Sells and colleagues found that Par-4 was specific to apoptosis response, but also indicated that other family members are involved in growth regulation [161].

We investigated how Par-4 may contribute to CLL pathogenesis and growth by knocking down the expression of Par-4 in the Mec-1 CLL cell line. Additionally, we crossed the E $\mu$ -Tcl1 mice to a Par4<sup>-/-</sup> animal to examine the role of Par-4 in the development of CLL. Our results lead us to hypothesize that intrinsic Par-4 is not a pro-apoptotic factor in the context of CLL but rather may be a growth factor that is a potential therapeutic target.

## **Results**

### ***5a) Knockdown of Par-4 leads to reduced CLL growth***

We sought to determine the role of Par-4 in CLL growth by knocking down Par-4 expression in the human Mec-1 CLL line. There was a decrease in Par-4 protein and mRNA levels after lentiviral shRNA mediated knockdown in Mec-1 cells (Figure 5.1A). Cell Signaling lysis buffer and RIPA buffer were used to lyse Mec-1 cells treated with control and Par-4 shRNA to confirm knockdown. Par-4 is known to inhibit Akt phosphorylation and reduce Bcl2 levels, which were increased in Par-4 knockdown Mec-1 cells, confirming specific Par-4 knockdown (Figure 5.1A) [178, 190]. We repeated the knockdown experiment and generated several clones from a single infection with two different Par-4 shRNA constructs (Figure 5.1B). After we confirmed Par-4 knockdown, we tested the importance of Par-4 for CLL growth by culturing cells with continuous puromycin selection for 14 days and counting total cell numbers to generate a growth curve with four clones of control shRNA and five clones of hPar-4 shRNA (Figure 5.1C). Surprisingly, Par-4 knockdown resulted in an overall reduction in the growth of Mec-1 cells *in vitro* (Figure 5.1D,  $p = 0.0024$ ).

Subcutaneous injection of control shRNA and Par-4 shRNA knockdown cells into left and right flanks of NSGS mice induced tumors which were followed for a period of 3 weeks, at which time they had to be euthanized as per IACUC protocol (Figure 5.1E). Par-4 knockdown Mec-1 cells grew more slowly *in vivo*, mimicking the *in vitro* results (Figure 5.1F). Injected tumors retained their knockdown of Par-4 expression *in vivo* as shown through immunoblot analysis (Figure 5.1G).

### ***5b) Par-4 knockdown leads to increased p21 expression***

The unexpected result of Par-4 knockdown reducing the growth rate of Mec-1 CLL cells (Figure 5.1) and an increase in known pro-survival and anti-apoptotic proteins of phospho-Akt



and Bcl2, led us to investigate if Par-4 knockdown affected the cell cycle in CLL cells. Interestingly, Par-4 knockdown Mec-1 cells had fewer cells entering S phase but more cells in G1 phase suggesting a halt in the G1 to S transition (Figure 5.2A). We initially probed a panel of cell cycle regulators and kinases in the Par-4 knockdown cells and made an interesting discovery that p21 expression is increased in cells with reduced Par-4 (Figure 5.2B). We did not observe significant changes in CDK1 expression, but did find a slight increase in CDK4 expression. CDK4 is found to be prominent in the G1 phase while CDK2 is active in the G1 to S phase transition followed by CDK1 which is active in G2/M phase [262]. Cell cycle analysis indicates that a greater number of Par-4 knockdown cells are present in the G1 phase supporting the increase in CDK4 expression. Slightly less CDK2 expression is consistent with the proposal that the Mec-1 cells are remaining in G1 and not able to proceed through the cell cycle. There was no significant change in p27 levels between control and Par-4 knockdown. We additionally probed for Hsp90 as many cell cycle regulators are clients of Hsp90 chaperone activity to confirm that changes are not due to cell stress. Hsp70 is an excellent indicator of loss of Hsp90 function and we did not see changes in that expression of either protein. p21 is involved in different phases of the cell cycle, but primarily works to control the transition from G1 to S [263]. Increase in p21 levels is likely to be responsible for the G1/S halt observed in Par-4 knockdown cells. Clones generated from a second shRNA infection reproduced the results of increased p21 expression. An average of three control shRNA clones and 7 Par-4 shRNA clones are represented in the histogram. Elevated levels of Par-4 expression in the control shRNA levels result in decreased p21 levels with reciprocal results shown in the Par-4 shRNA knockdown cells (Figure 5.2C). We then examined Par-4 and p21 mRNA levels in cells knocked down with the human Par-4 shRNA construct. mRNA levels mirrored results observed at the protein level with increased p21 expression in cells with reduced Par-4 (Figure 5.2D,E).

### 5c) Loss of Par-4 delays development of CLL in vivo

To determine the effect of Par-4 in the development of CLL, we crossed E $\mu$ -Tcl1 mice with mice deficient for Par-4 (Figure 5.3A). We tested several tissues including, spleen, peripheral blood, peritoneal cavity, lymph nodes, bone marrow cells, and liver in the Par-4<sup>-/-</sup> E $\mu$ Tcl1 mice and confirmed that they were deficient for Par-4, but positive for Tcl1 expression (Figure 5.3B). We monitored CLL progression in the Par-4<sup>+/+</sup>E $\mu$ Tcl1 and Par-4<sup>-/-</sup>E $\mu$ Tcl1 by periodic submandibular bleeding and measuring the percentage of CD5+CD19+ CLL cells in the blood by flow cytometry. Mice were considered to be CLL if there was a distinct population of CD5+CD19+ (>15-20%) cells defined on the FACS profile. Figure 5.3C shows that CLL development is significantly delayed in Par-4<sup>-/-</sup> mice compared to wild type mice ( $p < 0.0003$ ). Figure 5.3D represents the survival analysis for Par-4<sup>+/+</sup>E $\mu$ Tcl1 and Par-4<sup>-/-</sup>E $\mu$ Tcl1 mice. The average age of death of Par-4<sup>+/+</sup>E $\mu$ Tcl1 was 8.9mo versus the 11.97mo for Par-4<sup>-/-</sup>E $\mu$ Tcl1 mice ( $p < 0.05$ ). Par-4<sup>-/-</sup>E $\mu$ Tcl1 mice still developed CLL like disease as indicated by CD5+CD19+ staining and gross pathology of the disease indicated by splenomegaly (Figure 5.3E). The total spleen cell number was similar in Par-4<sup>-/-</sup>E $\mu$ Tcl1, Par-4<sup>+/+</sup>E $\mu$ Tcl1, and the adoptive transfer recipient spleen of Par-4<sup>+/+</sup>E $\mu$ Tcl1 cells. Adoptive transfer of  $7.6 \times 10^6$  Par-4<sup>-/-</sup>E $\mu$ Tcl1 CLL cells into WT and Par4 null recipients resulted in similar rates of growth measured through submandibular bleeding (Figure 5.3F). This indicated that Par-4 was not required in the microenvironment for the growth of CLL, but loss of Par-4 in the de novo mouse model delays disease development supporting a cell intrinsic role for Par-4.

We discovered that Par-4<sup>-/-</sup>E $\mu$ Tcl1 spleen cells expressed higher p21 protein levels compared to Par-4<sup>+/+</sup>E $\mu$ Tcl1 spleen cells providing in vivo confirmation of p21 upregulation observed *in vitro* using Par-4 knockdown cell lines (Figure 5.4A). Additional comparison showed

that p21 is present in spleens of Par-4<sup>+/+</sup>E $\mu$ Tcl1 mice but the majority of Par-4<sup>-/-</sup>E $\mu$ Tcl1 spleens express 2-23 fold more p21 (Figure 5.4B). In order for p21 to execute its function to block the cell cycle from G1 to S phase, p21 must be found in the nucleus of the cell [264]. Therefore we looked at nuclear and cytoplasmic fractions of Par-4<sup>+/+</sup>E $\mu$ Tcl1 and Par-4<sup>-/-</sup>E $\mu$ Tcl1 spleen cells and found that Par-4<sup>-/-</sup>E $\mu$ Tcl1 cells had greater nuclear p21 levels compared to Par-4<sup>+/+</sup>E $\mu$ Tcl1 cells, further confirming that Par-4 knockout led to increased levels of functional p21 (Figure 5.4C).

**Figure 5.1A**

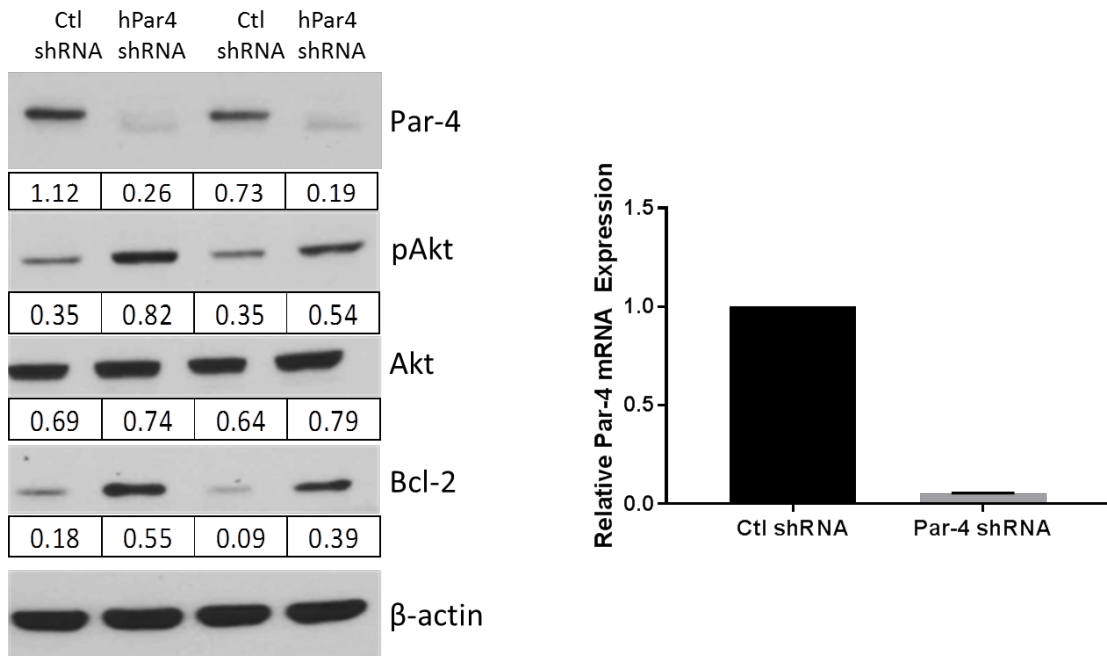


**Figure 5.1B**

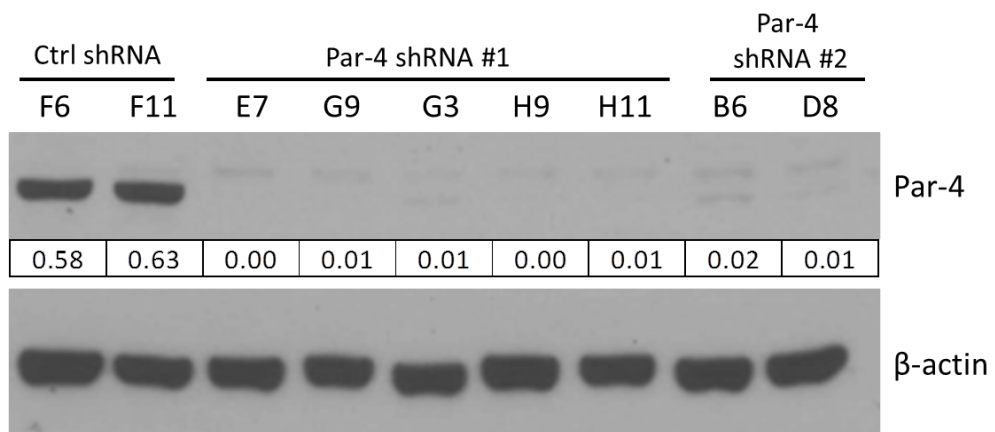


Figure 5.1C

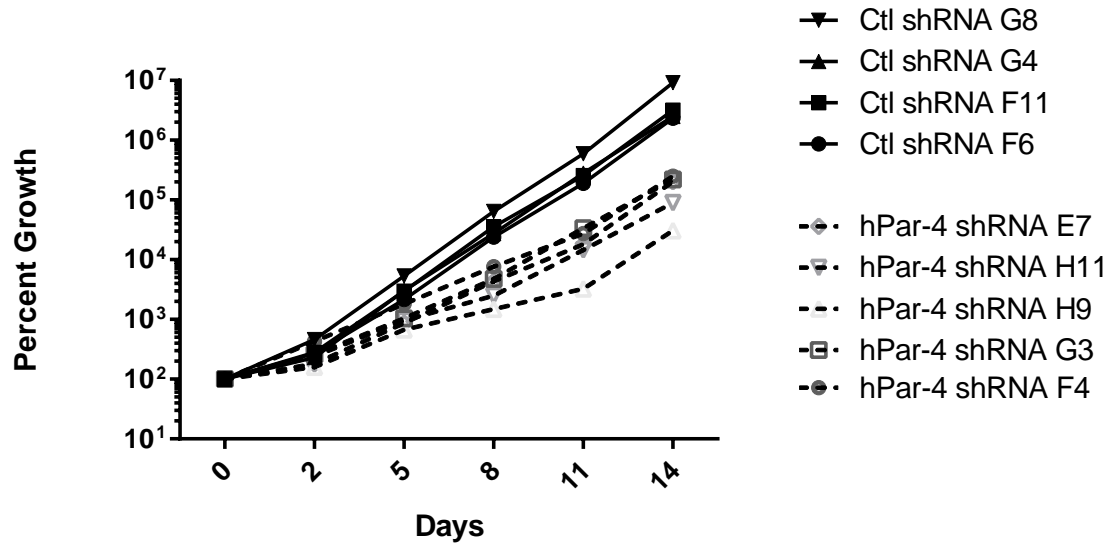
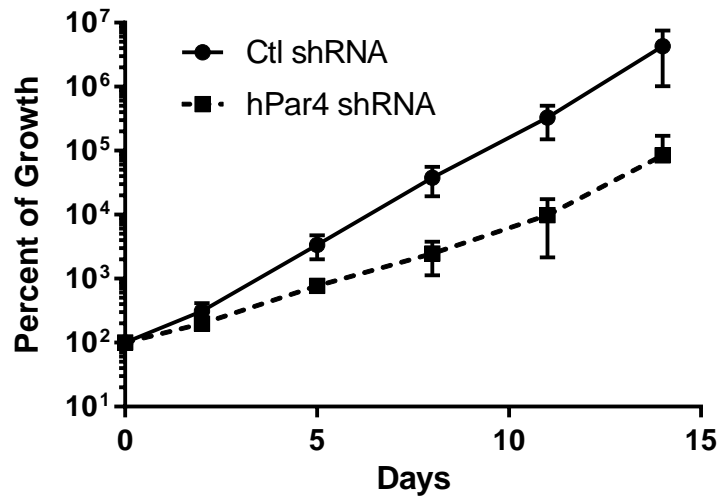


Figure 5.1D



**Figure 5.1E**



338



339



340

**Left: Ctrl shRNA**

**Right: hPar-4 shRNA**



341



342



343

Figure 5.1F

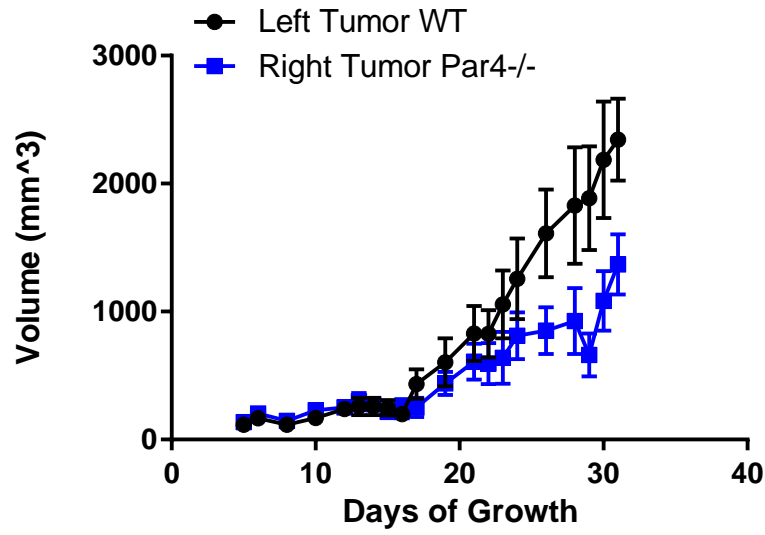


Figure 5.1G

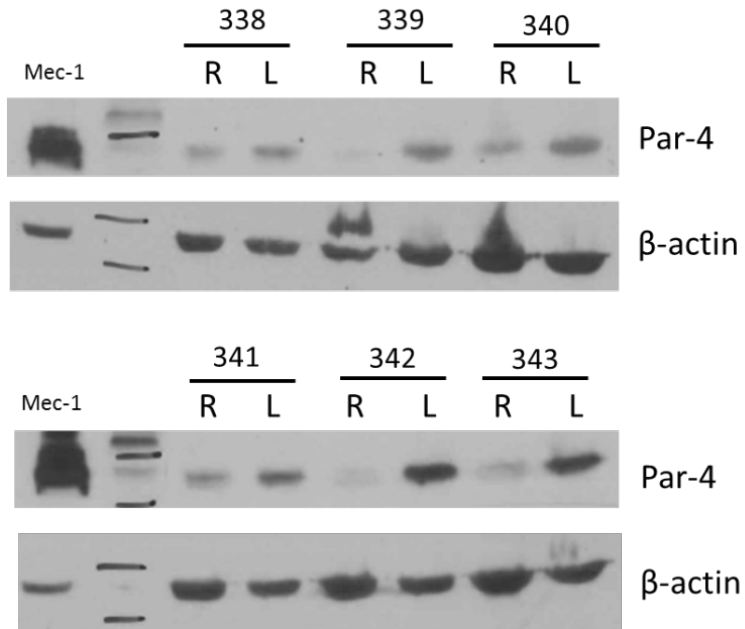


Figure 5.1 Knockdown of Par-4 in vitro leads to reduced CLL growth

A) Left panel: Western blot of proteins in the lysates of Mec-1 cells expressing human Par-4 specific shRNA or control shRNA, which was probed for Par-4, pAkt, Akt, Bcl-2, and  $\beta$ -actin. Par-4 protein band intensities were normalized to Actin. Lanes 1 & 2 are cells lysed with Cell signaling lysis buffer and lanes 3 & 4 are cells lysed with RIPA buffer. Right panel: Quantification of Par-4 mRNA in Mec-1 cells expressing Par-4 shRNA compared to those expressing a control shRNA by qRT-PCR. Par-4 mRNA expression was normalized to human 18S RNA. B) Multiple clones of Par-4 knockdown Mec-1 cells were obtained by limiting dilution cloning in the presence of puromycin. Lysates of these clones were analyzed for Par-4 expression by Western blot. Par-4 protein band intensities were normalized to  $\beta$ -Actin. C) Growth curves of several clones of Mec-1 cells (indicated by letter and number) expressing control or human Par-4 specific shRNA in the presence of puromycin (1.5 $\mu$ g/ml). Cell counts were determined by trypan blue exclusion. D) Growth curve of Mec-1 cells expressing control or Par-4 specific shRNA, with each representing mean and SE for four clones for control shRNA and five clones for Par-4shRNA expressing clones. Slopes of the curves are different ( $P= 0.0024$ ) as calculated by linear regression analysis. E) Mec-1 cells ( $2 \times 10^6$ ) expressing control or Par-4 specific shRNA were engrafted into NSGS mice subcutaneously with matrigel. Pictures show tumors on flanks after 35 days of growth. F) Tumor volumes were calculated by measuring the length and the width with a caliper. Tumor volumes are plotted as a function of time. Difference between the slopes of the two lines is found to be statistically significant ( $P \leq 0.001$ ) by linear regression analysis. G) After 35 days of growth the tumors were excised and Western blot analysis was performed on tumor cell lysates to confirm tumors retained Par-4 knockdown in each mouse throughout the experiment. Lane 2 in each blot is the protein ladder control marker.



Figure 5.2A

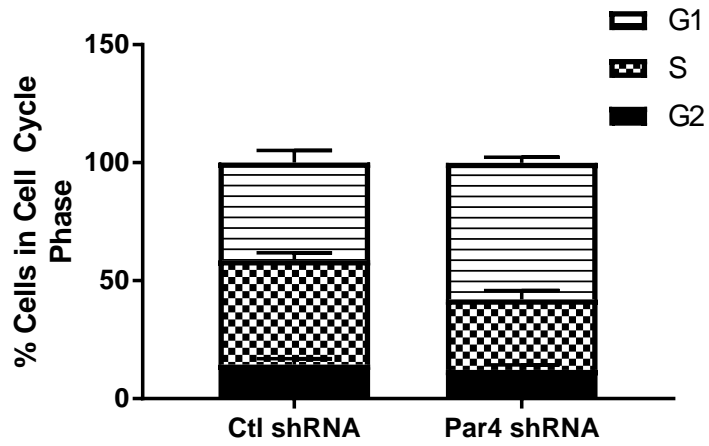


Figure 5.2B

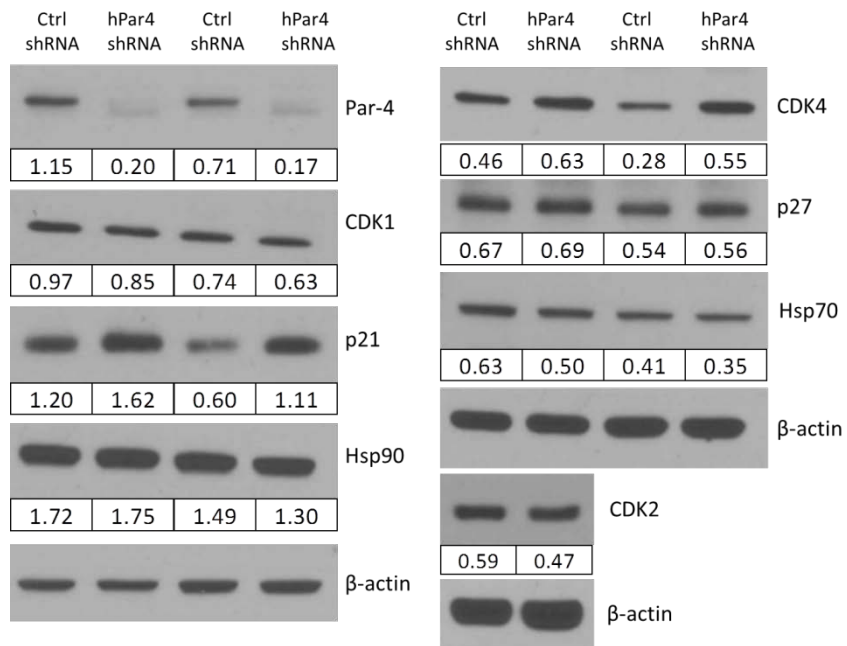


Figure 5.2C

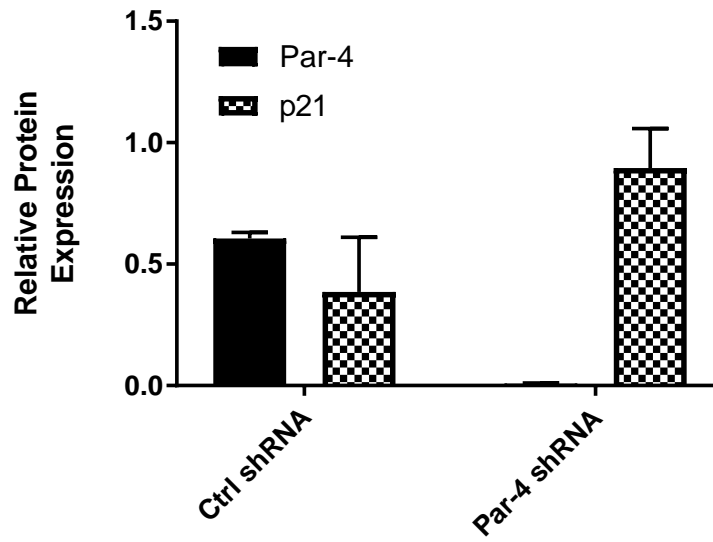
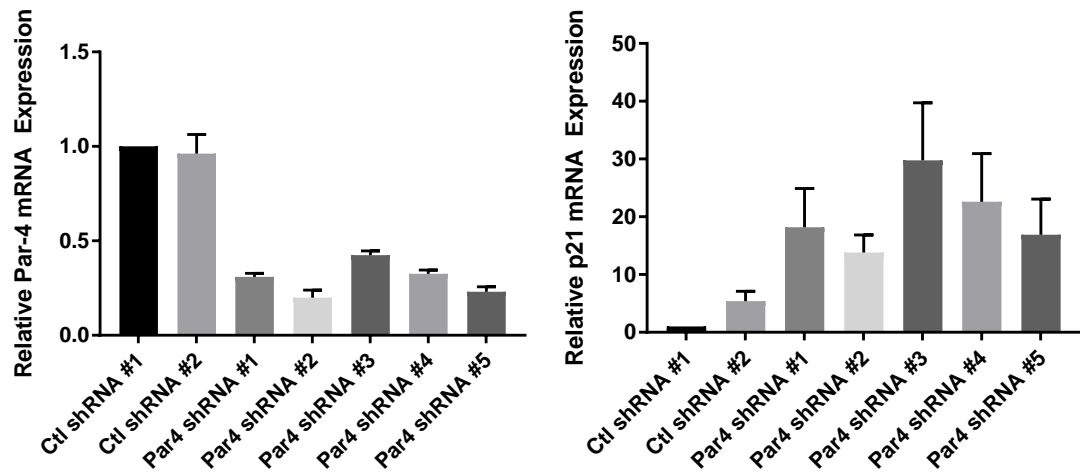


Figure 5.2D



**Figure 5.2E**

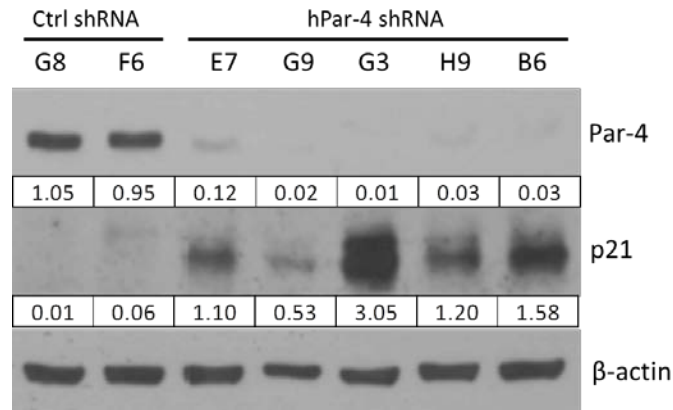


Figure 5.2 Par-4 knockdown leads to G1 cell cycle arrest and increased p21 expression

A) Mec-1 cells infected with control or Par-4 specific shRNA lentivirus were collected and stained with propidium iodide. Cell cycle analysis was performed by flow cytometry. Histograms represent mean  $\pm$  SE of four control shRNA clones and 5 Par-4 shRNA clones. B) Cell lysates from control and Par-4 shRNA expressing Mec-1 cell clones were analyzed by immunoblot for proteins involved in cell cycle. Lanes 1 & 2 are cells lysed with Cell signaling lysis buffer and lanes 3 & 4 are cells lysed with RIPA buffer. Protein values are expression normalized to  $\beta$ -actin. C) Mean  $\pm$  SE of band intensities of Par-4 and p21 expression normalized to  $\beta$ -actin in 3 control shRNA and 7Par-4 shRNA clones. Densitometry values determine by Image J analysis. P value = 0.00003 for Par-4 expression and p= 0.05 for p21 expression determined by student t-test. D) Control and Par-4 shRNA expressing Mec-1 clones were collected and RNA was isolated. Par-4 mRNA (left) and p21 mRNA (right) were quantified by qRT-PCR and were normalized to human 18S RNA expression. E) Immunoblots of proteins from Par-4 and control shRNA infected Mec-1 clones (indicated by letter followed by a number) used for QRT-PCR assays in panel D.

Figure 5.3A

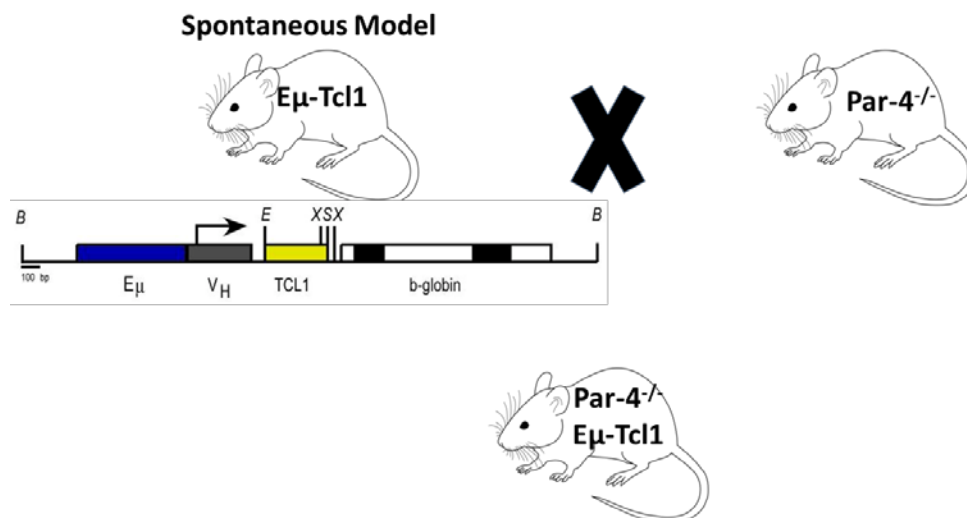


Figure 5.3B

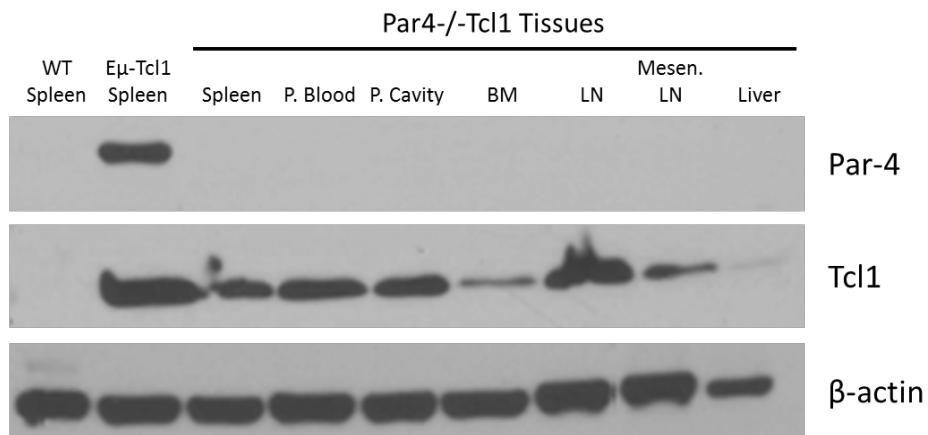


Figure 5.3C

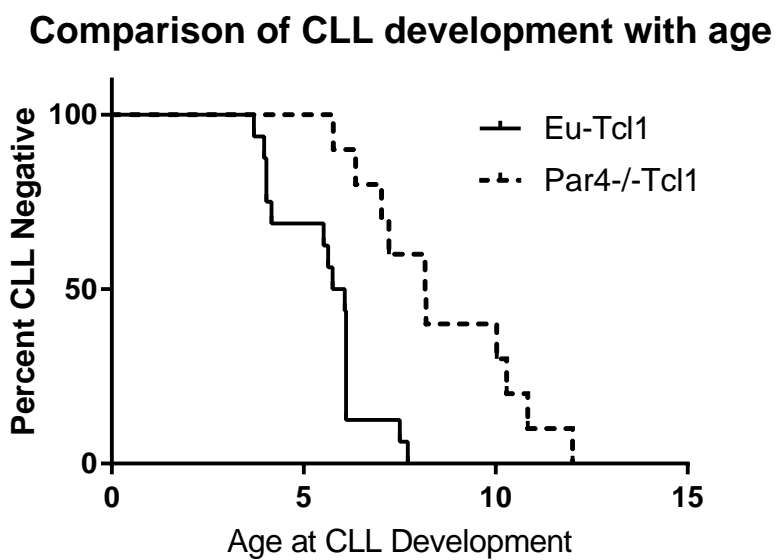


Figure 5.3D

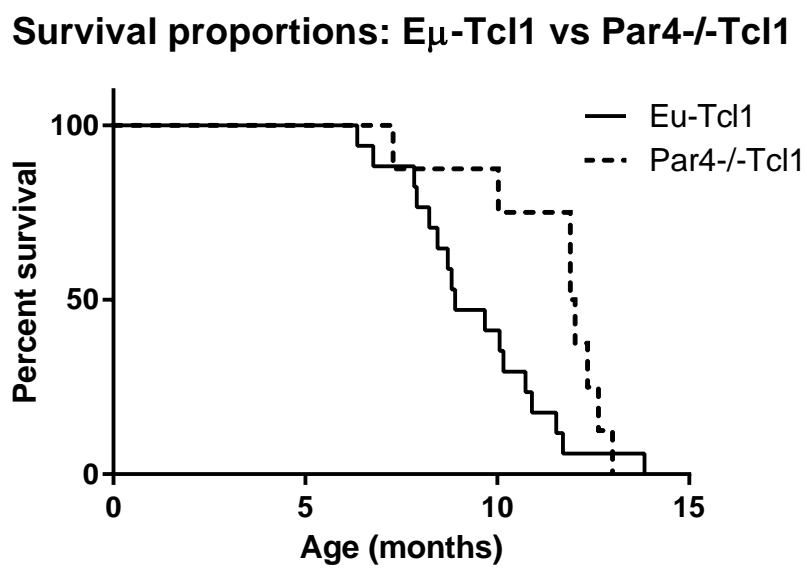


Figure 5.3E

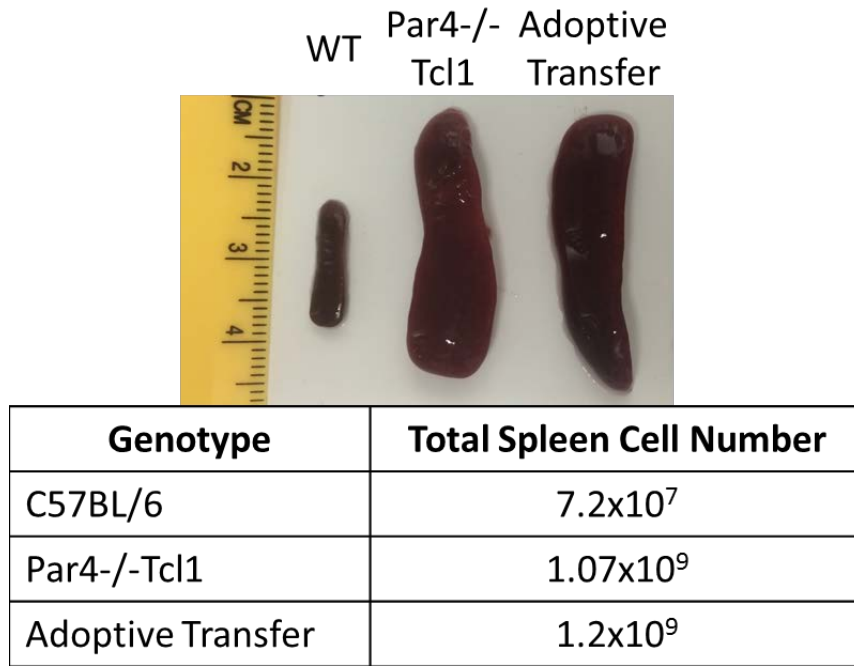


Figure 5.3F

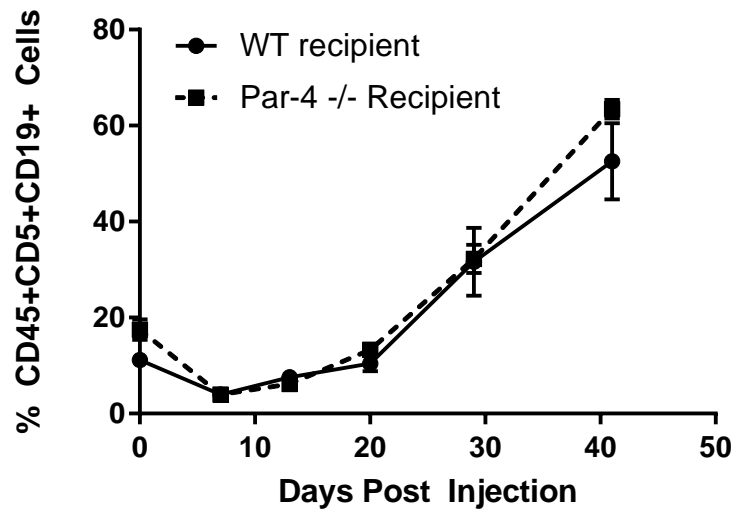
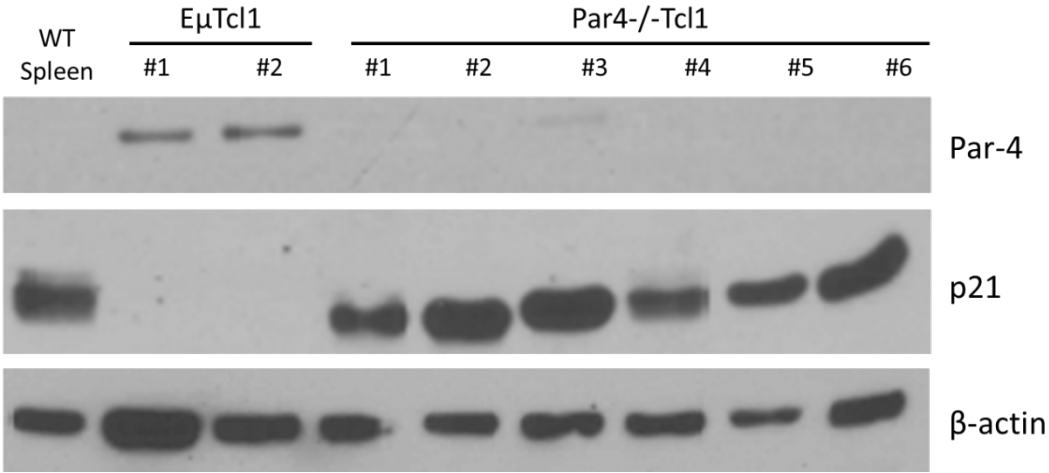


Figure 5.3 Loss of Par-4 delays development of CLL in vivo

A) Breeding scheme of the E $\mu$ -Tcl1 CLL mice crossed with animals deficient for Par-4, both on C57BL/6 background. F1 generation was then intercrossed to get complete Par-4 knockout with the expression of the human Tcl1 gene in B cells. B) Tissues from Par4<sup>-/-</sup>Tcl1 mice (Mouse 2057, Age 13mo, 18days) were harvested and expression of Par-4 and Tcl1 was determined by Western blot analysis. C) Percent of Par-4<sup>+/+</sup> E $\mu$ -Tcl1 and Par-4<sup>-/-</sup>E $\mu$ Tcl1 cohorts that developed CLL over time. P value = 0.0002 determined by Log-Rank test. (n=16 E $\mu$ -Tcl1, n=10 Par4<sup>-/-</sup>Tcl1). Mice were defined as CLL positive if they have  $\geq$  15-20% of CD5+CD19+ cells in their peripheral blood. D) Effect of Par-4 loss on the survival of E $\mu$ Tcl1 mice. Survival curve represents a total of 17 E $\mu$ -Tcl1 Par-4<sup>+/+</sup> mice and 9 E $\mu$ Tcl1Par4<sup>-/-</sup> mice. P value = 0.0472 determined by Log-Rank test. Mice were euthanized according to their body condition score. E) Comparison of spleens sizes and total cell number in C57BL/6 WT (13.1mo), Par-4<sup>-/-</sup>E $\mu$ Tcl1 (11.9mo), and adoptive transfer recipient injected with E $\mu$ Tcl1 cells. F) Kinetics of CLL development in WT and Par4 null mice injected with Par-4<sup>-/-</sup>E $\mu$ Tcl1 CLL cells obtained from the cohort described in previous panels. n = 6/group. There was no statistically significant difference in the % of CLL cells in the two groups of recipients at all time points tested.

**Figure 5.4A**



**Figure 5.4B**

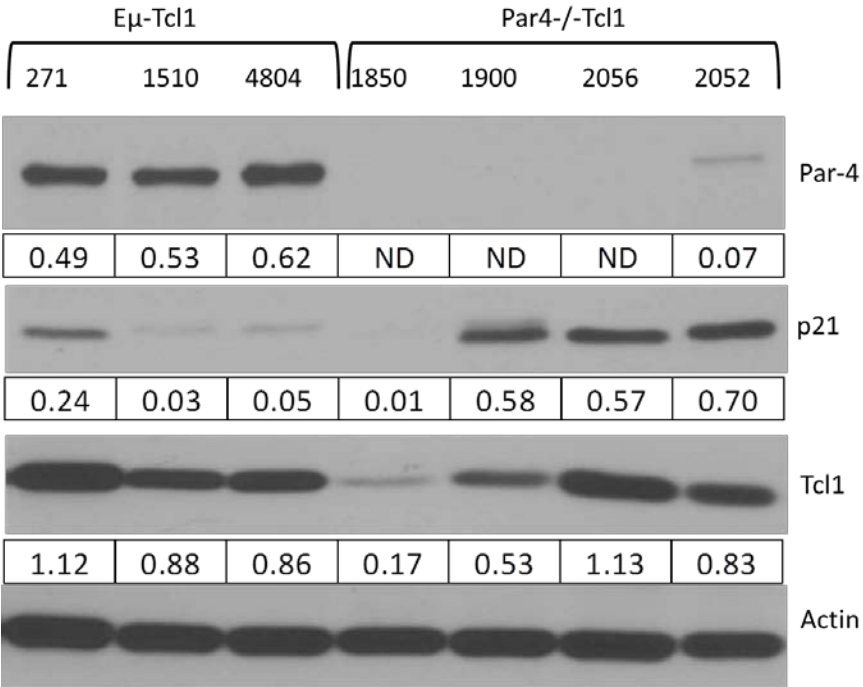




Figure 5.4C

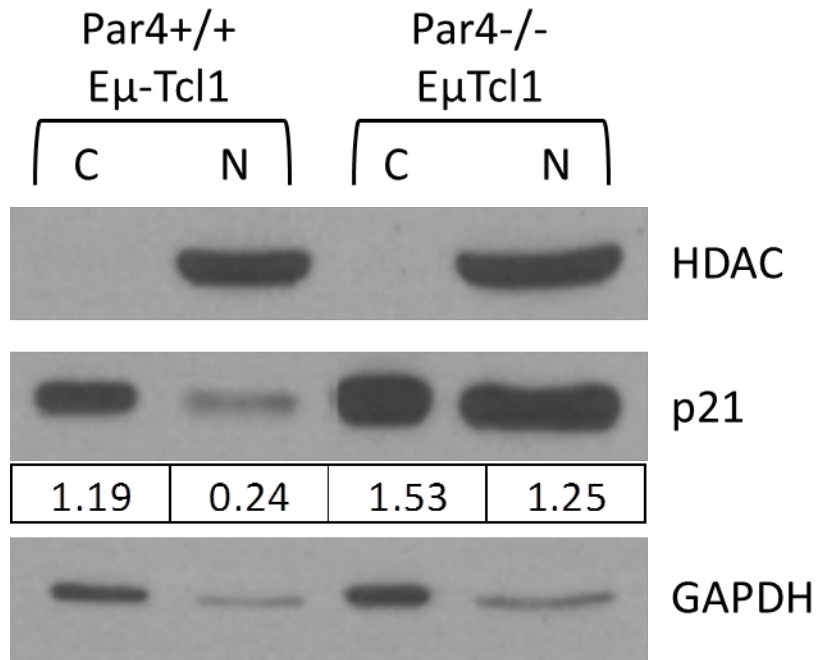


Figure 5.4 Par-4<sup>-/-</sup> Eμ-Tcl1 spleen CLL cells have increased levels of p21 expression

A) Splens from multiple Par-4<sup>+/+</sup> Eμ-Tcl1 and Par-4<sup>-/-</sup> Tcl1 mice (individual mice numbered 1 through 6) were harvested, total protein was isolated and analyzed by SDS PAGE followed by Western blots. . Immunoblots were probed for Par-4 and p21. Protein expression was normalized to β-Actin. B) Spleen cell lysates from Eμ-Tcl1 mice and Par-4<sup>-/-</sup> Tcl1 mice were analyzed by immunoblots, which were probed for Par-4, p21, and Tcl1. C) Proteins from nuclear and cytoplasmic fractions of cell lysates from Par-4<sup>+/+</sup> EμTcl1 and Par-4<sup>-/-</sup> EμTcl1 CLL cells were analyzed by Western blots, which were probed for p21 expression. Nuclear (N) loading control is HDAC and cytoplasmic (C) control is GAPDH. p21 densitometry values were normalized to respective controls.

## Summary

A valuable way to verify the importance of a gene product in molecular biology is to knock out the gene and determine if there is an effect on the phenomenon of interest. Hence, we knocked down Par-4 in the Mec-1 cell line. We found that Par-4 is not critical for the survival of CLL cells, as Mec-1 cells persisted with a dramatic down regulation of Par-4 protein and mRNA expression. Additionally, Par-4 is not required for the development and growth of CLL cells as animals lacking Par-4 with the Tcl1 oncogene continued to develop a CLL like disease.

Loss of Par-4 did result in a decrease in growth suggesting that it is involved in CLL cell proliferation. Decreased Par-4 levels resulted in a reduction in the G1 to S phase transition of the cell cycle with a reciprocal induction of p21 expression. This is a novel finding as CLL cells in the periphery of patients are in a quiescent state. The knockdown studies are done in a transformed cell line that proliferates, which could be responsible for the retardation in cell cycle, as infection with a scrambled shRNA construct did not change the growth pattern of the Mec-1 CLL cells. While a proliferative cell line may not be the best model of quiescent CLL cells, it does allow us to establish mechanisms in which these cells avoid apoptosis. It would be interesting to investigate the cell cycle status of cells in spleens of Par4<sup>-/-</sup>Eμ-Tcl1 and Par4<sup>+/-</sup>Eμ-Tcl1 mice at similar stages of disease to see if Par4<sup>-/-</sup>Eμ-Tcl1 CLL exhibit a reduced G1 to S transition to confirm our cell line data. Results were comparable in the Mec-1 Par-4 shRNA knockdown cells and the spleens of Par4<sup>-/-</sup>Eμ-Tcl1 mice that showed delayed CLL development and increased p21 expression. This is a clinically relevant finding as a study investigating the expression of p21 in CLL cases and patients with Richter's syndrome found that 80% of CLL cases did not express detectable levels of p21 [265]. 43% of patients with Richter's syndrome did express detectable levels of p21. Cobo et al. analyzed the sequence of p21 in three CLL cases and 6 Richter's syndrome to find a germline configuration in all of them indicating that it was

not mutated. We did not sequence the *p21* gene in our Par-4 knockdown and knockout cells to confirm that it was not mutated, but our observed increase in nuclear p21 levels in Par4<sup>-/-</sup>Eμ-Tcl1 CLL cells suggests that it is still able to translocate to the nucleus and function in the regulation of the cell cycle that occurs in the nucleus.

## CHAPTER 6

### **Splenic microenvironment and Par-4 expression is important for the development of CLL in the mouse**

B cell receptor signaling has been proven to be critical for the survival of CLL. The microenvironment was found to support CLL B cell activation and provide a proliferative niche for malignant cells to expand [9, 154, 266]. CLL cells that circulate within the peripheral blood are characterized to be quiescent and resistant to apoptosis. A small population of CLL cells exists that is actively proliferating, but the site of new growth is currently being debated [148]. A recent study in CLL patients has provided direct in vivo evidence that the lymph node microenvironment is the site of new cells with higher Ki67 staining expression compared to the peripheral blood and bone marrow [143]. Other studies examining gene expression profiles have suggested that the lymph node shows elevated BCR signaling gene signatures [142] and may have enhanced immune suppressive markers [141]. In human patients, the spleen has not been examined carefully as a site of CLL growth during early stages of CLL disease nor in most of the molecular analyses, due to the difficulty of accessing spleen tissue. This limitation can be overcome in an animal model. In the E $\mu$ -Tcl1 transgenic mouse model, some studies utilized intravital imaging to visualize sites to which CLL cells home for their clonal expansion [154]. Heinig et al. suggest that CLL cells travel to splenic B cell follicles to interact with follicular dendritic cells (FDCs) to accelerate disease progression. Other studies have indicated that E $\mu$ -Tcl1 CLL cells require interaction with macrophages in order to survive and proliferate, but the site of interaction was not well defined [152, 153]. Further characterization of the CLL microenvironment is essential to understand how CLL cells avoid apoptosis, become resistant to cytotoxic therapies, and progress towards a more aggressive disease. Our initial studies to establish an adoptive transfer model with E $\mu$ -Tcl1 cells led us to question where the CLL cells

home for their *in vivo* growth. Severe splenomegaly is a well-defined marker of CLL progression in the E $\mu$ -Tcl1 de novo and adoptive transfer models, suggesting that this splenic microenvironment needs to be investigated further.

We have shown that CLL cells overexpress Par-4 compared to levels in normal B cell subsets. Additionally, CLL cells secrete Par-4 that can induce apoptosis of other cancer cell lines. Hence we investigated if Par-4 secreted from CLL cells is able to manipulate the microenvironment's ability to promote or delay CLL growth. Studies in this chapter investigate the role of spleen and Par-4 in the splenic microenvironment using primary and adoptive transfer models.

## **Results**

### *6a) Spleen is the primary site of CLL growth in mouse models*

The E $\mu$ -Tcl1 mouse is an excellent model to study CLL as these mice progressively develop an accumulation of CD5+CD19+ cells within the peripheral blood, spleen, lymph nodes, and bone marrow [144]. The E $\mu$ -Tcl1 mouse exhibits splenomegaly, hepatomegaly, enlarged lymph nodes, and anemia as disease progresses. We monitored the growth of the spleen in the E $\mu$ -Tcl1 mouse over time through ultrasonographic analysis and found that the spleen size increases with age and disease progression (Figure 6.1A). Representative ultrasound images are shown in Figure 6.1B. Staining of the peripheral blood and spleen cells from E $\mu$ Tcl1 mice euthanized at different ages indicates that the spleen has a slightly higher percentage of CD5+CD19+ cells compared to the blood (Figure 6.1C). In terms of absolute numbers spleen has more CLL cells than any other tissue (data not shown).

We also utilized the adoptive transfer model to monitor the growth of CLL cells in the peripheral blood and spleen (Figure 6.2A). Ultrasound imaging of the recipient mouse after CLL injection shows an increase in spleen size. Total volume of the spleen is calculated by 3-D imaging and tracing with the Vevo 2100 software (Figure 6.2B). We compared the change in spleen size to the peripheral blood CD5+CD19+ staining and detected a notable increase in spleen size at day 7 while we were able to detect CD5+CD19+ population in the blood only at day 21 (Figure 6.2C). This result indicates that the CLL cells grow first in spleen before they egress to the periphery. We also noted that recipient mice developed CLL with tumor burden primarily in the spleen irrespective of the route of injection (IV, IP, or SQ) (Figure 6.2D).

To determine if the spleen is a preferred site of CLL growth we measured the localization and the growth of CLL cells in various lymphoid organs after adoptive transfer. In order to monitor the homing and growth of injected CLL cells, we utilized E $\mu$ Tcl1 CLL cells that

expressed the human ROR1 cell surface molecule (C57BL/6 background) to differentiate injected cells from resident CD5+CD19+ cells. Spleen, peritoneal cavity, bone marrow, and lymph node tissues were collected after adoptive transfer of  $10 \times 10^6$  hROR1+CD5+CD19+ cells into WT recipients (Figure 6.3A). Total hROR1+CD5+CD19+ numbers were calculated by hemocytometer trypan blue counts and percentage of hROR1 positive cells through flow cytometry (Figure 6.3B). After 24hrs, CLL cells were found within the spleen but were not detected in the peritoneal cavity until day 6 and bone marrow, liver, and lymph nodes until day 30 or longer (Figure 6.3C). Spleen histology at each time point indicates an expansion of the white pulp and loss of follicular structure as time progresses post- adoptive transfer (Figure 6.3D).

We also performed xenograft studies with primary human peripheral blood samples injected into NSG mice. After 5 days of growth, we were able to detect human CLL cells in the peripheral blood and spleen of NSG mice (Figure 6.4A). The spleen contained the greatest number of human CLL cells (p#11:  $3.1 \times 10^5$ ; p#14:  $3.3 \times 10^5$ ) further confirming that the adoptively transferred cells home to the spleen for proliferation and survival (Figure 6.4B).

#### *6b) Splenectomy delays CLL development*

Results indicate that the spleen is the primary site of CLL growth in the E $\mu$ -Tcl1 de novo and adoptive transfer models. To further confirm that this site is important in the growth and development of CLL we surgically removed the spleens of E $\mu$ -Tcl1 mice to measure its importance for CLL (Figure 6.5A). Splenectomy of E $\mu$ -Tcl1 mice at both 4mo and 8mo of age delayed the development and/or progression of CLL as indicated by peripheral blood CD5+CD19+ staining (Figure 6.5B). The overall survival of E $\mu$ -Tcl1 mice splenectomized at both ages was significantly increased with a median survival age increasing to 12.06mo compared to 9.68mo of animals with a spleen (Figure 6.5C, p value = 0.024 determined by Log-Rank test).

Breakdown of animal survival that were splenectomized at each age is depicted in Figure 6.5D. Mice splenectomized at 4mo had an average median survival age of 12.33mo (p value = 0.068 Log-Rank test, p=0.0103 Gehan-Breslow-Wilcoxon test) and mice splenectomized at 8mo resulted in a median survival age of 11.81mo (p value = 0.043 Log-Rank test, p = 0.0192 Gehan-Breslow-Wilcoxon test). We detected CD5+CD19+ cells within different compartments of the body including the peripheral blood, peritoneal cavity, bone marrow, lymph nodes, liver, thymus, and omental tissue (Figure 6.5E). The majority of the tumor burden in splenectomized E $\mu$ -Tcl1 mice was located in the peritoneal cavity and liver (Figure 6.5F).

Animals were euthanized when their body condition score diminished or showed elevated CD5+CD19+ peripheral blood staining. A majority of the splenectomized mice still showed signs of CLL with positive staining in the blood and other tissues at the time of sacrifice. However, there were some specific cases (6/18) where the splenectomized mice did not develop CLL (absence of detectable numbers of CD5+CD19+ cells) suggesting that splenectomy potentially cured the disease (Table 6.1). These mice developed poor body condition, presumably due to secondary effects of splenectomy (bowel obstruction etc.). Because some mice still developed CLL, splenectomy does not cure, but does delay the progression. We also tested the effect of removing the spleen in the adoptive transfer model. We splenectomized six recipient mice and after recovery, injected CLL cells intravenously. We monitored CLL development through peripheral blood staining over time and found that removal of the spleen resulted in a highly significant delay in CLL growth, such that none of the splenectomized mice developed disease even at day 200, whereas the eusplenic mice in the cohort developed disease by day 25 (Figure 6.6A). Mice were euthanized at day 200 to determine if there was CLL in internal organs even though no CLL cells were detected in the blood. An additional experiment replicated the results of delayed CLL growth in splenectomized recipients and we were only able



to detect a clean CD5+CD19+ stain in 2/10 mice as compared to ≈90% of eusplenic recipients that developed disease (Figure 6.6B). We performed additional splenectomy experiments on WT mice to determine if spleen removal altered the population of B1 cells without CLL injection. We did not observe a change in the total population resident CD5+CD19+ B cells in any tissues.

*6c) CLL cells do not require B, T, and NK cells present in the microenvironment*

Splenectomy of both the de novo E $\mu$ -Tcl1 and adoptive transfer models of CLL led to a dramatic delay in CLL growth and development. We next tried to determine what cell types present in the spleen are supporting the growth of CLL. We utilized the NSG (NOD-scid IL2R $\gamma$ null) mouse strain that is lacking B, T and NK cells as the adoptive transfer recipients. The NSG mice adoptively transferred with E $\mu$ -Tcl1 CLL cells all developed CLL like disease at a slightly quicker rate than WT C57BL/6 recipients (Figure 6.7A; p value = 0.026 determined by linear regression analysis). This indicates that B, T, and NK cells are not required to support the growth of CLL cells, but may suggest the occurrence of an immune response that slows the growth of CLL cells in WT mice (Alhakeem, S. 2017 Dissertation). Additionally, we adoptively transferred CLL cells into splenectomized NSG mice to determine if the requirement for spleen for CLL growth will hold true in the absence of the adaptive immune system. (Figure 6.7B). As in BL/6 mice splenectomy considerably delayed CLL growth in Sp $\alpha$  NSG mice. However, CLL cells grew faster in the splenectomized NSG background compared to the splenectomized WT background. CLL cells were isolated consistently from the peritoneal cavity, liver, and peripheral blood of splenectomized NSG mice (Figure 6.7C). Two of three mice showed positive staining of CLL cells within the bone marrow compartment and lymph node, but were absent from the third, though all the mice had CLL cells in the blood, peritoneal cavity and liver. This suggests

that the lack of B, T, and NK cells in other organs allowed the growth of CLL cells, suggesting a role for adaptive immunity in controlling the spread of disease to other lymphoid organs.

*6d) Splenectomy of Par-4<sup>-/-</sup> mice results in delayed CLL growth*

We have shown that Par-4 is secreted by CLL cells and that the secreted Par-4 is effective in inducing apoptosis of other cancer cell lines (Figure 3.4C, 3.4F). We were therefore curious to test if Par-4 in the microenvironment played a role in the growth of CLL cells. Par4<sup>-/-</sup>Eμ-Tcl1 mice lack Par-4 in CLL cells themselves as well as Par-4 that is sourced from other cell types in the microenvironment. As shown in chapter 5, Par4<sup>-/-</sup>Eμ-Tcl1 mice still developed CLL but at a delayed rate compared to Par4<sup>+/+</sup>Eμ-Tcl1 mice (Figure 5.3C). Par4<sup>-/-</sup>Eμ-Tcl1 mice also had an improved lifespan compared to Par4<sup>+/+</sup>Eμ-Tcl1 suggesting that the lack of Par-4 intrinsically and/or extracellularly reduced the aggressiveness of the disease.

We first wanted to determine if Par4<sup>+/+</sup>Eμ-Tcl1 CLL cells grow at similar rates within the Par4<sup>-/-</sup> background versus C57BL/6 background. Initial experiments were promising showing that the lack of Par-4 in recipient mice led to more rapid growth of CLL, but results could not be repeated. An average of all three adoptive transfer experiments in Par4 null and WT recipients is shown in Figure 6.8A. There was no significant difference in the growth rate of CLL cells between the two recipient backgrounds (p value = 0.3441). Next we transferred the Par4<sup>-/-</sup>Eμ-Tcl1 cells into WT and Par4<sup>-/-</sup> animals and measured their expansion overtime, allowing us to see if Par-4 in the microenvironment affected the growth rate of CLL cells lacking endogenous Par-4. We did not observe a change in the rate of CLL growth between the Par-4 null and WT recipients (Figure 6.8B). There is variability in the growth rate of CLL samples derived from de novo mouse models that may be contributing to this result, further experiments using different Par4<sup>-/-</sup>Eμ-Tcl1 CLL

samples are required to confirm these results as these particular primary CLL cells could have been more aggressive than others.

Due to the significant difference in CLL development between the Par4<sup>-/-</sup>Eμ-Tcl1 and Par4<sup>+/+</sup>Eμ-Tcl1 mice, we further investigated the effect of Par-4 on CLL growth. Since elimination of the primary site of CLL growth with splenectomy results in delayed CLL development, we splenectomized Par4<sup>-/-</sup> mice to see if the lack of spleen and Par-4 may contribute to changes in CLL growth. Interestingly, we find that absence of the spleen in the Par-4 null background allows for faster growth of CLL cells in the Spx environment (Figure 6.9A). Repeated experiments found that the lack of Par-4 in splenectomized animals results in CLL growth in 50% of recipients, whereas only 20% of Par-4<sup>+/+</sup> Spx mice develop CLL (Figure 6.9B). This result suggests that Par-4 present in the WT splenectomized animals is preventing the growth of CLL in other tissue microenvironments. Further studies must be completed to determine how Par-4 is preventing growth, but appears that it may be acting as a tumor suppressor in the secondary CLL microenvironments.

Figure 6.1A

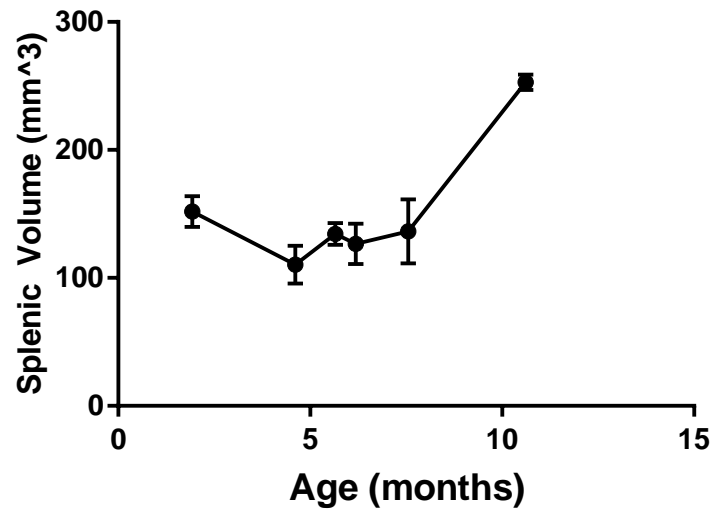


Figure 6.1B

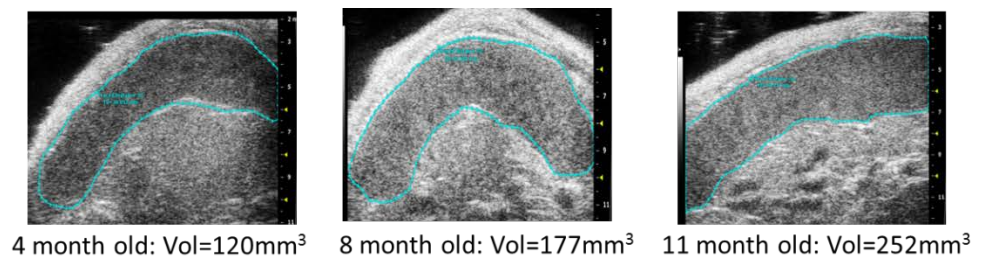


Figure 6.1C

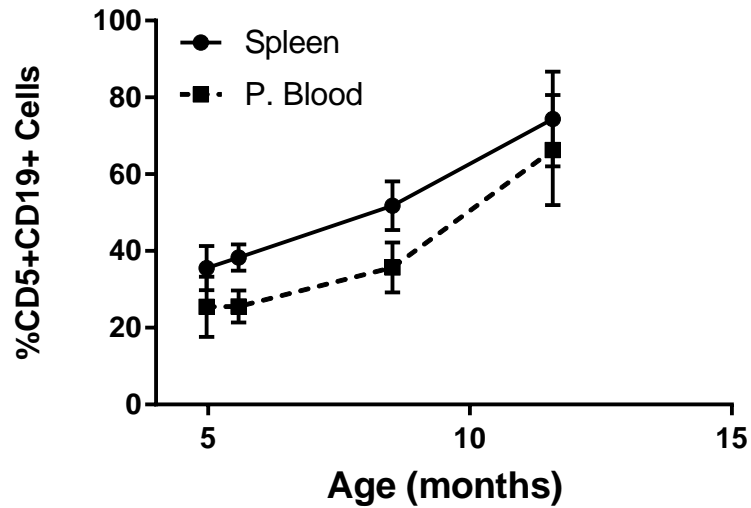


Figure 6.1: Spleen is the primary site of CLL growth in CLL in the E $\mu$ Tcl1 mouse model

A) Spleen volumes were measured through ultrasound imaging of E $\mu$ -Tcl1 mice at different ages.

Each point represents an average of three spleens. Wildtype 3mo C57BL/6 mice have a spleen size of 96.6mm<sup>3</sup>. B) Representative ultrasound images of E $\mu$ -Tcl1 mouse spleens at each age. C)

Percentage of peripheral blood and spleen CD5+CD19+ cells in E $\mu$ -Tcl1 mice at the indicated ages. Values represent mean  $\pm$  SD of three mice,  $p = 0.567$  determined by 2 way ANOVA

comparing the spleen and peripheral blood at different ages.

Figure 6.2A

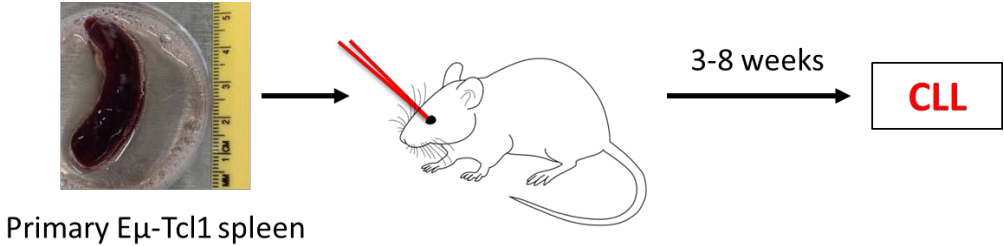


Figure 6.2B

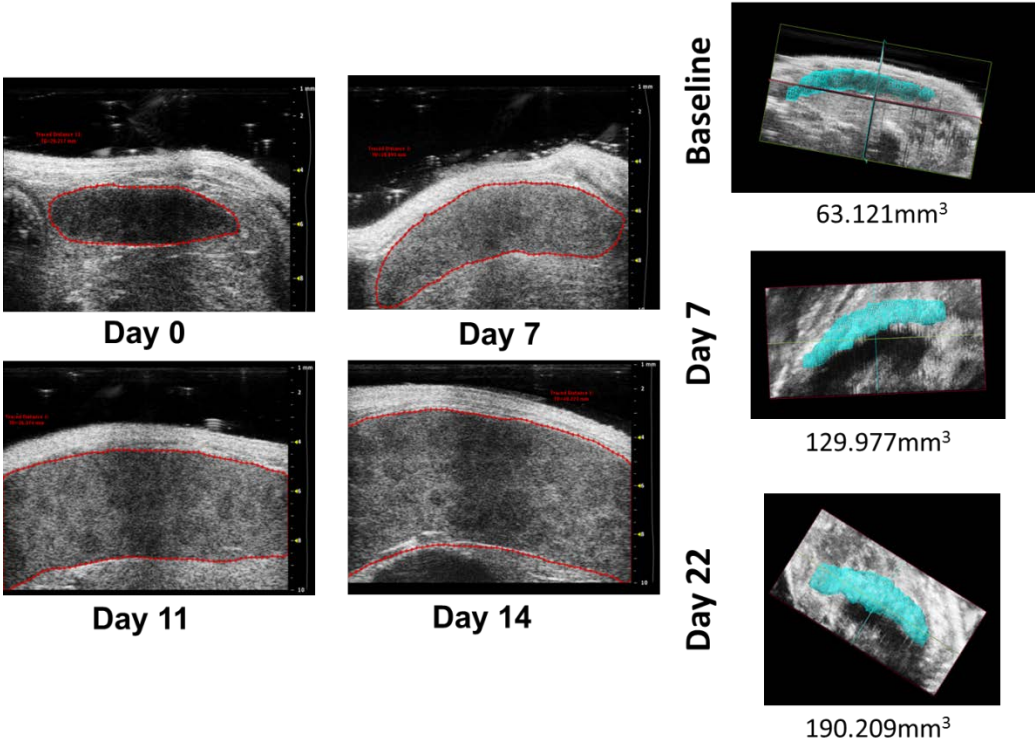


Figure 6.2C

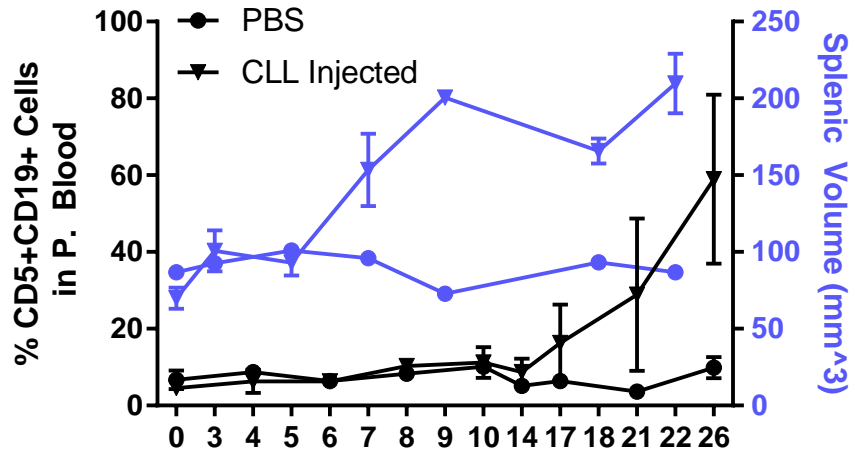


Figure 6.2D

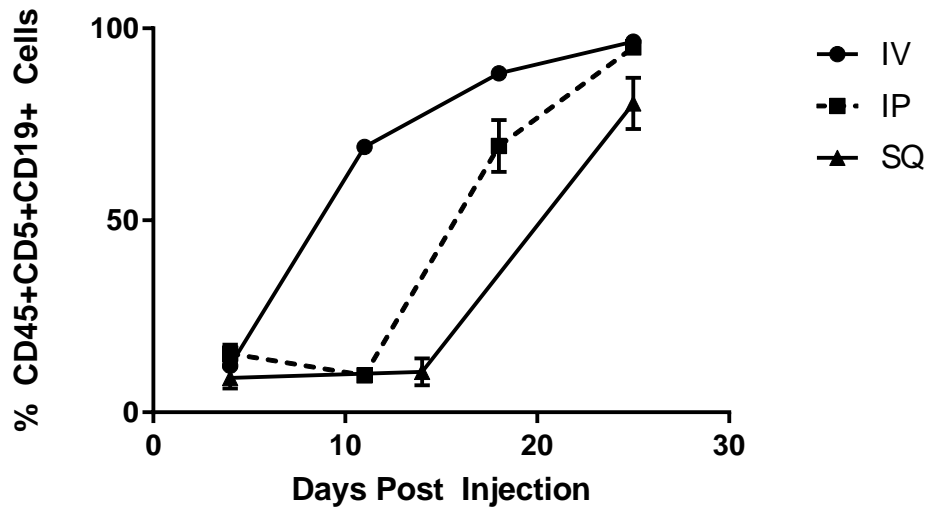


Figure 6.2 Growth of CLL in spleen in the adoptive transfer model

A) Scheme of adoptive transfer for CLL development.  $10 \times 10^6$  Emu-Tcl1 CLL cells were injected into eusplenic or splenctomized C57BL/6 mice. B) Ultrasound imaging of spleen in an adoptive transfer recipient after CLL injection at different times after CLL injection. Splenic volumes are calculated after 3-D imaging and trace modeling using the Vevo 2100 ultrasound system and software (Right). C) Comparison of peripheral blood CD5+CD19+ staining and spleen volume in the adoptive transfer model. Average values of two mice are shown for each group except the splenic volume of the PBS injection represents one mouse. D)  $10 \times 10^6$  CLL cells were injected intravenously (IV, n=1), intraperitoneal (IP, n=2), and subcutaneously (SQ, n=3). CLL growth was monitored by submandibular cheek bleeding and flow cytometry analysis of CD45+CD5+CD19+ staining. Mean  $\pm$  SD values are graphed



Figure 6.3A

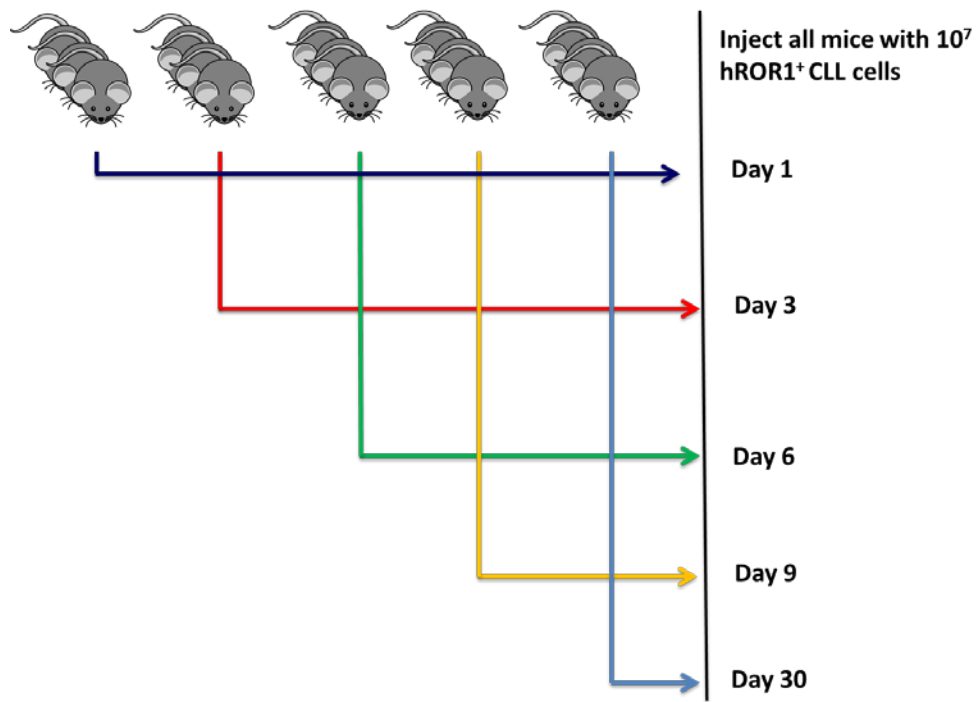


Figure 6.3B

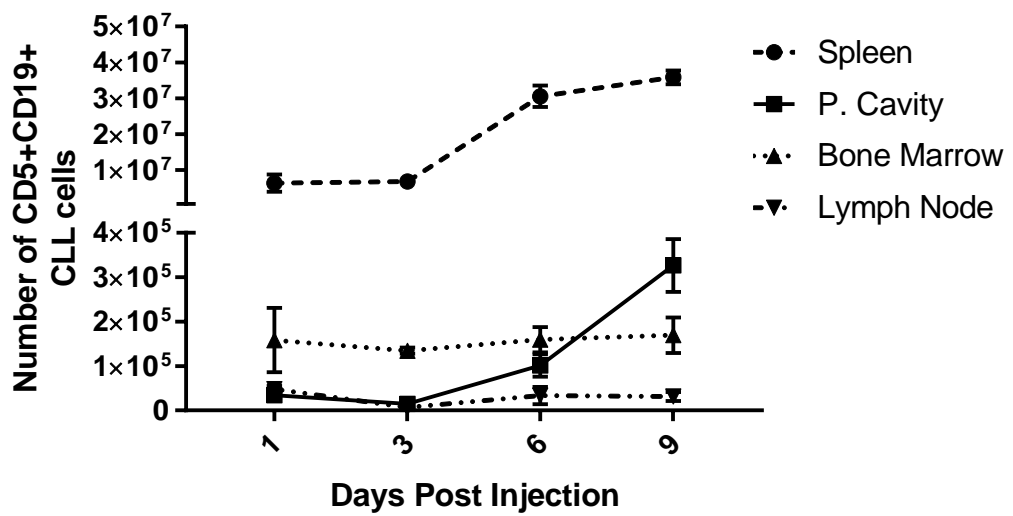
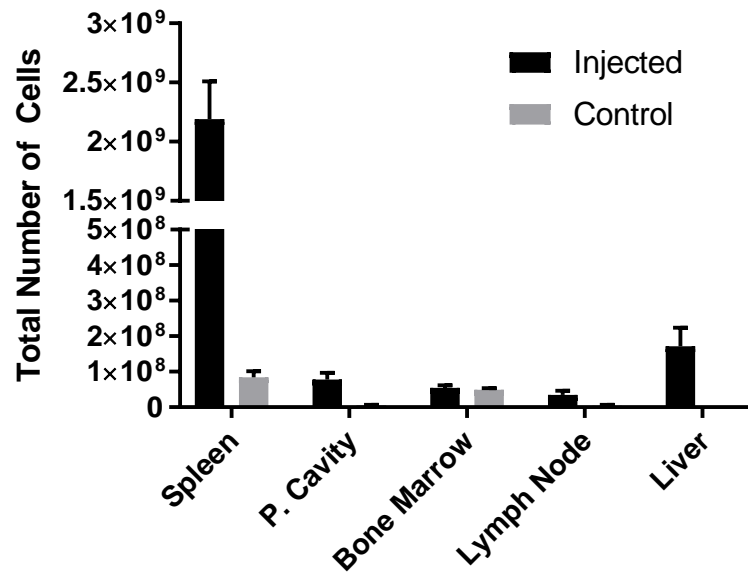


Figure 6.3C



**Figure 6.3D**

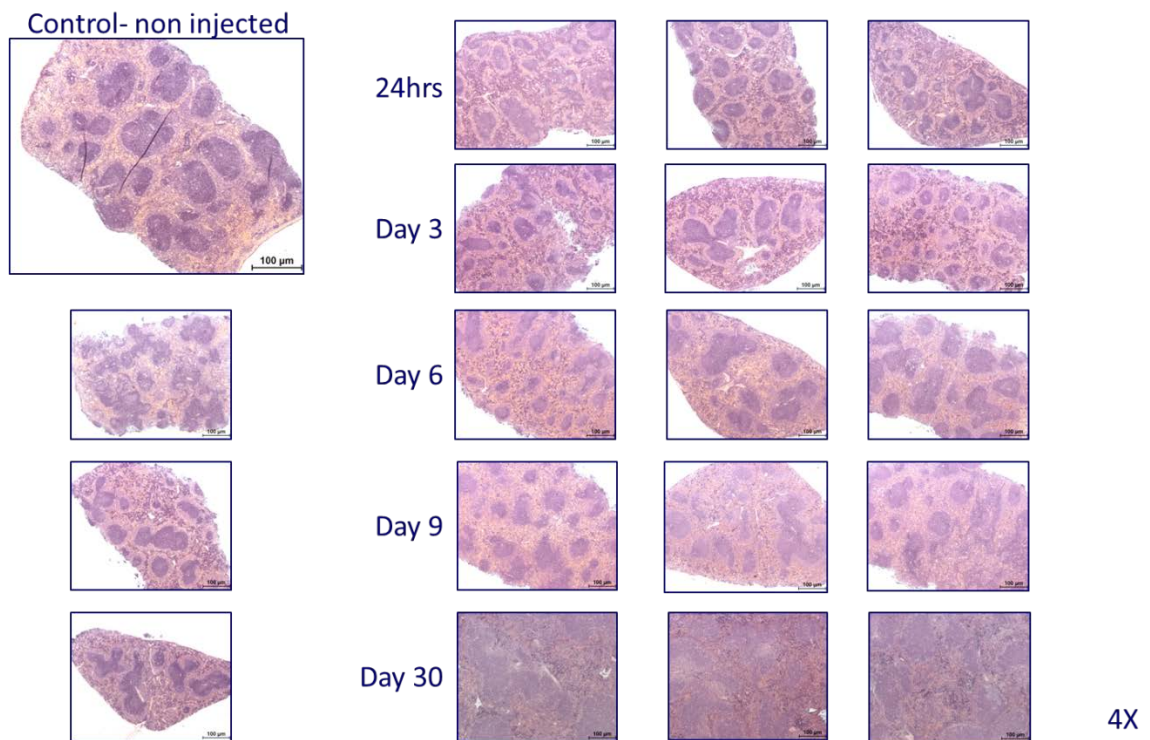


Figure 6.3 Injection of hROR1+CLL cells to monitor localization of CLL in the adoptive transfer model

A) Scheme of the experiment. C57BL/6.hROR1+ve CLL cells ( $10 \times 10^6$ ) were injected intravenously into C57BL/6 recipients. Three mice per group with an additional noninjected WT mouse were euthanized at each time point to detect CLL in different lymphoid organs. B) Total number of hROR1+CD5+CD19+ cells detected by FACS analysis in each tissue at different times after CLL transfer are shown. C) Total number of CLL cells in each tissue at day 30 post injection. D) H&E staining of spleen tissues at each time point of euthanasia. All image magnifications were at 10x.

Figure 6.4A

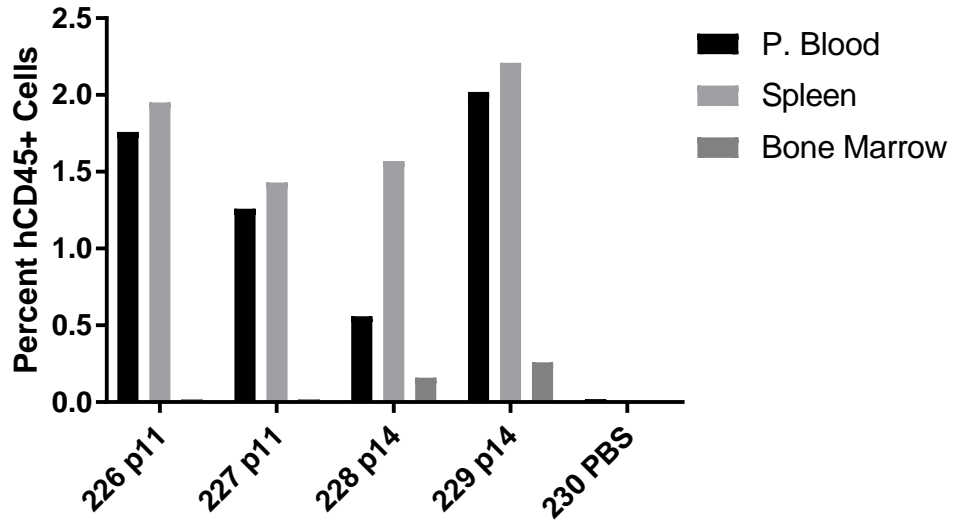
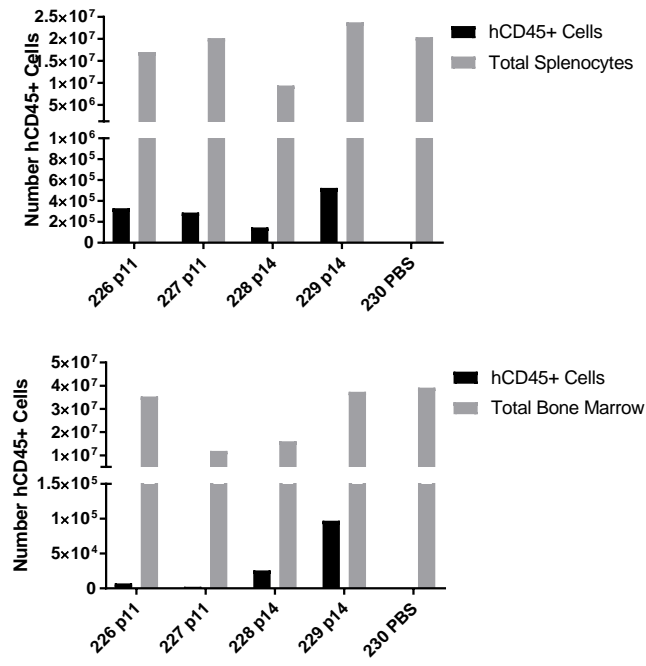


Figure 6.4B



#### 6.4 Human xenograft in NSG mice

A)  $20 \times 10^6$  human peripheral blood CLL cells (p#11 and p#14) were injected into two recipient NSG mice. After 5 days of growth, tissues were collected and stained for human CD45+ cells. The numbers refer to individual patients. Numbers 226 to 230 refer to individual NSG mouse recipients. B) Total numbers of viable cells were calculated by hemocytometer counts and the percentage of human CD45+ cells were used to calculate the total number of cells present in the spleen (top) and bone marrow (bottom).

Figure 6.5A

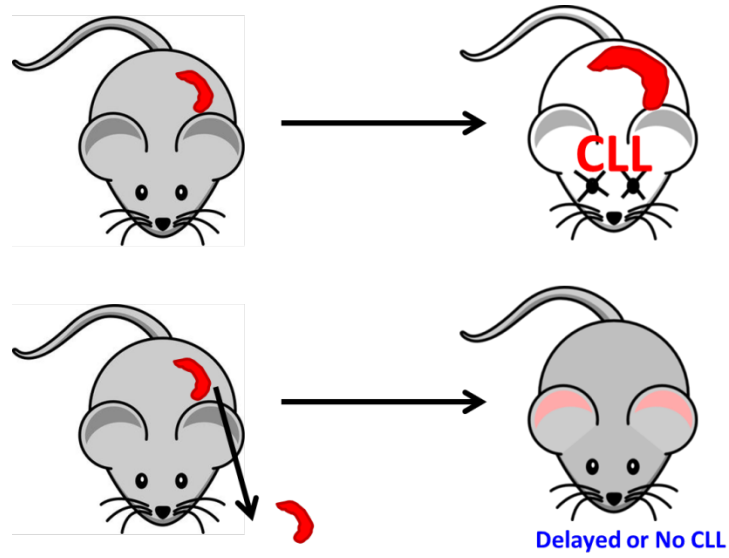


Figure 6.5B

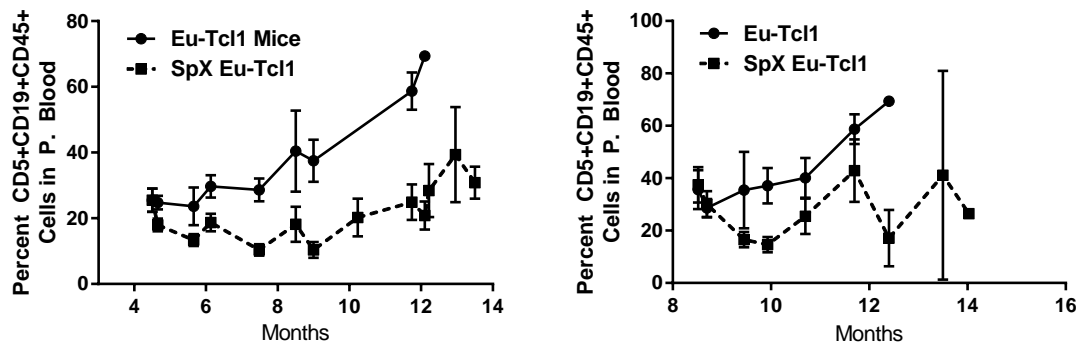


Figure 6.5C

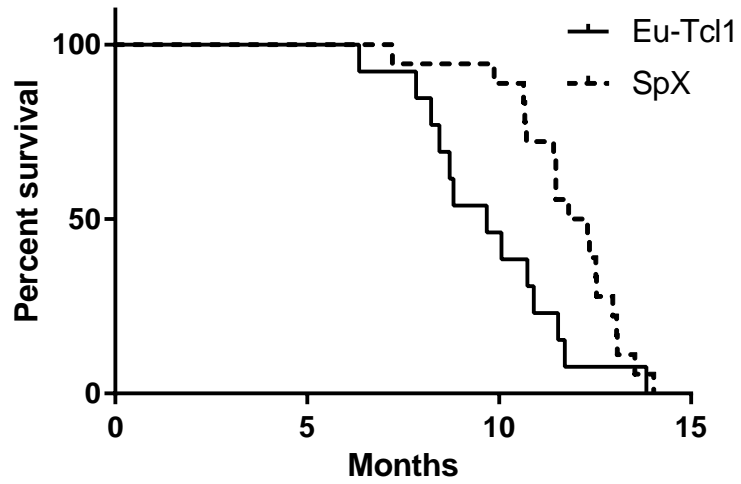


Figure 6.5D

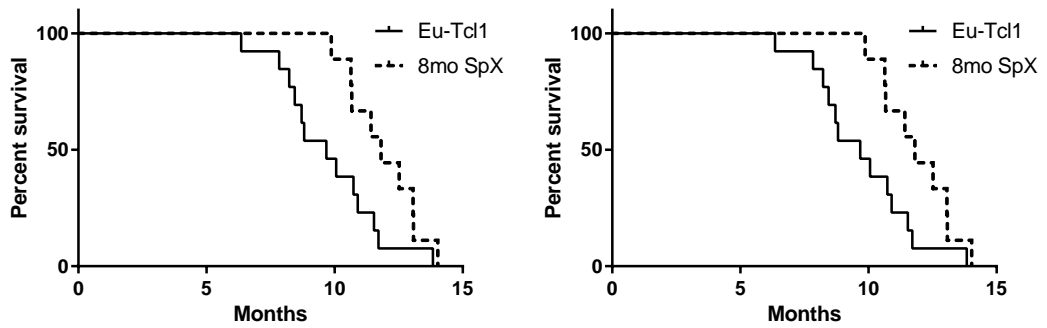


Figure 6.5E

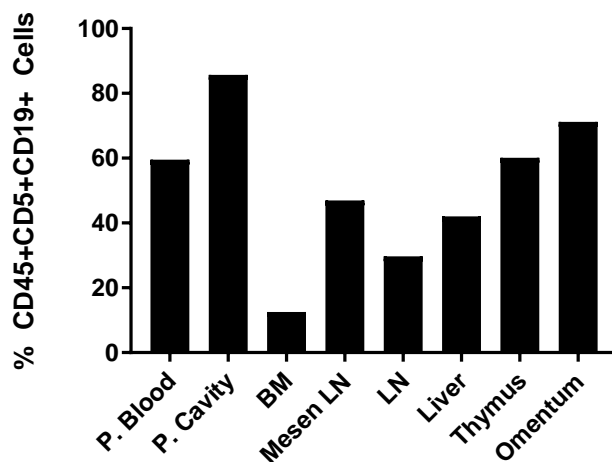


Figure 6.5F

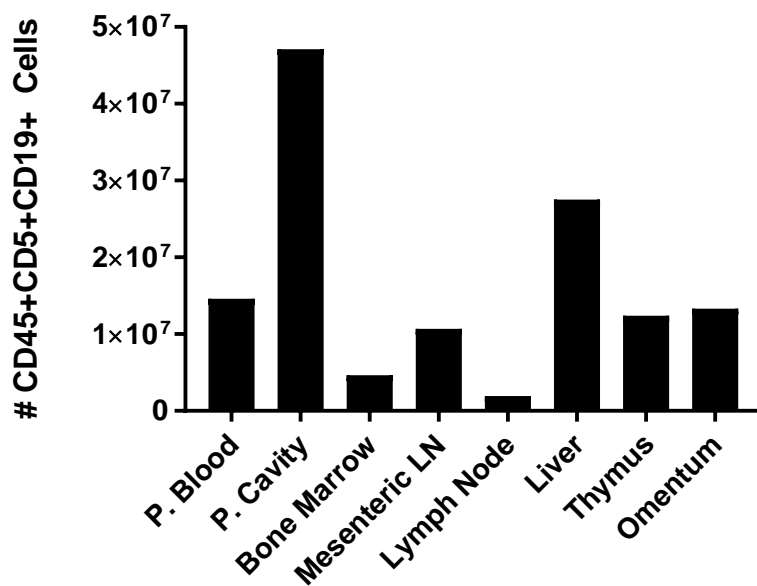




Figure 6.5 Splenectomy delays the development and growth of CLL

A) Schematic diagram of the effect of splenectomy on CLL development in the E $\mu$ -Tcl1 mouse model. B) Percentage of CD45+CD5+CD19+ cells in the peripheral blood of E $\mu$ -Tcl1 CLL cells over time with and without splenectomy. Left: animals splenectomized at 4mo, Right: animals splenectomized at 8mo. Values represent mean  $\pm$  SE. SpX n=9, Eusplenic n=13 C) Overall survival of E $\mu$ -Tcl1 mice with (n=13) and without spleen (n=18). P value = 0.02 determined by Log-Rank test. D) Breakdown of overall survival of animals splenectomized at 4mo (left) and 8mo (right) to E $\mu$ -Tcl1 mice with spleens. Nine animals in each age group are included compared to 13 animals with spleen. 4mo p value = 0.06, 8mo p value = 0.043 determined by Log-Rank test. E) CD45+CD5+CD19+ cells within the tissues of a representative splenectomized E $\mu$ -Tcl1 mouse. F) Tumor burden of CLL cells within different tissues of a representative splenectomized mouse.

Table 7: Summary of splenectomized Eμ-Tcl1 mice.

#	Age at Spx	Tag	Age at Death	Status	At Death: P. Blood CD5+CD19+ Cells %	Diagnosis
1	4Months,30Days	1614	12mo 11, days	Euthanized 4-21-16	9.97	no CLL
2	4Months,30Days	1611	10 mo, 27 Days	Euthanized 3-8-16	65.4	CLL
3	4Months,23Days	1618	11mo, 15 days	Euthanized 4-1-16	13.78	start CLL
4	5Months,18Days	1561	12 mo, 30 days	Euthanized 4-21-16	25.93	CLL
5	5Months,18Days	1565	12 mo, 10 days	Euthanized 4-1-16	41.99	CLL
6	5Months,18Days	NT	12mo, 17 days	Euthanized 4-8-16	93.45	CLL
7	5Months,16Days	1569	13mo, 17 days	Euthanized 4-21-16	35.68	CLL
8	5Months,16Days	1562	11 mo, 15 days	Euthanized 2-17-16	26.77	CLL
9	5Months,16Days	1566	7 mo,7Days	Died		missed
10	8Months,16Days	1351	11 mo, 25 Days	Euthanized 12-18-15	7.58	no CLL
11	8Months,16Days	1358	13mo, 2 days	Euthanized 1-26-16	1.32	no CLL
12	8Months,12Days	1360	9mo, 27 days	Euthanized 10-23-15	11.71	no CLL
13	8Months,12Days	1361	13 mo,1Days	Euthanized 1-26-16	80.99	CLL
14	8Months,14Days	1355	11 mo, 25 Days	Died		missed
15	8Months,14Days	1353	12 mo, 16 days	Euthanized 1-20-16	56.78	CLL
16	8Months,14Days	1357	10 mo,19Days	Euthanized 11-12-15	4.76	no CLL
17	8Months,14Days	1352	10 mo,20Days	Died		CLL
18	11Months,18Days	B3809	14 mo, 1Days	Euthanized 11-23-15	26.47	no CLL



Figure 6.7A

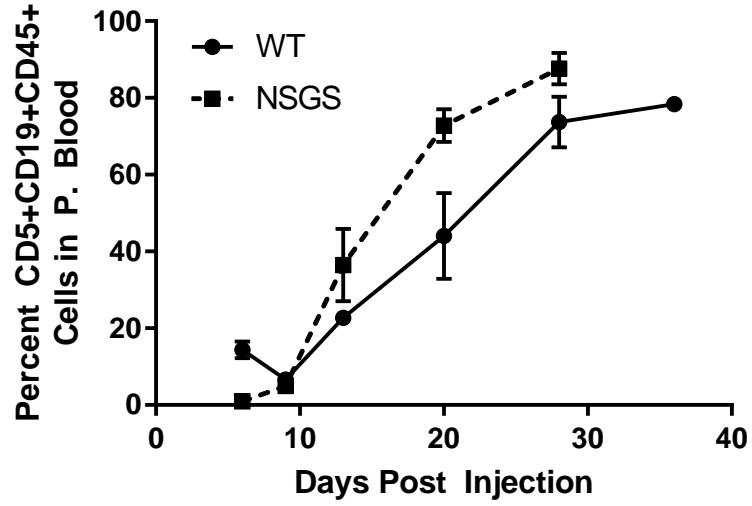


Figure 6.7B

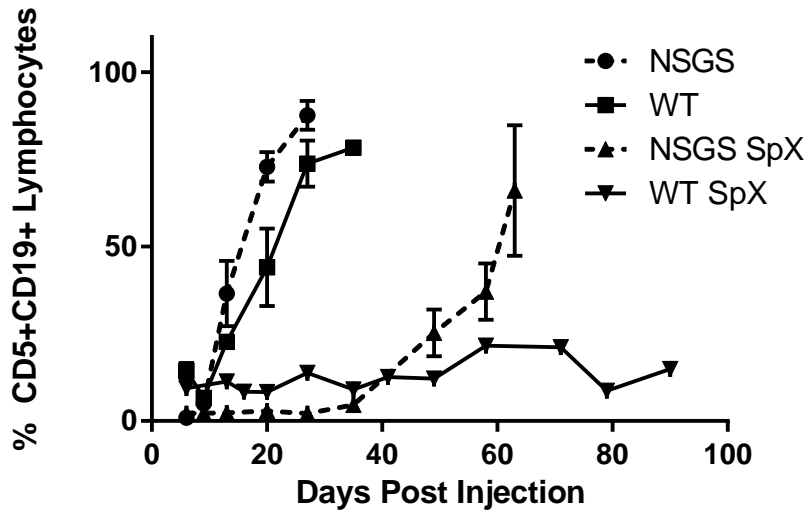


Figure 6.7C

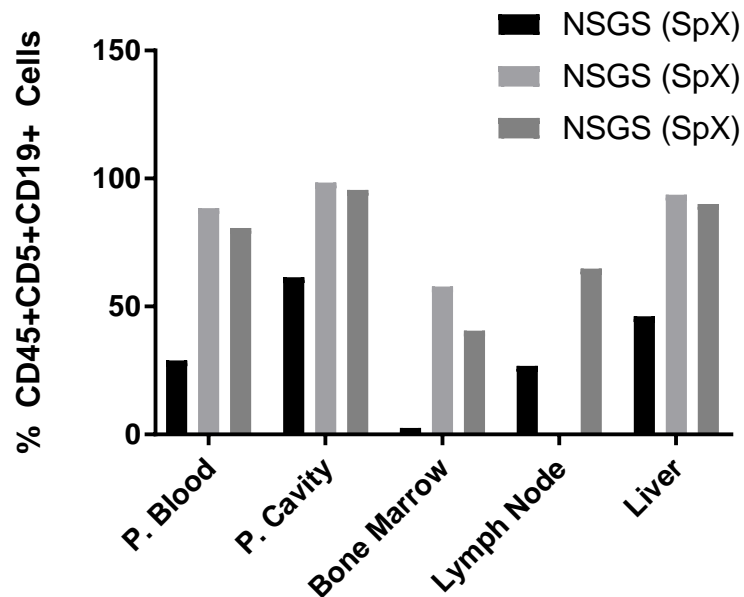


Figure 6.7 CLL cells do not require B, T, or NK cells in the microenvironment niche

A)  $5.0 \times 10^6$  E $\mu$ -Tcl1 CLL cells were adoptively transferred into BL/6 or NSGS mice (n=4 each) and the recipients were monitored for CD5+CD19+ cells in the blood at various times after CLL cell injection. The differences in the slopes of two lines of CLL kinetics in the two groups of recipients are statistically significant (p value= 0.026 as determined by linear regression analysis). B) Experiment described in panel A is repeated with SpX BL/6 and NSGS (figure legend says NSGS) mice. C) Tissues from three SpX NSG mice were collected once CLL was detected in the blood. Values represent the % of CD5+CD19+ cells gated on CD45+ in the peripheral blood, peritoneal cavity, bone marrow, lymph node, and liver. Each bar represents one mouse.

Figure 6.8A

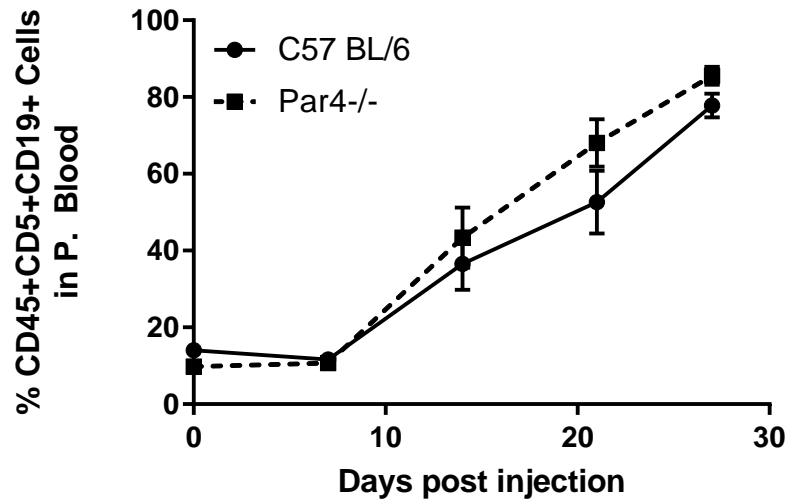


Figure 6.8B

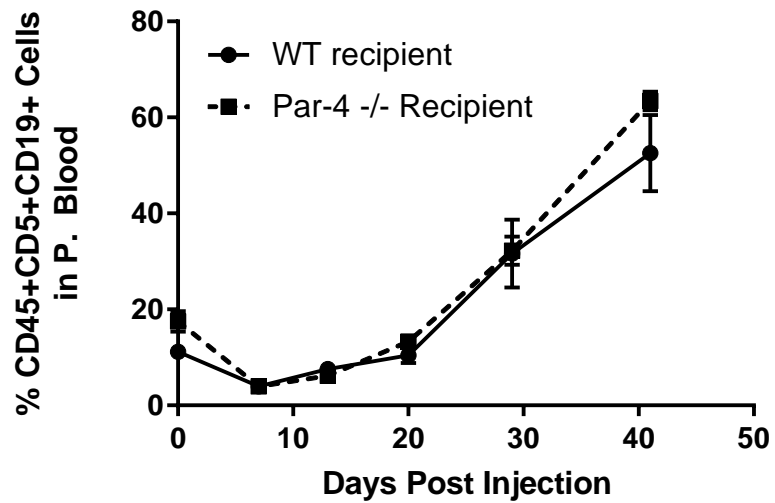


Figure 6.8 Adoptive transfer of CLL cells into Par4<sup>-/-</sup> vs Par4<sup>+/+</sup> recipient mice

A)  $10 \times 10^6$  Par4<sup>+/+</sup> E $\mu$ Tcl1 CLL cells were injected (i.v.) into WT BL/6 and BL/6.Par4<sup>-/-</sup> recipients. Values represent mean  $\pm$  SEM of results from three experiments with a total of n=12 recipients per group. P value = 0.3441 determined by linear regression analysis. B) Par4<sup>-/-</sup> E $\mu$ Tcl1 CLL cells ( $10 \times 10^6$ ) were adoptively transferred (i.v. route) into WT and Par4<sup>-/-</sup> recipients. n=5/group. P value = 0.79 determined by linear regression analysis. Graphs show the change in % CD45+CD5+CD19+ cells in blood as a function of time.





Figure 6.9 CLL develops faster in splenectomized Par-4<sup>-/-</sup> recipients

Par4<sup>+/+</sup>E $\mu$ Tcl1 CLL cells ( $7.8 \times 10^6$ ) were transferred into splenectomized Par4<sup>-/-</sup> and WT recipients via the i.v. route. 3/6 of Par-4<sup>-/-</sup> splenectomized animals, but only 1/6 WT SpX mice developed CLL 70 days after transfer. B) Endpoint percent CD5+CD19+ cells in peripheral blood of all adoptive transfer studies to Par-4<sup>-/-</sup> and WT splenectomized recipients. 50% of splenectomized Par-4<sup>-/-</sup> recipients developed CLL compared to 20% of WT splenectomized recipients.

## Summary

Defining the CLL microenvironment is critical in order to understand how leukemic cells evade apoptosis and continue to proliferate. The spontaneous apoptosis of primary CLL cells observed in tissue culture provides evidence for the necessity of supportive stromal cells and other factors required to promote survival. Due to the difficulty in culturing CLL cells, mouse models have proven to be an excellent tool to study the growth regulatory mechanisms of CLL. We and others have shown that the E $\mu$ -Tcl1 mouse model develops CLL-like disease characterized by an accumulation of CD5+CD19+ lymphocytes in secondary lymphoid organs, including the spleen as it progresses with age [144, 211]. The expansion of leukemic cells is consistently reproduced in the adoptive transfer model which we have now characterized by ultrasound imaging. CLL cells are first detected within the spleen and not in other lymphoid tissues or liver until later time points after adoptive transfer. Utilizing the human ROR1-expressing CLL cells, we confirmed that the spleen is the initial site for CLL homing after transfer. This phenomenon is also not dependent on the route of injection as studies in the laboratory have found that CLL cells are prominent in the spleen of recipient mice after intravenous, intraperitoneal, and subcutaneous injections of mouse CLL cells. This observation is also made when transferring primary human peripheral blood cells into NSG mice. Five days after transfer, human cells are detected primarily within the spleen.

Splenectomy of both the de novo E $\mu$ -Tcl1 and adoptive transfer recipients dramatically delayed the development of CLL. In healthy hosts, the spleen stores more than a quarter of the entire lymphocyte population and can expand to hold more red blood cells or WBCs when needed during an immune response. The spleen's ability to expand contributes to the gross pathology that is observed in mouse models. Therefore, removal of the spleen initially relieves the animal of the bulk of the tumor load. The surprising finding in the de novo E $\mu$ -Tcl1 model

after splenectomy is that some mice never developed CLL and were essentially cured of leukemia. This was not true for all cases, but further studies to determine why CLL progression occurs in some, but not all mice after splenectomy would be of interest.

Initial removal of the spleen before adoptive transfer of CLL cells dramatically prevents CLL growth in C57Bl/6 WT mice. This is thought to be due to the loss of the primary site of growth and CLL cells cannot establish another site for proliferation. To further support our observations, it would be of interest to adoptively transfer CLL cells to recipient mice and to perform splenectomy after CLL cells are established in the spleen for 2-3 days. This would more closely represent what is seen in many patients that are likely to have CLL in the spleen before disease is detected in peripheral blood.

CLL growth was detected in 50% of splenectomized Par-4 deficient animals as compared to 20% of CLL growth observed in splenectomized C57Bl/6 animals. This is a surprising finding as our preceding studies have indicated that intrinsic Par-4 does not act as a tumor suppressor in the context of CLL. The lack of Par-4 in secondary sites of proliferation allows for the growth of CLL which suggests that intrinsic and extracellular Par-4 may play different roles in CLL. The studies presented here investigating the role of Par-4 in the microenvironment are preliminary and primarily observational. Studies to define the mechanism by which Par-4 prevents CLL growth in sites other than the spleen are underway.

## CHAPTER 7

### Discussion

Par-4 is a well-known tumor suppressor that is down regulated in several cancers and can selectively induce and sensitize cancer cells to apoptosis[267]. This quality has made Par-4 an attractive therapeutic target in a variety of cancers, yet there are very few studies investigating its regulation. However, there are several studies that have investigated Par-4 expression in CLL. Human peripheral blood CLL samples express Par-4 but these studies did not confirm if it is functional. Chow et al. suggested that Par-4 could be responsible for a patient's ability to respond to imatinib treatment but did not confirm if Par-4 was functionally inducing apoptosis of neoplastic cells after treatment [202]. Other studies indicate that Par-4's interactions with other proteins such as Bcl-2 is not consistent in CLL as it is in solid tumors [190, 203]. These results suggest that Par-4 is regulated differently in CLL than what is currently known from other tumor studies. This proposed difference could potentially contribute to one of the many defects in the apoptotic pathway that is found to characterize CLL. In this study, I originally aimed to define the tumor suppressive role of Par-4 in CLL, but made an unexpected and exciting discovery that intrinsic Par-4 rather promotes CLL growth. My studies found that BCR signaling pathway plays a surprising role in regulating Par-4 expression in CLL cells. I have shown that Par-4 secreted from CLL cells is functional in inducing apoptosis of other cancer cells leading to question why a pro-survival pathway is regulating the expression of a pro-apoptotic factor. My studies knocking down intrinsic Par-4 expression in CLL cells suggest Par-4 has a novel role in regulating cell growth mechanisms that include induction of p21 expression. Additionally, I found that Par-4 in the secondary CLL microenvironments may act to prevent the growth of CLL. These findings imply that Par-4 has pleiotropic roles within the context of CLL making it an interesting protein to investigate.

In this thesis I characterized the expression of Par-4 in CLL. This is the first investigation of the role of Par-4 in CLL using the E $\mu$ -Tcl1 mouse model to compare levels of expression in malignant CLL cells against normal B1a cells. I have identified a novel regulation of Par-4 through the BCR signaling pathway that was previously unknown. I have also confirmed much of our findings in the mouse model with primary human CLL samples allowing my results to be translated to patients.

### 7.1 Increased expression of Par-4 in CLL and novel regulation through BCR signaling

Both mouse E $\mu$ -Tcl1 CLL cells and primary human CLL cells express high levels of Par-4 compared to normal B cell subsets and whole peripheral blood samples. Increased expression levels led to concerns if Par-4 expressed in CLL cells was mutated, but I confirmed that Par-4 was found in both the cytoplasm and the nucleus of CLL cells and that secreted Par-4 functionally induced apoptosis of other cancer cell lines. Additionally, knockdown studies of Par-4 in the Mec-1 CLL cell line confirmed that Par-4 was functionally interacting with well-defined targets such as activated AKT and regulated Bcl2 expression [178, 193]. This was an interesting finding since Par-4 knockdown cells were growing more slowly in culture than the control shRNA infected cells leading me to hypothesize about how Par-4 may support growth in CLL. Previous studies in CLL could not replicate the inverse relationship between Par-4 and Bcl2 that have initially been proposed in transformed fibroblasts and PC-3 cells [190, 191]. More specifically, one study found a positive correlation between expression of Par-4 and Bcl-2 in CLL patient samples ( $R=0.7$ ) [203]. Cheema and colleagues discovered that Par-4, along with WT-1 (Wilm's tumor suppressor-1) binds to the Bcl-2 promoter to prevent its expression and pro-survival activity [268]. Ectopic expression of Par-4 in androgen-independent prostate cell lines resulted in decreased Bcl-2 protein and transcript levels along with an increase in WT-1 expression. Par-4 has previously been shown to interact with the WT-1 promoter [162]. WT-1 is an interesting

protein as it has been classified as both a tumor suppressor and oncogene [269]. WT-1 is found to be required for normal development but when mutated, is associated with development of kidney tumors and urogenital disease. Conversely, high WT-1 expression has been found in nearly 74% of AML and 66% of ALL patients and is associated with a worse prognosis and poor response to therapy. Cosialls and colleagues concluded that the WT-1 promoter region is silenced by hypermethylation in 78.4% of CLL cases [270]. Consistent with this, another study screening for tumor associated antigens in CLL did not detect WT-1 mRNA in 43 human CLL cases [271]. The lack of WT-1 expression detected in CLL cases could be responsible for the discrepancy of the Par-4-Bcl-2 relationship in human CLL cases. Without the co-interaction of WT-1 in CLL, Par-4 may not be able to downregulate Bcl-2 expression as shown in studies by Boehrer and Borjarska-Junak [190, 203]. With those points in mind, I still observed an increase in Bcl-2 expression in Par-4 shRNA mediated knockdown in Mec-1 cells (Figure 5.1B). It would be of interest to determine the status of WT-1 in the Mec-1 cell line to determine if the requirement of WT-1 is essential for Bcl-2 regulation by Par-4 in CLL cells. We are currently investigating if Bcl-2 expression is changed in the Par4<sup>-/-</sup>E $\mu$ -Tcl1 versus Par4<sup>+/+</sup>E $\mu$ -Tcl1 cells to be certain that the inverse expression is not specific to Mec-1 cells.

We are currently sequencing Par-4 to confirm that it is not mutated in CLL. As noted previously, our studies indicate that Par-4 is functional by its ability to localize within the cytoplasm and nucleus. Detection of phosphorylation at Thr155 (rat) or Thr163 (human) would confirm that the PKA phosphorylation site is intact which is required for Par-4 mediated apoptosis [169]. The Par-4 nuclear location sequence 2 (NLS2) enables Par-4 to translocate to the nucleus, but NF- $\kappa$ B inhibition is only observed after Thr163 phosphorylation. PKA is known to be active in CLL cells and it would be ideal to determine that the threonine site is still intact in CLL Par-4 [272].

Additionally, I have utilized the online database CBioPortal for cancer genomics to investigate if there are known mutations of the Par-4 gene in banked CLL patient samples. CBioPortal provides exploration of multi-dimensional cancer genomic data sets to determine mutation status of particular genes within individual patients [273, 274]. This program classifies a gene alteration in a patient if it is mutated, deleted, amplified, or if its expression deviates from the user-defined normal threshold [273]. I analyzed the status of the *PAWR* gene within two available data sets: Chronic Lymphocytic Leukemia, Broad Cell 2013 that consisted of 160 samples and IUOPA Nature 2015 consisting of 506 samples [275, 276]. No *PAWR* gene alterations were detected in these two studies. I confirmed that the program could indeed identify *PAWR* gene alterations in known tumor models by investigating its status in the Pan-Lung Cancer TCGA Nature Genetics 2016 study comprised of 1144 samples which indicated a combination of mutations, deletions, and amplifications of *PAWR* [277]. This brief analysis suggests that the *PAWR* gene is currently not found to be mutated in human CLL patients but our current studies are will further confirm this conclusion.

It is well accepted that CLL cells contain activated Akt which is pivotal in maintaining cell survival [278]. Akt is also known to phosphorylate Par-4 at Ser249 (rat)/ Ser230 (human) that prevents nuclear translocation and Par-4 mediated apoptosis [170]. We do observe activated levels of Akt in primary mouse E $\mu$ -Tcl1 CLL cells consistent with what has been published previously [228]. Tcl1 is a known co-activator of Akt and is a contributing factor in Akt activity in the E $\mu$ -Tcl1 mouse model [217]. Tcl1 has been found to interact with Akt through the pleckstrin homology domain of Akt which alters the cellular localization of the kinase. Tcl1 helps facilitate Akt phosphorylation at both Thr308 and Ser473 sites by translocating it to the cell membrane for PI3K signaling [279]. Transfection of cells with Akt and Tcl1 also results in Akt translocation to the nucleus [217]. Akt nuclear localization has recently been described to inhibit chromatin

condensation, regulate cell cycle progression, cell survival and double stranded DNA break repair [280]. We observed elevated levels of Tcl1 expression in the mouse E $\mu$ -Tcl1 CLL cells and activated levels of Akt suggesting that this may be another level of regulation of Par-4. As mentioned earlier, Akt and Par-4 act on each other to regulate their functions in many different solid tumor models. We have not investigated the interaction of Akt and Par-4 in the E $\mu$ -Tcl1 mouse, but because of the interactions described with Tcl1-Akt and Akt-Par-4, it is possible that Par-4 could be regulated by this pathway as well. We do see Par-4 is within the nucleus of CLL cells, but we do not know the mechanism of action. According to Pekarsky and colleagues, Tcl1 complexes with Akt to translocate to the nucleus and one possibility is that Par-4 could be found within this complex as well. Immunoprecipitation studies could determine if all three of these proteins are interacting. CLL survival does not appear to depend on Par-4 nuclear location, suggesting that Par-4 may not be inhibiting NF- $\kappa$ B. A tripartite complex of Tcl1-Akt-Par-4 may prevent Par-4 mediated NF- $\kappa$ B inhibition. However, this hypothesis is not supported by the observation that Mec-1 cells do not express high levels of Tcl1 and neither does every human CLL clone, despite increased expression of Par-4.

The Tcl1 oncogene has been found to interact directly with de novo DNA methyltransferases DNMT3a and DNMT3b in CLL [281]. DNA methyltransferases are enzymes that methylate CpG islands that result in silencing of a target gene. Some hematological cancers have mutations that inactivate DNA methyltransferases leading to over expression of driver genes that promote disease [282]. Studies utilizing the E $\mu$ -Tcl1 mouse found a two to four fold increase in hypomethylated CpG islands and promoter regions in B cells expressing Tcl1 compared to WT mouse B cells [281]. These results suggest that overexpression of Tcl1 blocks DNMT3a enzyme activity and therefore promotes expression of other genes. Interestingly, Par-4 promoter methylation and silencing has been detected in 30% of endometrial cancers [283].



Other studies have found Par-4 promoter hypermethylation in Ras-transformed cells which is attributed to an upregulation in DNMT3a expression and activity [284]. It is possible that the Par-4 upregulation that I observed in E $\mu$ -Tcl1 cells is due to the lack of DNMT3a activity. I do not have consistent results suggesting the Tcl1 is regulated through BCR signaling so it is not likely that the promoter hypomethylation observed in E $\mu$ -Tcl1 CLL cells is due to BCR signaling regulation. It would be interesting to first confirm if Par-4 promoter is regulated by DNMT3a methylation in CLL and then to measure protein levels in Tcl1+ and Tcl1- CLL cells to see if there is a change in Par-4.

Immunoblot analysis indicated that E $\mu$ -Tcl1 CLL cells expressed high levels of Par-4 compared to normal B cell subsets. Normal B1a cells that express CD5+CD19+ markers expressed the highest level of Par-4 and had slightly higher basal levels of phosphorylated SFK and Lyn compared to B1b and B2 cells, but less than CLL cells. We are the first group to compare CLL BCR signaling and Par-4 expression with the correct B cell subset controls. I conclude that increased Par-4 levels are not caused by Tcl1 expression as discussed earlier. B1a cells have increased Par-4 expression compared to other B cell subsets and also differ in expression of CD5 uniquely. Is CD5 expression related to Par-4? I did not study this closely but could examine the effect of anti-CD5 antibody treatment to CLL cells or siRNA targeting CD5 to determine the effect on Par-4 expression. CD5 has been shown to negatively regulate BCR signaling by recruiting SHP-1 (Src homology 2 containing phosphatase 1) to the BCR signaling complex [75]. Similarly in CLL, studies have found that Lyn is able to phosphorylate CD5 leading to the recruitment of SHP-1 to inhibit BCR signaling [108]. Lyn is known to be involved in both activation and inhibition of B cells. My studies link Lyn expression and Par-4 in CLL and regulation of Par-4 expression through CD5 could be a potential mechanism that requires further study.

Based on my findings and the importance of BCR signaling in the survival of CLL, this was a likely pathway to be involved in Par-4 regulation [48, 127, 250]. Inhibitors of kinases involved in BCR signaling and shRNA mediated knockdown of Lyn kinase in the Mec-1 cell line as well as in the B cell lymphoma line, LY-3 (Figure 4.3D) clearly demonstrate regulation of Par-4 expression through the BCR signaling pathway. Studies utilizing siRNA targeting CD79a (Ig $\alpha$ ) further confirm that Par-4 expression is regulated by the BCR signaling pathway avoiding the off target effects of kinase inhibitors (Figure 4.3G).

We also investigated if BCR signaling inhibition led to a decrease in Tcl1 oncogene expression to determine if it's down regulation was a contributing factor to CLL cell death. We did not observe consistent down regulation of Tcl1 after BCR inhibition until very late time points when most of the cells were dead ( $\geq$  48hrs). Hence it is unlikely that Par-4 down regulation involves the effect of BCR signaling on Tcl1 expression. However, as discussed briefly in Chapter 4, the delayed downregulation of Par-4 observed after BCR kinase inhibition may result from Par-4 being bound in a tripartite complex of proteins. The potential interactions of Par-4 and Akt as well as Akt-Tcl1 in primary CLL could create a ternary complex that provides stability of protein expression after cytotoxic treatment with BCR inhibitors. Immunoprecipitation assays of Par-4 would be required to see if Akt and Tcl1 are both bound to further develop this hypothesis.

When BCR signaling is engaged, Src family and Syk protein kinases are activated which triggers activation of complex downstream signaling networks that include phospholipase C $\gamma$  to PI3-K pathway and Ras-MAPK (ERK) pathway [132]. My finding that targeting ERK1/2 in E $\mu$ -Tcl1 CLL cells results in a decrease in Par-4 expression further confirms that Par-4 is regulated by survival signaling in malignant CLL cells. This is an interesting finding compared to studies investigating Par-4 regulation via Ras in fibroblasts where it was shown that Par-4 works to block

ERK2 expression in order to prevent oncogenic transformation [181]. In my studies it is conceivable that Par-4 is regulated directly by SFKs and/or Akt. Thus, the difference in Par-4/ERK regulation in CLL B cells and fibroblasts could be due to tissue specific effects.

Kline et al. previously reported that c-Src and Par-4 interact independently of Akt1 [285]. Treatment of HT29 colon cancer cells with PP2, an SFK inhibitor, and 5-FU (5-fluorouracil) a chemotherapeutic agent, led to increased Par-4 activation by preventing the negative regulation of Par-4 by Akt1 and 14-3-3 $\sigma$ . Direct inhibition of c-Src reduced interactions of Par-4 with Src which was predicted to be through three tyrosine residues on Par-4. This suggests a novel regulation of Par-4 in colon cancer cells. Oncogenic SFKs as well as activated Akt are well established in CLL, suggesting that these interactions could be responsible for Par-4 regulation [109, 278, 286]. Studies to observe the effect of AKT inhibition in CLL on Par-4 expression would be of interest to confirm the novel regulation of Par-4 through survival pathways in CLL.

A recent study investigating the mechanism of Par-4 regulation in pancreatic cancer suggests that Par-4 is negatively regulated by TRIM21(Ro52) [287]. TRIM21 is an E3 ubiquitin ligase that functions to ubiquitinate protein substrates, targeting them to proteosomal degradation. In response to cisplatin treatment, TRIM21 downregulated Par-4 expression in a pancreatic cancer cell line. TRIM21 has also been identified as a target of autoantibodies in Sjogren's Syndrome and Systemic Lupus Erythematosus (SLE) where increased levels of TRIM21 resulted in increased apoptosis of B cells [288]. Of the tripartite motif (TRIM) family members, currently TRIM13 (also known as Leu5) has been associated with CLL, as it is contained in the chromosome 13q14 region deleted in many CLL cases. Hence it will be interesting to investigate TRIM21 expression and the effect of BCR signaling on TRIM21 in CLL [289].

Another potential mechanism of Par-4 regulation in CLL is through Casein Kinase 2 (CK2). CK2 is a serine/threonine kinase that has been found to phosphorylate Par-4 at Ser231,

which inhibits its pro-apoptotic activity in prostate cancer cells [290]. CK2 has also been found to be hyper-activated and overexpressed in CLL cells [291]. Investigating Par-4 phosphorylation at Ser231 could also explain why we do not observe the pro-apoptotic actions of intrinsic Par-4.

## 7.2 Role of p21 in pro-growth function of Par-4 in CLL

Knockdown studies targeting Par-4 in CLL generated a novel phenotype of delayed CLL growth *in vitro* and *in vivo*, which led us to investigate roles of Par-4 other than its tumor suppressor function. Because I observed an increase in pro-survival (pAkt) and anti-apoptotic factors (Bcl-2), my first hypothesis was cell cycle regulation. I initially looked at cell cycle inhibitors and indeed found an increase in p21 expression (Figure 5.2B). I also probed for p27 expression, and while there may be a slight increase in expression, it is not as significant as for p21. Studies in human CLL patient samples have looked for expression of p21 and p27. 80% of CLL cases were negative for basal levels of p21 expression while the majority of CLL cases expressed high p27 levels [265]. The low levels of p21 in CLL could potentially be due to increased levels of Par-4 in CLL. Along with *in vitro* studies using Par-4 knockdown Mec-1 cells we crossed Par-4<sup>-/-</sup> animals with the de novo E $\mu$ -Tcl1 mouse model of CLL to determine the role of Par-4 in the development of CLL *in vivo*. The Par-4 deficiency delayed CLL development in the E $\mu$ Tcl1 mice and also prolonged their survival compared to Par-4<sup>+/+</sup> E $\mu$ Tcl1 mice. The Par-4<sup>-/-</sup> CLL cells also exhibited an increase in p21 expression.

Recently, cyclin dependent kinase inhibitors are being investigated for the treatment of leukemia due to their success in solid tumors [292]. Dinaciclib, a CDK1, CDK2, CDK4 and CDK5 inhibitor, reduced survival of CLL cells by inhibiting key oncogenic pathways vital for CLL survival [293]. Our studies identify Par-4 as a factor involved in the cell cycle through connection with p21 in CLL cells as reduced expression of Par-4 led to a halt in the G1/S transition of the cell cycle and a reciprocal induction of p21 expression. Interestingly, Igawa et al. observed that CLL

cells in the proliferation centers located in the lymph node highly expressed cyclin D2 which is involved in the transition between G0/G1, a stage at which p21 activity is down regulated in cycling cells [294, 295]. Studies investigating the interaction of Par-4 and Cyclin D2 are warranted to elucidate the potential role that Par-4 is playing in promoting growth of CLL cells. P21 expression is regulated by p53 in most cases, although p53 independent p21 expression has been observed [296, 297]. Since p53 is mutated in Mec-1 cells, p21 expression in Par-4 knockdown and knockout cells may be using alternate pathways [298].

Another recent study investigated the relationship between Par-4 and p21 after inducing ER stress with the treatment of a natural compound derivative 3-AWA (3-Azido withaferin A) [299]. Depending on the dose of 3-AWA administered, induction of ER stress in prostate and colon cancer cells led to an increase in Par-4 expression and down regulation of p21. The authors suggested that the loss of activated Akt allowed for increased Par-4 expression which then promoted apoptosis. The reduced expression of p21 after treatment was found to be mediated by pro-apoptotic JNK (Jun N-terminal kinase) activation. JNK has been found to be a key player in stress induced cell death in both normal cells and solid tumor cancers [300]. Conversely our lab has discovered that JNK is required for survival and proliferation of malignant B lymphoma cells suggesting a dual role for the kinase in solid versus hematological cancers [301]. The pro-survival role of JNK in B cell lymphoma was further confirmed in two recent studies that examined CARD11 and DUSP4 deficiencies in B cell lymphoma [302, 303]. The diverse roles that JNK potentially has in CLL versus endothelial based tumors may be contributing to the pro-growth function of Par-4 in CLL via p21 suppression. The AKT/Par-4/JNK/p21 axis defined by Rasool et. al. provides direction to investigate this pathway further in CLL due to the pro-growth roles we have found for JNK and Par-4 in B cell malignancies.

### 7.3 Par-4 in the tumor microenvironment

Introducing the Par-4 knockout allele into E $\mu$ -Tcl1 mice delayed progression of CLL and prolonged mouse survival compared to Par-4<sup>+/+</sup>E $\mu$ Tcl1 mice. Par-4<sup>-/-</sup>E $\mu$ Tcl1 mice are deficient for Par-4 in all tissues, not specifically in B cells (Figure 5.3B). My finding that CLL cells are able to secrete functional Par-4 introduces a level of complexity within the in vivo tumor microenvironment. I do not know if Par-4 secreted from the CLL cells is manipulating the microenvironment to further enhance the growth in Par-4<sup>+/+</sup> E $\mu$ Tcl1. In order to test, one could treat the Par-4<sup>+/+</sup> E $\mu$ Tcl1 mouse with an anti-Par-4 antibody to see if extracellular Par-4 in the mouse model is promoting or preventing the growth of CLL. In my splenectomy studies, the lack of Par-4 in the secondary tumor microenvironments appears to allow the growth of CLL suggesting that the presence of Par-4 is acting to prevent CLL growth in the sites which fits with its known tumor suppressor function. But this is only observed in splenectomized mice. This is important since I have shown spleen to be the primary niche where the CLL cells grow (Figure 6.1). While CLL cells do not appear to be sensitive to Par-4 sourced from an autocrine fashion, I do not know if Par-4 sourced from other cells results in CLL apoptosis. Studies investigating E $\mu$ -Tcl1 CLL cells treated with secreted Par-4 from other cancer cell lines or recombinant Par-4 have been performed by our collaborators. Results show that human CLL cells are not sensitive to recombinant Par-4 mediated apoptosis. Additionally, I observed slightly lower levels of total GRP78 expressed in CLL cells compared to other cancer cells. Experiments with antibody towards cell surface GRP78 must be performed to confirm that extracellular Par-4 is able to functionally bind its receptor and induce apoptosis in the proposed FADD dependent manner.

Injection of CLL cells into splenectomized C57BL/6 and Par-4 null mice resulted in a surprising finding that the lack of Par-4 enhanced the growth of CLL. This is a dramatic difference compared to WT mice where very few splenectomized recipients developed disease as opposed

to 50% of the Par-4 null mice that develop CLL. It is important to note that of the splenectomized Par-4<sup>-/-</sup> mice that did develop CLL, all recipients were females. This is an interesting finding as both female and male mice lacking Par-4 leads to the development of endometrial or prostate hyperplasia respectively [172]. 56% of males develop prostate hyperplasia while 36% of females develop endometrial tumors, suggesting that Par-4<sup>-/-</sup> males actually have a greater likelihood to develop tumors. Because of the gender difference in splenectomized mice, we question if hormone levels play a role in regulating the development of CLL. Could elevated testosterone levels in male mice prevent CLL growth in the Par-4<sup>-/-</sup> background? This can be tested by castrating male Par-4<sup>-/-</sup> mice, followed by splenectomy and injection of CLL to see if changes in hormone level result in differential CLL growth rate. Or could ovariectomy in female mice lead to reduced development of CLL in splenectomized recipients? Interestingly, a 2005 study found the oestradiol injection into mice resulted in decreased Par-4 levels suggesting that estradiol regulates Par-4 [172]. Additionally estradiol has been found to promote NOTCH signaling which can promote VEGF and tumor development [304-306]. The elevated levels of estradiol in female mice could be promoting the growth of CLL cells when lacking Par-4. CLL is more prevalent in men than women, suggesting a gender bias and it would be curious to see if Par-4 is regulating this effect [307].

My findings suggest that the spleen is the primary site of growth in the CLL mouse model. In the clinic, physicians currently rely primarily on peripheral blood, lymph node and bone marrow involvement to evaluate patient status. Because I find that the majority of CLL cells are located within the spleen of mice in early stages of disease, physicians could be overlooking an initial proliferative setting with important prognostic implications. More importantly, if we are able to identify the cell types found within the mouse splenic microenvironment that are required for the growth of CLL we could also identify them in the

human for potential therapeutic targets. I have established a splenic stromal cell line derived from the E $\mu$ -Tcl1 mouse spleen. Preliminary studies suggest that co-culture of splenic stromal cells with CLL improves *in vitro* proliferation of CLL. This new stromal cell line could be of great use to help mimic the *in vivo* tumor microenvironment. These stromal cells are more effective than bone marrow stromal cell line or fibroblast cell line. Currently we are making efforts to establish a Par4<sup>-/-</sup> splenic stromal cell line.

#### **7.4 Summary**

My study of BCR signaling in CLL has provided important insights in CLL growth and led to development of new promising therapeutics [37]. Findings from our laboratory suggest that B cell lymphomas and other B cell malignancies are reliant on the BCR signaling pathway and therefore provides multiple targets for therapy [36]. I have used approved inhibitors to target kinases within the BCR pathway to find that BCR signaling regulates Par-4 expression, a well-defined tumor suppressor. Unlike the down regulation that is observed in many solid tumors including prostate, lung, breast, and pancreatic, Par-4 is highly expressed in CLL. This finding markedly suggested that Par-4 regulation is altered in CLL and indeed, we find its expression is reliant on the BCR survival pathway in CLL. My studies showed that endogenous Par-4 is regulating the growth of CLL cells and loss of expression delays CLL development. Upregulated p21 expression is likely responsible for reduced growth in Par-4 knockdown cells. Additionally, I find that Par-4 plays a role in secondary microenvironments of CLL by preventing CLL growth in splenectomy models (summarized in Figure 7.1). This initial study is the first to closely examine Par-4 and its regulation in CLL and its contribution to the complexity of the disease.



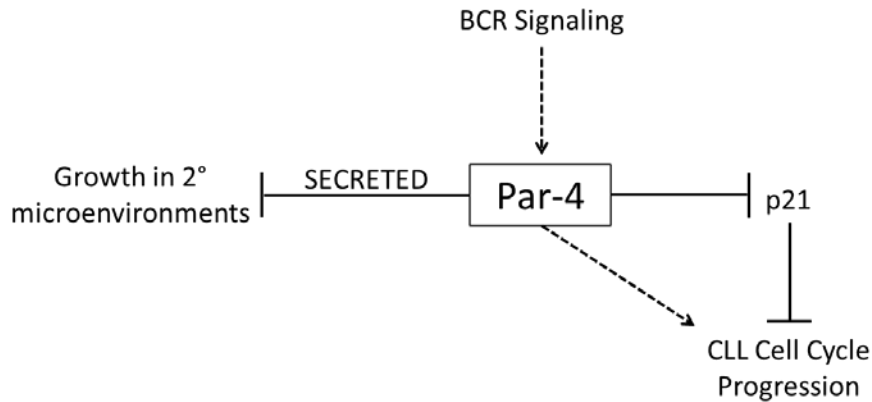


Figure 7.1 Summary of the Role of Par-4 in B-cell Chronic Lymphocytic Leukemia

Par-4 has pleiotropic roles within CLL. BCR signaling regulates Par-4 expression in CLL. Inhibition of BCR signaling results in CLL cell death and therefore prevents growth. Par-4 inhibits the expression of p21 which is known to block cell cycle progression. The inhibition of p21 by Par-4 leads to enhanced cell cycle progression and cell growth. Additionally, Par-4 has been found to be secreted from cells. The absence of spleen, the primary microenvironment of CLL, leads to reduced CLL growth and development.

Par-4 has been defined as a tumor suppressor and pro-apoptotic factor in many solid tumors but we propose a different role for intrinsic Par-4 in this hematologic disease. This is unconventional, but not the first case in which a molecule has variable roles in different diseases, especially between solid and hematological-based tumors. As mentioned earlier, JNK was defined as a pro-apoptotic factor that is activated in response to UV damage and stress leading to apoptosis in fibroblasts, prostate cancer, and neuronal cells [301]. Other studies then found that JNK is involved in survival signaling of BCR/ABL transformed leukemic cells leading to increased B cell transformation [308]. The dual role in apoptotic and survival signaling makes the function of JNK complex and dependent on the cellular context [301]. The additional role of Par-

4 in CLL also makes it a complex protein and potentially provides another target for CLL-specific therapy.

Additionally, this study is important as I have identified intrinsic Par-4 as a pro growth factor in CLL which could have implications since Par-4 is currently a target of a clinical trial [246]. Studies have found that the treatment of normal mouse and human cells with the anti-malarial drug, chloroquine, induces Par-4 secretion [309]. Induced paracrine secreted Par-4 triggered apoptosis of cancer cells in a mouse lung tumor model. These results led to a clinical trial where patients will receive hydroxychloroquine orally every day after tumor resection for 90 days. This clinical trial is still in the phase of recruiting patients and we are eager to see the promising outcomes of Par-4 secretion for the treatment of solid tumors. I find that loss of Par-4 in the secondary microenvironments allows for CLL growth which would further support the need for the clinical trial to prevent cancer growth. Also, the SAC transgenic animals that over express the cancer specific pro-apoptotic domain of Par-4 do not show any signs of developing leukemia [310]. Although this study did not quantify levels of the SAC domain in the plasma of the animals, it is known that the SAC domain is secreted from normal cells [199]. Because my studies prove only intrinsic Par-4 is responsible for promoting cell growth and I do not have evidence to suggest that extracellular Par-4 is taken up by CLL cells to further promote transformation or growth, I do not think inducing Par-4 secretion in the clinical trial would increase that patient's chance to develop CLL.

I find that Par-4 promotes the growth of CLL in the E $\mu$ Tcl1 mouse model and human Mec-1 cell line. It would be interesting to identify an inhibitor of Par-4 directly to see if a chemical modulator specific to this protein would result in decreased CLL progression in vivo as well. BCR inhibition has been proven effective in the treatment of CLL, but combination treatment towards other molecules that promote CLL growth could result in an improved

response. If inhibitors towards Par-4 could enhance the effectiveness of BCR inhibition, lower doses would be necessary and therefore minimize any adverse side effects. Continued work to identify other potential targets is critical to help patients fight CLL.

## REFERENCES

1. Institute, N.C. *Understanding Cancer*. What is Cancer? 2017 [cited 2017; Available from: <https://www.cancer.gov>.
2. Institute, N.C. *Understanding Cancer*. Cancer Statistics 2017 [cited 2017; Available from: <https://www.cancer.gov>.
3. Ferlay J, S.I., Ervik M, Dikshit R, Eser S, Mathers C, Rebelo M, Parkin DM, Forman D, Bray, F. *Cancer Incidence and Mortality Worldwide*. 2013 [cited 2017; GLOBOCAN 2012 v1.0:[Available from: <http://globocan.iarc.fr>.
4. Institute, N.C. *Surveillance, Epidemiology, and End Results Program*. Cancer Statistics 2017 [cited 2017; Available from: <https://seer.cancer.gov>.
5. Society, A.C., *Cancer Facts and Figures, 2017*. 2017: Atlanta.
6. Hanahan, D. and R.A. Weinberg, *The hallmarks of cancer*. Cell, 2000. **100**(1): p. 57-70.
7. Hanahan, D. and R.A. Weinberg, *Hallmarks of cancer: the next generation*. Cell, 2011. **144**(5): p. 646-74.
8. Whiteside, T.L., *The tumor microenvironment and its role in promoting tumor growth*. Oncogene, 2008. **27**(45): p. 5904-12.
9. Burger, J.A. and J.G. Gribben, *The microenvironment in chronic lymphocytic leukemia (CLL) and other B cell malignancies: insight into disease biology and new targeted therapies*. Semin Cancer Biol, 2014. **24**: p. 71-81.
10. Murphy, K. and C. Weaver, *Janeway's immunobiology*. 9th edition. ed. 2017, New York, NY: Garland Science/Taylor & Francis Group, LLC. xx, 904 pages.
11. Asma, G.E., R. Langlois van den Bergh, and J.M. Vossen, *Development of pre-B and B lymphocytes in the human fetus*. Clin Exp Immunol, 1984. **56**(2): p. 407-14.
12. Montecino-Rodriguez, E. and K. Dorshkind, *B-1 B cell development in the fetus and adult*. Immunity, 2012. **36**(1): p. 13-21.
13. Tumang, J.R., et al., *Peritoneal and splenic B-1 cells are separable by phenotypic, functional, and transcriptomic characteristics*. Eur J Immunol, 2004. **34**(8): p. 2158-67.
14. Hayakawa, K., et al., *The "Ly-1 B" cell subpopulation in normal immunodeficient, and autoimmune mice*. J Exp Med, 1983. **157**(1): p. 202-18.
15. Ray, A. and B.N. Dittel, *Isolation of mouse peritoneal cavity cells*. J Vis Exp, 2010(35).
16. Sindhava, V.J. and S. Bondada, *Multiple regulatory mechanisms control B-1 B cell activation*. Front Immunol, 2012. **3**: p. 372.
17. Griffin, D.O. and T.L. Rothstein, *Human b1 cell frequency: isolation and analysis of human b1 cells*. Front Immunol, 2012. **3**: p. 122.
18. Herzenberg, L.A. and L.A. Herzenberg, *Toward a layered immune system*. Cell, 1989. **59**(6): p. 953-4.
19. Pieper, K., B. Grimbacher, and H. Eibel, *B-cell biology and development*. J Allergy Clin Immunol, 2013. **131**(4): p. 959-71.
20. Bondada, S.C., Ralph L; and Gururajan, Murali, *B Lymphocytes*. eLS. John Wiley & Sons, Ltd, 2013.
21. Kraus, M., et al., *Survival of resting mature B lymphocytes depends on BCR signaling via the Igalpha/beta heterodimer*. Cell, 2004. **117**(6): p. 787-800.
22. Shaffer, A.L., A. Rosenwald, and L.M. Staudt, *Lymphoid malignancies: the dark side of B-cell differentiation*. Nat Rev Immunol, 2002. **2**(12): p. 920-32.

23. Howlader N, N.A., Krapcho M, Miller D, Bishop K, Kosary CL, Yu M, Ruhl J, Tatalovich Z, Mariotto A, Lewis DR, Chen HS, Feuer EJ, Cronin KA, *SEER Cancer Statistics Review, 1975-2014*, N.C. Institute, Editor. 2016: Bethesda, MD.
24. Institute, N.C. *Adult Hodgkin Lymphoma Treatment (PDQ)*. 2017 7/5/2017; Available from: <https://www.cancer.gov/types/lymphoma/hp/adult-hodgkin-treatment-pdq>.
25. Society, L.L. *Non Hodgkin's Lymphoma*. 2017; Available from: <https://www.lls.org/lymphoma/>.
26. Nordqvist, C., *Leukemia: Causes, symptoms, and treatment*, in *Medical News Today*. 2017, MediLexicon, Intl.
27. Sherbenou, D.W. and B.J. Druker, *Applying the discovery of the Philadelphia chromosome*. *J Clin Invest*, 2007. **117**(8): p. 2067-74.
28. Short, N.J. and F. Ravandi, *Acute Myeloid Leukemia: Past, Present, and Prospects for the Future*. *Clin Lymphoma Myeloma Leuk*, 2016. **16 Suppl**: p. S25-9.
29. Terwilliger, T. and M. Abdul-Hay, *Acute lymphoblastic leukemia: a comprehensive review and 2017 update*. *Blood Cancer J*, 2017. **7**(6): p. e577.
30. Institute, N.C. *Childhood Acute Lymphoblastic Leukemia Treatment (PDQ®)—Health Professional Version*. 2017 4/14/2017; Available from: <https://www.cancer.gov/types/leukemia/hp/child-all-treatment-pdq>.
31. *Chronic Lymphocytic Leukemia Treatment (PDQ(R)): Health Professional Version*, in *PDQ Cancer Information Summaries*. 2002: Bethesda (MD).
32. Dighiero, G. and T.J. Hamblin, *Chronic lymphocytic leukaemia*. *Lancet*, 2008. **371**(9617): p. 1017-29.
33. Institute, N.C. *SEER Cancer Stat Facts*. Chronic Lymphocytic Leukemia 2017; Available from: <http://seer.cancer.gov/statfacts/html/clyl.html>.
34. Ghia, P., A.M. Ferreri, and F. Caligaris-Cappio, *Chronic lymphocytic leukemia*. *Crit Rev Oncol Hematol*, 2007. **64**(3): p. 234-46.
35. Chiorazzi, N., K.R. Rai, and M. Ferrarini, *Chronic lymphocytic leukemia*. *N Engl J Med*, 2005. **352**(8): p. 804-15.
36. Gururajan, M., C.D. Jennings, and S. Bondada, *Cutting edge: constitutive B cell receptor signaling is critical for basal growth of B lymphoma*. *J Immunol*, 2006. **176**(10): p. 5715-9.
37. Burger, J.A. and N. Chiorazzi, *B cell receptor signaling in chronic lymphocytic leukemia*. *Trends Immunol*, 2013. **34**(12): p. 592-601.
38. Burger, J.A., et al., *The microenvironment in mature B-cell malignancies: a target for new treatment strategies*. *Blood*, 2009. **114**(16): p. 3367-75.
39. Hamblin, T., *Historical aspects of chronic lymphocytic leukaemia*. *Br J Haematol*, 2000. **111**(4): p. 1023-34.
40. Rai, K.R., et al., *Chronic lymphocytic leukemia*. *Med Clin North Am*, 1984. **68**(3): p. 697-711.
41. Faguet, G.B., *Chronic lymphocytic leukemia: an updated review*. *J Clin Oncol*, 1994. **12**(9): p. 1974-90.
42. Rai, K.R. and P. Jain, *Chronic lymphocytic leukemia (CLL)—Then and now*. *Am J Hematol*, 2016. **91**(3): p. 330-40.
43. Hamblin, T.J., et al., *Unmutated Ig V(H) genes are associated with a more aggressive form of chronic lymphocytic leukemia*. *Blood*, 1999. **94**(6): p. 1848-54.
44. Society, A.C. *Chronic Lymphocytic Leukemia*. Key Statistics for Chronic Lymphocytic Leukemia 2016; Available from: <https://www.cancer.org/cancer/chronic-lymphocytic-leukemia>.

45. Rai, K.R., et al., *Clinical staging of chronic lymphocytic leukemia*. Blood, 1975. **46**(2): p. 219-34.
46. Binet, J.L., et al., *A new prognostic classification of chronic lymphocytic leukemia derived from a multivariate survival analysis*. Cancer, 1981. **48**(1): p. 198-206.
47. Hallek, M., et al., *Guidelines for the diagnosis and treatment of chronic lymphocytic leukemia: a report from the International Workshop on Chronic Lymphocytic Leukemia updating the National Cancer Institute-Working Group 1996 guidelines*. Blood, 2008. **111**(12): p. 5446-56.
48. Kipps, T.J., et al., *Chronic lymphocytic leukaemia*. Nat Rev Dis Primers, 2017. **3**: p. 17008.
49. Berndt, S.I., et al., *Meta-analysis of genome-wide association studies discovers multiple loci for chronic lymphocytic leukemia*. Nat Commun, 2016. **7**: p. 10933.
50. Malek, S., *Advances in chronic lymphocytic leukemia*. Advances in experimental medicine and biology,. 2013, New York: Springer. xi, 334 pages.
51. Puiggros, A., G. Blanco, and B. Espinet, *Genetic abnormalities in chronic lymphocytic leukemia: where we are and where we go*. Biomed Res Int, 2014. **2014**: p. 435983.
52. Veronese, A., et al., *Allele-specific loss and transcription of the miR-15a/16-1 cluster in chronic lymphocytic leukemia*. Leukemia, 2015. **29**(1): p. 86-95.
53. Dohner, H., et al., *Genomic aberrations and survival in chronic lymphocytic leukemia*. N Engl J Med, 2000. **343**(26): p. 1910-6.
54. Dohner, H., et al., *p53 gene deletion predicts for poor survival and non-response to therapy with purine analogs in chronic B-cell leukemias*. Blood, 1995. **85**(6): p. 1580-9.
55. Finlay, C.A., P.W. Hinds, and A.J. Levine, *The p53 proto-oncogene can act as a suppressor of transformation*. Cell, 1989. **57**(7): p. 1083-93.
56. Ouillette, P., et al., *Incidence and clinical implications of ATM aberrations in chronic lymphocytic leukemia*. Genes Chromosomes Cancer, 2012. **51**(12): p. 1125-32.
57. Law, P.J., et al., *Genome-wide association analysis of chronic lymphocytic leukaemia, Hodgkin lymphoma and multiple myeloma identifies pleiotropic risk loci*. Sci Rep, 2017. **7**: p. 41071.
58. Law, P.J., et al., *Genome-wide association analysis implicates dysregulation of immunity genes in chronic lymphocytic leukaemia*. Nat Commun, 2017. **8**: p. 14175.
59. Rossi, D., M. Fangazio, and G. Gaidano, *The spectrum of genetic defects in chronic lymphocytic leukemia*. Mediterr J Hematol Infect Dis, 2012. **4**(1): p. e2012076.
60. Rosati, E., et al., *Constitutively activated Notch signaling is involved in survival and apoptosis resistance of B-CLL cells*. Blood, 2009. **113**(4): p. 856-65.
61. Kopan, R., *Notch signaling*. Cold Spring Harb Perspect Biol, 2012. **4**(10).
62. De Falco, F., et al., *Notch signaling sustains the expression of Mcl-1 and the activity of eIF4E to promote cell survival in CLL*. Oncotarget, 2015. **6**(18): p. 16559-72.
63. Rossi, D., et al., *Integrated mutational and cytogenetic analysis identifies new prognostic subgroups in chronic lymphocytic leukemia*. Blood, 2013. **121**(8): p. 1403-12.
64. Gianfelici, V., *Activation of the NOTCH1 pathway in chronic lymphocytic leukemia*. Haematologica, 2012. **97**(3): p. 328-30.
65. Wang, L., et al., *Transcriptomic Characterization of SF3B1 Mutation Reveals Its Pleiotropic Effects in Chronic Lymphocytic Leukemia*. Cancer Cell, 2016. **30**(5): p. 750-763.
66. Alhourani, E., et al., *BIRC3 alterations in chronic and B-cell acute lymphocytic leukemia patients*. Oncol Lett, 2016. **11**(5): p. 3240-3246.
67. Zhang, S. and T.J. Kipps, *The pathogenesis of chronic lymphocytic leukemia*. Annu Rev Pathol, 2014. **9**: p. 103-18.

68. Nadeu, F., et al., *Clinical impact of clonal and subclonal TP53, SF3B1, BIRC3, NOTCH1, and ATM mutations in chronic lymphocytic leukemia*. *Blood*, 2016. **127**(17): p. 2122-30.
69. Baumann Kreuziger, L.M., G. Tarchand, and V.A. Morrison, *The impact of Agent Orange exposure on presentation and prognosis of patients with chronic lymphocytic leukemia*. *Leuk Lymphoma*, 2014. **55**(1): p. 63-6.
70. Schinasi, L.H., et al., *Insecticide exposure and farm history in relation to risk of lymphomas and leukemias in the Women's Health Initiative observational study cohort*. *Ann Epidemiol*, 2015. **25**(11): p. 803-10.
71. Hulkkonen, J., et al., *Surface antigen expression in chronic lymphocytic leukemia: clustering analysis, interrelationships and effects of chromosomal abnormalities*. *Leukemia*, 2002. **16**(2): p. 178-85.
72. Wang, K., G. Wei, and D. Liu, *CD19: a biomarker for B cell development, lymphoma diagnosis and therapy*. *Exp Hematol Oncol*, 2012. **1**(1): p. 36.
73. Azzam, H.S., et al., *CD5 expression is developmentally regulated by T cell receptor (TCR) signals and TCR avidity*. *J Exp Med*, 1998. **188**(12): p. 2301-11.
74. Werner-Favre, C., et al., *Cell surface antigen CD5 is a marker for activated human B cells*. *Eur J Immunol*, 1989. **19**(7): p. 1209-13.
75. Bikah, G., et al., *CD5-mediated negative regulation of antigen receptor-induced growth signals in B-1 B cells*. *Science*, 1996. **274**(5294): p. 1906-9.
76. DiRaimondo, F., et al., *The clinical and diagnostic relevance of CD23 expression in the chronic lymphoproliferative disease*. *Cancer*, 2002. **94**(6): p. 1721-30.
77. Damle, R.N., et al., *B-cell chronic lymphocytic leukemia cells express a surface membrane phenotype of activated, antigen-experienced B lymphocytes*. *Blood*, 2002. **99**(11): p. 4087-93.
78. Gaidano, G., R. Foa, and R. Dalla-Favera, *Molecular pathogenesis of chronic lymphocytic leukemia*. *J Clin Invest*, 2012. **122**(10): p. 3432-8.
79. Seifert, M., et al., *Cellular origin and pathophysiology of chronic lymphocytic leukemia*. *J Exp Med*, 2012. **209**(12): p. 2183-98.
80. Carsetti, R., M.M. Rosado, and H. Wardmann, *Peripheral development of B cells in mouse and man*. *Immunol Rev*, 2004. **197**: p. 179-91.
81. Rossi, D. and G. Gaidano, *Biological and clinical significance of stereotyped B-cell receptors in chronic lymphocytic leukemia*. *Haematologica*, 2010. **95**(12): p. 1992-5.
82. Slupsky, J.R., *Does B cell receptor signaling in chronic lymphocytic leukaemia cells differ from that in other B cell types?* *Scientifica (Cairo)*, 2014. **2014**: p. 208928.
83. Agathangelidis, A., et al., *Stereotyped B-cell receptors in chronic lymphocytic leukemia*. *Leuk Lymphoma*, 2014. **55**(10): p. 2252-61.
84. Baliakas, P., et al., *Clinical effect of stereotyped B-cell receptor immunoglobulins in chronic lymphocytic leukaemia: a retrospective multicentre study*. *Lancet Haematol*, 2014. **1**(2): p. e74-84.
85. Chu, C.C., et al., *Chronic lymphocytic leukemia antibodies with a common stereotypic rearrangement recognize nonmuscle myosin heavy chain IIA*. *Blood*, 2008. **112**(13): p. 5122-9.
86. Alhakeem, S.S., et al., *Role of B cell receptor signaling in IL-10 production by normal and malignant B-1 cells*. *Ann N Y Acad Sci*, 2015. **1362**: p. 239-49.
87. Lam, K.P. and K. Rajewsky, *B cell antigen receptor specificity and surface density together determine B-1 versus B-2 cell development*. *J Exp Med*, 1999. **190**(4): p. 471-7.

88. Baumgarth, N., et al., *B-1 and B-2 cell-derived immunoglobulin M antibodies are nonredundant components of the protective response to influenza virus infection*. J Exp Med, 2000. **192**(2): p. 271-80.
89. Alugupalli, K.R. and R.M. Gerstein, *Divide and conquer: division of labor by B-1 B cells*. Immunity, 2005. **23**(1): p. 1-2.
90. Haas, K.M., et al., *B-1a and B-1b cells exhibit distinct developmental requirements and have unique functional roles in innate and adaptive immunity to S. pneumoniae*. Immunity, 2005. **23**(1): p. 7-18.
91. Hayakawa, K., et al., *B cells generated by B-1 development can progress to chronic lymphocytic leukemia*. Ann N Y Acad Sci, 2015. **1362**: p. 250-5.
92. Hayakawa, K., et al., *Early generated B1 B cells with restricted BCRs become chronic lymphocytic leukemia with continued c-Myc and low Bmf expression*. J Exp Med, 2016. **213**(13): p. 3007-3024.
93. Chiorazzi, N. and M. Ferrarini, *Cellular origin(s) of chronic lymphocytic leukemia: cautionary notes and additional considerations and possibilities*. Blood, 2011. **117**(6): p. 1781-91.
94. Rothstein, T.L., et al., *Human B-1 cells take the stage*. Ann N Y Acad Sci, 2013. **1285**: p. 97-114.
95. Foster, A.E., et al., *Selective depletion of a minor subpopulation of B-chronic lymphocytic leukemia cells is followed by a delayed but progressive loss of bulk tumor cells and disease regression*. Mol Cancer, 2009. **8**: p. 106.
96. Reya, T., et al., *Stem cells, cancer, and cancer stem cells*. Nature, 2001. **414**(6859): p. 105-11.
97. Rheingold, S.R., et al., *Role of the BCR complex in B cell development, activation, and leukemic transformation*. Immunol Res, 2003. **27**(2-3): p. 309-30.
98. Lam, K.P., R. Kuhn, and K. Rajewsky, *In vivo ablation of surface immunoglobulin on mature B cells by inducible gene targeting results in rapid cell death*. Cell, 1997. **90**(6): p. 1073-83.
99. Bojarczuk, K., et al., *B-cell receptor signaling in the pathogenesis of lymphoid malignancies*. Blood Cells Mol Dis, 2015. **55**(3): p. 255-65.
100. Hallek, M., *Signaling the end of chronic lymphocytic leukemia: new frontline treatment strategies*. Hematology Am Soc Hematol Educ Program, 2013. **2013**: p. 138-50.
101. Niemann, C.U. and A. Wiestner, *B-cell receptor signaling as a driver of lymphoma development and evolution*. Semin Cancer Biol, 2013. **23**(6): p. 410-21.
102. Packham, G., et al., *The outcome of B-cell receptor signaling in chronic lymphocytic leukemia: proliferation or anergy*. Haematologica, 2014. **99**(7): p. 1138-48.
103. Orchard, J.A., et al., *ZAP-70 expression and prognosis in chronic lymphocytic leukaemia*. Lancet, 2004. **363**(9403): p. 105-11.
104. Gauld, S.B. and J.C. Cambier, *Src-family kinases in B-cell development and signaling*. Oncogene, 2004. **23**(48): p. 8001-6.
105. Ingley, E., *Functions of the Lyn tyrosine kinase in health and disease*. Cell Commun Signal, 2012. **10**(1): p. 21.
106. Xu, Y., et al., *Lyn tyrosine kinase: accentuating the positive and the negative*. Immunity, 2005. **22**(1): p. 9-18.
107. Malbec, O., et al., *Fc epsilon receptor I-associated lyn-dependent phosphorylation of Fc gamma receptor IIB during negative regulation of mast cell activation*. J Immunol, 1998. **160**(4): p. 1647-58.



108. Tibaldi, E., et al., *Lyn-mediated SHP-1 recruitment to CD5 contributes to resistance to apoptosis of B-cell chronic lymphocytic leukemia cells*. *Leukemia*, 2011. **25**(11): p. 1768-81.
109. Contri, A., et al., *Chronic lymphocytic leukemia B cells contain anomalous Lyn tyrosine kinase, a putative contribution to defective apoptosis*. *J Clin Invest*, 2005. **115**(2): p. 369-78.
110. Wang, Y.H., et al., *Expression levels of Lyn, Syk, PLCgamma2 and ERK in patients with chronic lymphocytic leukemia, and higher levels of Lyn are associated with a shorter treatment-free survival*. *Leuk Lymphoma*, 2013. **54**(6): p. 1165-70.
111. Herishanu, Y. and A. Polliack, *B-cell receptor signaling in chronic lymphocytic leukemia leans on Lyn*. *Leuk Lymphoma*, 2013. **54**(6): p. 1125-6.
112. Dong, S. and J.C. Byrd, *A New Role for Lyn in the CLL Microenvironment*. *Cancer Cell*, 2016. **30**(4): p. 511-512.
113. Nguyen, P.H., et al., *LYN Kinase in the Tumor Microenvironment Is Essential for the Progression of Chronic Lymphocytic Leukemia*. *Cancer Cell*, 2016. **30**(4): p. 610-622.
114. Ke, J., et al., *Anomalous constitutive Src kinase activity promotes B lymphoma survival and growth*. *Mol Cancer*, 2009. **8**: p. 132.
115. Blake, R.A., et al., *SU6656, a selective src family kinase inhibitor, used to probe growth factor signaling*. *Mol Cell Biol*, 2000. **20**(23): p. 9018-27.
116. Lombardo, L.J., et al., *Discovery of N-(2-chloro-6-methyl-phenyl)-2-(6-(4-(2-hydroxyethyl)-piperazin-1-yl)-2-methylpyrimidin-4-ylamino)thiazole-5-carboxamide (BMS-354825), a dual Src/Abl kinase inhibitor with potent antitumor activity in preclinical assays*. *J Med Chem*, 2004. **47**(27): p. 6658-61.
117. Zauli, G., et al., *Dasatinib plus Nutlin-3 shows synergistic antileukemic activity in both p53 wild-type and p53 mutated B chronic lymphocytic leukemias by inhibiting the Akt pathway*. *Clin Cancer Res*, 2011. **17**(4): p. 762-70.
118. Cornall, R.J., et al., *Role of Syk in B-cell development and antigen-receptor signaling*. *Proc Natl Acad Sci U S A*, 2000. **97**(4): p. 1713-8.
119. Feng, G. and X. Wang, *Role of spleen tyrosine kinase in the pathogenesis of chronic lymphocytic leukemia*. *Leuk Lymphoma*, 2014. **55**(12): p. 2699-705.
120. Mocsai, A., J. Ruland, and V.L. Tybulewicz, *The SYK tyrosine kinase: a crucial player in diverse biological functions*. *Nat Rev Immunol*, 2010. **10**(6): p. 387-402.
121. Zarbock, A., C.A. Lowell, and K. Ley, *Spleen tyrosine kinase Syk is necessary for E-selectin-induced alpha(L)beta(2) integrin-mediated rolling on intercellular adhesion molecule-1*. *Immunity*, 2007. **26**(6): p. 773-83.
122. Benkisser-Petersen, M., et al., *Spleen Tyrosine Kinase Is Involved in the CD38 Signal Transduction Pathway in Chronic Lymphocytic Leukemia*. *PLoS One*, 2016. **11**(12): p. e0169159.
123. Parente-Ribes, A., et al., *Spleen tyrosine kinase inhibitors reduce CD40L-induced proliferation of chronic lymphocytic leukemia cells but not normal B cells*. *Haematologica*, 2016. **101**(2): p. e59-62.
124. Buchner, M., et al., *Spleen tyrosine kinase inhibition prevents chemokine- and integrin-mediated stromal protective effects in chronic lymphocytic leukemia*. *Blood*, 2010. **115**(22): p. 4497-506.
125. Maddocks, K. and J.A. Jones, *Bruton tyrosine kinase inhibition in chronic lymphocytic leukemia*. *Semin Oncol*, 2016. **43**(2): p. 251-9.
126. Maas, A. and R.W. Hendriks, *Role of Bruton's tyrosine kinase in B cell development*. *Dev Immunol*, 2001. **8**(3-4): p. 171-81.

127. Woyach, J.A., et al., *Bruton's tyrosine kinase (BTK) function is important to the development and expansion of chronic lymphocytic leukemia (CLL)*. *Blood*, 2014. **123**(8): p. 1207-13.
128. Koehrer, S. and J.A. Burger, *B-cell receptor signaling in chronic lymphocytic leukemia and other B-cell malignancies*. *Clin Adv Hematol Oncol*, 2016. **14**(1): p. 55-65.
129. Woyach, J.A., et al., *Prolonged lymphocytosis during ibrutinib therapy is associated with distinct molecular characteristics and does not indicate a suboptimal response to therapy*. *Blood*, 2014. **123**(12): p. 1810-7.
130. Jamroziak, K., B. Pula, and J. Walewski, *Current Treatment of Chronic Lymphocytic Leukemia*. *Curr Treat Options Oncol*, 2017. **18**(1): p. 5.
131. Werner, M., E. Hobeika, and H. Jumaa, *Role of PI3K in the generation and survival of B cells*. *Immunol Rev*, 2010. **237**(1): p. 55-71.
132. Jacob, A., et al., *Convergence of signaling pathways on the activation of ERK in B cells*. *J Biol Chem*, 2002. **277**(26): p. 23420-6.
133. Adem, J., et al., *ERK1/2 has an essential role in B cell receptor- and CD40-induced signaling in an in vitro model of germinal center B cell selection*. *Mol Immunol*, 2015. **67**(2 Pt B): p. 240-7.
134. Montagut, C. and J. Settleman, *Targeting the RAF-MEK-ERK pathway in cancer therapy*. *Cancer Lett*, 2009. **283**(2): p. 125-34.
135. Fecteau, J.F., et al., *Sorafenib-induced apoptosis of chronic lymphocytic leukemia cells is associated with downregulation of RAF and myeloid cell leukemia sequence 1 (Mcl-1)*. *Mol Med*, 2012. **18**: p. 19-28.
136. Davids, M.S. and J.R. Brown, *Targeting the B cell receptor pathway in chronic lymphocytic leukemia*. *Leuk Lymphoma*, 2012. **53**(12): p. 2362-70.
137. Mongini, P.K., et al., *TLR-9 and IL-15 Synergy Promotes the In Vitro Clonal Expansion of Chronic Lymphocytic Leukemia B Cells*. *J Immunol*, 2015. **195**(3): p. 901-23.
138. Slinger, E., et al., *Targeting antigen-independent proliferation in chronic lymphocytic leukemia through differential kinase inhibition*. *Leukemia*, 2017.
139. Pascutti, M.F., et al., *IL-21 and CD40L signals from autologous T cells can induce antigen-independent proliferation of CLL cells*. *Blood*, 2013. **122**(17): p. 3010-9.
140. Ansell, S.M. and R.H. Vonderheide, *Cellular composition of the tumor microenvironment*. *Am Soc Clin Oncol Educ Book*, 2013.
141. Mittal, A.K., et al., *Chronic lymphocytic leukemia cells in a lymph node microenvironment depict molecular signature associated with an aggressive disease*. *Mol Med*, 2014. **20**: p. 290-301.
142. Herishanu, Y., et al., *The lymph node microenvironment promotes B-cell receptor signaling, NF-kappaB activation, and tumor proliferation in chronic lymphocytic leukemia*. *Blood*, 2011. **117**(2): p. 563-74.
143. Herndon, T.M., et al., *Direct in vivo evidence for increased proliferation of CLL cells in lymph nodes compared to bone marrow and peripheral blood*. *Leukemia*, 2017. **31**(6): p. 1340-1347.
144. Bichi, R., et al., *Human chronic lymphocytic leukemia modeled in mouse by targeted TCL1 expression*. *Proc Natl Acad Sci U S A*, 2002. **99**(10): p. 6955-60.
145. Munk Pedersen, I. and J. Reed, *Microenvironmental interactions and survival of CLL B-cells*. *Leuk Lymphoma*, 2004. **45**(12): p. 2365-72.
146. Messmer, B.T., et al., *In vivo measurements document the dynamic cellular kinetics of chronic lymphocytic leukemia B cells*. *J Clin Invest*, 2005. **115**(3): p. 755-64.

147. Herreros, B., et al., *Proliferation centers in chronic lymphocytic leukemia: the niche where NF-kappaB activation takes place*. *Leukemia*, 2010. **24**(4): p. 872-6.
148. Caligaris-Cappio, F., M.T. Bertilaccio, and C. Scielzo, *How the microenvironment wires the natural history of chronic lymphocytic leukemia*. *Semin Cancer Biol*, 2014. **24**: p. 43-8.
149. Herishanu, Y., et al., *Biology of chronic lymphocytic leukemia in different microenvironments: clinical and therapeutic implications*. *Hematol Oncol Clin North Am*, 2013. **27**(2): p. 173-206.
150. Burger, J.A., *Nurture versus nature: the microenvironment in chronic lymphocytic leukemia*. *Hematology Am Soc Hematol Educ Program*, 2011. **2011**: p. 96-103.
151. Burger, J.A., et al., *Blood-derived nurse-like cells protect chronic lymphocytic leukemia B cells from spontaneous apoptosis through stromal cell-derived factor-1*. *Blood*, 2000. **96**(8): p. 2655-63.
152. Galletti, G., et al., *Targeting Macrophages Sensitizes Chronic Lymphocytic Leukemia to Apoptosis and Inhibits Disease Progression*. *Cell Rep*, 2016. **14**(7): p. 1748-60.
153. Reinart, N., et al., *Delayed development of chronic lymphocytic leukemia in the absence of macrophage migration inhibitory factor*. *Blood*, 2013. **121**(5): p. 812-21.
154. Heinig, K., et al., *Access to follicular dendritic cells is a pivotal step in murine chronic lymphocytic leukemia B-cell activation and proliferation*. *Cancer Discov*, 2014. **4**(12): p. 1448-65.
155. Scarfo, L., A.J. Ferreri, and P. Ghia, *Chronic lymphocytic leukaemia*. *Crit Rev Oncol Hematol*, 2016. **104**: p. 169-82.
156. Jain, N. and S. O'Brien, *Targeted therapies for CLL: Practical issues with the changing treatment paradigm*. *Blood Rev*, 2016. **30**(3): p. 233-44.
157. Fraietta, J.A., R.D. Schwab, and M.V. Maus, *Improving therapy of chronic lymphocytic leukemia with chimeric antigen receptor T cells*. *Semin Oncol*, 2016. **43**(2): p. 291-9.
158. Thyagarajan, B., et al., *Richter's transformation presenting as splenic rupture after 6 years of complete remission of chronic lymphocytic leukaemia*. *BMJ Case Rep*, 2016. **2016**.
159. Benjamini, O., et al., *Second cancers in patients with chronic lymphocytic leukemia who received frontline fludarabine, cyclophosphamide and rituximab therapy: distribution and clinical outcomes*. *Leuk Lymphoma*, 2015. **56**(6): p. 1643-50.
160. !!! INVALID CITATION !!! [158, 159].
161. Sells, S.F., et al., *Commonality of the gene programs induced by effectors of apoptosis in androgen-dependent and -independent prostate cells*. *Cell Growth Differ*, 1994. **5**(4): p. 457-66.
162. Johnstone, R.W., et al., *A novel repressor, par-4, modulates transcription and growth suppression functions of the Wilms' tumor suppressor WT1*. *Mol Cell Biol*, 1996. **16**(12): p. 6945-56.
163. Diaz-Meco, M.T., et al., *The product of par-4, a gene induced during apoptosis, interacts selectively with the atypical isoforms of protein kinase C*. *Cell*, 1996. **86**(5): p. 777-86.
164. Johnstone, R.W., et al., *Mapping of the human PAWR (par-4) gene to chromosome 12q21*. *Genomics*, 1998. **53**(2): p. 241-3.
165. Hebbar, N., C. Wang, and V.M. Rangnekar, *Mechanisms of apoptosis by the tumor suppressor Par-4*. *J Cell Physiol*, 2012. **227**(12): p. 3715-21.
166. El-Guendy, N. and V.M. Rangnekar, *Apoptosis by Par-4 in cancer and neurodegenerative diseases*. *Exp Cell Res*, 2003. **283**(1): p. 51-66.

167. Boghaert, E.R., et al., *Immunohistochemical analysis of the proapoptotic protein Par-4 in normal rat tissues*. Cell Growth Differ, 1997. **8**(8): p. 881-90.
168. El-Guendy, N., et al., *Identification of a unique core domain of par-4 sufficient for selective apoptosis induction in cancer cells*. Mol Cell Biol, 2003. **23**(16): p. 5516-25.
169. Gurumurthy, S., et al., *Phosphorylation of Par-4 by protein kinase A is critical for apoptosis*. Mol Cell Biol, 2005. **25**(3): p. 1146-61.
170. Goswami, A., et al., *Binding and phosphorylation of par-4 by akt is essential for cancer cell survival*. Mol Cell, 2005. **20**(1): p. 33-44.
171. Diaz-Meco, M.T., et al., *Inactivation of the inhibitory kappaB protein kinase/nuclear factor kappaB pathway by Par-4 expression potentiates tumor necrosis factor alpha-induced apoptosis*. J Biol Chem, 1999. **274**(28): p. 19606-12.
172. Garcia-Cao, I., et al., *Tumour-suppression activity of the proapoptotic regulator Par4*. EMBO Rep, 2005. **6**(6): p. 577-83.
173. Mundi, P.S., et al., *AKT in cancer: new molecular insights and advances in drug development*. Br J Clin Pharmacol, 2016. **82**(4): p. 943-56.
174. Cantley, L.C., *The phosphoinositide 3-kinase pathway*. Science, 2002. **296**(5573): p. 1655-7.
175. Bayascas, J.R. and D.R. Alessi, *Regulation of Akt/PKB Ser473 phosphorylation*. Mol Cell, 2005. **18**(2): p. 143-5.
176. Goswami, A., P. Ranganathan, and V.M. Rangnekar, *The phosphoinositide 3-kinase/Akt1/Par-4 axis: a cancer-selective therapeutic target*. Cancer Res, 2006. **66**(6): p. 2889-92.
177. Lee, T.J., et al., *Overexpression of Par-4 sensitizes TRAIL-induced apoptosis via inactivation of NF-kappaB and Akt signaling pathways in renal cancer cells*. J Cell Biochem, 2010. **109**(5): p. 885-95.
178. Joshi, J., et al., *Par-4 inhibits Akt and suppresses Ras-induced lung tumorigenesis*. EMBO J, 2008. **27**(16): p. 2181-93.
179. Fernandez-Marcos, P.J., et al., *Simultaneous inactivation of Par-4 and PTEN in vivo leads to synergistic NF-kappaB activation and invasive prostate carcinoma*. Proc Natl Acad Sci U S A, 2009. **106**(31): p. 12962-7.
180. Diaz-Meco, M.T. and S. Abu-Baker, *The Par-4/PTEN connection in tumor suppression*. Cell Cycle, 2009. **8**(16): p. 2518-22.
181. Qiu, S.G., et al., *Negative regulation of Par-4 by oncogenic Ras is essential for cellular transformation*. Oncogene, 1999. **18**(50): p. 7115-23.
182. Goswami, A., et al., *Par-4 binds to topoisomerase 1 and attenuates its DNA relaxation activity*. Cancer Res, 2008. **68**(15): p. 6190-8.
183. Champoux, J.J., *DNA topoisomerases: structure, function, and mechanism*. Annu Rev Biochem, 2001. **70**: p. 369-413.
184. Garcia-Cao, I., et al., *Genetic inactivation of Par4 results in hyperactivation of NF-kappaB and impairment of JNK and p38*. EMBO Rep, 2003. **4**(3): p. 307-12.
185. Eckelman, B.P., G.S. Salvesen, and F.L. Scott, *Human inhibitor of apoptosis proteins: why XIAP is the black sheep of the family*. EMBO Rep, 2006. **7**(10): p. 988-94.
186. Lafuente, M.J., et al., *Regulation of mature T lymphocyte proliferation and differentiation by Par-4*. EMBO J, 2003. **22**(18): p. 4689-98.
187. Elmore, S., *Apoptosis: a review of programmed cell death*. Toxicol Pathol, 2007. **35**(4): p. 495-516.
188. Zhao, Y. and V.M. Rangnekar, *Apoptosis and tumor resistance conferred by Par-4*. Cancer Biol Ther, 2008. **7**(12): p. 1867-74.

189. Shrestha-Bhattarai, T. and V.M. Rangnekar, *Cancer-selective apoptotic effects of extracellular and intracellular Par-4*. *Oncogene*, 2010. **29**(27): p. 3873-80.
190. Boehrer, S., et al., *Deregulated expression of prostate apoptosis response gene-4 in less differentiated lymphocytes and inverse expressional patterns of par-4 and bcl-2 in acute lymphocytic leukemia*. *Hematol J*, 2001. **2**(2): p. 103-7.
191. Qiu, G., et al., *Mutually exclusive expression patterns of Bcl-2 and Par-4 in human prostate tumors consistent with down-regulation of Bcl-2 by Par-4*. *Oncogene*, 1999. **18**(3): p. 623-31.
192. Gaulard, P., et al., *Expression of the bcl-2 gene product in follicular lymphoma*. *Am J Pathol*, 1992. **140**(5): p. 1089-95.
193. Boehrer, S., et al., *In lymphatic cells par-4 sensitizes to apoptosis by down-regulating bcl-2 and promoting disruption of mitochondrial membrane potential and caspase activation*. *Cancer Res*, 2002. **62**(6): p. 1768-75.
194. Chendil, D., et al., *Par-4, a pro-apoptotic gene, inhibits radiation-induced NF kappa B activity and Bcl-2 expression leading to induction of radiosensitivity in human prostate cancer cells PC-3*. *Cancer Biol Ther*, 2002. **1**(2): p. 152-60.
195. Chakraborty, M., et al., *Par-4 drives trafficking and activation of Fas and FasL to induce prostate cancer cell apoptosis and tumor regression*. *Cancer Res*, 2001. **61**(19): p. 7255-63.
196. Chaudhry, P., et al., *Prostate apoptosis response 4 (Par-4), a novel substrate of caspase-3 during apoptosis activation*. *Mol Cell Biol*, 2012. **32**(4): p. 826-39.
197. Treude, F., et al., *Caspase-8-mediated PAR-4 cleavage is required for TNFalpha-induced apoptosis*. *Oncotarget*, 2014. **5**(10): p. 2988-98.
198. Boosen, M., et al., *Par-4 is an essential downstream target of DAP-like kinase (Dlk) in Dlk/Par-4-mediated apoptosis*. *Mol Biol Cell*, 2009. **20**(18): p. 4010-20.
199. Burikhanov, R., et al., *The tumor suppressor Par-4 activates an extrinsic pathway for apoptosis*. *Cell*, 2009. **138**(2): p. 377-88.
200. Lee, A.S., *GRP78 induction in cancer: therapeutic and prognostic implications*. *Cancer Res*, 2007. **67**(8): p. 3496-9.
201. Lee, A.S., *The Par-4-GRP78 TRAIL, more twists and turns*. *Cancer Biol Ther*, 2009. **8**(22): p. 2103-5.
202. Chow, K.U., et al., *Imatinib induces apoptosis in CLL lymphocytes with high expression of Par-4*. *Leukemia*, 2005. **19**(6): p. 1103-5; author reply 1105-6; discussion 1106-7.
203. Bojarska-Junak, A., et al., *Assessment of the pathway of apoptosis involving PAR-4, DAXX and ZIPK proteins in CLL patients and its relationship with the principal prognostic factors*. *Folia Histochem Cytobiol*, 2011. **49**(1): p. 98-103.
204. Simonetti, G., et al., *Mouse models in the study of chronic lymphocytic leukemia pathogenesis and therapy*. *Blood*, 2014. **124**(7): p. 1010-9.
205. Phillips, J.A., et al., *The NZB mouse as a model for chronic lymphocytic leukemia*. *Cancer Res*, 1992. **52**(2): p. 437-43.
206. Salerno, E., et al., *The New Zealand black mouse as a model for the development and progression of chronic lymphocytic leukemia*. *Cytometry B Clin Cytom*, 2010. **78 Suppl 1**: p. S98-109.
207. Calin, G.A., et al., *Frequent deletions and down-regulation of micro- RNA genes miR15 and miR16 at 13q14 in chronic lymphocytic leukemia*. *Proc Natl Acad Sci U S A*, 2002. **99**(24): p. 15524-9.
208. Planelles, L., et al., *APRIL promotes B-1 cell-associated neoplasm*. *Cancer Cell*, 2004. **6**(4): p. 399-408.

209. Widhopf, G.F., 2nd, et al., *ROR1 can interact with TCL1 and enhance leukemogenesis in Emu-TCL1 transgenic mice*. Proc Natl Acad Sci U S A, 2014. **111**(2): p. 793-8.
210. Zapata, J.M., et al., *TNF receptor-associated factor (TRAF) domain and Bcl-2 cooperate to induce small B cell lymphoma/chronic lymphocytic leukemia in transgenic mice*. Proc Natl Acad Sci U S A, 2004. **101**(47): p. 16600-5.
211. Pekarsky, Y., et al., *The long journey of TCL1 transgenic mice: lessons learned in the last 15 years*. Gene Expr, 2015. **16**(3): p. 129-35.
212. Russo, G., et al., *Molecular analysis of a t(14;14) translocation in leukemic T-cells of an ataxia telangiectasia patient*. Proc Natl Acad Sci U S A, 1989. **86**(2): p. 602-6.
213. Narducci, M.G., et al., *Regulation of TCL1 expression in B- and T-cell lymphomas and reactive lymphoid tissues*. Cancer Res, 2000. **60**(8): p. 2095-100.
214. Said, J.W., et al., *TCL1 oncogene expression in B cell subsets from lymphoid hyperplasia and distinct classes of B cell lymphoma*. Lab Invest, 2001. **81**(4): p. 555-64.
215. Teitell, M.A., *The TCL1 family of oncoproteins: co-activators of transformation*. Nat Rev Cancer, 2005. **5**(8): p. 640-8.
216. Weng, J., et al., *TCL1: a shared tumor-associated antigen for immunotherapy against B-cell lymphomas*. Blood, 2012. **120**(8): p. 1613-23.
217. Pekarsky, Y., et al., *Tcl1 enhances Akt kinase activity and mediates its nuclear translocation*. Proc Natl Acad Sci U S A, 2000. **97**(7): p. 3028-33.
218. Noguchi, M., et al., *Proto-oncogene TCL1: more than just a coactivator for Akt*. FASEB J, 2007. **21**(10): p. 2273-84.
219. Pekarsky, Y., et al., *Tcl1 functions as a transcriptional regulator and is directly involved in the pathogenesis of CLL*. Proc Natl Acad Sci U S A, 2008. **105**(50): p. 19643-8.
220. Herling, M., et al., *TCL1 shows a regulated expression pattern in chronic lymphocytic leukemia that correlates with molecular subtypes and proliferative state*. Leukemia, 2006. **20**(2): p. 280-5.
221. Hamblin, T.J., *The TCL1 mouse as a model for chronic lymphocytic leukemia*. Leuk Res, 2010. **34**(2): p. 135-6.
222. Herling, M., et al., *High TCL1 levels are a marker of B-cell receptor pathway responsiveness and adverse outcome in chronic lymphocytic leukemia*. Blood, 2009. **114**(21): p. 4675-86.
223. Pekarsky, Y., et al., *Animal models for chronic lymphocytic leukemia*. J Cell Biochem, 2007. **100**(5): p. 1109-18.
224. Bresin, A., et al., *TCL1 transgenic mouse model as a tool for the study of therapeutic targets and microenvironment in human B-cell chronic lymphocytic leukemia*. Cell Death Dis, 2016. **7**: p. e2071.
225. Virgilio, L., et al., *Deregulated expression of TCL1 causes T cell leukemia in mice*. Proc Natl Acad Sci U S A, 1998. **95**(7): p. 3885-9.
226. Hoyer, K.K., et al., *Dysregulated TCL1 promotes multiple classes of mature B cell lymphoma*. Proc Natl Acad Sci U S A, 2002. **99**(22): p. 14392-7.
227. Yan, X.J., et al., *B cell receptors in TCL1 transgenic mice resemble those of aggressive, treatment-resistant human chronic lymphocytic leukemia*. Proc Natl Acad Sci U S A, 2006. **103**(31): p. 11713-8.
228. Johnson, A.J., et al., *Characterization of the TCL-1 transgenic mouse as a preclinical drug development tool for human chronic lymphocytic leukemia*. Blood, 2006. **108**(4): p. 1334-8.

229. Gorgun, G., et al., *E(mu)-TCL1 mice represent a model for immunotherapeutic reversal of chronic lymphocytic leukemia-induced T-cell dysfunction*. Proc Natl Acad Sci U S A, 2009. **106**(15): p. 6250-5.
230. Hofbauer, J.P., et al., *Development of CLL in the TCL1 transgenic mouse model is associated with severe skewing of the T-cell compartment homologous to human CLL*. Leukemia, 2011. **25**(9): p. 1452-8.
231. Bagnara, D., et al., *A novel adoptive transfer model of chronic lymphocytic leukemia suggests a key role for T lymphocytes in the disease*. Blood, 2011. **117**(20): p. 5463-72.
232. Bertilaccio, M.T., et al., *Xenograft models of chronic lymphocytic leukemia: problems, pitfalls and future directions*. Leukemia, 2013. **27**(3): p. 534-40.
233. Stacchini, A., et al., *MEC1 and MEC2: two new cell lines derived from B-chronic lymphocytic leukaemia in prolymphocytoid transformation*. Leuk Res, 1999. **23**(2): p. 127-36.
234. Rasul, E., et al., *The MEC1 and MEC2 lines represent two CLL subclones in different stages of progression towards prolymphocytic leukemia*. PLoS One, 2014. **9**(8): p. e106008.
235. Hertlein, E., et al., *Characterization of a new chronic lymphocytic leukemia cell line for mechanistic in vitro and in vivo studies relevant to disease*. PLoS One, 2013. **8**(10): p. e76607.
236. Kellner, J., et al., *Isolation of a novel chronic lymphocytic leukemic (CLL) cell line and development of an in vivo mouse model of CLL*. Leuk Res, 2016. **40**: p. 54-9.
237. ter Brugge, P.J., et al., *A mouse model for chronic lymphocytic leukemia based on expression of the SV40 large T antigen*. Blood, 2009. **114**(1): p. 119-27.
238. Singh, S.P., et al., *Cell lines generated from a chronic lymphocytic leukemia mouse model exhibit constitutive Btk and Akt signaling*. Oncotarget, 2017.
239. Wiestner, A., *Emerging role of kinase-targeted strategies in chronic lymphocytic leukemia*. Blood, 2012. **120**(24): p. 4684-91.
240. Yardeni, T., et al., *Retro-orbital injections in mice*. Lab Anim (NY), 2011. **40**(5): p. 155-60.
241. Golde, W.T., P. Gollobin, and L.L. Rodriguez, *A rapid, simple, and humane method for submandibular bleeding of mice using a lancet*. Lab Anim (NY), 2005. **34**(9): p. 39-43.
242. Ullman-Cullere, M.H. and C.J. Foltz, *Body condition scoring: a rapid and accurate method for assessing health status in mice*. Lab Anim Sci, 1999. **49**(3): p. 319-23.
243. Plumb, J.A., *Cell sensitivity assays: the MTT assay*. Methods Mol Med, 2004. **88**: p. 165-9.
244. Shrestha-Bhattarai, T. and V.M. Rangnekar, *Cancer-selective apoptotic effects of extracellular and intracellular Par-4*. Oncogene, 2010. **29**(27): p. 3873.
245. Boehrer, S., et al., *Expression and function of prostate-apoptosis-response-gene-4 in lymphatic cells*. Leuk Lymphoma, 2002. **43**(9): p. 1737-41.
246. Wang, P. *Biological Effects of Agent on PAR-4 Levels With Resected Solid Tumors*. 2016 July 5, 2017; Available from: <https://clinicaltrials.gov/ct2/show/NCT03015324>.
247. Riches, J.C., et al., *Trisomy 12 chronic lymphocytic leukemia cells exhibit upregulation of integrin signaling that is modulated by NOTCH1 mutations*. Blood, 2014. **123**(26): p. 4101-10.
248. Parker, T.L. and M.P. Strout, *Chronic lymphocytic leukemia: prognostic factors and impact on treatment*. Discov Med, 2011. **11**(57): p. 115-23.
249. Herzenberg, L.A. and A.M. Stall, *Conventional and Ly-1 B-cell lineages in normal and mu transgenic mice*. Cold Spring Harb Symp Quant Biol, 1989. **54 Pt 1**: p. 219-25.

250. Song, Z., et al., *Activities of SYK and PLCgamma2 predict apoptotic response of CLL cells to SRC tyrosine kinase inhibitor dasatinib*. Clin Cancer Res, 2010. **16**(2): p. 587-99.
251. Vitale, C. and J.A. Burger, *Chronic lymphocytic leukemia therapy: new targeted therapies on the way*. Expert Opin Pharmacother, 2016. **17**(8): p. 1077-89.
252. Palacios, E.H. and A. Weiss, *Function of the Src-family kinases, Lck and Fyn, in T-cell development and activation*. Oncogene, 2004. **23**(48): p. 7990-8000.
253. Ke, J., et al., *The role of MAPKs in B cell receptor-induced down-regulation of Egr-1 in immature B lymphoma cells*. J Biol Chem, 2006. **281**(52): p. 39806-18.
254. Veldurthy, A., et al., *The kinase inhibitor dasatinib induces apoptosis in chronic lymphocytic leukemia cells in vitro with preference for a subgroup of patients with unmutated IgVH genes*. Blood, 2008. **112**(4): p. 1443-52.
255. Tiruttani Subhramanyam, U.K., et al., *Structural basis for the regulatory interactions of proapoptotic Par-4*. Cell Death Differ, 2017. **24**(9): p. 1540-1547.
256. Chang, S., J.H. Kim, and J. Shin, *p62 forms a ternary complex with PKCzeta and PAR-4 and antagonizes PAR-4-induced PKCzeta inhibition*. FEBS Lett, 2002. **510**(1-2): p. 57-61.
257. Liu, W.J., et al., *p62 links the autophagy pathway and the ubiquitin-proteasome system upon ubiquitinated protein degradation*. Cell Mol Biol Lett, 2016. **21**: p. 29.
258. Le, X.F., et al., *Dasatinib induces autophagic cell death in human ovarian cancer*. Cancer, 2010. **116**(21): p. 4980-90.
259. Xie, N., et al., *Autophagy contributes to dasatinib-induced myeloid differentiation of human acute myeloid leukemia cells*. Biochem Pharmacol, 2014. **89**(1): p. 74-85.
260. Stewart, J.R. and C.A. O'Brian, *Protein kinase C- $\alpha$  mediates epidermal growth factor receptor transactivation in human prostate cancer cells*. Mol Cancer Ther, 2005. **4**(5): p. 726-32.
261. Alkan, S., et al., *Survival role of protein kinase C (PKC) in chronic lymphocytic leukemia and determination of isoform expression pattern and genes altered by PKC inhibition*. Am J Hematol, 2005. **79**(2): p. 97-106.
262. Hochegger, H., S. Takeda, and T. Hunt, *Cyclin-dependent kinases and cell-cycle transitions: does one fit all?* Nat Rev Mol Cell Biol, 2008. **9**(11): p. 910-6.
263. Deng, C., et al., *Mice lacking p21CIP1/WAF1 undergo normal development, but are defective in G1 checkpoint control*. Cell, 1995. **82**(4): p. 675-84.
264. Cmielova, J. and M. Rezacova, *p21Cip1/Waf1 protein and its function based on a subcellular localization [corrected]*. J Cell Biochem, 2011. **112**(12): p. 3502-6.
265. Cobo, F., et al., *Multiple cell cycle regulator alterations in Richter's transformation of chronic lymphocytic leukemia*. Leukemia, 2002. **16**(6): p. 1028-34.
266. ten Hacken, E. and J.A. Burger, *Microenvironment dependency in Chronic Lymphocytic Leukemia: The basis for new targeted therapies*. Pharmacol Ther, 2014. **144**(3): p. 338-48.
267. Ranganathan, P. and V.M. Rangnekar, *Regulation of cancer cell survival by Par-4*. Ann N Y Acad Sci, 2005. **1059**: p. 76-85.
268. Cheema, S.K., et al., *Par-4 transcriptionally regulates Bcl-2 through a WT1-binding site on the bcl-2 promoter*. J Biol Chem, 2003. **278**(22): p. 19995-20005.
269. Yang, L., et al., *A tumor suppressor and oncogene: the WT1 story*. Leukemia, 2007. **21**(5): p. 868-76.
270. Cosialls, A.M., et al., *Epigenetic profile in chronic lymphocytic leukemia using methylation-specific multiplex ligation-dependent probe amplification*. Epigenomics, 2012. **4**(5): p. 491-501.



271. Giannopoulos, K., et al., *Expression of RHAMM/CD168 and other tumor-associated antigens in patients with B-cell chronic lymphocytic leukemia*. *Int J Oncol*, 2006. **29**(1): p. 95-103.
272. Meyers, J.A., D.W. Su, and A. Lerner, *Chronic lymphocytic leukemia and B and T cells differ in their response to cyclic nucleotide phosphodiesterase inhibitors*. *J Immunol*, 2009. **182**(9): p. 5400-11.
273. Cerami, E., et al., *The cBio cancer genomics portal: an open platform for exploring multidimensional cancer genomics data*. *Cancer Discov*, 2012. **2**(5): p. 401-4.
274. Gao, J., et al., *Integrative analysis of complex cancer genomics and clinical profiles using the cBioPortal*. *Sci Signal*, 2013. **6**(269): p. pl1.
275. Landau, D.A., et al., *Evolution and impact of subclonal mutations in chronic lymphocytic leukemia*. *Cell*, 2013. **152**(4): p. 714-26.
276. Puente, X.S., et al., *Non-coding recurrent mutations in chronic lymphocytic leukaemia*. *Nature*, 2015. **526**(7574): p. 519-24.
277. Campbell, J.D., et al., *Distinct patterns of somatic genome alterations in lung adenocarcinomas and squamous cell carcinomas*. *Nat Genet*, 2016. **48**(6): p. 607-16.
278. Zhuang, J., et al., *Akt is activated in chronic lymphocytic leukemia cells and delivers a pro-survival signal: the therapeutic potential of Akt inhibition*. *Haematologica*, 2010. **95**(1): p. 110-8.
279. Laine, J., et al., *The protooncogene TCL1 is an Akt kinase coactivator*. *Mol Cell*, 2000. **6**(2): p. 395-407.
280. Martelli, A.M., et al., *The emerging multiple roles of nuclear Akt*. *Biochim Biophys Acta*, 2012. **1823**(12): p. 2168-78.
281. Palamarchuk, A., et al., *Tcl1 protein functions as an inhibitor of de novo DNA methylation in B-cell chronic lymphocytic leukemia (CLL)*. *Proc Natl Acad Sci U S A*, 2012. **109**(7): p. 2555-60.
282. Yang, L., R. Rau, and M.A. Goodell, *DNMT3A in haematological malignancies*. *Nat Rev Cancer*, 2015. **15**(3): p. 152-65.
283. Moreno-Bueno, G., et al., *Inactivation of the candidate tumor suppressor par-4 in endometrial cancer*. *Cancer Res*, 2007. **67**(5): p. 1927-34.
284. Pruitt, K., et al., *Ras-mediated loss of the pro-apoptotic response protein Par-4 is mediated by DNA hypermethylation through Raf-independent and Raf-dependent signaling cascades in epithelial cells*. *J Biol Chem*, 2005. **280**(24): p. 23363-70.
285. Kline, C.L. and R.B. Irby, *The pro-apoptotic protein Prostate Apoptosis Response Protein-4 (Par-4) can be activated in colon cancer cells by treatment with Src inhibitor and 5-FU*. *Apoptosis*, 2011. **16**(12): p. 1285-94.
286. Ghosh, A.K., et al., *The novel receptor tyrosine kinase Axl is constitutively active in B-cell chronic lymphocytic leukemia and acts as a docking site of nonreceptor kinases: implications for therapy*. *Blood*, 2011. **117**(6): p. 1928-37.
287. Nguyen, J.Q. and R.B. Irby, *TRIM21 is a novel regulator of Par-4 in colon and pancreatic cancer cells*. *Cancer Biol Ther*, 2017. **18**(1): p. 16-25.
288. Espinosa, A., et al., *The Sjogren's syndrome-associated autoantigen Ro52 is an E3 ligase that regulates proliferation and cell death*. *J Immunol*, 2006. **176**(10): p. 6277-85.
289. Bullrich, F., et al., *Characterization of the 13q14 tumor suppressor locus in CLL: identification of ALT1, an alternative splice variant of the LEU2 gene*. *Cancer Res*, 2001. **61**(18): p. 6640-8.

290. de Thonel, A., et al., *Regulation of the proapoptotic functions of prostate apoptosis response-4 (Par-4) by casein kinase 2 in prostate cancer cells*. *Cell Death Dis*, 2014. **5**: p. e1016.
291. Martins, L.R., et al., *Targeting CK2 overexpression and hyperactivation as a novel therapeutic tool in chronic lymphocytic leukemia*. *Blood*, 2010. **116**(15): p. 2724-31.
292. Ghelli Luserna di Rora, A., I. Iacobucci, and G. Martinelli, *The cell cycle checkpoint inhibitors in the treatment of leukemias*. *J Hematol Oncol*, 2017. **10**(1): p. 77.
293. Chen, Y., et al., *Pro-survival signal inhibition by CDK inhibitor dinaciclib in Chronic Lymphocytic Leukaemia*. *Br J Haematol*, 2016. **175**(4): p. 641-651.
294. Igawa, T., et al., *Cyclin D2 is overexpressed in proliferation centers of chronic lymphocytic leukemia/small lymphocytic lymphoma*. *Cancer Sci*, 2011. **102**(11): p. 2103-7.
295. Donjerkovic, D. and D.W. Scott, *Regulation of the G1 phase of the mammalian cell cycle*. *Cell Res*, 2000. **10**(1): p. 1-16.
296. Galanos, P., et al., *Chronic p53-independent p21 expression causes genomic instability by deregulating replication licensing*. *Nat Cell Biol*, 2016. **18**(7): p. 777-89.
297. Theerakitthanakul, K., et al., *Senescence Process in Primary Wilms' Tumor Cell Culture Induced by p53 Independent p21 Expression*. *J Cancer*, 2016. **7**(13): p. 1867-1876.
298. Agnoletto, C., et al., *The anti-leukemic activity of sodium dichloroacetate in p53mutated/null cells is mediated by a p53-independent ILF3/p21 pathway*. *Oncotarget*, 2015. **6**(4): p. 2385-96.
299. Rasool, R.U., et al., *AKT is indispensable for coordinating Par-4/JNK cross talk in p21 downmodulation during ER stress*. *Oncogenesis*, 2017. **6**(5): p. e341.
300. Dhanasekaran, D.N. and E.P. Reddy, *JNK signaling in apoptosis*. *Oncogene*, 2008. **27**(48): p. 6245-51.
301. Gururajan, M., et al., *c-Jun N-terminal kinase (JNK) is required for survival and proliferation of B-lymphoma cells*. *Blood*, 2005. **106**(4): p. 1382-91.
302. Knies, N., et al., *Lymphomagenic CARD11/BCL10/MALT1 signaling drives malignant B-cell proliferation via cooperative NF-kappaB and JNK activation*. *Proc Natl Acad Sci U S A*, 2015. **112**(52): p. E7230-8.
303. Schmid, C.A., et al., *DUSP4 deficiency caused by promoter hypermethylation drives JNK signaling and tumor cell survival in diffuse large B cell lymphoma*. *J Exp Med*, 2015. **212**(5): p. 775-92.
304. Arevalo, M.A., et al., *Estradiol meets notch signaling in developing neurons*. *Front Endocrinol (Lausanne)*, 2011. **2**: p. 21.
305. Fan, J.Z., et al., *Estrogen improves the proliferation and differentiation of hBMSCs derived from postmenopausal osteoporosis through notch signaling pathway*. *Mol Cell Biochem*, 2014. **392**(1-2): p. 85-93.
306. Guo, P., et al., *Overexpression of vascular endothelial growth factor by MCF-7 breast cancer cells promotes estrogen-independent tumor growth in vivo*. *Cancer Res*, 2003. **63**(15): p. 4684-91.
307. Kipps, T.J., et al., *Chronic lymphocytic leukaemia*. *Nat Rev Dis Primers*, 2017. **3**: p. 16096.
308. Hess, P., et al., *Survival signaling mediated by c-Jun NH(2)-terminal kinase in transformed B lymphoblasts*. *Nat Genet*, 2002. **32**(1): p. 201-5.
309. Burikhanov, R., et al., *Chloroquine-Inducible Par-4 Secretion Is Essential for Tumor Cell Apoptosis and Inhibition of Metastasis*. *Cell Rep*, 2017. **18**(2): p. 508-519.
310. Zhao, Y., et al., *Cancer resistance in transgenic mice expressing the SAC module of Par-4*. *Cancer Res*, 2007. **67**(19): p. 9276-85.

Vita

**Mary Kathryn (Katie) McKenna**

Date and Place of Birth: 07/31/1988, Mt. Sterling, Kentucky, USA

Education:

2012-2017 PhD, Department of Microbiology, Immunology and Molecular Genetics  
University of Kentucky, Lexington, KY

2006-2010 Bachelors of Science, Biology  
Centre College, Danville, KY

Professional Positions:

08/12-9/17 Graduate Research Assistant, University of Kentucky, Lexington, KY

01/12-08/12 Lab Technician, Dr. John Yannelli, University of Kentucky

06/10-5/11 Lab Technician, FermSolutions Inc., Danville, KY

Scholastic and Professional Honors:

08/12-9/17 Graduate Research Assistantship, University of Kentucky

07/2014-03/16 T32 National Cancer Institute Supported National Research Service Award  
Trainee: Continuing Umbrella of Research Experiences (CURE) Program

08/2012 Appalachian Student Minority Award

2007-2010 Tri Beta Honors Society

2006-2010 Centre College Faculty Scholarship

Leadership/Awards:

2013-2015 MEPPs, Microbiology Educational Policies and Practices Committee  
Student Representative

2014-2016 University of Kentucky Graduate Student Congress  
Microbiology, Immunology, and Molecular Genetics Student Representative

2013-2017 District Science Fair Judge, Morton Middle School  
Fayette County Science Fair

- 2015-2017 BRIDGE Program Mentor  
Eastern Kentucky University – University of Kentucky
- 11/2015 University of Kentucky Graduate School Three-Minute Thesis Competition  
2<sup>nd</sup> Place
- 05/2017 Markey Cancer Center Research Day  
1<sup>st</sup> Place Graduate Student Poster Awardee

Publications:

**McKenna MK**, Gachuki BW, Alhakeem SS, Oben KN, Rangnekar VM, Gupta RC, Bondada S. Anti-cancer activity of withaferin a in B-cell lymphoma. *Cancer biology & therapy* 2015:1088-1098.

Alhakeem, S. S., Sindhava, V. J., **McKenna, M. K.**, Gachuki, B. W., Byrd, J. C., Muthusamy, N. and Bondada, S. (2015), Role of B cell receptor signaling in IL-10 production by normal and malignant B-1 cells. *Annals of the New York Academy of Sciences* p239-249.

Oben, K.Z., Gachuki, B.W., Alhakeem, S.A., **McKenna, M.K.**, Liang, Y., St. Clair, D.K., Rangnekar, V.M., Bondada, S Radiation Induced Apoptosis of Murine Bone Marrow Cells Is Independent of Early Growth Response 1 (EGR1). *PLoS One*, 2017. 12(1): p. e0169767.

Karine Z. Oben, Sara S. Alhakeem, **Mary K. McKenna**, et al. Withaferin A induces selective apoptosis of myelodysplastic syndrome but not normal bone marrow cells via elevation of reactive oxygen species. *Oncotarget*. (*Manuscript Accepted*).

**McKenna et al.** Novel pro-growth role for the tumor suppressor Prostate Apoptosis Response-4 in Chronic Lymphocytic Leukemia (*to be submitted*)

Sara S. Alhakeem, **Mary K. McKenna**, Karine Z. Oben, et al. Suppression of Anti-tumor Immunity in Chronic Lymphocytic Leukemia Mouse Model via Interleukin-10 Production (*submitted, Leukemia*)

Abstracts and Presentations:

- 2017 Markey Cancer Center Symposium, University of Kentucky  
Poster Presentation, May 2017
- 2016 International Congress of Immunology. Melbourne, Australia  
Invited Oral Presentation, August 2016

- 2016 Markey Cancer Center Symposium, University of Kentucky  
Invited Oral Presentation, May 2016
- 2016 Markey Cancer Center Symposium, University of Kentucky  
Poster Presentation, May 2016
- 2016 Immunology: American Association for Immunologists, Seattle, WA  
Poster Presentation, May 2016
- 2015 American Association for Hematology, Orlando, FL  
Poster Co-Authorship, December 2015
- 2015 Immunology: American Association for Immunologists, New Orleans, LA  
Poster Presentation, May 2015
- 2015 Markey Cancer Center Symposium, University of Kentucky  
Poster Presentation, May 2015
- 2015 Microbiology, Immunology, and Molecular Genetics Department Retreat; Poster  
Presentation, May 2015
- 2015 Graduate Student Day at the Capitol, Frankfort, KY  
Poster Presentation, October 2015
- 2014 Markey Cancer Center Symposium, University of Kentucky  
Poster Presentation, May 2014
- 2014 Center for Clinical and Translational Science Spring Conference, University of  
Kentucky; Poster Presentation, April 2014
- 2014 Microbiology, Immunology, and Molecular Genetics Department Retreat; Poster  
Presentation, May 2014
- 2013 Autumn Immunology Conference, Chicago, IL  
Oral and Poster Presentation, November 2013
- 2013 Center for Clinical and Translational Science Spring Conference  
Poster Presentation, April 2013
- 2013 Microbiology, Immunology, and Molecular Genetics Department Retreat; Oral  
and Poster Presentation, May 2013